REGULATION OF CHROMATIN STRUCTRE AND TRANSCRIPTION BY POLY(ADP-RIBOSE) POLYMERASE -1

A Dissertation

Presented to the Faculty of the Graduate School

of Cornell University

in Partial Fulfillment of the Requirements for the Degree of

Doctor in Philosophy

by

Raga Krishnakumar

May 2010

REGULATION OF CHROMATIN STRUCTRE AND TRANSCRIPTION BY POLY(ADP-RIBOSE) POLYMERASE -1

Raga Krishnakumar, Ph.D.

Cornell University 2010

The process of transcription, which is a vital step in the cellular response to physiological and environmental stimuli, is highly regulated at multiple levels. Many proteins are involved in orchestrating transcriptional responses, including proteins that modulate the physiological template for transcription, chromatin. One such protein is the highly abundant nuclear enzyme Poly(ADP-ribose) Polymerase-1 , or PARP-1. Although PARP-1 has classically been studied with relation to its role in the detection and repair of DNA damage, recent work has uncovered physiological functions of PARP-1 in regulating transcription. PARP-1 has been shown to have a range of functions in transcriptional regulating, including acting as a co-activator and as a modulator of chromatin structure. Although there are increasing numbers of studies revealing roles for PARP-1 in many processes, the molecular mechanisms of PARP-1 action in most pathways is largely unknown. In this study, I have investigated transcriptional regulation by PARP-1 *in vivo*, using both genomic and gene-specific analyses in breast cancer cells and human cardiomyocytes.

Using chromatin immunoprecipitation coupled with DNA microarrays (ChIP-chip), I show that PARP-1 binds to active promoters in MCF-7 breast cancer cells, and that at genes that are positively-regulated by PARP-1, it acts to exclude the binding of linker histone H1. Further analysis revealed that exclusion of H1 from promoters allows for a favorable chromatin structure which in turn permits the binding of RNA Polymerase II at target genes. This open chromatin conformation also requires methylated histones, which PARP-1 maintains by PARylating and preventing

recruitment of the demethylase KDM5B, a pathway which is also utilized by signal-dependent transcription.

Besides breast cancer, PARP-1 plays a prominent role in other pathologies, one of which is the progression of cardiovascular disease (CVD). I use a human cardiomyocyte cell line to show that TNFα can drastically increase the binding of the transcription factor NFκB to chromatin, and that this causes changes in the gene expression profile of these cells. PARP-1 is known to cooperate with NFκB at target genes. I show that in human cardiomyocytes, PARP-1 is required for NFκB up-regulated genes, but not for down-regulated genes, confirming its role as an activator of NFκB-dependent transcription. Interestingly, I see that the majority of NFκB binding in the presence of TNFα is not to canonical NFκB binding sites, suggesting the the majority of the NFκB response is intricately dependent on other transcription factors, and I show that one of these factors, ATF2, is vital for recruiting NFκB to promoters and regulating transcription. It will be interesting to further investigate how PARP-1 and ATF2 may be collaborating at target genes. Together, these data demonstrate a conserved binding pattern of PARP-1 on chromatin across cell types, and establish novel connections between PARP-1, signaling pathways, chromatin and gene expression.

BIOGRAPHICAL SKETCH

Raga Krishnakumar was born in Chennai, India. At age 2, she moved to Geneva, Switzerland, where she lived until she graduated from the International School of Geneva. In 2001, she joined St. John's College in Cambridge University, UK, where she gained a strong background in general biology, including topics in biochemistry, physiology, pathology, genetics and molecular biology. In 2004, she completed her undergraduate studies and received a B.A. with honors. In the same year, she joined the Graduate Field of Biochemistry, Molecular and Cell Biology at Cornell University, and in 2005, she joined the lab of Dr. W. Lee Kraus. During her graduate studies, Raga studied the molecular mechanisms by which the nuclear enzyme Poly(ADP-ribose) Polymerase – 1 regulates chromatin structure and transcription in mammalian cells. She received multiple awards, including the American Heart Association Pre-doctoral Fellowship in 2008. In 2009, she successfully defended her Ph.D. thesis.

To my parents, for supporting me in every way, and always believing in me

ACKNOWLEDGMENTS

I would like to thank my advisor, Dr. Lee Kraus, for taking a chance on me and accepting me as his student, despite my lack of experience at the start. It is never easy to take such a gamble, and I am grateful that he did. Additionally, I wish to thank him for all his support during my graduate studies, teaching me the importance of dedication and hard work, and always leading by example. I am also grateful to my committee members, Dr. John Lis and Dr. Barbara Baird for following my research, providing scientific insights and for all their advice throughout the years.

I cannot express in words how much gratitude I have toward my parents, Velamur and Jaya Krishnakumar, for everything that they have done for me. They have always stood by me, through good and bad, and have given me everything without ever expecting anything in return. Any success I have is a testament to their unconditional love and support. அம்மா, அப்பா, எல்லாத்துக்கும் ரொம்ப தேங்க்ஸ்! I love you!

Thank you to my brother, Rajiv, who despite being younger than me is taller, smarter and more accomplished than I ever will be. You teach me to be better every day, leet. Thank you to my grandmother, ரமணி பட்டி, who despite the hardships in her life, has always been by my side, and on my side. And thanks to the rest of my family, especially to my aunt Prabha Siddarth, my uncle S. Siddarth and my adorable cousin Divya for being my home away from home, and to my parents (in law) Semyon and Bella Bronevetsky for taking me into their family and making me feel like their own daughter.

I would like to thank all my lab-mates in the Kraus lab for great scientific interactions, and for creating such a stimulating work environment. First of all, thank you to my fellow classmate, my "partner in crime" and one of my closest friends,

Nasun Hah. We went through it all together, from classes to A-exams to the stress of graduating. Nasun, you know I would not have made it this far without your support, and it scares me to think of being in a lab without you. I'll miss you tons, and you know I will keep convincing you to meet me on the West Coast! A special thanks to previous lab members Dr. Miltos Kininis and Dr. Tong Zhang for being my teachers in lab when I first joined and for continued help throughout my studies. Also thanks to Dr. Matt Gamble for a very fruitful collaboration, and for imparting so much knowledge on me. I was lucky to have had such a great bay-mate and friend in Xin Luo. She helped me get through a lot of tough times (with fruit and candy always ready!) and she always has a smile on her face, no matter what. Thank you to my undergraduate researcher, Michelle DuMond, for helping me to be a better teacher, and for the great conversations about science and life. I want to thank present lab members Kris Frizzell (fellow PARPer), Dr. Don Ruhl (for his help and patience, despite my million questions), Liz Fogarty, Miao Sun, Bryan Gibson, Dr. Charles Danko and Fang Ye. I am also grateful to have worked with past lab members Dr. Dave Wacker, Dr. Gary Isaacs, Dr. Nina Heldring, Jhoanna Berrocal and Molly Shook. Also thanks to our rotation students, undergraduate researchers and undergraduate helpers. I wish you all the best of luck. I will miss everyone in the lab a lot, and hope that we will have the chance to meet often in the future.

Thank you to all my friends at Cornell and around the world, especially Priyanka Saksena, Daria Gavriouchkina (je vous aime, les filles!), Miltos Kininis (bananas!) and my gang: Nasun Hah, Xin Li, Shamoni Maheshwari, Ram Viswanatha and Srich Murugesan. Friendships like these last a lifetime, and I am fortunate to have met each end every one of you. I know we have many reunions to look forward to.

A little shout-out to my two kitties, Loki and Kali: they were my Ph.D. companions and loved me unconditionally during the good and bad times. Love you, babies.

Lastly and mostly, I want to thank my husband, Greg Bronevetsky. Not only has he been my rock these last five years, but only he could put up with me so patiently, and support me through everything. Grego, I am more grateful than you will ever know, and I am the luckiest person in the world to have a life partner like you. Я тебя люблю!

Having completed this challenging journey through graduate school, I truly believe that nothing is impossible if you put all of your mind and your heart into it. Ph.D. always seemed to me like an exclusive club with members-only access. I'm honored and excited to have finally earned the entrance pass! And so it begins.

TABLE OF CONTENTS

LIST OF FIGURES

LIST OF TABLES

LIST OF ABBREVIATIONS

AP1	Activating Protein 1
AP2	Activating Protein 2
APLF	Aprataxin PNK-like Factor
ATCC	American Type Culture Collection
ATF	Activating Transcription Factor
BER	Base Excision Repair
BP	Base Pairs
BRCA1	Breast Cancer 1
CARM1	Coactivator-associated Arginine Methyltransferase 1
CBP	CREB Binding Protein
CHFR	Checkpoint protein with FHA and RING domains
ChIP	Chromatin Immunoprecipitation
CREB	cAMP Response Element Binding
CTCF	CCTC-binding Factor
CVD	Cardiovascular Disease
DNA	Deoxyribonucleic Acid
EED	Embryonic Ectoderm Development
ENCODE	Encyclopedia of DNA Elements
ES cells	Embryonic Stem Cells
EZH2	Enhancer of Zeste
FISH	Fluoresent In-Situ Hybridization
FPR	False Positive Rate
Fwd	Forward
GO	Gene Ontology

GTF	General Transcription Factor
H3K4me3	Histone 3 Lysine 4 Trimethylation
HDAC	Histone Deacetylase
HP1	Heterochromatic Protein 1
HUVEC	Human Umbilical Vein Endothelial Cells
IkB	Inhibitor of NFkB
IKK	IkB Kinase
KB	Kilobase Pairs
KDM5B	Lysine Demethylase 5B
LM-PCR	Ligantion-Mediated PCR
LPS	Lipopolysaccharide
Luc	Luciferase
MCF-7	Michigan Cancer Foundation - 7
MHC	Major Histocompatibility Complex
MLL	Mixed Lineage Leukemia
MNase	Micrococcal Nuclease
mRNA	Messenger RNA
NAD+	Nicotinamide Adenine Dinucleotide
NAMPT	Nicotinamide Phosphoribosyltransferase
NFkB	Nuclear Factor Kappa-Light-Chain-Enhancer of Activated B Cells
NMNAT-1	Nicotinamide Mononucleotide Adenylyl Transferase - 1
PAR	Poly(ADP-ribose)
PARG	Poly(ADP-ribose) Glycohydrolase
PARP-1	Poly(ADP-ribose) Polymerase - 1
PBZ	PAR-Binding Zinc finger
PCR	Polymerase Chain Reaction

PHD	Pleckstrin Homology Domain
Pol II	RNA Polymerase II
PPARg	Peroxisome Proliferator-Activated Receptor Gamma
qPCR	Quantitative PCR
Rev	Reverse
RNA	Ribonucleic Acid
RT	Reverse Transcription
SEM	Standard Error of the Mean
shRNA	Short Hairpin RNA
SIRT1	Sirtuin 1
SIRT6	Sirtuin 6
SUMO	Small Ubiquitin-like Molecule
SV40	Simian Virus 40
TAF3	TBP-Associated Factor 3
TBP	TATA-Binding Protein
TFIIB	Transcription Factor IIB
TFIID	Transcription Factor IID
TIF1b	Transcriptional Intermediary Factor 1beta
TNFa	Tumor Necrosis Factor Alpha
TPA	12-O-Tetradecanoylphorbol-13-acetate
TRX	Trithorax
TSS	Transcription Start Site

CHAPTER 1

PARP-1: Molecular Actions, Physiological Outcomes, and Clinical Targets*

* This chapter was written by R. Krishnakumar and W. L. Kraus, and will be published as a review article in *Molecular Cell*

1.1 Summary

The abundant nuclear enzyme PARP-1, a multifunctional regulator of chromatin structure, transcription, and genomic integrity, plays key roles in a wide variety of molecular processes in the nucleus. Recent studies have begun to connect the molecular functions of PARP-1 to specific physiological and pathological outcomes, many of which can be altered by an expanding array of chemical inhibitors of PARP enzymatic activity.

1.2 Introduction

Nuclear processes involving access to or modification of the genome, such as transcription and DNA repair, require a host of structural and regulatory proteins. Poly(ADP-ribose) polymerase-1 (PARP-1), a ubiquitous and abundant nuclear protein and the founding member of the PARP family, has a number of distinct biochemical activities that make it well suited for both structural and regulatory roles across the genome (Hassa and Hottiger, 2008; Kim et al., 2005; Schreiber et al., 2006). As discussed below, PARP-1 can bind to various DNA structures and nucleosomes, and it possesses an NAD^+-dependent catalytic activity that synthesizes a negatively charged polymer on target proteins called poly(ADP-ribose) or PAR. Although historically studied in the context of DNA damage detection and repair, PARP-1 has more recently been linked to the regulation of chromatin structure and transcription, DNA methylation and imprinting, insulator activity, and chromosome organization. In this review, I provide an overview of PARP-1's structure and activities, as well as an in depth review of papers published in the past few years that have provided new insights into the molecular functions of PARP-1 in the nucleus. In addition, I highlight

emerging information about the roles of PARP-1 in physiological and pathological outcomes, its interplay with nuclear NAD^+ metabolic enzymes, and the chemical biology of PAR.

1.3 PARP-1 and the PARP family

Poly(ADP-ribosyl)ation reactions and PARP-like genes have been identified in a wide variety of single and multicellular eukaryotes, from fungi to mammals (but surprisingly not the yeasts *S. cerevisae* and *S. pombe*), as well as eubacteria, archaebacteria, and double stranded DNA viruses (Hassa et al., 2006; Otto et al., 2005). In mammalian cells, the bulk of the PAR production is catalyzed by PARP-1, although recent studies have begun to characterize the structure and function of related PARP proteins.

1.3.1 PARP-1 structure and biochemical activities

PARP-1 is a highly conserved protein of ~116 kDal (D'Amours et al., 1999). Like many other chromatin- and transcription- related proteins, it has a modular structure comprising multiple independently folded domains. The major functional units of PARP-1 are an amino terminal DNA binding domain (DBD), a central automodification domain (AMD), and a carboxyl-terminal catalytic domain (CD) (Hakme et al., 2008; Schreiber et al., 2006) (**Fig. 1.1A**, top). The DBD contains two Cys-Cys-His-Cys zinc fingers (FI/Zn1 and FII/Zn2) that mediate binding to DNA, a newly discovered third zinc binding domain (Zn3) that mediates inter-domain contacts important for DNA-dependent enzyme activation (Langelier et al., 2008), a nuclear localization signal (NLS), and a caspase-3 (C3) cleavage site (Hakme et al., 2008; Schreiber et al., 2006). The AMD contains a BRCT (BRCA1 C-terminus) fold, which

mediates protein-protein interactions (e.g., with DNA repair enzymes). The CD, which is the most conserved domain across the PARP superfamily, contains a PARP signature motif, which binds NAD^+, as well as a "WGR" motif, which is named after the most conserved amino acid sequence in the motif (Trp, Gly, Arg) and has an unknown function. The structures of all of these domains and motifs from have now been determined, providing new insights about the structure and function of PARP-1 (**Fig. 1.1B**). Together, the structural and functional domains of PARP-1 confer the activities required for the broad range of functions of PARP-1 in the nucleus. ***1.3.2***

Other PARP family members

Although much of the focus has been on PARP-1, studies over the past decade have identified a family of as many as 17 proteins that share homology to the catalytic domain of PARP-1 (Ame et al., 2004; Hakme et al., 2008; Hassa and Hottiger, 2008; Schreiber et al., 2006). Recently, a new unified nomenclature referring to this family of proteins as (ADP-ribosyl) transferases (ARTs) has been proposed to recognize that fact that: (1) PARPs catalyze a transferase reaction, not a template-dependent polymerization reaction and (2) not all family members have PARP activity; some are likely to function as mono(ADP-ribosyl) transferases (mARTs) (Hottiger et al., 2010). In addition to the PARP-like domain, the PARP family members are "functionalized" with a wide variety of other structural and functional domains (e.g., DNA-binding domains, RNA-binding domains, subcellular localization signals, macrodomains, BRCT motifs, ankyrin repeats, zinc fingers) that dictate their overall biological activities. A recent structural analysis has classified members of the PARP family into three groups based on their catalytic domains: (1) PARPs 1-5, which are bona fide PARPs containing a conserved glutamate (Glu 988 in PARP-1) that defines the PARP catalytic activity, (2) PARPs 6-8, 10-12, and 14-16,

Figure 1.1. Structural and functional organization of PARP-1 and PARP-2.

(A) Schematic representation of human PARP-1 and PARP-2 with the functional domains noted in the text.

(B) Structures of the six structural and functional domains in human PARP-1. FI (PDB 2DMJ), FII (PDB 2CS2), ZnIII (PDB 2RIQ), BRCT (PDB 2COK), WGR (PDB: 2CR9), catalytic domain (PDB 1UK1; structure shown in complex with a quinazoline inhibitor).

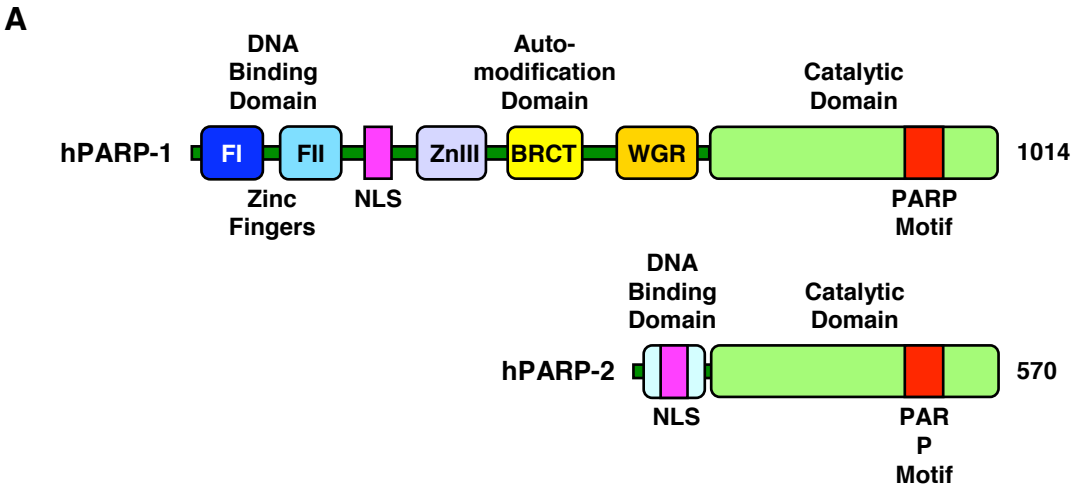
A
DNA Binding Domain
Auto-modification Domain
Catalytic Domain
hPARP-1
FI
FII
ZnIII
BRCT
WGR
1014
Zinc Fingers
NLS
PARP Motif
DNA Binding Domain
Catalytic Domain
hPARP-2
570
NLS
PAR P Motif

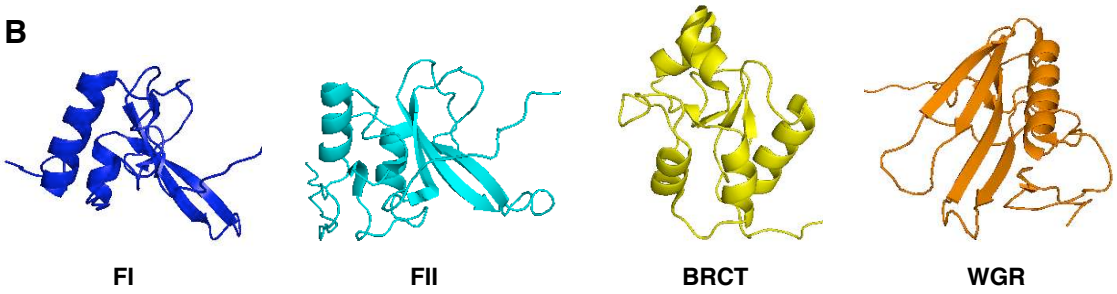
B
FI
FII
BRCT
WGR

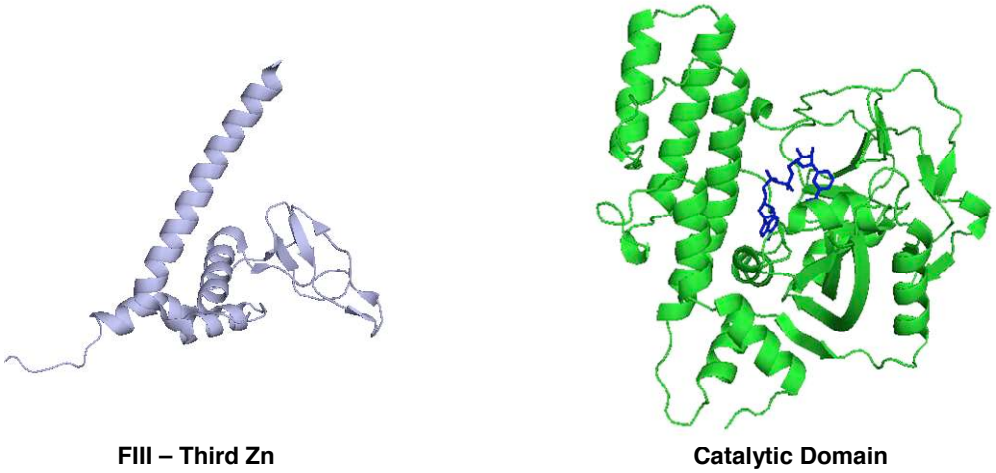
FIII – Third Zn
Catalytic Domain

which are confirmed or putative mARTs, and (3) PARPs 9 and 13, which lack key NAD^+-binding residues and the catalytic glutamate, and are likely inactive (Kleine et al., 2008) (**Fig. 1.2**).

PARP family members localize to various cellular compartments, including the nucleus, cytoplasm, mitochondria, and vault particles, although the subcellular localization and function of many of the PARPs are unknown (Ame et al., 2004; Hassa and Hottiger, 2008). The primary nuclear PARPs are PARP-1, PARP-2 (the closest paralog to PARP-1), PARP-3, and tankyrase 1 and 2 (PARP-5a and -5b) (Ame et al., 2004; Hakme et al., 2008; Hassa and Hottiger, 2008; Schreiber et al., 2006). Also found in the nucleus, although not exclusively, are v-PARP (PARP-4), PARP-6, PARP-8, PARP-9, the Bal proteins Bal 1-3 (PARP-13, -14, -15), and PARP-10. The known functions of the PARP family members span a wide range of cellular processes, including DNA repair, transcription, cellular signaling, cell cycle regulation, and mitosis (Ame et al., 2004; Hakme et al., 2008; Hassa and Hottiger, 2008; Schreiber et al., 2006). This diverse array of processes plays key roles in a wide variety of biological outcomes, including differentiation, development, stress responses, inflammation, and cancer. Although the focus of this review is on PARP-1, I draw parallels to other PARP family members when applicable.

1.4 Molecular Biology and Biochemistry of PARP-1

1.4.1 DNA binding, chromatin binding, and genomic localization

Studies over the past few decades have shown that PARP-1 associates with chromatin in specific patterns that relate to its function (Kraus, 2008; Kraus and Lis, 2003; Tulin et al., 2003). This association is driven by interactions with DNA, nucleosomes, or other chromatin-associated proteins, which are not mutually

Figure 1.2. The PARP catalytic domain is highly conserved across the PARP family.

(A) Alignment of the catalytic domain structures from mammalian PARP-1 (PDB 1UK1), PARP-2, and PARP-3.

(A) Alignment of the catalytic domain structures from mammalian PARPs 1, 2, 3, 5a, 5b, 10, 12, 14, 15 (PDB 1A26, 1GSO, 3FHB, 2RF5, 3KR7, 3HKV, 2PQF, 3GOY, 3GEY, respectively).

In (A) and (B), NAD^+ has been modeled in based on a structure of diptheria toxin (PDB 1TOX).

[Figure courtesy of Bryan Gibson]

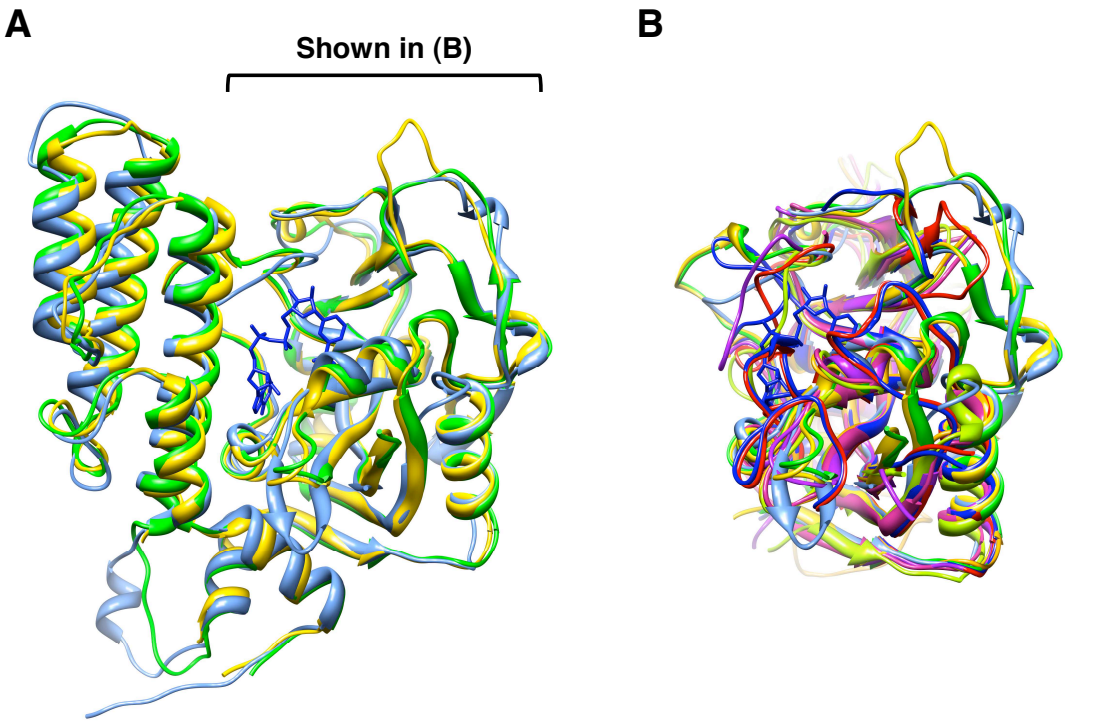
A
Shown in (B)
B
PARPs 1, 2, 3
PARPs 1, 2, 3, 5a, 5b, 10, 12, 14, 15

exclusive. PARP-1 binds to a variety of DNA structures, including single- and double-strand breaks, crossovers, cruciforms, and supercoils, as well as some specific double-stranded DNA sequences (Kraus, 2008; Kraus and Lis, 2003). PARP-1 also binds to nucleosomes in a specific manner, interacting with both DNA and histones at or near the dyad axis where the DNA enters and exits the nucleosome (Kim et al., 2004). Finally, PARP-1 can interact with a wide variety of chromatin-associated proteins, including components of the transcription machinery, sequence-specific DNA-binding transcription factors, chromatin modifying enzymes, and histone variants (e.g., macroH2A; see below) (Kim et al., 2005; Kraus, 2008; Kraus and Lis, 2003; Tulin et al., 2003). Interactions with these proteins allows for indirect association of PARP-1 with chromatin. By binding to chromatin, PARP-1 can alter the structure of nucleosomes or the composition of chromatin (Kim et al., 2004; Kraus, 2008; Kraus and Lis, 2003; Tulin et al., 2003; Wacker et al., 2007). This may occur through target protein modification by PARP-1's enzymatic activity, as well as competition for binding sites on nucleosomes. For example, PARP-1 may displace the linker histone H1 from nucleosomes by PARylating it or for competing for overlapping binding sites on the nucleosomes (Ju et al., 2006; Kim et al., 2004; Krishnakumar et al., 2008).

Recent genomic localization studies have provided new insights about PARP-1 function, showing that PARP-1 binds at the promoters of most actively transcribed genes (Krishnakumar et al., 2008). The binding of PARP-1 at promoters correlates with the binding of Pol II, gene expression, and the presence of histone H3 lysine 4 trimethylation (H3K4me3), a histone modification that marks active promoters (**Fig. 1.3**). PARP-1 also binds to chromatin outside of promoter regions, including enhancers (Krishnakumar et al., 2008). In response to genotoxic stress, PARP-1 relocalizes to sites of DNA damage (i.e., nicks, breaks) (El-Khamisy et al., 2003;

Huber et al., 2004; Malanga and Althaus, 2005; Petermann et al., 2005; Pleschke et al., 2000). Whether this DNA damage-induced relocalization results in a global redistribution of PARP-1 away from promoters, as was shown recently for the NAD^+-dependent chromatin regulator SIRT1 (Oberdoerffer et al., 2008), remains to be determined. This is an attractive model that fits well with the global reduction in transcription observed in response to DNA damage.

1.4.2 Catalytic activity, binding partners, and targets

PAR is a large, negatively charged polymer that functions as a post-translational modification, as well as a free polymer. Most of the PAR in the cell is produced by the catalytic activity of PARP-1, which catalyzes the polymerization of ADP-ribose units from donor NAD^+ molecules on target proteins (D'Amours et al., 1999) (**Fig. 1.4**). The ADP-ribose units are linked to each other via glycosidic ribose-ribose 1' → 2' bonds, and the resulting PAR polymers may be linear or branched (D'Amours et al., 1999). The modification most likely occurs on glutamate, aspartate, or lysine residues, although historically the evidence for covalent modification of specific residues has been weak (D'Amours et al., 1999; Hassa and Hottiger, 2008). In fact, some have even argued for strong non-covalent binding of free PAR polymers, rather than covalent modification (Hassa and Hottiger, 2008). Recent studies, however, have begun to make progress on defining specific sites of PAR attachment on target proteins (Altmeyer et al., 2009; Haenni et al., 2008; Kanai et al., 2007) (see below).

PARP-1 catalytic activity is regulated through allosteric mechanisms involving a range of binding partners, including damaged DNA, histones, nucleosomes, and an assortment of nuclear proteins (D'Amours et al., 1999; Kraus and Lis, 2003; Tulin et al., 2003). PARP-1 catalytic activity is also regulated by post-translational modifications; autoPARylation of PARP-1 inhibits its catalytic activity, while

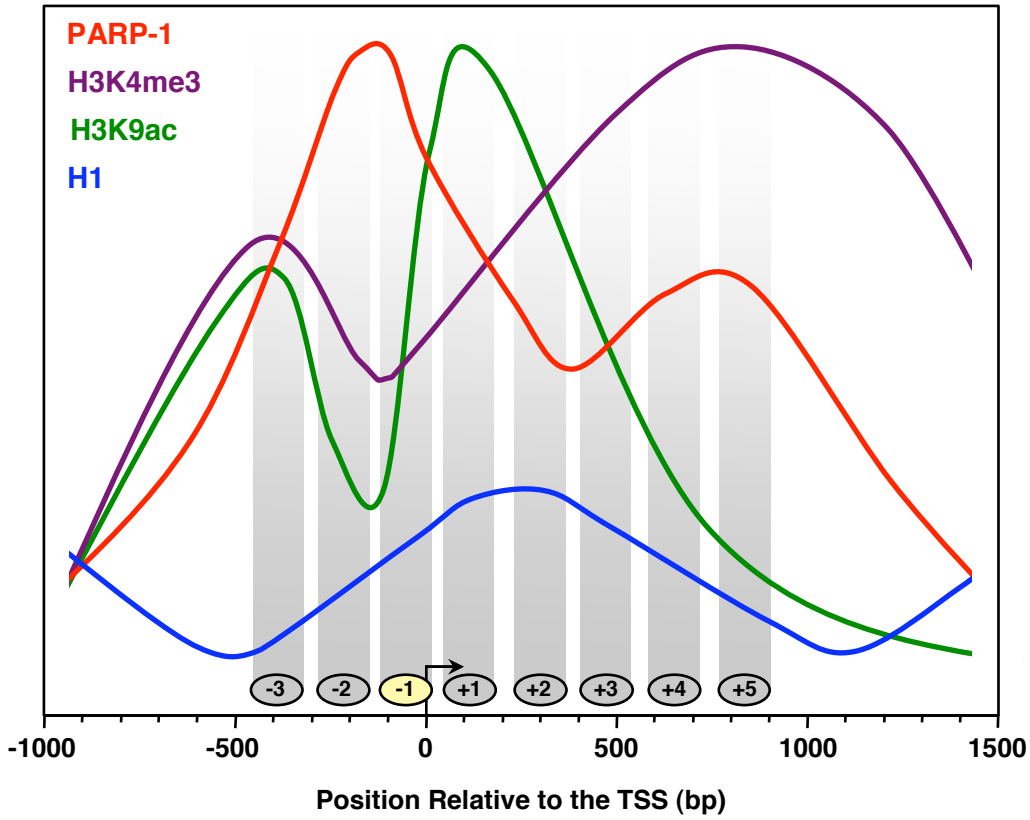

Figure 1.3. The chromatin landscape at the promoters of highly expressed genes. Schematic of average genomic ChIP and nucleosome mapping data across the promoters of the most highly expressed genes (top quartile) in cells. The graphs are based on data from the literature: PARP- 1 and H1 (Krishnakumar et al., 2008), H3K4me3 (Barski et al., 2007), H3K9ac (Wang et al., 2008b), and nucleosome positioning (Schones et al., 2008).

phosphorylation by Erk1/2 enhances its catalytic activity (Kauppinen et al., 2006). PARP-1 catalytic activity may also be regulated by nicotinamide mononucleotide adenylyltransferase-1 (NMNAT-1), a nuclear NAD^+ synthase that interacts with PARP-1 and can produce NAD^+ locally for use by nuclear enzymes that require NAD^+, such as PARP-1 and SIRT1 (Kim et al., 2004; Zhang et al., 2009; Zhang and Kraus, 2009). Regulated catalysis, such as that exhibited by PARP-1, may be a more common mode of action for chromatin-modifying enzymes than has generally been considered, and there are likely to be some general principles that can be learned from the study of PARP-1's catalytic activity. PARP-1, which has many protein binding partners in the nucleus, has been identified as a component of a wide variety of protein complexes, including those that (1) repair DNA damage (e.g., condensin I/XRCC1), (2) regulate transcription (e.g., Mediator; TLE corepressor), (3) function as insulators (e.g., CTCF), and (4) methylate DNA (e.g., DNMT-1) (**Fig. 1.5**) (Caiafa et al., 2009; Caiafa and Zlatanova, 2009; El-Khamisy et al., 2003; Guastafierro et al., 2008; Hassa et al., 2005; Heale et al., 2006; Ju et al., 2004; Malanga and Althaus, 2005; Pavri et al., 2005; Pleschke et al., 2000; Zampieri et al., 2009). Many of these binding partners have been reported to be PARylated as targets of PARP-1 catalytic activity (Kim et al., 2005; Kraus, 2008; Kraus and Lis, 2003). Covalent attachment of PAR is thought to alter the activity of target proteins through both steric and charge effects, ultimately preventing protein-protein interactions, protein-nucleic acid interactions, enzymatic activity, or subcellular localization (Hassa and Hottiger, 2008; Schreiber et al., 2006).

Known or suspected targets of PARP-1 catalytic activity include histones, transcription factors, nuclear enzymes, and nuclear structural proteins. For example, PARP-1 can PARylate histones, especially H1, H2A and H2B, which may play a role in the regulation of chromatin structure, although the extent of histone

Figure 1.4. Biosynthesis of NAD^+ and PAR.

Chemical structures of NAD^+, PAR, and metabolites. The enzymes that catalyze the synthesis of NAD^+ in the mammalian salvage pathway are shown. The enzymatic actions of PARP, PARG, (ADP-ribosyl) protein hydrolase, and (ADP-ribosyl) protein lyase are also indicated.

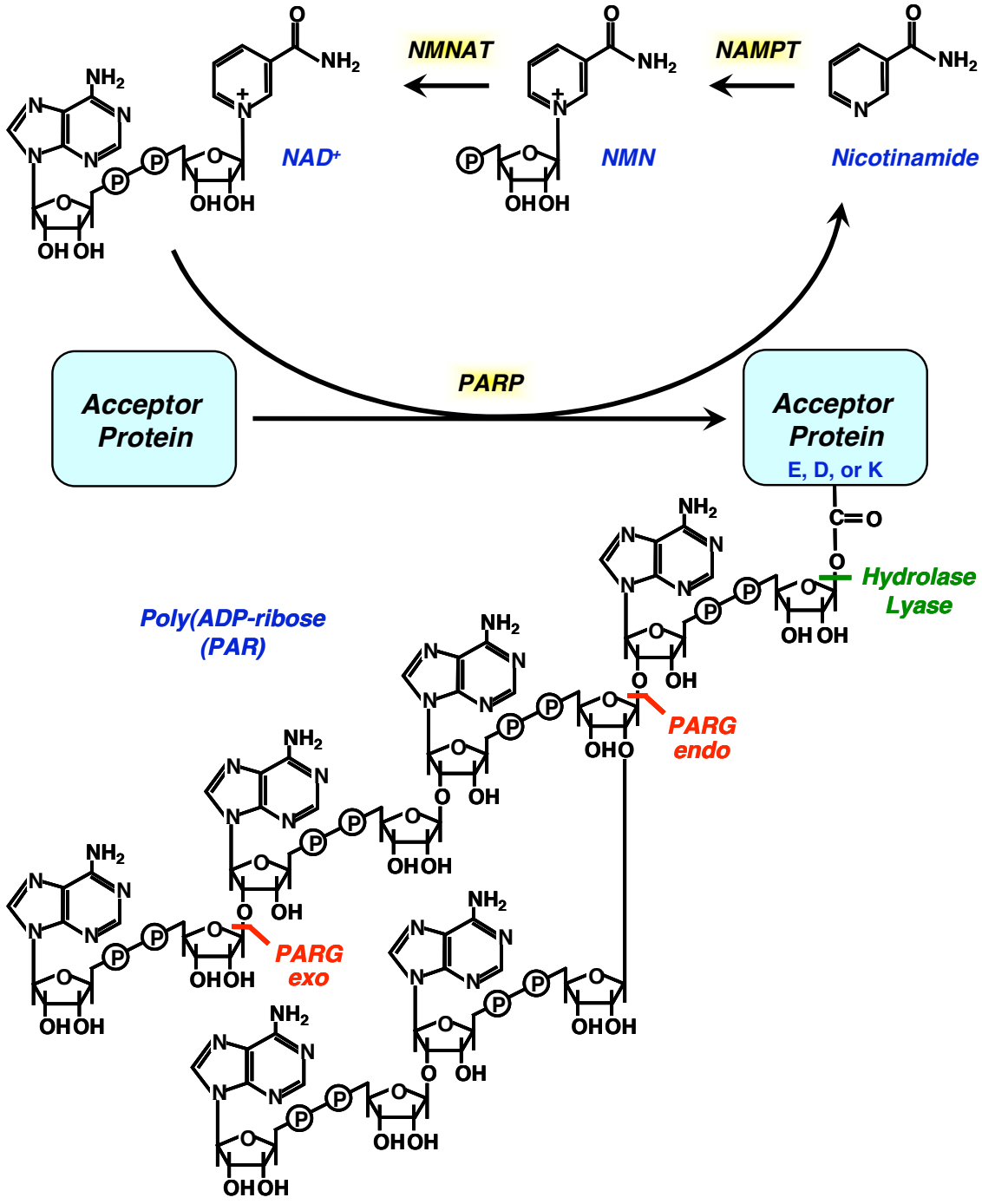
NMNAT
NAMPT
NAD+
NMN
Nicotinamide
PARP
Acceptor Protein
Acceptor Protein
E, D, or K
Hydrolase
Lyase
Poly(ADP-ribose (PAR)
PARG endo
PARG exo

modification and its relevance to nuclear processes remains to be clarified (D'Amours et al., 1999; Kim et al., 2005; Kraus, 2008; Kraus and Lis, 2003). PARP-1 also PARylates a number of DNA repair proteins, including p53 (Kanai et al., 2007; Mendoza-Alvarez and Alvarez-Gonzalez, 2001), which is not surprising given PARP-1's well characterized role in DNA repair. Although the functional significance of p53 PARylation has been elusive, a recent study suggests that PARylation of p53 on specific sites (likely Glu 255, Asp 256 and Glu 268) can prevent p53 export from the nucleus by blocking its interaction with the nuclear export receptor Crm1 (Kanai et al., 2007). PARP-1 has also been reported to PARylate and alter the function of numerous other transcription factors, including CTCF, AP-1, YY1 and NF-κB (Kraus, 2008), as well as nuclear enzymes, such as Aurora B kinase (Monaco et al., 2005), thereby inhibiting their function. Finally, PARP-1-dependent PARylation of target proteins is required for the normal function of centromeres, centrosomes, and the mitotic spindle (Kim et al., 2005). As these examples suggest, the PARylation of target proteins by PARP-1 plays a central role in determining the cellular functions of PARP-1.

1.4.3 Post-translational modifications of PARP-1

Like other nuclear proteins that play key roles in regulatory processes, PARP-1 is subject to a variety of covalent post-translational modifications as endpoints of cellular signaling pathways. These include PARylation, acetylation, phosphorylation, ubiquitylation, and SUMOylation (**Fig. 1.6**); the latter two were more recently discovered and are less well characterized (Cohen-Armon et al., 2007; Hassa et al., 2005; Kauppinen et al., 2006; Martin et al., 2009; Messner et al., 2009; Wang et al., 2008a)

• ***PARylation.*** PARP-1 is PARylated by itself, PARP-2, and possibly other PARPs. Automodification of PARP-1 (i.e., autoPARylation) may occur as an

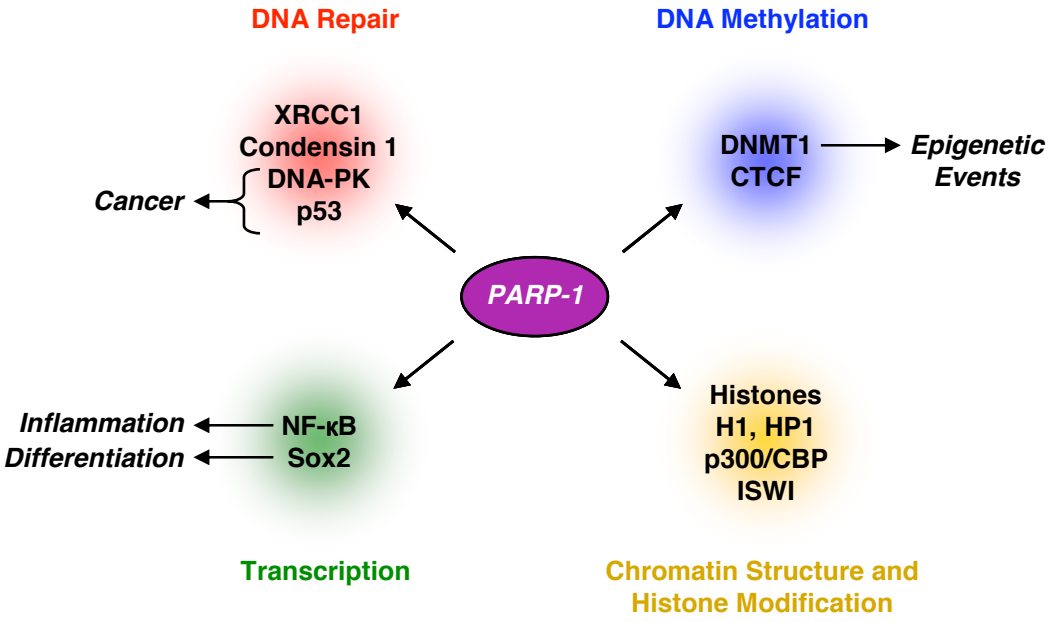

Figure 1.5. Interactions and functions of PARP-1 in the nucleus.

PARP-1 interacts with and PARylates proteins involved in DNA repair, Transcription, DNA methylation, and the regulation of chromatin structure and histone modification to control physiological and pathological outcomes.

extensive addition of ADP-ribose in chains >200 units in length or as a more modest addition of a single unit or chains up to 20 units in length (i.e., mono- or oligoPARylation, respectively) (D'Amours et al., 1999; Mendoza-Alvarez and Alvarez-Gonzalez, 1999). Whether this occurs primarily in cis or in trans (i.e., intra- or inter-molecularly, respectively) has been debated in the literature, but is typically considered intermolecular (Altmeyer et al., 2009; Alvarez-Gonzalez and Mendoza-Alvarez, 1995; Mendoza-Alvarez and Alvarez-Gonzalez, 1993, 1999). Extensive autoPARylation of PARP-1 (e.g., in response to DNA damage) inhibits its DNA binding and catalytic activities (D'Amours et al., 1999). Biochemical and cell-based assays have shown that activation and autoPARylation of PARP-1 results in its release from chromatin (Kim et al., 2004; Petesch and Lis, 2008; Tulin and Spradling, 2003; Wacker et al., 2007). The effect of less extensive autoPARylation of PARP-1 is not clear; modestly modified PARP-1 may have altered activities, but retain its association with chromatin.

Initial reports suggested that PARylation of PARP-1 occurred on as many as 28 glutamate residues, primarily in the AMD and DBD (D'Amours et al., 1999; Schreiber et al., 2006). In contrast, a recent study has shown that the glutamate residues in the AMD are not required for PARylation of PARP-1 (Altmeyer et al., 2009). Rather, based on amino acid substitutions (i.e., Lys to Arg), the authors conclude that at least three lysines residues in the AMD (Lys 498, 521, and 524) are sites of automodification on PARP-1 (Altmeyer et al., 2009). A similar approach was used to identify lysines 36 and 37 of PARP-2 as sites of auto-mono(ADP-ribosyl)ation (Haenni et al., 2008). Although these results could significantly change the expectations of the field both in terms of PARP-1 autoregulation, as well as sites of modification on other PARP target proteins, they should be interpreted with caution. Mutation of specific residues in PARP-1 or PARP-2 could reduce automodification

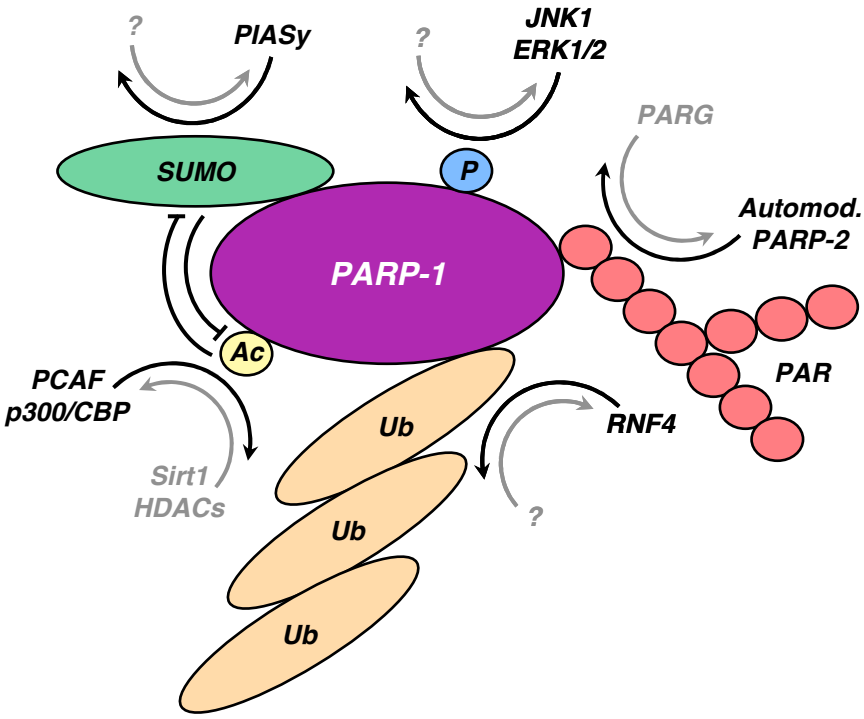

Figure 1.6. Covalent post-translational modifications of PARP-1.

Schematic representation of PARP-1 modifications: PARylation, phosphorylation, acetylation, SUMOylation, ubiquitylation, as described in the text.

without necessarily being sites for covalent attachment of PAR. Furthermore, PARylation seems to be promiscuous; deletion or mutation of one site may allow for modification of another site. The identification of adducts on targets residues by mass spectrometry will be required to conclusively address this issue.

• ***Phosphorylation and acetylation.*** PARP-1 is phosphorylated by ERK1/2 at Ser 372 and Thr 373, and JNK1 at undetermined sites (Kauppinen et al., 2006; Zhang et al., 2007). The former is required for maximal PARP-1 activation after DNA damage (Kauppinen et al., 2006), whereas the latter promotes sustained PARP-1 activation during H_2O_2-induced non-apoptotic cell death (Zhang et al., 2007). PARP-1 is acetylated by the acetyltransferases p300/CBP and PCAF (Hassa et al., 2003; Hassa et al., 2005; Rajamohan et al., 2009). The acetylation of PARP-1 is reversed by a number of deacetylases, including Sirt1 (Hassa et al., 2005; Rajamohan et al., 2009). Acetylation of PARP-1 was first identified in the context of NF-κB-dependent transcription, where it plays a critical role in regulating NF-κB target genes in immune cells (Hassa et al., 2003; Hassa et al., 2005). In cardiomyocytes, PARP1 is acetylated as an endpoint of stress responses, resulting in the DNA damage-independent activation of PARP-1 (Rajamohan et al., 2009). PARP-2 is also acetylated at Lys 36 and 37 in the NLS, which are the same sites that are mono(ADP-ribosyl)ated. Acetylation of PARP-2 reduces its DNA binding and enzymatic activities, and presumably the extent of mono(ADP-ribosyl)ation (Haenni et al., 2008).

• ***SUMOylation and ubiquitylation.*** Recent studies have shown that PARP-1 is SUMOylated and ubiquitylated, modulating its role as a regulator of chromatin structure and transcription (Martin et al., 2009; Messner et al., 2009). PARP-1 interacts with and is SUMOylated by PIASy, a SUMO E3 ligase (Martin et al., 2009; Stilmann et al., 2009). In *Drosophila*, dPARP (a homolog of mammalian PARP-1) is SUMOylated in response to heat shock, which is required for the full activation of the

Hsp70 gene (Martin et al., 2009). PIASy is recruited and released at the *Hsp70* locus during the heat shock response with kinetics that mirror those of both PARP-1 and the SUMO-conjugating enzyme Ubc9 (Martin et al., 2009). Interestingly, the SUMO-targeted ubiquitin ligase RNF4 polyubiquitylates dPARP and presumably causes its clearance from the *Hsp70* promoter via degradation (Martin et al., 2009). These results fit well with the fact that dPARP regulates the chromatin structure at the *Drosophila Hsp70* locus upon heat shock (Petesch and Lis, 2008; Tulin and Spradling, 2003). In mammalian cells, SUMOylation and p300/CBP-dependent acetylation at Lys 486 of PARP-1 are mutually exclusive (Messner et al., 2009). Since acetylation of PARP-1 is required for activated transcription at some target promoters (Hassa et al., 2003; Hassa et al., 2005), SUMOylation of PARP-1 might modulate the transcriptional outcome in this PARP-1-dependent pathway. Similar to what is observed in *Drosophila*, polyubiquitylation of PARP-1, likely in the DBD, promotes the degradation of PARP-1, thereby regulating its overall activity (Wang et al., 2008a).

1.5 Nuclear Actions of PARP-1

PARP-1 contributes in many unique ways to the molecular biology of nuclear processes, playing key roles in the maintenance of genomic integrity, the regulation of chromatin structure and transcription, and the establishment of DNA methylation patterns, as well as a host of other processes (e.g., mitotic apparatus function, cell death pathways) (**Fig. 1.5**) (Hassa and Hottiger, 2008; Kim et al., 2005). Below, I highlight the newest results related to some of the key aspects of PARP-1 function.

1.5.1 DNA damage detection and repair

The earliest functions ascribed to PARP-1 were related to DNA damage detection and repair, and much of the PARP-1 literature has been devoted to this aspect of PARP-1 biology (D'Amours et al., 1999). PARP-1 has been implicated in at least three distinct DNA repair pathways: base excision repair (BER), single-strand break (SSB) repair, and double-strand break (DSB) repair (Bouchard et al., 2003; Woodhouse and Dianov, 2008). PARP-2 has also been implicated in DNA repair pathways, including BER (Schreiber et al., 2002; Yelamos et al., 2008). Although neither PARP-1 nor PARP-2 is individually required for viability in mice, *Parp-1*$^{-/-}$ or *Parp-2*$^{-/-}$ mice or embryonic fibroblasts exhibit a variety of DNA repair defects and chromosomal abnormalities (de Murcia et al., 1997; Menissier de Murcia et al., 2003; Wang et al., 1997). *Parp-1*$^{-/-}$/*Parp-2*$^{-/-}$ mice show embryonic lethality with considerable genomic instability (Menissier de Murcia et al., 2003), indicating both overlapping and non-redundant functions of PARP-1 or PARP-2 in the maintenance of genomic integrity.

As with other cellular stresses, DNA damage (e.g., SSBs, DSBs, oxidation, alkylation) elicits an immediate and dramatic PARP-1-dependent PARylation response targeting a variety of nuclear proteins. This response may be transient or sustained depending on the extent of damage and the pathway activated (Bouchard et al., 2003; D'Amours et al., 1999; Woodhouse and Dianov, 2008). The link between DNA damage and enhancement of PARP-1 enzymatic activity makes PARP-1 an excellent DNA damage sensor. In response to low levels of DNA damage, PARP-1 promotes cell survival and DNA repair. With severe DNA damage, PARP-1 promotes cell death through at least two distinct pathways: (1) energy failure-induced necrosis, which results from depletion of NAD^+ (and ultimately ATP) and (2) apoptosis-inducing factor-dependent apoptosis (Bouchard et al., 2003; Kim et al., 2005). Thus,

PARP-1 has a vital role in determining cellular outcomes in response to DNA damage.

As might be expected, PARP-1 interacts physically and functionally with other key DNA damage detection and response proteins, including the ATM kinase and p53 (Bouchard et al., 2003). For example, PARP-1 deficient cells exhibit impaired ATM-kinase activity and reduced formation H2AXγ foci (Aguilar-Quesada et al., 2007; Menisser-de Murcia et al., 2001). PARP-1-dependent PARylation of the Spt6 component of the histone chaperone FACT inhibits the exchange of variant H2AX with conventional H2A in the context of the nucleosome (Heo et al., 2008). PARP-1 also interacts with proteins involved in the DNA repair pathways noted above and may play a role in recruiting these proteins to sites of DNA damage (Woodhouse and Dianov, 2008). These include XRCC-1 in the BER pathway, which requires PARP-1 for its recruitment to sites of DNA damage (El-Khamisy et al., 2003; Heale et al., 2006; Masson and Caldwell, 1998; Okano et al., 2003). Some BER proteins (e.g., XRCC1, DNA ligase III) may also bind PAR (Pleschke et al., 2000), although the functional consequences of this binding are not clear. PARP-2 has also been shown to interact with XRCC1, as well as DNA polymerase β and DNA ligase III (Schreiber et al., 2002), which suggests contributions of PARP-2 to the BER process. Although an initial set of PARP-1 and PARP-2 interactions with genome maintenance factors has been determined, this list is unlikely to be complete. In addition, although these interactions are suggestive of possible mechanisms, the detailed mechanisms that might underlie the contributions of PARP-1 and PARP-2 to DNA damage detection and repair have not yet been revealed.

1.5.2 Chromatin structure and transcription

Although historically the focus has been on PARP-1's role in DNA damage detection and repair, studies over the past decade have revealed important roles for

PARP-1 in transcriptional regulation (Kim et al., 2005; Kraus, 2008; Kraus and Lis, 2003; Tulin et al., 2003). The ability of PARP-1 to modulate chromatin structure and function underlies its contributions to this process. In fact, the ability to disrupt chromatin structure by PARylating histones (e.g., H1 and H2B) and destabilizing nucleosomes was one of the earliest functional effects of PARP-1 to be characterized (Huletsky et al., 1989; Mathis and Althaus, 1987; Poirier et al., 1982). More recent biochemical studies have shown that, in the absence of NAD^+ or significant autoPARylation, PARP-1 binds to nucleosomes and promotes the compaction of chromatin by bringing together neighboring nucleosomes (Kim et al., 2004; Wacker et al., 2007). In the presence saturating levels of NAD^+, which lead to considerable autoPARylation of PARP-1 in the presence of nucleosomes, the compaction is nearly completely reversed (Kim et al., 2004; Wacker et al., 2007).

PARP-1 localizes to the promoters of almost all actively transcribed genes (Krishnakumar et al., 2008), which suggests that it plays a role in promoting the formation of chromatin structures that are permissive to transcription. In this regard, PARP-1 has been shown to block the binding of the linker histone H1, a repressive chromatin architectural protein, to promoter chromatin (Ju et al., 2006; Kim et al., 2004; Krishnakumar et al., 2008). PARP-1 also PARylates DEK, another repressive chromatin-associated protein, and promotes its release from chromatin (Gamble and Fisher, 2007). Yet, PARP-1 only regulates a subset of the genes to which it binds and it has both positive and negative effects of transcription (Frizzell et al., 2009; Krishnakumar et al., 2008). Thus, gene regulation by PARP-1 is a complex process that is likely to involve multiple mechanisms and be modulated by additional inputs.

PARP-1 regulates transcription in multiple ways, including (1) regulating chromatin structure and composition (as discussed in the preceding paragraph), (2) functioning as a classical coregulator with a wide variety of signal-regulated,

sequence-specific DNA binding transcriptional activators, (3) functioning as a direct enhancer-binding factor, and (4) regulating the actions of insulators and insulator-binding factors, such as CTCF. These aspects of PARP-1 function have been reviewed extensively elsewhere (Kim et al., 2005; Kraus, 2008; Kraus and Lis, 2003; Tulin et al., 2003). In the 'coregulator' mode, PARP-1 may be recruited to target promoters as a functional endpoint of signaling pathways to regulate components of the transcription complex assembled at the promoter. In some cases, the enzymatic activity of PARP-1 is required (e.g., with HES1 and Elk1) (Cohen-Armon et al., 2007; Ju et al., 2004), while in others it is not (e.g., NF-κB and RAR) (Hassa and Hottiger, 2002; Kraus and Lis, 2003; Pavri et al., 2005). When acting as a coregulator during signal-regulated transcriptional responses, PARP-1 can function as a promoter-specific 'exchange factor' that promotes the release of inhibitory factors and the recruitment of stimulatory. In this regard, PARP-1 has been shown to promote the exchange of (1) a TLE1 corepressor complex for a HAT-containing coactivator complex during signal-dependent gene regulation in neuronal cells (Ju et al., 2004) (2) an inactive cdk8-positive Mediator for an active cdk8-negative Mediator during retinoic acid-regulated activation (Pavri et al., 2005). PARP-1 has also been reported to promote the recruitment of topoisomerase IIβ (TopoIIβ) to hormone-regulated promoters, leading to promoter DNA cleavage, factor exchange, and transcriptional activation (Ju et al., 2006). The DNA cleavage has been proposed to resolve a topological barrier and allow for favorable structural changes at the promoter (Ju et al., 2006), but this model has yet to be proven.

Drosophila has been a useful model organism for studying the role of PARP-1 in the regulation of chromatin structure and transcription because flies only have two genes encoding PARPs: PARP-1 like (dPARP), which is expressed as three isoforms, and tankyrase-like (Hanai et al., 1998; Miwa et al., 1999). In *Drosophila* larvae,

inhibition of PARP activity or disruption of dPARP gene expression blocks PAR accumulation, chromatin decondensation, and transcription at loci containing highly inducible genes, such as those regulated by heat shock or ecdysone) (Tulin et al., 2003). dPARP may also play a role in maintaining the compaction of heterochromatin (Tulin et al., 2002). Interestingly, in the case of the *Hsp70* gene in *Drosophila* S2 cells, dPARP (as well as heat shock factor and GAGA factor) is required for a heat shock-dependent, transcription-independent disruption of nucleosomes across the entire gene, which occurs within 30 seconds of activation - faster than the rate of Pol II transcription (Petesch and Lis, 2008). dPARP exhibits ecdysteroid-regulated localization to Cajal bodies and histone locus bodies, where it PARylates resident proteins and maintains organelle integrity (Kotova et al., 2009). dPARP can also PARylate the nucleosome remodeling ATPase, ISWI, leading to its inactivation (Sala et al., 2008). Together, these studies in *Drosophila* have helped to uncover and clarify the roles of PARP-1 in regulating chromatin structure and transcription.

1.5.3 DNA methylation

Studies over the past decade have begun to link PARP-1-dependent PARylation with DNA methylation, a stable epigenetic mark that can be passed to daughter cells upon cell division and is associated with the repression of gene expression (Attwood et al., 2002; Caiafa and Zampieri, 2005). One of the ways in which PARP-1 affects DNA methylation is by regulating the expression and activity of the DNA methyltransferase Dnmt1 (Caiafa et al., 2009; Caiafa and Zlatanova, 2009). PARP-1 binds to the promoter of the Dnmt1 gene and can protect it from DNA methylation-induced silencing in a PAR-dependent manner (Zampieri et al., 2009). In this regard, overexpression of poly(ADP-ribose) glycohydrolase (PARG), an enzyme that degrades PAR (see below), leads to aberrant methylation of a CpG island in the

promoter of the Dnmt1 gene in mouse fibroblasts, which in turn inhibits its transcription (Zampieri et al., 2009). The loss of Dnmt1 expression leads to widespread passive hypomethylation of genomic DNA.

In addition to PARP-1's role in regulating Dnmt1 gene expression, PARP-1 also been shown to interact with Dnmt1 in a complex that contains PAR (Reale et al., 2005). The non-covalent binding of PAR polymers by Dnmt1 within the complex inhibits Dnmt1 DNA methyltransferase activity, probably through an inhibitory steric mechanism (Reale et al., 2005). Interestingly, the effects of PARP-1 on DNA methylation are modulated by CTCF, which may promote PARP-1 automodification, CTCF PARylation, the accumulation of PAR polymers, and ultimately the inhibition of Dnmt1 DNA methyltransferase activity (Guastafierro et al., 2008). Future studies will be required to determine the extent to which PARP-1 plays a role in the dynamic regulation of DNA methylation in different physiological and disease states.

1.5.4 Functional interplay with Sirt1

Recent studies have identified functional interplay between PARP-1 and the NAD^+-dependent protein deacetylase Sirt1. Sirt1 is an important regulator of metabolism, cell differentiation and senescence, stress responses, and cancer, which is does by regulating chromatin structure and gene expression (Zhang and Kraus, 2009). PARP-1 and Sirt1 have been shown to function antagonistically; chemical activation of SIRT1 leads to reduced PARP-1 activity and knockout of Sirt1 increases PARP-1 activity (Kolthur-Seetharam et al., 2006). PARP-1 and Sirt1 are thought to compete for nuclear NAD^+, and a byproduct of the reactions they catalyze, nicotinamide, can inhibit both of their activities (Kim et al., 2005; Zhang and Kraus, 2009). This sets the stage for a tightly regulated interplay between these two proteins.

Recent studies have begun to elucidate the mechanisms of this interplay that go beyond simple competition for NAD^+. As noted above, acetylation of PARP-1 by PCAF is required for stress-induced cell death pathways. Deacetylation of PARP-1 by Sirt1 promotes cell survival (Rajamohan et al., 2009). In mice, double knockout of PARP-1 in a Sirt1 background increases the late post-natal lethality before weaning that is observed in Sirt1 knockout animals, but also rescues the abnormal pericentric heterochromatin formation, nucleolar disorganization, and mitotic defects that are observed in Sirt1-deficient cells (El Ramy et al., 2009). Unchecked PARP-1 activity in the absence of Sirt1 results in apoptosis inducing factor-mediated cell death. In mammalian cells, Sirt1 inhibits the expression of the PARP-1 gene, adding another layer of complexity to the functional interplay (Rajamohan et al., 2009). In *Drosophila*, dPARP and dPARG may promote chromatin silencing by regulating the localization and function of dSir2 (the *Drosophila* homolog of mammalian Sirt1) (Tulin et al., 2006). These results establish a functional link between PARP-1 and Sirt1 that plays key roles in chromatin structure, the maintenance of genomic integrity, and cell viability.

1.6 Chemical Biology and Dynamics of PAR

PAR is a negatively charged molecule that resembles single stranded nucleic acid polymers. As described above, it functions as a covalent post-translational modification, as well as a protein-binding matrix. Much of the focus on PAR to date has been on its synthesis and degradation, both of which occur on the time scale of minutes in the cell.

1.6.1 Dynamic synthesis and degradation of PAR

PAR is synthesized rapidly in response to a variety of physiologic (e.g., hormone signaling) and stress-related (e.g., heat shock, DNA damage) stimuli (D'Amours et al., 1999; Hakme et al., 2008). As noted above, these stimuli ultimately result in the allosteric activation of PARP-1 catalytic activity, which in turn can lead to the autoPARylation of PARP-1, as well as the transmodification of other protein targets. If extensive, autoPARylation can inhibit PARP-1 enzymatic activity, which can block further PAR synthesis (D'Amours et al., 1999; Hakme et al., 2008). Very rapidly after synthesis (within seconds to minutes), PAR is degraded to ADP-ribose monomers, which may have signaling functions in the nucleus (see below) (Gagne et al., 2006; Min and Wang, 2009). Structurally different types of PAR are degraded at different rates (i.e., short more rapidly than long, linear more rapidly than branched), which may influence their biological functions (Hassa and Hottiger, 2008).

Most PAR in the cell is degraded by the enzyme poly(ADP-ribose) glycohydrolase PARG), an enzyme with both exo and endoglycosidase activities (actually a family of isoforms all encoded by the same gene) (Gagne et al., 2006; Min and Wang, 2009) (**Fig. 1.4**). In mice, targeted deletion of the 110 kDal PARG isoforms results in increased lethality in response to genotoxin exposure and septic shock relative to wild-type animals (Cortes et al., 2004). Mice with complete deletion of all PARG isoforms are embryonic lethal. Trophoblast stem cells from these animals are viable only when cultured in the presence of a PARP inhibitor and they exhibit reduced growth, accumulation of PAR, and increased sensitivity genotoxic stress (Koh et al., 2004). In *Drosophila*, increasing or decreasing dPARG levels phenocopies dPARP mutation, supporting a role for dPARG in removing PAR and, perhaps, facilitating multiple cycles of catalysis by individual PARP molecules (Tulin et al., 2006). The available data highlight the importance of PAR catabolism for

embryonic development, the maintenance of normal physiological states, and protection against genotoxic stress (Cortes et al., 2004; Fisher et al., 2007; Koh et al., 2004; St-Laurent et al., 2007).

Recently, the enzyme ADP-ribose-protein-hydrolase-3 (ARH3) was also shown to possesses intrinsic PARG activity (Oka et al., 2006), suggesting that the mammalian genome may encode several additional proteins with PARG activities. Other enzymatic activities, such as poly and mono (ADP-ribosyl) protein hydrolase, as well as mono(ADP-ribosyl) protein lyase, may also act to remove PAR polymers and ADP-ribose monomers from target proteins (Hassa and Hottiger, 2008). Although the dynamic nature of PAR synthesis and degradation has been elucidated, the function of the PAR polymer itself and the nature of its biomolecular interactions have remained elusive. Recent studies, however, have begun to shed new light in this area, especially with the discovery of PAR-binding motifs and domains in proteins.

1.6.2 PAR-binding motifs/domains

Recent studies have begun to reveal the interactions and functions of PAR in the cell. These studies have lead to the identification of three different motifs or domains that bind PAR, which are found in a variety of proteins involved in DNA repair or chromatin regulation (**Fig. 1.7**) (Kleine and Luscher, 2009; Kraus, 2009).

- ***A short motif.*** A series of studies have lead to the experimental and computational identification of an eight amino acid PAR-binding motif found in PAR-binding proteins: $[HKR]_1$-X_2-X_3-$[AIQVY]_4$-$[KR]_5$-$[KR]_6$-$[AILV]_7$-$[FILPV]_8$, (**Fig. 1.7A**) (Gagne et al., 2008; Pleschke et al., 2000). Although the function of this motif has not been extensively verified in functional assays, its identification in a large set of proteins suggests a potentially broad role for PAR in regulating the function of nuclear proteins. For example, PAR-binding motifs in the *Drosophila* hnRNPs Squid/hrp40 and Hrb98DE/hrp38 may play a role in regulating alternative splicing of RNA

transcripts (Ji and Tulin, 2009). The prominent role that basic amino acids play as determinants of this consensus sequence, however, raises questions about the specificity of PAR binding or whether the binding reflects the general affinity of the basic amino acids for charged polymers (Kleine and Luscher, 2009).

• ***PAR-binding zinc finger (PBZ).*** The (PBZ), a C2H2 zinc finger, represents another motif that can bind PAR (**Fig. 1.7B**) (Ahel et al., 2008; Eustermann et al., 2010; Isogai et al., 2010; Rulten et al., 2008). It was originally identified in CHFR (checkpoint protein with FHA and RING domains), APLF (aprataxin PNK-like factor), and other proteins involved in DNA repair and checkpoint control proteins (Ahel et al., 2008; Rulten et al., 2008). Functional analyses have demonstrated that the actions of CHFR in the antephase checkpoint are blocked by mutations in the PBZ motif or by inhibition of poly(ADP-ribose) synthesis (Ahel et al., 2008). PAR binding by the PBZ in APLF is required for targeting the protein to DNA strand breaks and may also serve to suppress further PAR synthesis (Rulten et al., 2008). These results provided the first evidence of functional consequences for PAR binding through a specific motif.

• ***Macrodomains.*** The macrodomain, an ancient and highly conserved structural domain (Kraus, 2009), represents a third type of motif that can bind PAR, as well as other metabolites of NAD^+ (e.g., ADP-ribose, see above; O-acetyl-ADP-ribose, which is generated as a by product of sirtuin-mediated deacetylation reactions (Zhang and Kraus, 2009)) (**Fig. 1.7C**) (Karras et al., 2005; Kustatscher et al., 2005; Neuvonen and Ahola, 2009). Prior reports have suggested a physical and functional link between PARP-1 and the macrodomain-containing histone variant macroH2A (Nusinow et al., 2007; Ouararhni et al., 2006). Three recent papers have gone farther to examine the mechanisms and functions of PAR binding by macrodomain-containing proteins in the control of nuclear functions (Kraus, 2009).

Figure 1.7. PAR-binding motifs.

(A) PAR binding motifs, as found in dHrp38, a protein that regulates alternative splicing of RNA transcripts.

(B) PAR-binding zinc fingers (PBZs), as found in hAPLF, a protein involved in DNA damage checkpoints. The structures of the two PBZs from hAPLF are shown.

(C) Macrodomains, as found in macroH2A1.1, a histone variant involved in setting the chromatin environment. The structure of the macrodomain of macroH2A1.1 bound to ADP-ribose is shown.

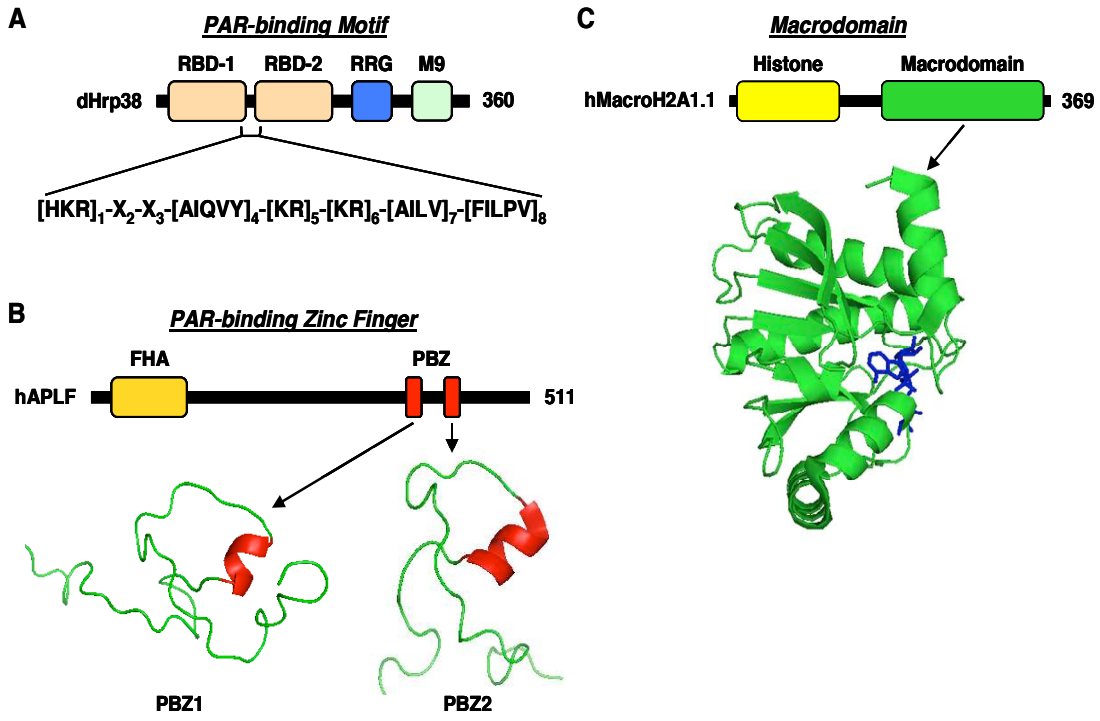
A
PAR-binding Motif
RBD-1
RBD-2
RRG
M9
dHrp38
360
[HKR]1-X2-X3-[AIQVY]4-[KR]5-[KR]6-[AILV]7-[FILPV]8
B
PAR-binding Zinc Finger
FHA
PBZ
hAPLF
511
PBZ1
PBZ2
C
Macrodomain
Histone
Macrodomain
hMacroH2A1.1
369

The macrodomain of macroH2A1.1 is required for the localization of macroH2A1.1 to sites of DNA damage-induced PARP-1 activation and PAR formation in the nucleus (Timinszky et al., 2009). One outcome of macroH2A1.1 localization to PARylated loci is the transient compaction of chromatin, an effect that might play a role in regulating DNA repair responses (Timinszky et al., 2009). The macrodomain of ALC1 (a.k.a. Chd1L), an ATP-dependent nucleosome remodeling enzyme, is required for PAR-dependent interactions with PARP-1 and targeting to sites of PAR formation in the nucleus (Ahel et al., 2009; Gottschalk et al., 2009). Interestingly, the ATPase and nucleosome-remodeling activities of ALC1 are dependent on NAD^+-dependent PAR synthesis by PARP-1 (Ahel et al., 2009; Gottschalk et al., 2009). Thus, PAR binding through the macrodomain of ALC1 represents another mechanism by which PARP-1 can alter chromatin structure.

The PAR-binding motifs/domains described herein are likely share at least two common functions: (1) targeting of the proteins that contain them to sites of PAR synthesis and (2) regulating the activity of the proteins that contain them upon PAR-binding. Whether there are additional PAR-binding motifs/domains present in the eukaryotic proteome has yet to be determined, but the future identification any such motifs/domains will give immediate clues as to the function of the proteins that contain them.

1.7 PARP-1 and NAD^+ Metabolism

As the substrate for PARP-1-catalyzed PARylation reactions, NAD^+ plays a central role in determining the function and activity of PARP-1. The synthesis of NAD^+ occurs in multiple cellular compartments, including the nucleus, which may be the most relevant source of NAD^+ for PARP-1 (Berger et al., 2004; Rongvaux et al.,

2003). In mammals, NAD^+ is synthesized de novo in a pathway leading from tryptophan, as well as through a salvage pathway leading from nicotinamide and catalyzed by the enzymes nicotinamide phosphoribosyltransferase (NAMPT) and nicotinamide mononucleotide adenylyltransferase (NMNAT; NMNAT-1 is the nuclear form) (**Fig. 1.4**) (Berger et al., 2004; Rongvaux et al., 2003). Interestingly, nicotinamide is natural endogenous inhibitor of PARP-1 (and Sirt1). Thus, the salvage pathway supports PARP-1 activity by depleting nicotinamide and producing of NAD^+.

Recent studies have illustrated how the enzymatic activities of PARP-1, NAMPT, and NMNAT are functionally linked. For example, stress-induced cell death due to PARP-1-dependent NAD^+ depletion in cardiomyocytes can be reversed by overexpression of NAMPT (Pillai et al., 2005), supporting the conclusion that NAMPT catalyzes the rate-limiting step in NAD^+ synthesis (Revollo et al., 2004). Furthermore, in addition to producing NAD^+ to support PARP-1 catalytic activity, NMNAT-1 also stimulates PARP-1 catalytic activity by binding to activated, automodified PARP-1 (Berger et al., 2007). A recent study has shown that Sirt1 recruits NMNAT-1 to target gene promoters, presumably to supply NAD^+ for protein deacetylase reactions at the promoter (Zhang et al., 2009). It is likely that a similar mechanism involving PARP-1 and NMNAT-1 supports PARylation of proteins at the promoters of PARP-1-regulated genes. The enzymatic activities of PARP-1 and Sirt1 may also be linked through competition for limiting supplies of nuclear NAD^+ (review?). Difficulty in accurately determining the concentrations of nuclear NAD^+, however, has hampered verification of this conclusion. Although functional interplay between PARP-1 and NAD^+-metabolizing enzymes in the nucleus has been established, the molecular mechanisms remain to be clarified.

1.8 Cellular Signaling through PARP-1

PARP-1 is a targeted endpoint of a number of distinct cellular signaling pathways, including those regulated by hormones, stress, and DNA damage. As noted above, PARP-1 is subject to a variety of post-translational modifications in response to these pathways, and these modification are likely to play a key role in regulating PARP-1 activity and generating specificity of signaling endpoints.

1.8.1 Cellular signaling pathways and functional outcomes

The ultimate functional outcomes of PARP-1-dependent signaling pathways are varied. For example, PARP-1 can act as an integrator in a number of pathways, including stress-dependent gene regulatory pathways, where it facilitates the recruitment of chromatin- and transcription-regulating proteins, and promotes the reorganization of chromatin at PARP-1 target genes (Frizzell et al., 2009; Hassa et al., 2003; Petesch and Lis, 2008; Tulin and Spradling, 2003). PARP-1 can also act as an "exchange factor" at target gene promoters in response to cellular signals, promoting a switch from the binding of repressive complexes to activating complexes at target gene promoters (Ju et al., 2006; Ju et al., 2004; Pavri et al., 2005). The most well characterized signaling pathways in which PARP-1 plays a role are NF-κB-dependent pro-inflammatory responses, heat shock, cellular kinase-dependent pathways, and hormone signaling, although the involvement of PARP-1 in a number of other pathways seems likely.

• ***NF-κB-dependent pro-inflammatory pathways.*** PARP-1 plays a key role in pro-inflammatory gene expression responses. Much of PARP-1's function in this regard is as a transcriptional coregulator of NF-κB in signaling pathways leading from Toll-like receptors (Hassa and Hottiger, 2002). In this regard, PARP-1 functions as a

coactivator of NF-κB to regulate the expression of pro-inflammatory target genes. This involves the acetylation of PARP-1 by p300/CBP, which is required for the interaction of PARP-1 with NF-κB and coactivation by the Mediator complex in response to inflammatory stimuli (Hassa et al., 2003; Hassa et al., 2005). PARP-1 was recently shown to be required for DNA damage-induced activation of IκB kinase (IKK), a key protein in the pathway leading to activation of NF-κB. In this regard, PARP-1 promotes the PAR-dependent assembly of a complex containing PIASy and ATM, both of which contain PAR-binding motifs, as well as IKKγ, which is subsequently SUMOylated (Stilmann et al., 2009).

• ***Heat shock.*** In *Drosophila*, PAR rapidly accumulates at heat shock loci in response to heat shock (Tulin and Spradling, 2003). dPARP is required for heat shock-induced "puffing" (i.e., chromatin decondensation) at these loci, as described above (Tulin and Spradling, 2003, Petesch, 2008 #7). Knockdown of dPARP or treatment with a PARP inhibitor prevents heat shock-induced nucleosome loss and enhanced transcription at the *Hsp70* gene (Petesch and Lis, 2008). In fact, with dPARP knockdown or in the presence of the PARP inhibitor, the nucleosomes remain in a non-heat shock state even after heat shock (Petesch and Lis, 2008). Currently, the mechanisms by which PARP-1 senses the heat shock signal is unknown, but it may involve interactions with heat shock factor, a DNA-binding transcription factor that is phosphorylated in response to heat shock.

• ***Hormone- and kinase-dependent signaling.*** PARP-1 plays critical roles in signal-dependent gene regulation as an endpoint of neurogenic, steroid, retinoid, and other hormone signaling pathways (Ju et al., 2006; Ju et al., 2004; Kim et al., 2004; Kim et al., 2005; Kraus, 2008; Pavri et al., 2005). PARP-1 alters the chromatin structure and the set of factors bound at the promoters of the target genes whose expression is regulated by these signaling pathways. Some of these pathways involve

cellular kinases, such as ERK1/2, JNK1, PKC, and CaMKIIδ (Berger et al., 2007; Cohen-Armon et al., 2007; Ju et al., 2004; Kauppinen et al., 2006; Zhang et al., 2007). Signaling through ERK1/2 enhances PARP-1 activity, although phosphorylation of PARP-1 does not occur in all contexts (Cohen-Armon et al., 2007; Kauppinen et al., 2006). The stress-activated kinase JNK1 phosphorylates PARP-1, which promotes the sustained activation of PARP-1 when cells are stressed with hydrogen peroxide (Zhang et al., 2007). Furthermore, PKC phosphorylates NMNAT-1, reducing its ability to bind PAR, providing yet another level of PARP-1 regulation by the NAD^+ metabolic pathway (Berger et al., 2007).

1.8.2 Convergence of signaling pathways: transcription and DNA repair

A number of parallels exist between PARP-1's roles in transcription and DNA repair. For example, PARP-1 (1) interacts with and PARylates components of both the transcription and DNA repair machineries, (2) directs components of both machineries to specific sites in chromatin, and (3) is covalently modified in response to the signaling pathways that regulate these processes (Kim et al., 2005). The transcription- and repair-related aspects of PARP-1 function may converge in some contexts. For example, a recent study has suggested that upon estrogen treatment, a topoisomerase IIβ- and PARP-1-containing complex is recruited to target promoters, causing the formation of a double strand break in the promoter DNA (Ju et al., 2006). The function of the double strand break is not known, but it may resolve a topological constraint allowing a critical structural change in the promoter. Alternatively, it may serve as a signal to activate PARP-1 and stimulate its factor exchange functions at the promoter. Whether PARP-1 plays a role in the obligate post-transcription DNA repair process has not been determined, but it might explain the presence of PARP-1 at nearly all actively transcribed genes (Krishnakumar et al., 2008). Another recent

paper has proposed a related model of estrogen-dependent gene regulation involving transcription-induced oxidative damage of promoter DNA, although the role of PARP-1 in this process was not determined (Perillo et al., 2008).

Controlled transcription-coupled DNA damage as means of regulating signal-dependent gene expression might seem to be an inefficient and dangerous way for cells to respond to signals, but this is a conceptually interesting and novel view. These results should be evaluated carefully and are in need of additional confirmation and mechanistic analyses.

1.9 Physiology and Pathology of PARP-1

Studies over the past decade have begun to reveal the ways in which the nuclear functions of PARP-1 contribute to specific physiological and pathological outcomes. However, a much greater understanding of the specific biological roles of PARP-1 and how they are regulated is needed. Based on studies in animal models, PARP-1 has been implicated in development, the function of the immune and nervous systems, aging, and cancer, all of which have been reviewed in detail previously (Beneke and Burkle, 2004; Burkle et al., 2004; Kim et al., 2005; Peralta-Leal et al., 2008). Below I highlight some of the key results from animal models, as well as discuss the roles of PARP-1 in inflammation and development.

1.9.1 Animal models of PARP-1 function

PARP-1 knockout mice are viable and show only mild phenotypes (Wang et al., 1995), although some interesting phenotypes have been revealed in response to certain chemical agents and in some genetic backgrounds. For example, *Parp-1*$^{-/-}$ mice are more sensitive to chemically-induced genotoxic stress (de Murcia et al.,

1997; Wang et al., 1995; Wang et al., 1997). They also show resistance in various models of inflammation (Ha, 2004; Mabley et al., 2001; Oliver et al., 1999), as well as increased tumor formation in some genetic backgrounds (e.g., *p53*$^{-/-}$ and SCID) and in chemically-induced models of cancer (Masutani et al., 2005; Morrison et al., 1997; Tong et al., 2001). The mild phenotypes observed in the PARP-1 knockout mice may be due to redundancy with other PARP family members. In this regard, genetic ablation of dPARP in *Drosophila*, which has only one PARP-1-like gene, causes lethality at the larval stage (Miwa et al., 1999; Tulin et al., 2003; Tulin et al., 2002). Furthermore, double knockout of PARP-1 and PARP-2 in mice causes embryonic lethality (Menissier de Murcia et al., 2003). Likewise, individual tankyrase 1/PARP-5a and tankyrase 2/PARP-5b knockout mice (i.e., *Tnks1*$^{-/-}$ and *Tnks2*$^{-/-}$) are largely normal, but double knockout causes early embryonic lethality, indicating redundancy in mouse development (Chiang et al., 2008; Hsiao et al., 2006).

1.9.2 Inflammatory responses

PARP-1 has long been recognized as a key component of innate immunity and inflammatory responses, and these are the best characterized PARP-1-dependent biological responses (Cuzzocrea, 2005). PARP-1 is heavily automodified in response to bacterial infection (Nossa et al., 2009) and PARP inhibitors inhibit lymphocyte proliferation and lymphokine induction (Weltin et al., 1995). *Parp-1*$^{-/-}$ mice are resistance to inflammation in various experimental models, including LPS-induced septic shock and streptozotocin-induced diabetes (Ha, 2004; Mabley et al., 2001; Oliver et al., 1999). Moreover, PARP-deficient *Drosophila* exhibit defects in innate immunity and are more susceptible to bacterial infection that their wild-type counterparts (Tulin and Spradling, 2003). As these results indicate, PARP-1 plays a central role in supporting inflammatory responses. In pathological states, this can

have dire consequences, leading to tissue damage. Hence the potential utility of PARP inhibitors in treating inflammatory disorders (Graziani and Szabo, 2005).

Interestingly, PARP-1-dependent pro-inflammatory responses are not limited to cells of the immune system. Recent studies have implicated PARP-1 in pathological pro-inflammatory stress responses in cells of the central nervous and cardiovascular systems (Moroni, 2008; Pacher and Szabo, 2007). In a mouse model of multiple sclerosis, PARP-1 knockout reduces the severity of the disease outcome (Farez et al., 2009; Selvaraj et al., 2009). Furthermore, PARP-1 knockout has been shown to improve various aspects of cardiac function in mice (Pacher and Szabo, 2007). These results suggest a number of exciting potential therapeutic applications for PARP inhibitors.

1.9.3 Development: stem cells and differentiation

Although PARP-1 knockout mice develop normally (Wang et al., 1995), the embryonic lethal phenotype of PARP-1/PARP-2 double knockout mice indicate that PARPs are critical for embryonic development (Menissier de Murcia et al., 2003). The requirement for PARP-1 and PARP-2 in development is due, at least in part, to the roles they play in the maintenance of genomic stability (Menissier de Murcia et al., 2003). The extent to which they control other specific developmental processes is not clear, although new studies have suggested roles for PARP-1 in stem cells and during differentiation.

• ***Stem cell function.*** In embryonic stem (ES) cells from *Parp-1*$^{-/-}$ mice, about 10% of genes analyzed showed altered expression compared to about 3% of genes in livers from the same animals (Ogino et al., 2007). The number of genes down-regulated by PARP-1 knockout was about two-fold more than the number of up-regulated genes in both cases, indicating a major role for PARP-1 in keeping genes

active in ES and liver cells (Ogino et al., 2007). The large panel of genes whose expression is dependent on PARP-1 in ES cells suggests a role for PARP-1 in the developmental programming of these cells. A recent study has revealed some of the molecular mechanisms whereby PARP-1 might help to promote the differentiation of stem cells (Gao et al., 2009). Specifically, PARP-1 antagonizes the DNA-binding transcription factor Sox2 to stimulate expression of the gene encoding fibroblast growth factor 4 (FGF4), a growth factor that promotes differentiation. PARP1 binds to the FGF4 enhancer and interacts with Sox2. In response to appropriate cellular signals, PARP-1 PARylates Sox2, which promotes its dissociation and degradation. Knockdown or chemical inhibition of PARP-1 PARylation of Sox2 decreases and association its binding to the FGF4 enhancers increases, leading to reduced expression of FGF4. These results indicate that PARP-1 can regulate the pluripotent state of ES cells by controlling the activity of key stem cell transcription factors.

• ***Cellular differentiation programs.*** PARP-1, as well as PARP-2, has been implicated in the differentiation of other cell types as well. For example, in a model of neuronal differentiation, PARP-1 is required for the exchange of corepressors for coactivators at the promoters of genes regulated by the transcription factor HES1 (Ju et al., 2004). PARP-1 is also required for T-cell dependent immunoglobulin class switching in B-cells (Ambrose et al., 2009; Morrison et al., 1997). In a model of endodermal differentiation, PARP-1 and PARP-2 play distinct roles in a pathway involving physical and functional interactions with the heterochromatin-associated proteins HP1 and TIF1β: PARP-2 is required for differentiation of mouse embryonal carcinoma cells into primitive endoderm-like cells in response to retinoic acid, while PARP-1 is required for subsequent differentiation into parietal endoderm-like cells in response to retinoic acid and dibutyryl cAMP (Quenet et al., 2008).

PARP-2 is required for adipogenesis (Bai et al., 2007) and spermiogenesis (Dantzer et al., 2006), and T-cell survival during thymopoiesis (Yelamos et al., 2006). During adipogenesis, PARP-2 functions as a coactivator of the adipogenic transcription factor PPARγ (Bai et al., 2007). During thymopoiesis, PARP-2 prevents the activation of a DNA damage-dependent apoptotic response through multiple rounds of T-cell receptor gene rearrangements (Yelamos et al., 2006). Whether PARP-1 plays a similar, or perhaps an antagonistic role, in these same differentiation pathways has yet to be determined.

1.10 PARP Inhibitors

With the identification of PARP-1 and other PARP family members as key players in cellular pathways that contribute to disease (Kim et al., 2005), the development of specific, potent, effective, and safe PARP inhibitors has become an area of active research and much recent excitement in the PARP field (Rouleau et al., 2010). The focus has been on competitive inhibitors of PARP catalytic activity (**Fig. 1.8**) that may be useful as research tools, as well as clinical therapies.

1.10.1 Pharmacology

3-aminobenzamide (3-AB) (**Fig. 1.8**) was the first PARP inhibitor to be extensively characterized, but it lacks the requisite selectivity and potency to be useful as a research tool or in the clinic (Rouleau et al., 2010). Over the past decade, a large number of compounds with the ability to inhibit one or more PARP family members have been synthesized and screened by various laboratories and companies (Pacher and Szabo, 2007; Ratnam and Low, 2007; Rouleau et al., 2010). These include

compounds derived from isoquinolines, phenanthridines, phthalazines, and other structural derivatives (**Fig. 1.8**), and a number of them are currently being tested in clinical trials as cancer therapies (Ratnam and Low, 2007; Rouleau et al., 2010). Although these inhibitors are highly specific for PARPs and most have nanomolar affinities, developing inhibitors that are specific for a single specific PARP has proven to be considerably more difficult given the high level of conservation of PARP catalytic domains (Hakme et al., 2008; Schreiber et al., 2006) (**Fig. 1.2**). Although quinazolinone and quinoxaline derivatives may be more selective for PARP-1 and PARP-2, respectively (Hassa and Hottiger, 2008), increasing specificity is an important area focus for the future. PARP inhibitors are likely to be useful for treating a wide variety of diseases related to genome integrity (e.g., cancers; (Ratnam and Low, 2007)), as well as stress and acute inflammatory responses (e.g., cardiovascular disease; (Pacher and Szabo, 2007)).

1.10.2 Clinical trials: focus on cancers

A number of clinical trials are now underway examining the safety and efficacy of PARP inhibitors as treatments for a variety of cancers, including breast, uterine, and ovarian cancers (Rouleau et al., 2010). In many cases, this may be due to synthetic lethality between PARP inhibition and a genetic lesion in the cancer cells. For example, p53-deficient breast cancer cells treated with a PARP inhibitor lose resistance to doxorubicin, a clinically active antitumor anthracycline antibiotic that promotes apoptosis (Munoz-Gamez et al., 2005). Similarly, germline mutations in the familial breast cancer genes *BRCA1* or *BRCA2* sensitize breast cancer cells to PARP inhibitors in a PARP-1-dependent manner (Bryant et al., 2005; Farmer et al., 2005). The goal of this approach is to target cells defective in one DNA repair pathway by

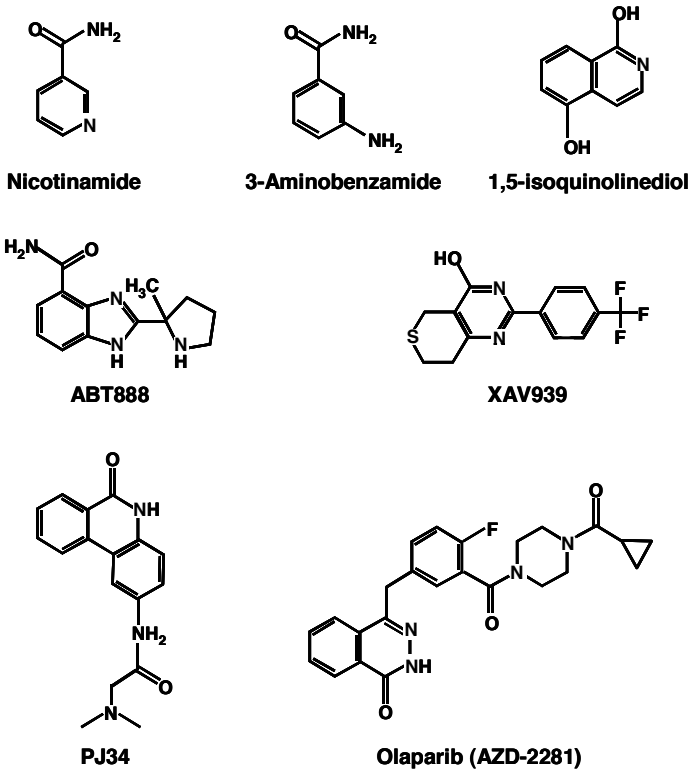

Figure 8. Structures of PARP inhibitors.

inhibiting another. A clinical trial based on this approach has shown selective anti-tumor activity for the PARP inhibitor, olaparib (**Fig. 1.8**), in breast and ovarian cancers containing *BRCA1* and *BRCA2* mutations at safely administrable doses with minimal side-effects (Fong et al., 2009). RNAi-based synthetic lethal screens may be a useful way of identifying other genes that mediate sensitivity to a PARP inhibitors; a recent study has identified a set of kinases whose silencing sensitized cells to a PARP inhibitor (Turner et al., 2008). Another study has suggested that breast cancer cells may be generally sensitive to the PARP inhibitor, PJ34 (Inbar-Rozensal et al., 2009) (**Fig. 1.8**), although this may be due synthetic lethality with unknown genetic alterations in the cells examined.

Tankyrase may also be a useful target for the treatment of cancers. In this regard, chemical inhibition of tankyrase shows synthetic lethality with *BRCA1* or *BRCA2* mutations in breast cancer cells, much like inhibition of PARP-1 (McCabe et al., 2009). Furthermore, XAV939 (**Fig. 1.8**), an inhibitor of tankyrases 1 and 2 regulates Wnt signaling in colon cancer cells by prolonging the half-life of axin and promote β-catenin degradation, a target that may be useful for treating Wnt pathway-dependent cancers (Huang et al., 2009). These and other related clinical discoveries have moved PARP-1 and other PARP family members from interesting subjects of molecular analyses to the forefront as clinical targets for cancer treatment (Rouleau et al., 2010).

1.11 Future Directions

Based on the literature reviewed herein, it is evident that the functions of PARP-1 are as diverse as they are numerous. In many cases, however, I lack a clear mechanistic understanding of how PARP-1 contributes to the nuclear processes in which it

participates. There are many questions and issues that remain to be addressed in future studies. For example, our knowledge of PARP-1 structure is incomplete. A structure of full length PARP-1, alone or in combination with its binding partners (e.g., DNA, nucleosomes, transcription factors), will be required to achieve a full understanding of PARP-1 function. In addition, our understanding of the physiological functions of PARP-1 is limited. More sophisticated and specific animal models, such as tissue-specific knockout mice, will be required to address this issue. Furthermore, our understanding of how the diverse functions of PARP-1 are integrated and controlled is limited. In this regard, the field must reconcile the roles played by PARP-1 plays in distinct, but inter-related biological processes, such as transcription and DNA repair. Finally, more specific PARP inhibitors will be required both as tools and therapeutics. The next decade promises to be an exciting one for the field.

REFERENCES

Aguilar-Quesada, R., Munoz-Gamez, J.A., Martin-Oliva, D., Peralta, A., Valenzuela, M.T., Matinez-Romero, R., Quiles-Perez, R., Menissier-de Murcia, J., de Murcia, G., Ruiz de Almodovar, M., and Oliver, F.J. (2007). Interaction between ATM and PARP-1 in response to DNA damage and sensitization of ATM deficient cells through PARP inhibition. BMC Mol Biol *8*, 29.

Ahel, D., Horejsi, Z., Wiechens, N., Polo, S.E., Garcia-Wilson, E., Ahel, I., Flynn, H., Skehel, M., West, S.C., Jackson, S.P., *et al*. (2009). Poly(ADP-ribose)-dependent regulation of DNA repair by the chromatin remodeling enzyme ALC1. Science *325*, 1240-1243.

Ahel, I., Ahel, D., Matsusaka, T., Clark, A.J., Pines, J., Boulton, S.J., and West, S.C. (2008). Poly(ADP-ribose)-binding zinc finger motifs in DNA repair/checkpoint proteins. Nature *451*, 81-85.

Altmeyer, M., Messner, S., Hassa, P.O., Fey, M., and Hottiger, M.O. (2009). Molecular mechanism of poly(ADP-ribosyl)ation by PARP1 and identification of lysine residues as ADP-ribose acceptor sites. Nucleic Acids Res *37*, 3723-3738.

Alvarez-Gonzalez, R., and Mendoza-Alvarez, H. (1995). Dissection of ADP-ribose polymer synthesis into individual steps of initiation, elongation, and branching. Biochimie *77*, 403-407.

Ambrose, H.E., Willimott, S., Beswick, R.W., Dantzer, F., de Murcia, J.M., Yelamos, J., and Wagner, S.D. (2009). Poly(ADP-ribose) polymerase-1 (Parp-1)-deficient mice demonstrate abnormal antibody responses. Immunology *127*, 178-186.

Ame, J.C., Spenlehauer, C., and de Murcia, G. (2004). The PARP superfamily. Bioessays *26*, 882-893.

Attwood, J.T., Yung, R.L., and Richardson, B.C. (2002). DNA methylation and the regulation of gene transcription. Cell Mol Life Sci *59*, 241-257.

Bai, P., Houten, S.M., Huber, A., Schreiber, V., Watanabe, M., Kiss, B., de Murcia, G., Auwerx, J., and Menissier-de Murcia, J. (2007). Poly(ADP-ribose) polymerase-2 controls adipocyte differentiation and adipose tissue function through the regulation of the activity of the retinoid X receptor/peroxisome proliferator-activated receptor-gamma heterodimer. J Biol Chem *282*, 37738-37746.

Barski, A., Cuddapah, S., Cui, K., Roh, T.Y., Schones, D.E., Wang, Z., Wei, G., Chepelev, I., and Zhao, K. (2007). High-resolution profiling of histone methylations in the human genome. Cell *129*, 823-837.

Beneke, S., and Burkle, A. (2004). Poly(ADP-ribosyl)ation, PARP, and aging. Sci Aging Knowledge Environ *2004*, re9.

Berger, F., Lau, C., and Ziegler, M. (2007). Regulation of poly(ADP-ribose) polymerase 1 activity by the phosphorylation state of the nuclear NAD biosynthetic enzyme NMN adenylyl transferase 1. Proc Natl Acad Sci U S A *104*, 3765-3770.

Berger, F., Ramirez-Hernandez, M.H., and Ziegler, M. (2004). The new life of a centenarian: signalling functions of NAD(P). Trends Biochem Sci *29*, 111-118.

Bouchard, V.J., Rouleau, M., and Poirier, G.G. (2003). PARP-1, a determinant of cell survival in response to DNA damage. Exp Hematol *31*, 446-454.

Bryant, H.E., Schultz, N., Thomas, H.D., Parker, K.M., Flower, D., Lopez, E., Kyle, S., Meuth, M., Curtin, N.J., and Helleday, T. (2005). Specific killing of BRCA2-deficient tumours with inhibitors of poly(ADP-ribose) polymerase. Nature *434*, 913-917.

Burkle, A., Beneke, S., and Muiras, M.L. (2004). Poly(ADP-ribosyl)ation and aging. Exp Gerontol *39*, 1599-1601.

Caiafa, P., Guastafierro, T., and Zampieri, M. (2009). Epigenetics: poly(ADP-ribosyl)ation of PARP-1 regulates genomic methylation patterns. FASEB J *23*, 672-678.

Caiafa, P., and Zampieri, M. (2005). DNA methylation and chromatin structure: the puzzling CpG islands. J Cell Biochem *94*, 257-265.

Caiafa, P., and Zlatanova, J. (2009). CCCTC-binding factor meets poly(ADP-ribose) polymerase-1. J Cell Physiol *219*, 265-270.

Chiang, Y.J., Hsiao, S.J., Yver, D., Cushman, S.W., Tessarollo, L., Smith, S., and Hodes, R.J. (2008). Tankyrase 1 and tankyrase 2 are essential but redundant for mouse embryonic development. PLoS One *3*, e2639.

Cohen-Armon, M., Visochek, L., Rozensal, D., Kalal, A., Geistrikh, I., Klein, R., Bendetz-Nezer, S., Yao, Z., and Seger, R. (2007). DNA-independent PARP-1 activation by phosphorylated ERK2 increases Elk1 activity: a link to histone acetylation. Mol Cell *25*, 297-308.

Cortes, U., Tong, W.M., Coyle, D.L., Meyer-Ficca, M.L., Meyer, R.G., Petrilli, V., Herceg, Z., Jacobson, E.L., Jacobson, M.K., and Wang, Z.Q. (2004). Depletion of the 110-kilodalton isoform of poly(ADP-ribose) glycohydrolase increases sensitivity to genotoxic and endotoxic stress in mice. Mol Cell Biol *24*, 7163-7178.

Cuzzocrea, S. (2005). Shock, inflammation and PARP. Pharmacol Res *52*, 72-82.

D'Amours, D., Desnoyers, S., D'Silva, I., and Poirier, G.G. (1999). Poly(ADP-ribosyl)ation reactions in the regulation of nuclear functions. Biochem J *342 (Pt 2)*, 249-268.

Dantzer, F., Mark, M., Quenet, D., Scherthan, H., Huber, A., Liebe, B., Monaco, L., Chicheportiche, A., Sassone-Corsi, P., de Murcia, G., and Menissier-de Murcia, J. (2006). Poly(ADP-ribose) polymerase-2 contributes to the fidelity of male meiosis I and spermiogenesis. Proc Natl Acad Sci U S A *103*, 14854-14859.

de Murcia, J.M., Niedergang, C., Trucco, C., Ricoul, M., Dutrillaux, B., Mark, M., Oliver, F.J., Masson, M., Dierich, A., LeMeur, M.*, et al*. (1997). Requirement of poly(ADP-ribose) polymerase in recovery from DNA damage in mice and in cells. Proc Natl Acad Sci U S A *94*, 7303-7307.

El Ramy, R., Magroun, N., Messadecq, N., Gauthier, L.R., Boussin, F.D., Kolthur-Seetharam, U., Schreiber, V., McBurney, M.W., Sassone-Corsi, P., and Dantzer, F. (2009). Functional interplay between Parp-1 and SirT1 in genome integrity and chromatin-based processes. Cell Mol Life Sci.

El-Khamisy, S.F., Masutani, M., Suzuki, H., and Caldecott, K.W. (2003). A requirement for PARP-1 for the assembly or stability of XRCC1 nuclear foci at sites of oxidative DNA damage. Nucleic Acids Res *31*, 5526-5533.

Eustermann, S., Brockmann, C., Mehrotra, P.V., Yang, J.C., Loakes, D., West, S.C., Ahel, I., and Neuhaus, D. (2010). Solution structures of the two PBZ domains from human APLF and their interaction with poly(ADP-ribose). Nat Struct Mol Biol *17*, 241-243.

Farez, M.F., Quintana, F.J., Gandhi, R., Izquierdo, G., Lucas, M., and Weiner, H.L. (2009). Toll-like receptor 2 and poly(ADP-ribose) polymerase 1 promote central nervous system neuroinflammation in progressive EAE. Nat Immunol *10*, 958-964.

Farmer, H., McCabe, N., Lord, C.J., Tutt, A.N., Johnson, D.A., Richardson, T.B., Santarosa, M., Dillon, K.J., Hickson, I., Knights, C., *et al*. (2005). Targeting the DNA repair defect in BRCA mutant cells as a therapeutic strategy. Nature *434*, 917-921.

Fisher, A.E., Hochegger, H., Takeda, S., and Caldecott, K.W. (2007). Poly(ADP-ribose) polymerase 1 accelerates single-strand break repair in concert with poly(ADP-ribose) glycohydrolase. Mol Cell Biol *27*, 5597-5605.

Fong, P.C., Boss, D.S., Yap, T.A., Tutt, A., Wu, P., Mergui-Roelvink, M., Mortimer, P., Swaisland, H., Lau, A., O'Connor, M.J., *et al*. (2009). Inhibition of poly(ADP-ribose) polymerase in tumors from BRCA mutation carriers. N Engl J Med *361*, 123-134.

Frizzell, K.M., Gamble, M.J., Berrocal, J.G., Zhang, T., Krishnakumar, R., Cen, Y., Sauve, A.A., and Kraus, W.L. (2009). Global analysis of transcriptional regulation by poly(ADP-ribose) polymerase-1 and poly(ADP-ribose) glycohydrolase in MCF-7 human breast cancer cells. J Biol Chem *284*, 33926-33938.

Gagne, J.P., Hendzel, M.J., Droit, A., and Poirier, G.G. (2006). The expanding role of poly(ADP-ribose) metabolism: current challenges and new perspectives. Curr Opin Cell Biol *18*, 145-151.

Gagne, J.P., Isabelle, M., Lo, K.S., Bourassa, S., Hendzel, M.J., Dawson, V.L., Dawson, T.M., and Poirier, G.G. (2008). Proteome-wide identification of poly(ADP-ribose) binding proteins and poly(ADP-ribose)-associated protein complexes. Nucleic Acids Res *36*, 6959-6976.

Gamble, M.J., and Fisher, R.P. (2007). SET and PARP1 remove DEK from chromatin to permit access by the transcription machinery. Nat Struct Mol Biol *14*, 548-555.

Gao, F., Kwon, S.W., Zhao, Y., and Jin, Y. (2009). PARP1 poly(ADP-ribosyl)ates Sox2 to control Sox2 protein levels and FGF4 expression during embryonic stem cell differentiation. J Biol Chem *284*, 22263-22273.

Gottschalk, A.J., Timinszky, G., Kong, S.E., Jin, J., Cai, Y., Swanson, S.K., Washburn, M.P., Florens, L., Ladurner, A.G., Conaway, J.W., and Conaway, R.C.

(2009). Poly(ADP-ribosyl)ation directs recruitment and activation of an ATP-dependent chromatin remodeler. Proc Natl Acad Sci U S A *106*, 13770-13774.

Graziani, G., and Szabo, C. (2005). Clinical perspectives of PARP inhibitors. Pharmacol Res *52*, 109-118.

Guastafierro, T., Cecchinelli, B., Zampieri, M., Reale, A., Riggio, G., Sthandier, O., Zupi, G., Calabrese, L., and Caiafa, P. (2008). CCCTC-binding factor activates PARP-1 affecting DNA methylation machinery. J Biol Chem *283*, 21873-21880.

Ha, H.C. (2004). Defective transcription factor activation for proinflammatory gene expression in poly(ADP-ribose) polymerase 1-deficient glia. Proc Natl Acad Sci U S A *101*, 5087-5092.

Haenni, S.S., Hassa, P.O., Altmeyer, M., Fey, M., Imhof, R., and Hottiger, M.O. (2008). Identification of lysines 36 and 37 of PARP-2 as targets for acetylation and auto-ADP-ribosylation. Int J Biochem Cell Biol *40*, 2274-2283.

Hakme, A., Wong, H.K., Dantzer, F., and Schreiber, V. (2008). The expanding field of poly(ADP-ribosyl)ation reactions. 'Protein Modifications: Beyond the Usual Suspects' Review Series. EMBO Rep *9*, 1094-1100.

Hanai, S., Uchida, M., Kobayashi, S., Miwa, M., and Uchida, K. (1998). Genomic organization of Drosophila poly(ADP-ribose) polymerase and distribution of its mRNA during development. J Biol Chem *273*, 11881-11886.

Hassa, P.O., Buerki, C., Lombardi, C., Imhof, R., and Hottiger, M.O. (2003). Transcriptional coactivation of nuclear factor-kappaB-dependent gene expression by p300 is regulated by poly(ADP)-ribose polymerase-1. J Biol Chem *278*, 45145-45153.

Hassa, P.O., Haenni, S.S., Buerki, C., Meier, N.I., Lane, W.S., Owen, H., Gersbach, M., Imhof, R., and Hottiger, M.O. (2005). Acetylation of poly(ADP-ribose) polymerase-1 by p300/CREB-binding protein regulates coactivation of NF-kappaB-dependent transcription. J Biol Chem *280*, 40450-40464.

Hassa, P.O., Haenni, S.S., Elser, M., and Hottiger, M.O. (2006). Nuclear ADP-ribosylation reactions in mammalian cells: where are we today and where are we going? Microbiol Mol Biol Rev *70*, 789-829.

Hassa, P.O., and Hottiger, M.O. (2002). The functional role of poly(ADP-ribose)polymerase 1 as novel coactivator of NF-kappaB in inflammatory disorders. Cell Mol Life Sci *59*, 1534-1553.

Hassa, P.O., and Hottiger, M.O. (2008). The diverse biological roles of mammalian PARPS, a small but powerful family of poly-ADP-ribose polymerases. Front Biosci *13*, 3046-3082.

Heale, J.T., Ball, A.R., Jr., Schmiesing, J.A., Kim, J.S., Kong, X., Zhou, S., Hudson, D.F., Earnshaw, W.C., and Yokomori, K. (2006). Condensin I interacts with the PARP-1-XRCC1 complex and functions in DNA single-strand break repair. Mol Cell *21*, 837-848.

Heo, K., Kim, H., Choi, S.H., Choi, J., Kim, K., Gu, J., Lieber, M.R., Yang, A.S., and An, W. (2008). FACT-mediated exchange of histone variant H2AX regulated by phosphorylation of H2AX and ADP-ribosylation of Spt16. Mol Cell *30*, 86-97.

Hottiger, M.O., Hassa, P.O., Luscher, B., Schuler, H., and Koch-Nolte, F. (2010). Toward a unified nomenclature for mammalian ADP-ribosyltransferases. Trends Biochem Sci.

Hsiao, S.J., Poitras, M.F., Cook, B.D., Liu, Y., and Smith, S. (2006). Tankyrase 2 poly(ADP-ribose) polymerase domain-deleted mice exhibit growth defects but have normal telomere length and capping. Mol Cell Biol *26*, 2044-2054.

Huang, S.M., Mishina, Y.M., Liu, S., Cheung, A., Stegmeier, F., Michaud, G.A., Charlat, O., Wiellette, E., Zhang, Y., Wiessner, S., *et al*. (2009). Tankyrase inhibition stabilizes axin and antagonizes Wnt signalling. Nature *461*, 614-620.

Huber, A., Bai, P., de Murcia, J.M., and de Murcia, G. (2004). PARP-1, PARP-2 and ATM in the DNA damage response: functional synergy in mouse development. DNA Repair (Amst) *3*, 1103-1108.

Huletsky, A., de Murcia, G., Muller, S., Hengartner, M., Menard, L., Lamarre, D., and Poirier, G.G. (1989). The effect of poly(ADP-ribosyl)ation on native and H1-depleted chromatin. A role of poly(ADP-ribosyl)ation on core nucleosome structure. J Biol Chem *264*, 8878-8886.

Inbar-Rozensal, D., Castiel, A., Visochek, L., Castel, D., Dantzer, F., Izraeli, S., and Cohen-Armon, M. (2009). A selective eradication of human nonhereditary breast cancer cells by phenanthridine-derived polyADP-ribose polymerase inhibitors. Breast Cancer Res *11*, R78.

Isogai, S., Kanno, S., Ariyoshi, M., Tochio, H., Ito, Y., Yasui, A., and Shirakawa, M. (2010). Solution structure of a zinc-finger domain that binds to poly-ADP-ribose. Genes Cells *15*, 101-110.

Ji, Y., and Tulin, A.V. (2009). Poly(ADP-ribosyl)ation of heterogeneous nuclear ribonucleoproteins modulates splicing. Nucleic Acids Res *37*, 3501-3513.

Ju, B.G., Lunyak, V.V., Perissi, V., Garcia-Bassets, I., Rose, D.W., Glass, C.K., and Rosenfeld, M.G. (2006). A topoisomerase IIbeta-mediated dsDNA break required for regulated transcription. Science *312*, 1798-1802.

Ju, B.G., Solum, D., Song, E.J., Lee, K.J., Rose, D.W., Glass, C.K., and Rosenfeld, M.G. (2004). Activating the PARP-1 sensor component of the groucho/ TLE1 corepressor complex mediates a CaMKinase IIdelta-dependent neurogenic gene activation pathway. Cell *119*, 815-829.

Kanai, M., Hanashiro, K., Kim, S.H., Hanai, S., Boulares, A.H., Miwa, M., and Fukasawa, K. (2007). Inhibition of Crm1-p53 interaction and nuclear export of p53 by poly(ADP-ribosyl)ation. Nat Cell Biol *9*, 1175-1183.

Karras, G.I., Kustatscher, G., Buhecha, H.R., Allen, M.D., Pugieux, C., Sait, F., Bycroft, M., and Ladurner, A.G. (2005). The macro domain is an ADP-ribose binding module. Embo J *24*, 1911-1920.

Kauppinen, T.M., Chan, W.Y., Suh, S.W., Wiggins, A.K., Huang, E.J., and Swanson, R.A. (2006). Direct phosphorylation and regulation of poly(ADP-ribose) polymerase-1 by extracellular signal-regulated kinases 1/2. Proc Natl Acad Sci U S A *103*, 7136-7141.

Kim, M.Y., Mauro, S., Gevry, N., Lis, J.T., and Kraus, W.L. (2004). NAD+-dependent modulation of chromatin structure and transcription by nucleosome binding properties of PARP-1. Cell *119*, 803-814.

Kim, M.Y., Zhang, T., and Kraus, W.L. (2005). Poly(ADP-ribosyl)ation by PARP-1: 'PAR-laying' NAD+ into a nuclear signal. Genes Dev *19*, 1951-1967.

Kleine, H., and Luscher, B. (2009). Learning how to read ADP-ribosylation. Cell *139*, 17-19.

Kleine, H., Poreba, E., Lesniewicz, K., Hassa, P.O., Hottiger, M.O., Litchfield, D.W., Shilton, B.H., and Luscher, B. (2008). Substrate-assisted catalysis by PARP10 limits its activity to mono-ADP-ribosylation. Mol Cell *32*, 57-69.

Koh, D.W., Lawler, A.M., Poitras, M.F., Sasaki, M., Wattler, S., Nehls, M.C., Stoger, T., Poirier, G.G., Dawson, V.L., and Dawson, T.M. (2004). Failure to degrade poly(ADP-ribose) causes increased sensitivity to cytotoxicity and early embryonic lethality. Proc Natl Acad Sci U S A *101*, 17699-17704.

Kolthur-Seetharam, U., Dantzer, F., McBurney, M.W., de Murcia, G., and Sassone-Corsi, P. (2006). Control of AIF-mediated cell death by the functional interplay of SIRT1 and PARP-1 in response to DNA damage. Cell Cycle *5*, 873-877.

Kotova, E., Jarnik, M., and Tulin, A.V. (2009). Poly (ADP-ribose) polymerase 1 is required for protein localization to Cajal body. PLoS Genet *5*, e1000387.

Kraus, W.L. (2008). Transcriptional control by PARP-1: chromatin modulation, enhancer-binding, coregulation, and insulation. Curr Opin Cell Biol *20*, 294-302.

Kraus, W.L. (2009). New functions for an ancient domain. Nat Struct Mol Biol *16*, 904-907.

Kraus, W.L., and Lis, J.T. (2003). PARP goes transcription. Cell *113*, 677-683.

Krishnakumar, R., Gamble, M.J., Frizzell, K.M., Berrocal, J.G., Kininis, M., and Kraus, W.L. (2008). Reciprocal binding of PARP-1 and histone H1 at promoters specifies transcriptional outcomes. Science *319*, 819-821.

Kustatscher, G., Hothorn, M., Pugieux, C., Scheffzek, K., and Ladurner, A.G. (2005). Splicing regulates NAD metabolite binding to histone macroH2A. Nat Struct Mol Biol *12*, 624-625.

Langelier, M.F., Servent, K.M., Rogers, E.E., and Pascal, J.M. (2008). A third zinc-binding domain of human poly(ADP-ribose) polymerase-1 coordinates DNA-dependent enzyme activation. J Biol Chem *283*, 4105-4114.

Mabley, J.G., Suarez-Pinzon, W.L., Hasko, G., Salzman, A.L., Rabinovitch, A., Kun, E., and Szabo, C. (2001). Inhibition of poly (ADP-ribose) synthetase by gene disruption or inhibition with 5-iodo-6-amino-1,2-benzopyrone protects mice from multiple-low-dose-streptozotocin-induced diabetes. Br J Pharmacol *133*, 909-919.

Malanga, M., and Althaus, F.R. (2005). The role of poly(ADP-ribose) in the DNA damage signaling network. Biochem Cell Biol *83*, 354-364.

Martin, N., Schwamborn, K., Schreiber, V., Werner, A., Guillier, C., Zhang, X.D., Bischof, O., Seeler, J.S., and Dejean, A. (2009). PARP-1 transcriptional activity is regulated by sumoylation upon heat shock. EMBO J.

Masson, M.E., and Caldwell, J.I. (1998). Conceptually driven encoding episodes create perceptual misattributions. Acta Psychol (Amst) *98*, 183-210.

Masutani, M., Gunji, A., Tsutsumi, M., Ogawa, K., Kamada, N., Shirai, T., Jishage, K., Nakagama, H., and Sugimura, T. (2005). Role of poly-ADP-ribosylation in cancer development. In Poly(ADP-Ribosyl)ation, A. Burkle, ed. (Georgetown, TX: Landes Bioscience).

Mathis, G., and Althaus, F.R. (1987). Release of core DNA from nucleosomal core particles following (ADP-ribose)n-modification in vitro. Biochem Biophys Res Commun *143*, 1049-1054.

McCabe, N., Cerone, M.A., Ohishi, T., Seimiya, H., Lord, C.J., and Ashworth, A. (2009). Targeting Tankyrase 1 as a therapeutic strategy for BRCA-associated cancer. Oncogene *28*, 1465-1470.

Mendoza-Alvarez, H., and Alvarez-Gonzalez, R. (1993). Poly(ADP-ribose) polymerase is a catalytic dimer and the automodification reaction is intermolecular. J Biol Chem *268*, 22575-22580.

Mendoza-Alvarez, H., and Alvarez-Gonzalez, R. (1999). Biochemical characterization of mono(ADP-ribosyl)ated poly(ADP-ribose) polymerase. Biochemistry *38*, 3948-3953.

Mendoza-Alvarez, H., and Alvarez-Gonzalez, R. (2001). Regulation of p53 sequence-specific DNA-binding by covalent poly(ADP-ribosyl)ation. J Biol Chem *276*, 36425-36430.

Menisser-de Murcia, J., Mark, M., Wendling, O., Wynshaw-Boris, A., and de Murcia, G. (2001). Early embryonic lethality in PARP-1 Atm double-mutant mice suggests a functional synergy in cell proliferation during development. Mol Cell Biol *21*, 1828-1832.

Menissier de Murcia, J., Ricoul, M., Tartier, L., Niedergang, C., Huber, A., Dantzer, F., Schreiber, V., Ame, J.C., Dierich, A., LeMeur, M., *et al*. (2003). Functional interaction between PARP-1 and PARP-2 in chromosome stability and embryonic development in mouse. EMBO J *22*, 2255-2263.

Messner, S., Schuermann, D., Altmeyer, M., Kassner, I., Schmidt, D., Schar, P., Muller, S., and Hottiger, M.O. (2009). Sumoylation of poly(ADP-ribose) polymerase 1 inhibits its acetylation and restrains transcriptional coactivator function. FASEB J.

Min, W., and Wang, Z.Q. (2009). Poly (ADP-ribose) glycohydrolase (PARG) and its therapeutic potential. Front Biosci *14*, 1619-1626.

Miwa, M., Hanai, S., Poltronieri, P., Uchida, M., and Uchida, K. (1999). Functional analysis of poly(ADP-ribose) polymerase in Drosophila melanogaster. Mol Cell Biochem *193*, 103-107.

Monaco, L., Kolthur-Seetharam, U., Loury, R., Murcia, J.M., de Murcia, G., and Sassone-Corsi, P. (2005). Inhibition of Aurora-B kinase activity by poly(ADP-ribosyl)ation in response to DNA damage. Proc Natl Acad Sci U S A *102*, 14244-14248.

Moroni, F. (2008). Poly(ADP-ribose)polymerase 1 (PARP-1) and postischemic brain damage. Curr Opin Pharmacol *8*, 96-103.

Morrison, C., Smith, G.C., Stingl, L., Jackson, S.P., Wagner, E.F., and Wang, Z.Q. (1997). Genetic interaction between PARP and DNA-PK in V(D)J recombination and tumorigenesis. Nat Genet *17*, 479-482.

Munoz-Gamez, J.A., Martin-Oliva, D., Aguilar-Quesada, R., Canuelo, A., Nunez, M.I., Valenzuela, M.T., Ruiz de Almodovar, J.M., De Murcia, G., and Oliver, F.J. (2005). PARP inhibition sensitizes p53-deficient breast cancer cells to doxorubicin-induced apoptosis. Biochem J *386*, 119-125.

Neuvonen, M., and Ahola, T. (2009). Differential activities of cellular and viral macro domain proteins in binding of ADP-ribose metabolites. J Mol Biol *385*, 212-225.

Nossa, C.W., Jain, P., Tamilselvam, B., Gupta, V.R., Chen, L.F., Schreiber, V., Desnoyers, S., and Blanke, S.R. (2009). Activation of the abundant nuclear factor poly(ADP-ribose) polymerase-1 by Helicobacter pylori. Proc Natl Acad Sci U S A *106*, 19998-20003.

Nusinow, D.A., Hernandez-Munoz, I., Fazzio, T.G., Shah, G.M., Kraus, W.L., and Panning, B. (2007). Poly(ADP-ribose) polymerase 1 is inhibited by a histone H2A variant, MacroH2A, and contributes to silencing of the inactive X chromosome. J Biol Chem *282*, 12851-12859.

Oberdoerffer, P., Michan, S., McVay, M., Mostoslavsky, R., Vann, J., Park, S.K., Hartlerode, A., Stegmuller, J., Hafner, A., Loerch, P., *et al*. (2008). SIRT1 redistribution on chromatin promotes genomic stability but alters gene expression during aging. Cell *135*, 907-918.

Ogino, H., Nozaki, T., Gunji, A., Maeda, M., Suzuki, H., Ohta, T., Murakami, Y., Nakagama, H., Sugimura, T., and Masutani, M. (2007). Loss of Parp-1 affects gene expression profile in a genome-wide manner in ES cells and liver cells. BMC Genomics *8*, 41.

Oka, S., Kato, J., and Moss, J. (2006). Identification and characterization of a mammalian 39-kDa poly(ADP-ribose) glycohydrolase. J Biol Chem *281*, 705-713.

Okano, S., Lan, L., Caldecott, K.W., Mori, T., and Yasui, A. (2003). Spatial and temporal cellular responses to single-strand breaks in human cells. Mol Cell Biol *23*, 3974-3981.

Oliver, F.J., Menissier-de Murcia, J., Nacci, C., Decker, P., Andriantsitohaina, R., Muller, S., de la Rubia, G., Stoclet, J.C., and de Murcia, G. (1999). Resistance to endotoxic shock as a consequence of defective NF-kappaB activation in poly (ADP-ribose) polymerase-1 deficient mice. Embo J *18*, 4446-4454.

Otto, H., Reche, P.A., Bazan, F., Dittmar, K., Haag, F., and Koch-Nolte, F. (2005). In silico characterization of the family of PARP-like poly(ADP-ribosyl)transferases (pARTs). BMC Genomics *6*, 139.

Ouararhni, K., Hadj-Slimane, R., Ait-Si-Ali, S., Robin, P., Mietton, F., Harel-Bellan, A., Dimitrov, S., and Hamiche, A. (2006). The histone variant mH2A1.1 interferes with transcription by down-regulating PARP-1 enzymatic activity. Genes Dev *20*, 3324-3336.

Pacher, P., and Szabo, C. (2007). Role of poly(ADP-ribose) polymerase 1 (PARP-1) in cardiovascular diseases: the therapeutic potential of PARP inhibitors. Cardiovasc Drug Rev *25*, 235-260.

Pavri, R., Lewis, B., Kim, T.K., Dilworth, F.J., Erdjument-Bromage, H., Tempst, P., de Murcia, G., Evans, R., Chambon, P., and Reinberg, D. (2005). PARP-1 determines specificity in a retinoid signaling pathway via direct modulation of mediator. Mol Cell *18*, 83-96.

Peralta-Leal, A., Rodriguez, M.I., and Oliver, F.J. (2008). Poly(ADP-ribose)polymerase-1 (PARP-1) in carcinogenesis: potential role of PARP inhibitors in cancer treatment. Clin Transl Oncol *10*, 318-323.

Perillo, B., Ombra, M.N., Bertoni, A., Cuozzo, C., Sacchetti, S., Sasso, A., Chiariotti, L., Malorni, A., Abbondanza, C., and Avvedimento, E.V. (2008). DNA oxidation as triggered by H3K9me2 demethylation drives estrogen-induced gene expression. Science *319*, 202-206.

Petermann, E., Keil, C., and Oei, S.L. (2005). Importance of poly(ADP-ribose) polymerases in the regulation of DNA-dependent processes. Cell Mol Life Sci *62*, 731-738.

Petesch, S.J., and Lis, J.T. (2008). Rapid, transcription-independent loss of nucleosomes over a large chromatin domain at Hsp70 loci. Cell *134*, 74-84.

Pillai, J.B., Isbatan, A., Imai, S., and Gupta, M.P. (2005). Poly(ADP-ribose) polymerase-1-dependent cardiac myocyte cell death during heart failure is mediated by NAD+ depletion and reduced Sir2alpha deacetylase activity. J Biol Chem *280*, 43121-43130.

Pleschke, J.M., Kleczkowska, H.E., Strohm, M., and Althaus, F.R. (2000). Poly(ADP-ribose) binds to specific domains in DNA damage checkpoint proteins. J Biol Chem *275*, 40974-40980.

Poirier, G.G., de Murcia, G., Jongstra-Bilen, J., Niedergang, C., and Mandel, P. (1982). Poly(ADP-ribosyl)ation of polynucleosomes causes relaxation of chromatin structure. Proc Natl Acad Sci U S A *79*, 3423-3427.

Quenet, D., Gasser, V., Fouillen, L., Cammas, F., Sanglier-Cianferani, S., Losson, R., and Dantzer, F. (2008). The histone subcode: poly(ADP-ribose) polymerase-1 (Parp-1) and Parp-2 control cell differentiation by regulating the transcriptional intermediary factor TIF1beta and the heterochromatin protein HP1alpha. FASEB J *22*, 3853-3865.

Rajamohan, S.B., Pillai, V.B., Gupta, M., Sundaresan, N.R., Birukov, K.G., Samant, S., Hottiger, M.O., and Gupta, M.P. (2009). SIRT1 promotes cell survival under

stress by deacetylation-dependent deactivation of poly(ADP-ribose) polymerase 1. Mol Cell Biol *29*, 4116-4129.

Ratnam, K., and Low, J.A. (2007). Current development of clinical inhibitors of poly(ADP-ribose) polymerase in oncology. Clin Cancer Res *13*, 1383-1388.

Reale, A., Matteis, G.D., Galleazzi, G., Zampieri, M., and Caiafa, P. (2005). Modulation of DNMT1 activity by ADP-ribose polymers. Oncogene *24*, 13-19.

Revollo, J.R., Grimm, A.A., and Imai, S. (2004). The NAD biosynthesis pathway mediated by nicotinamide phosphoribosyltransferase regulates Sir2 activity in mammalian cells. J Biol Chem *279*, 50754-50763.

Rongvaux, A., Andris, F., Van Gool, F., and Leo, O. (2003). Reconstructing eukaryotic NAD metabolism. Bioessays *25*, 683-690.

Rouleau, M., Patel, A., Hendzel, M.J., Kaufmann, S.H., and Poirier, G.G. (2010). PARP inhibition: PARP1 and beyond. Nat Rev Cancer.

Rulten, S.L., Cortes-Ledesma, F., Guo, L., Iles, N.J., and Caldecott, K.W. (2008). APLF (C2orf13) is a novel component of poly(ADP-ribose) signaling in mammalian cells. Mol Cell Biol *28*, 4620-4628.

Sala, A., La Rocca, G., Burgio, G., Kotova, E., Di Gesu, D., Collesano, M., Ingrassia, A.M., Tulin, A.V., and Corona, D.F. (2008). The nucleosome-remodeling ATPase ISWI is regulated by poly-ADP-ribosylation. PLoS Biol *6*, e252.

Schones, D.E., Cui, K., Cuddapah, S., Roh, T.Y., Barski, A., Wang, Z., Wei, G., and Zhao, K. (2008). Dynamic regulation of nucleosome positioning in the human genome. Cell *132*, 887-898.

Schreiber, V., Ame, J.C., Dolle, P., Schultz, I., Rinaldi, B., Fraulob, V., Menissier-de Murcia, J., and de Murcia, G. (2002). Poly(ADP-ribose) polymerase-2 (PARP-2) is required for efficient base excision DNA repair in association with PARP-1 and XRCC1. J Biol Chem *277*, 23028-23036.

Schreiber, V., Dantzer, F., Ame, J.C., and de Murcia, G. (2006). Poly(ADP-ribose): novel functions for an old molecule. Nat Rev Mol Cell Biol *7*, 517-528.

Selvaraj, V., Soundarapandian, M.M., Chechneva, O., Williams, A.J., Sidorov, M.K., Soulika, A.M., Pleasure, D.E., and Deng, W. (2009). PARP-1 deficiency increases

the severity of disease in a mouse model of multiple sclerosis. J Biol Chem *284*, 26070-26084.

St-Laurent, J.F., Gagnon, S.N., Dequen, F., Hardy, I., and Desnoyers, S. (2007). Altered DNA damage response in Caenorhabditis elegans with impaired poly(ADP-ribose) glycohydrolases genes expression. DNA Repair (Amst) *6*, 329-343.

Stilmann, M., Hinz, M., Arslan, S.C., Zimmer, A., Schreiber, V., and Scheidereit, C. (2009). A nuclear poly(ADP-ribose)-dependent signalosome confers DNA damage-induced IkappaB kinase activation. Mol Cell *36*, 365-378.

Timinszky, G., Till, S., Hassa, P.O., Hothorn, M., Kustatscher, G., Nijmeijer, B., Colombelli, J., Altmeyer, M., Stelzer, E.H.K., Scheffzek, K.*, et al*. (2009). A macrodomain-containing histone rearranges chromatin upon sensing PARP1 activation.

Tong, W.M., Hande, M.P., Lansdorp, P.M., and Wang, Z.Q. (2001). DNA strand break-sensing molecule poly(ADP-Ribose) polymerase cooperates with p53 in telomere function, chromosome stability, and tumor suppression. Mol Cell Biol *21*, 4046-4054.

Tulin, A., Chinenov, Y., and Spradling, A. (2003). Regulation of chromatin structure and gene activity by poly(ADP-ribose) polymerases. Curr Top Dev Biol *56*, 55-83.

Tulin, A., Naumova, N.M., Menon, A.K., and Spradling, A.C. (2006). Drosophila poly(ADP-ribose) glycohydrolase mediates chromatin structure and SIR2-dependent silencing. Genetics *172*, 363-371.

Tulin, A., and Spradling, A. (2003). Chromatin loosening by poly(ADP)-ribose polymerase (PARP) at Drosophila puff loci. Science *299*, 560-562.

Tulin, A., Stewart, D., and Spradling, A.C. (2002). The Drosophila heterochromatic gene encoding poly(ADP-ribose) polymerase (PARP) is required to modulate chromatin structure during development. Genes Dev *16*, 2108-2119.

Turner, N.C., Lord, C.J., Iorns, E., Brough, R., Swift, S., Elliott, R., Rayter, S., Tutt, A.N., and Ashworth, A. (2008). A synthetic lethal siRNA screen identifying genes mediating sensitivity to a PARP inhibitor. EMBO J *27*, 1368-1377.

Wacker, D.A., Ruhl, D.D., Balagamwala, E.H., Hope, K.M., Zhang, T., and Kraus, W.L. (2007). The DNA binding and catalytic domains of poly(ADP-ribose) polymerase 1 cooperate in the regulation of chromatin structure and transcription. Mol Cell Biol *27*, 7475-7485.

Wang, T., Simbulan-Rosenthal, C.M., Smulson, M.E., Chock, P.B., and Yang, D.C. (2008a). Polyubiquitylation of PARP-1 through ubiquitin K48 is modulated by activated DNA, NAD+, and dipeptides. J Cell Biochem *104*, 318-328.

Wang, Z., Zang, C., Rosenfeld, J.A., Schones, D.E., Barski, A., Cuddapah, S., Cui, K., Roh, T.Y., Peng, W., Zhang, M.Q., and Zhao, K. (2008b). Combinatorial patterns of histone acetylations and methylations in the human genome. Nat Genet *40*, 897-903.

Wang, Z.Q., Auer, B., Stingl, L., Berghammer, H., Haidacher, D., Schweiger, M., and Wagner, E.F. (1995). Mice lacking ADPRT and poly(ADP-ribosyl)ation develop normally but are susceptible to skin disease. Genes Dev *9*, 509-520.

Wang, Z.Q., Stingl, L., Morrison, C., Jantsch, M., Los, M., Schulze-Osthoff, K., and Wagner, E.F. (1997). PARP is important for genomic stability but dispensable in apoptosis. Genes Dev *11*, 2347-2358.

Weltin, D., Picard, V., Aupeix, K., Varin, M., Oth, D., Marchal, J., Dufour, P., and Bischoff, P. (1995). Immunosuppressive activities of 6(5H)-phenanthridinone, a new poly(ADP-ribose)polymerase inhibitor. Int J Immunopharmacol *17*, 265-271.

Woodhouse, B.C., and Dianov, G.L. (2008). Poly ADP-ribose polymerase-1: an international molecule of mystery. DNA Repair (Amst) *7*, 1077-1086.

Yelamos, J., Monreal, Y., Saenz, L., Aguado, E., Schreiber, V., Mota, R., Fuente, T., Minguela, A., Parrilla, P., de Murcia, G., *et al*. (2006). PARP-2 deficiency affects the survival of CD4+CD8+ double-positive thymocytes. EMBO J *25*, 4350-4360.

Yelamos, J., Schreiber, V., and Dantzer, F. (2008). Toward specific functions of poly(ADP-ribose) polymerase-2. Trends Mol Med *14*, 169-178.

Zampieri, M., Passananti, C., Calabrese, R., Perilli, M., Corbi, N., De Cave, F., Guastafierro, T., Bacalini, M.G., Reale, A., Amicosante, G., *et al*. (2009). Parp1 localizes within the Dnmt1 promoter and protects its unmethylated state by its enzymatic activity. PLoS One *4*, e4717.

Zhang, S., Lin, Y., Kim, Y.S., Hande, M.P., Liu, Z.G., and Shen, H.M. (2007). c-Jun N-terminal kinase mediates hydrogen peroxide-induced cell death via sustained poly(ADP-ribose) polymerase-1 activation. Cell Death Differ *14*, 1001-1010.

Zhang, T., Berrocal, J.G., Frizzell, K.M., Gamble, M.J., DuMond, M.E., Krishnakumar, R., Yang, T., Sauve, A.A., and Kraus, W.L. (2009). Enzymes in the NAD+ salvage pathway regulate SIRT1 activity at target gene promoters. J Biol Chem *284*, 20408-20417.

Zhang, T., and Kraus, W.L. (2009). SIRT1-dependent regulation of chromatin and transcription: Linking NAD(+) metabolism and signaling to the control of cellular functions. Biochim Biophys Acta.

CHAPTER 2

Reciprocal Binding of PARP-1 and Histone H1 at Promoters Specifies Transcriptional Outcomes*

*This work was published as Krishnakumar R, Gamble MJ, Frizzell KM, Berrocal JG, Kininis M, Kraus WL. **Reciprocal binding of PARP-1 and histone H1 at promoters specifies transcriptional outcomes.** Science. 2008 Feb 8;319(5864):819-21. The text is reprinted here with permission from the publisher. Minor modifications have been made. Contributions by other authors to this work were as follows: M.J.G., ChIP-chip array design and data analysis (Figs 2.1, 2.2, 2.4, 2.6); K.M.F., gene expression analysis (Figs. 2.7, 2.8, 2.10); J.G.B, gene expression analysis (Figs. 2.7, 2.8, 2.10); M.K., nucleosome positioning analysis (Fig. 2.5).

2.1 Summary

Nucleosome-binding proteins act to modulate the promoter chromatin architecture and transcription of target genes. We use genomic and gene-specific approaches to show that two such factors, histone H1 and poly(ADP-ribose) polymerase-1 (PARP-1), exhibit a reciprocal pattern of chromatin binding at many RNA polymerase II-transcribed promoters. PARP-1 is enriched and H1 is depleted at these promoters. This pattern of binding is associated with actively transcribed genes. Furthermore, we show that PARP-1 acts to exclude H1 from a subset of PARP-1-stimulated promoters, suggesting a functional interplay between PARP-1 and H1 at the level of nucleosome binding. Thus, although H1 and PARP-1 have similar nucleosome-binding properties and effects on chromatin structure in vitro, they have distinct roles in determining gene expression outcomes in vivo.

2.2 Introduction

Gene expression outcomes are determined, in part, by the composition of promoter chromatin, including the post-translational modification state of nucleosomal histones (Berger, 2002), the incorporation of histone variants (Kamakaka and Biggins, 2005), and the presence of nucleosome-binding proteins (McBryant, et al., 2006). Linker histone H1 and poly(ADP-ribose) polymerase-1 (PARP-1) are examples of nucleosome-binding proteins that modulate the chromatin architecture and transcription of target genes (Kim, et al., 2005, Woodcock, et al., 2006). H1 and PARP-1 bind to overlapping sites on nucleosomes at or near the dyad axis where the DNA exits the nucleosome (Kim, et al., 2004, Vignali and Workman, 1998). Unlike H1, PARP-1 has an intrinsic NAD^+-dependent enzymatic activity that regulates its association with chromatin (Kim, et al., 2004). Previous work from our lab has shown that H1 and PARP-1 bind in a competitive and mutually exclusive manner to nucleosomes in vitro

and localize to distinct nucleosomal fractions in vivo (Kim, et al., 2004), suggesting distinct roles for these factors in the regulation of gene expression. However, little is known about how H1 and PARP-1 are distributed across the mammalian genome and how they interact to regulate global patterns of gene expression in vivo.

2.3 Results

To determine the patterns of H1 and PARP-1 localization across selected regions of the human genome, we performed chromatin immunoprecipitation (ChIP) in MCF-7 breast cancer cells using antibodies specific to PARP-1 and H1 (Kim et al.,; Kininis et al., 2007), coupled with hybridization of the enriched genomic DNA to custom microarrays (i.e., ChIP-chip) (Buck and Lieb, 2004). Each array represented 57 Mb of genomic DNA, including all 44 of the ENCODE regions (2004), as well as an additional 1117 promoter regions selected from genes regulated by enzymes in the nuclear NAD^+ signaling pathway (Kim, et al., 2005) (approximately -25 kb to +5 kb relative to the transcription start site (TSS)). The raw ChIP-chip signal to input ratios were processed and aligned to the TSSs for all 1517 RNA polymerase II (Pol II)-transcribed promoters on the array (i.e., ENCODE + selected). A single array error model was generated using a 1 kb moving window with 250 bp steps in which both the mean probe $\log_2$ ratio and p-values from a nonparametric Wilcoxon signed-rank test were calculated for each window. We observed an enrichment of PARP-1 and a depletion of H1 in the region surrounding the TSSs (Fig. 2.1A). Significant peaks were defined as the center of three consecutive windows with positive means, the center window with a mean greater than either adjacent window, and all windows having p-values less than 0.01 (Wilcoxon signed-rank test). Significant troughs were defined as the center of three consecutive windows with negative means, the center window with a mean less than either adjacent window, and all windows having p-values

Figure 2.1. Distinct patterns of genomic localization for H1 and PARP-1. **(A)** Heat maps of H1 and PARP-1 ChIP-chip data for 1517 promoters tiled from -25 kb to +5 kb relative to the TSS. The promoters are ordered top to bottom based on increasing intensity of the PARP-1 signal in a 10 kb window surrounding the TSS. **(B)** Histograms showing the number of statistically significant peaks and troughs of PARP-1 and H1 across the entire 30 kb tiled region for the 1517 promoters on the ChIP-chip array.

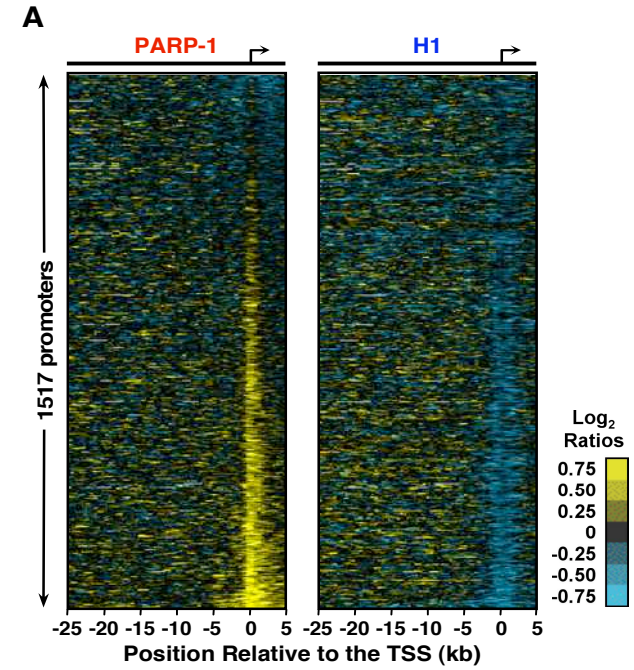
A
PARP-1
H1
1517 promoters
-25 -20 -15 -10 -5 0 5
-25 -20 -15 -10 -5 0 5
Position Relative to the TSS (kb)
Log2 Ratios
0.75
0.50
0.25
0
-0.25
-0.50
-0.75

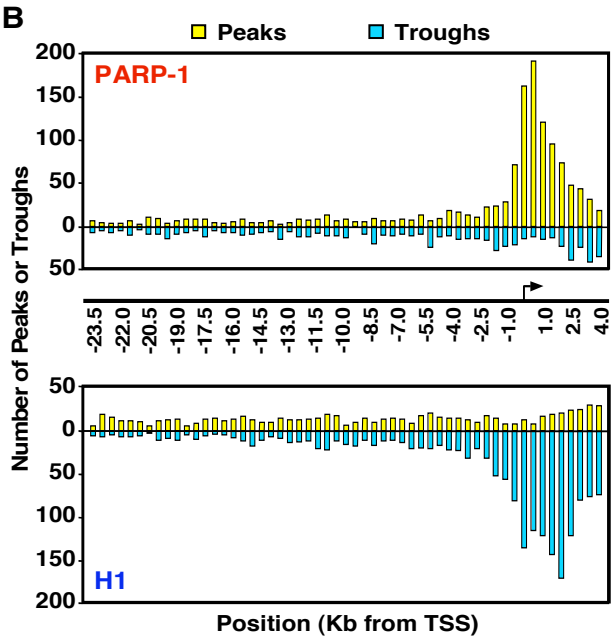
B
Peaks
Troughs
PARP-1
H1
Number of Peaks or Troughs
200
150
100
50
0
50
-23.5 -22.0 -20.5 -19.0 -17.5 -16.0 -14.5 -13.0 -11.5 -10.0 -8.5 -7.0 -5.5 -4.0 -2.5 -1.0 1.0 2.5 4.0
Position (Kb from TSS)

less than 0.01 (Wilcoxon signed-rank test). The use of our peak/trough selection criteria were justified by a low false positive rate (FPR) as determined by ChIP-qPCR (PARP-1 peak FPR = 0.11; H1 trough FPR = 0.08). Significant peaks of PARP-1 and troughs of H1 were clustered around the TSSs, but were also found in upstream and intergenic regions (Figs. 2.1B, 2.2A, 2.2B, and 2.3). This pattern of PARP-1 and H1 localization was also revealed by averaging the ChIP-chip data over the 30 kb tiled region for all promoters on the array or in a 20 kb region centered around significant PARP-1 peaks or H1 troughs (p-value < 0.01 from a Wilcoxon signed-rank test) (Fig. 2.4). Collectively, our ChIP-chip data identify a reciprocal relationship for chromatin binding by PARP-1 and H1 across the genome.

Although eukaryotic promoters generally show reduced nucleosome occupancy (Heintzman, et al., 2007, Mito, et al., 2007), this was not an important determinant for the reciprocal pattern of PARP-1 and H1 binding. Note, for example, that whereas PARP-1 peaks and H1 troughs are strongly correlated at promoters (Spearman correlation: -0.495, $p = 3.7 \times 10^{-94}$), they show little correlation with the presence of H3 (Fig. 2.6A). The Spearman correlation between PARP-1 and H1 was also determined for PARP-1-regulated genes only (108 genes total). These genes had a p value < 0.05, a fold change greater or less then 0.5 or -0.5, respectively, and were flagged present or marginal in two out of the three replicates for both PARP-1 knockdown and control cell lines. The correlation was as follows: -0.309, $p = 1.17 \times 10^{-3}$.

In addition, the pattern of PARP-1 and H1 binding at promoters (e.g., low versus high PARP-1/H1 ratios) is independent of the pattern of H3 occupancy at promoters (Fig. 2.6B). Finally, the reciprocal pattern of PARP-1 and H1 binding is observed in intergenic regions where H3 is not depleted (Fig. 2.4B). In spite of the reduced H3 occupancy at promoters, well-positioned nucleosomes are present at PARP-1-bound promoters that likely serve as targets for the binding of PARP-1 (Fig. 2.5). To

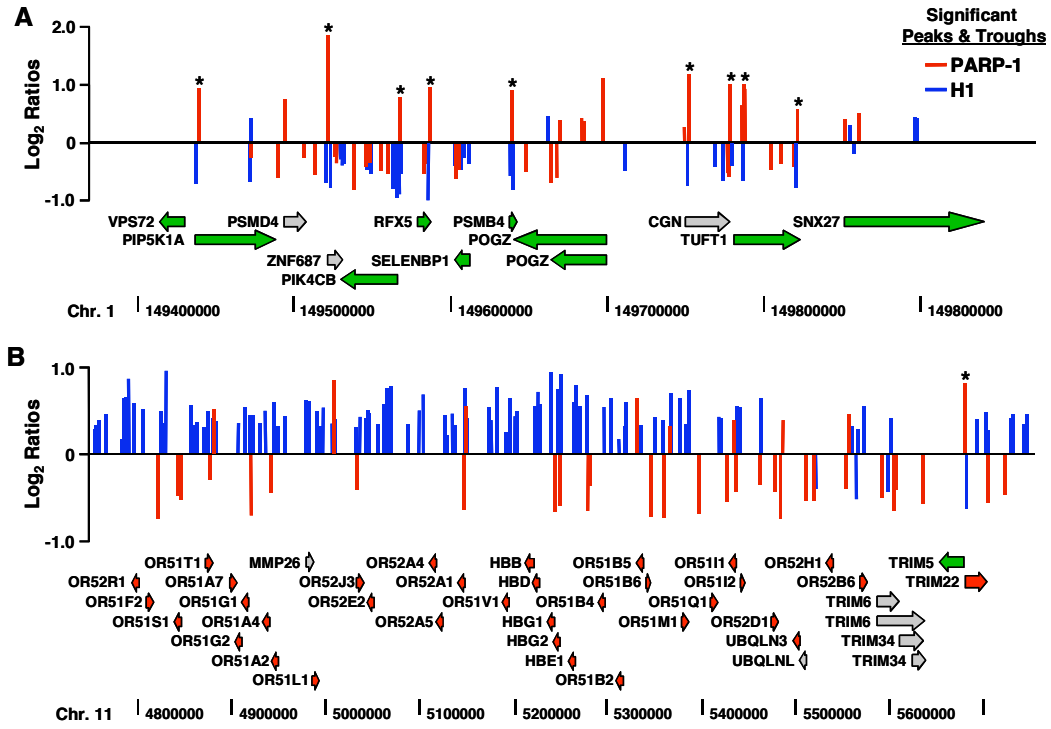

Figure 2.2. Diagram of statistically significant peaks and troughs of PARP-1 and H1 across ENCODE regions from Chr. 1 and Chr. 11. Annotated RefSeq genes are represented by arrows indicating the length of the gene, direction of transcription, and expression in MCF-7 cells (green = expressed, as determined by expression microarrays; red = unexpressed or highly unlikely to be expressed in MCF-7 cells; grey = ambiguous or no information available). Asterisks indicate genomic locations with a PARP-1 peak and a H1 trough.

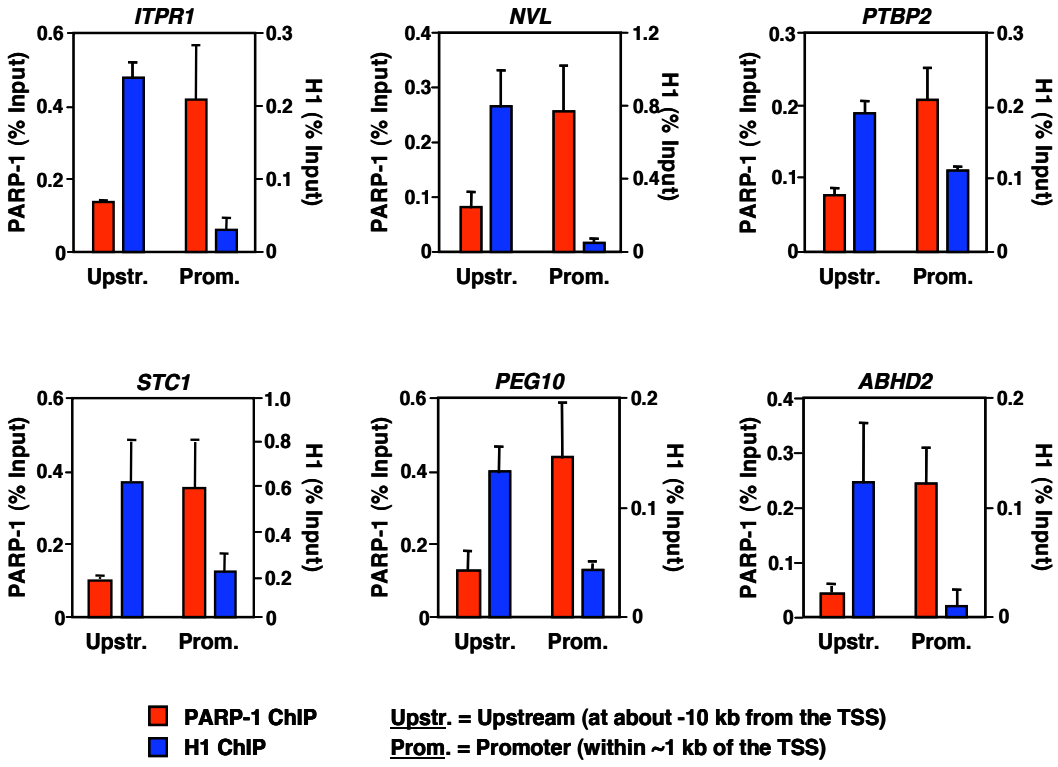

Figure 2.3. Gene-specific confirmation of PARP-1 and H1 ChIP-chip results. Gene-specific ChIP-qPCR analyses of H1 and PARP-1 binding at promoter (prom.) and upstream (upstr.; approx. -10 kb) regions for selected genes. Each bar = mean + SEM, $n = 3$.

explore the relationships between PARP-1, H1, and gene expression in more detail and under physiological NAD^+ concentrations, we coupled our ChIP-chip analyses with gene expression microarray analyses for MCF-7 cells grown under the same conditions. PARP-1 peaks showed a significant positive correlation with gene expression (Spearman rank correlation associated p-value of 7.1×10^{-49}), whereas H1 showed a significant negative correlation with gene expression (Spearman rank correlation associated p-value of 7.85×10^{-39}) (Fig. 2.6A). In addition, PARP-1 was enriched and H1 was depleted near the TSSs of expressed genes relative to unexpressed genes (Fig. 2.6B). For a gene to be classified as unambiguously expressed or unexpressed, all probe sets from all three replicates corresponding to the gene must have been flagged unanimously present or absent, respectively. Any genes not meeting these criteria were marked as ambiguous and were removed from the expression-based categorization analysis. We then grouped all genes containing both a significant PARP-1 peak and a significant H1 trough (p-value < 0.01 from a Wilcoxon signed-rank test), and compared them to a group that lacked both a PARP-1 peak and an H1 trough. For this analysis, peaks and troughs identified at p-values between 0.01 and 0.1 were labeled as ambiguous due to high false positive and false negative rates. More than 90 percent of the genes containing both a PARP-1 peak and an H1 trough at the promoter were expressed, whereas less than 45 percent of the genes lacking both a PARP-1 peak and an H1 trough at the promoter were expressed (Fig. 2.6C). This correlation was also observed when looking broadly across ENCODE regions enriched in expressed or unexpressed genes (Fig. 2.2; see asterisks). Together, these results indicate that the pattern of PARP-1 and H1 promoter localization is indicative of gene expression outcomes.

Figure 2.4. Reciprocal binding patterns for H1 and PARP-1 at promoter, upstream, and far distal sites. **(A)** Averaging analysis of the $\log_2$ enrichment ratios from H1, PARP-1, and H3 ChIP-chip for all 1517 genes on the array. **(B)** Averaging analysis of the $\log_2$ enrichment ratios from H1, PARP-1, and H3 ChIP-chip centered around significant PARP-1 peaks (left) or significant H1 troughs (right). The data are grouped based on the location of the defining peak relative to the TSS of the nearest gene ($\leq$ 2 kb or > 2 kb away). These data show that the reciprocal relationship for the binding of PARP-1 and H1 is observed: (1) whether the PARP-1 peak or H1 trough is located promoter-proximally (i.e., $\leq$ 2 kb from the TSS) or promoter-distally (i.e., > 2 kb from the TSS) and (2) in intergenic regions where H3 is not depleted.

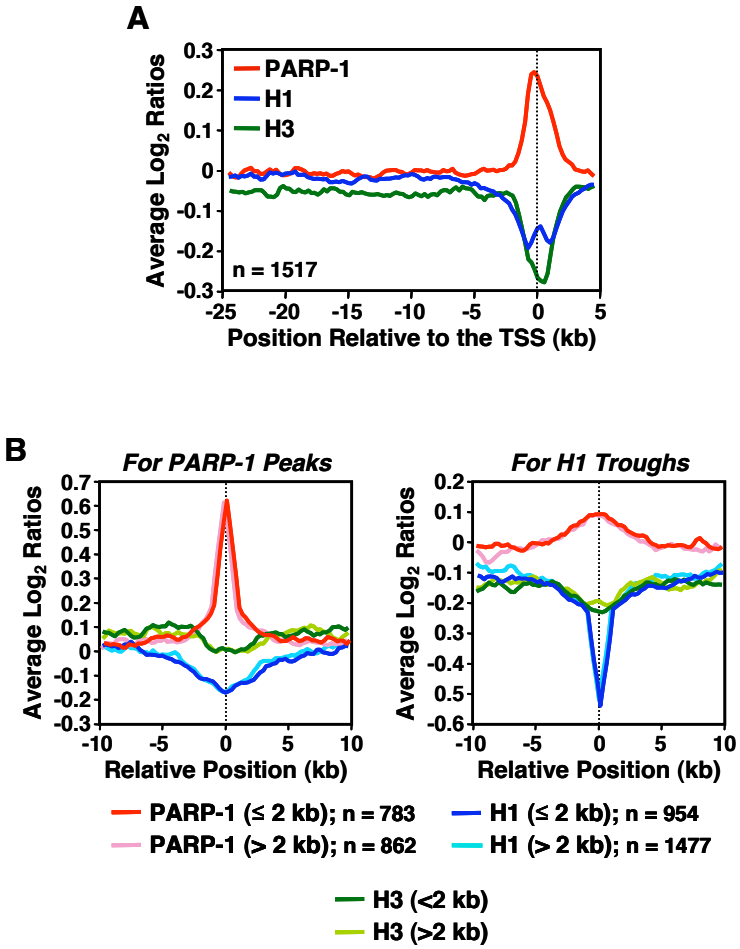
A
PARP-1
H1
H3
n = 1517
Average Log2 Ratios
Position Relative to the TSS (kb)
B
For PARP-1 Peaks
For H1 Troughs
Average Log2 Ratios
Relative Position (kb)
PARP-1 (≤ 2 kb); n = 783
PARP-1 (> 2 kb); n = 862
H1 (≤ 2 kb); n = 954
H1 (> 2 kb); n = 1477
H3 (<2 kb)
H3 (>2 kb)

Figure 2.5. Micrococcal nuclease mapping of positioned nucleosomes at PARP-1-occupied promoters. **(A)** Averaging analysis and alignment of PARP-1 and H3 ChIP-chip data with available MNase protection information (Ozsolak, et al., 2007) for 121 unambiguously bound genes. The yellow boxes highlight regions of significant protection and indicate the average location of positioned nucleosomes. These high-resolution mapping data demonstrate regions of significant MNase protection under the PARP-1 peak, indicating the presence of positioned nucleosomes. **(B)** A similar analyses to (A), but showing individual genes. The yellow ovals indicate the location of positioned nucleosomes. Together, these data indicate that in spite of the reduced occupancy of H3, PARP-1 bound promoters contain well-positioned nucleosomes that likely function as targets for PARP-1 binding.

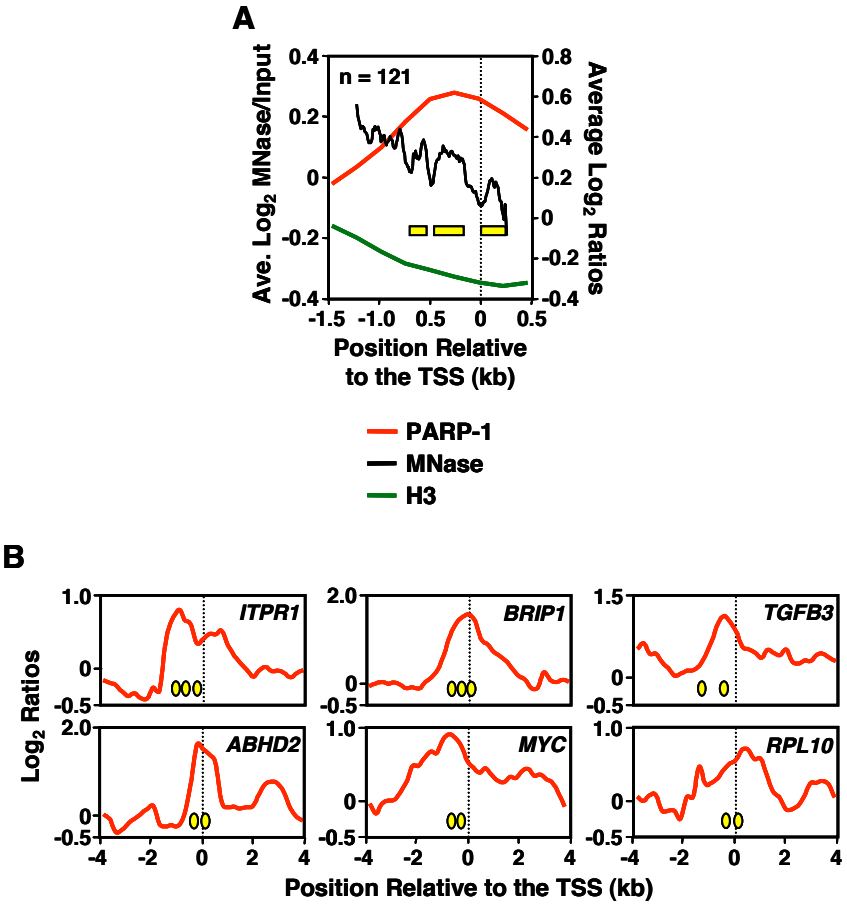
A
n = 121
Ave. Log2 MNase/Input
Average Log2 Ratios
Position Relative
to the TSS (kb)
PARP-1
MNase
H3
B
Log2 Ratios
ITPR1
BRIP1
TGFB3
ABHD2
MYC
RPL10
Position Relative to the TSS (kb)

Finally, to explore further the functional relationships between PARP-1, H1, and gene expression, we identified subsets of PARP-1-bound genes either down-regulated or up-regulated in MCF-7 cells by stable short hairpin RNA (shRNA)-mediated knockdown of PARP-1 (Fig. 2.7A). The target genes used for this analysis were identified in a microarray expression screen and were then confirmed by RT-qPCR as having either a two-fold reduction or two-fold increase in expression upon shRNA-mediated knockdown of PARP-1. For each gene, we assayed: (1) promoter binding by PARP-1 and H1 using ChIP-qPCR and (2) expression by RT-qPCR, with or without PARP-1 knockdown. The subset of genes positively regulated by PARP-1 (i.e., genes whose expression decreased upon PARP-1 knockdown) showed a 3- to 5-fold increase in H1 binding at the promoter in response to PARP-1 knockdown without changes in H3 occupancy (Figs. 2.7B, 2.8, and 2.9). These results provide a functional link between the chromatin binding and gene regulatory actions of PARP-1 and H1 at this subset of target promoters. Specifically, they suggest that PARP-1 acts to exclude H1 from these promoters and that upon PARP-1 knockdown, H1 is able to re-bind and inhibit transcription. In contrast, the subset of genes negatively regulated or not regulated by PARP-1 (i.e., genes whose expression decreased or was unchanged upon PARP-1 knockdown) showed little or no change in H1 binding at the promoter in response to PARP-1 knockdown (Figs. 2.7C and 2.10). These genes, some of which show a reciprocal pattern of PARP-1 and H1 localization at their promoters (Figs. 2.7C and 2.10), may be subject to other PARP-1-related transcriptional regulatory mechanisms (Kim, et al., 2005, Kraus and Lis, 2003) or indirect regulatory effects.

2.4 Discussion

Collectively, our data reveal the genomic localization patterns of H1 and PARP-1, highlighting the reciprocal relationship for their binding at promoters and other

Figure 2.6. A high PARP-1:H1 ratio specifies actively transcribed promoters. (A) Correlation analyses of PARP-1, H1, and H3 occupancy as determined by ChIP-chip (at the -250 bp-centered window) with gene expression as determined by microarrays (Expr.). **(B)** Averaging analysis of the $\log_2$ enrichment ratios from H1 and PARP-1 ChIP-chip for unambiguously expressed *(top)* or unambiguously unexpressed genes *(bottom)*. **(C)** *Top*, Averaging analysis of the $\log_2$ enrichment ratios from H1 and PARP-1 ChIP-chip for genes: (1) having both a PARP-1 peak and an H1 trough within 1.5 kb of the TSS *(left)*, or (2) unambiguously lacking both a PARP-1 peak and an H1 trough within 1.5 kb of the TSS *(right)*. *Bottom*, Percentage of expressed and unexpressed genes in each category. P-values are from a Chi-squared test and indicate significant differences relative to the total genes gene set (n = 878; percent expressed = 71.1).

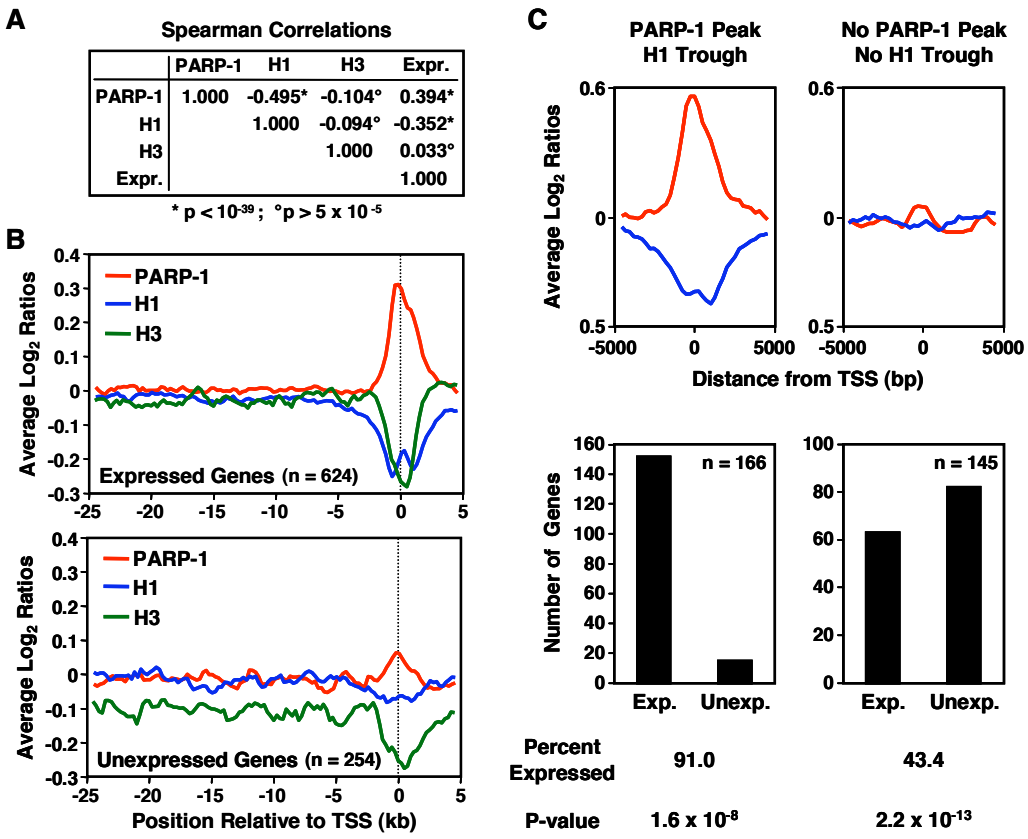
A
Spearman Correlations
PARP-1 H1 H3 Expr.
PARP-1 1.000 -0.495* -0.104° 0.394*
H1 1.000 -0.094° -0.352*
H3 1.000 0.033°
Expr. 1.000
* p < 10-39 ; °p > 5 x 10-5
B
Average Log2 Ratios
PARP-1
H1
H3
Expressed Genes (n = 624)
Unexpressed Genes (n = 254)
Position Relative to TSS (kb)
C
PARP-1 Peak
H1 Trough
No PARP-1 Peak
No H1 Trough
Distance from TSS (bp)
Number of Genes
n = 166
n = 145
Exp.
Unexp.
Percent Expressed
91.0
43.4
P-value
1.6 x 10-8
2.2 x 10-13

genomic locations. In addition, our results provide a functional link between chromatin binding by PARP-1 and H1 at a subset of target promoters and the corresponding gene expression outcomes. Finally, our results suggest that PARP-1 acts to exclude H1 from a subset of PARP-1-regulated promoters in vivo.

In a previous study (Kim, et al., 2004), we concluded that PARP-1 may act to repress Pol II transcription based on the observation that (1) PARP-1 represses in vitro transcription by Pol II with chromatin templates in the absence of NAD^+ and (2) PARP-1 does not colocalize with active Pol II (Ser5-P) on Drosophila polytene chromosomes. Although these results may seem at odds with our current data, a careful comparison of the two studies reveals that this is not the case, as described below.

(1) NAD^+ concentrations (in vivo versus in vitro)

The biochemical assays presented in our previous study (Kim, et al., 2004) examined the effects of PARP-1 on transcription at sub-physiological and supra-physiological extremes of NAD^+ (i.e., the absence of NAD^+ and saturating levels of NAD^+). Based on these results, we concluded that PARP-1 could (i) compact chromatin and repress transcription in the absence of NAD^+ and (ii) become auto(ADP-ribosyl)ated and release from chromatin in the presence of saturating concentrations of NAD^+ (i.e., >200 μM). In our current studies, we have examined PARP-1 localization and effects on transcription at physiological (in vivo) concentrations of nuclear NAD^+ (estimated in the literature to be ~70 μM; (Zhang, et al., 2002)). Under these conditions, PARP-1 clearly occupies the promoters of active genes, perhaps to exclude H1 and allow the binding of RNA Pol II.

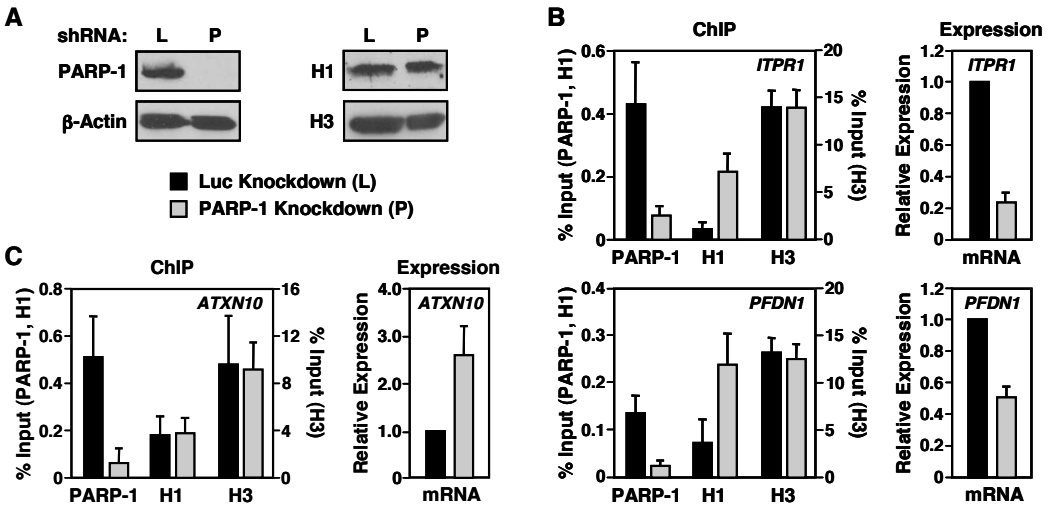

Figure 2.7. PARP-1 excludes H1 from PARP-1-regulated promoters. **(A)** Western blot showing the shRNA-mediated depletion of PARP-1 in MCF-7 cells versus control luciferase knockdown cells (Luc). **(B and C)** Gene-specific analysis of PARP-1, H1, and H3 promoter binding by ChIP-qPCR and mRNA expression by RT-qPCR in MCF-7 cells with or without PARP-1 knockdown. Expression data are standardized to β-actin transcripts. Each bar = mean + SEM, $n \geq 3$.

Figure 2.8. Additional gene-specific analyses showing that PARP-1 excludes H1 from genes down-regulated by PARP-1 knockdown. Gene-specific analysis of PARP-1 and H1 promoter binding by ChIP-qPCR and mRNA expression by RT-qPCR in MCF-7 cells with or without PARP-1 knockdown. Each bar = mean + SEM, $n \geq 3$.

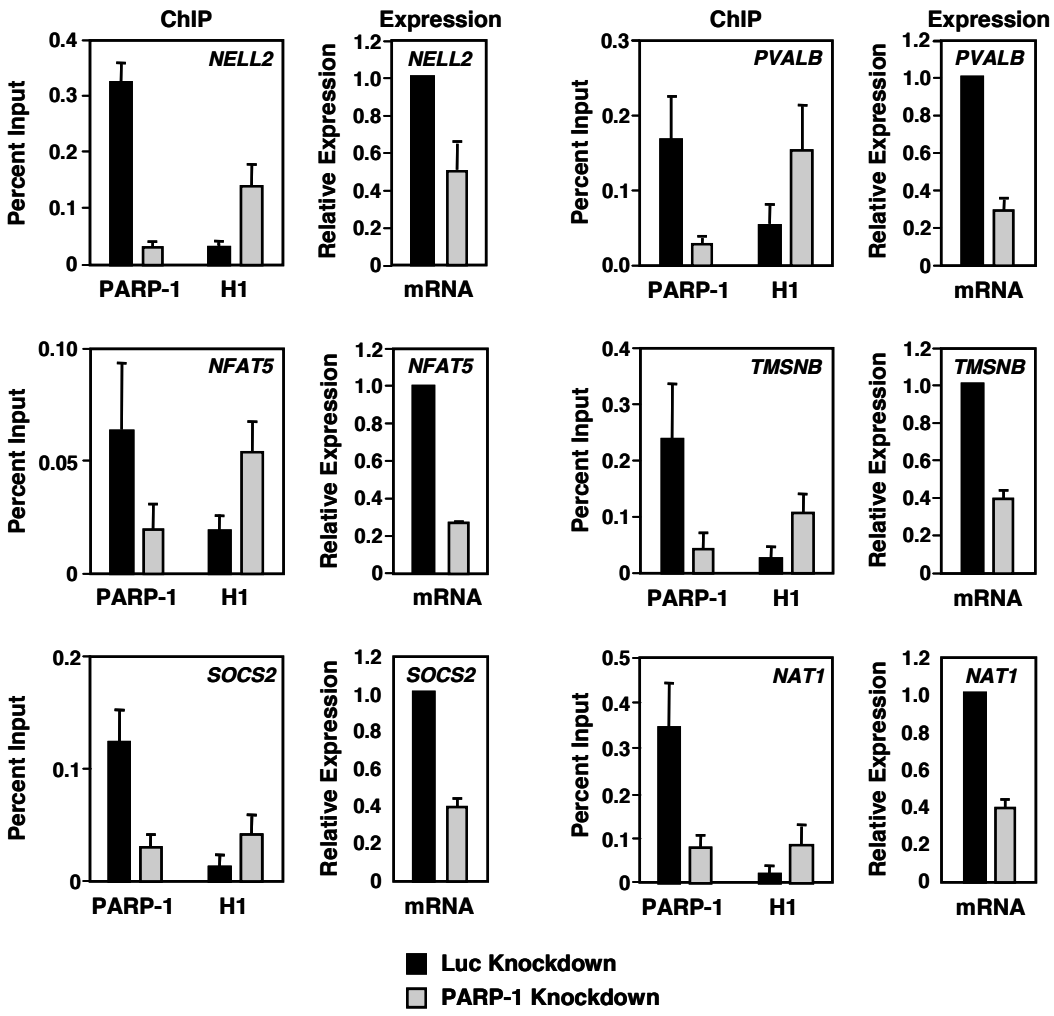
Genes Down-regulated by PARP-1 Knockdown
ChIP
Expression
ChIP
Expression
NELL2
NELL2
PVALB
PVALB
NFAT5
NFAT5
TMSNB
TMSNB
SOCS2
SOCS2
NAT1
NAT1
Percent Input
Relative Expression
PARP-1
H1
mRNA
Luc Knockdown
PARP-1 Knockdown

(2) Outcomes of nucleosome binding by PARP-1 (in vivo versus in vitro)

When comparing our current and previous results, one should consider how nucleosome binding by PARP-1 is "interpreted" in vivo. With chromatin templates in vitro, most factors that bind to nucleosomes and compact chromatin will repress transcription relative to a naked DNA template. From this view, chromatin compaction is a negative regulator of transcription. In vivo, the binding of PARP-1 to chromatin may promote the localized compaction of chromatin, but these structures may be less repressive than chromatin bound and compacted by H1. Thus, by excluding H1, PARP-1 may have a positive effect on Pol II binding and transcription.

(3) PARP-1 genomic localization on Drosophila polytene chromosomes

In our previous study, we showed that the immunofluorescent staining patterns of PARP-1 and Pol II Ser5-P on Drosophila polytene chromosomes were largely, but not completely, distinct (Kim, et al., 2004). From this initial analysis, we concluded that "PARP-1 occupies chromosomal domains that are distinct from transcriptionally active loci". These results, however may have had a higher resolution and revealed more information than we initially appreciated. A more careful analysis of these results, especially in the context of our current ChIP-chip results, suggests that we were detecting distinct localization patterns for PARP-1 and active RNA Pol II along the length of the gene (i.e., PARP-1 just upstream of the TSS and Pol II Ser5-P at the TSS and in the body of the gene). Previous studies have shown that this type of analysis can resolve transcription factors bound to DNA elements immediately upstream of the TSS and elongating Pol II in the body of the gene *(Boehm, et al., 2003, Simon, et al., 1985)*. Thus, PARP-1 and Pol II Ser5-P may not colocalize on *Drosophila* polytene chromosomes, but they can both localize to different regions of the same transcriptionally active gene.

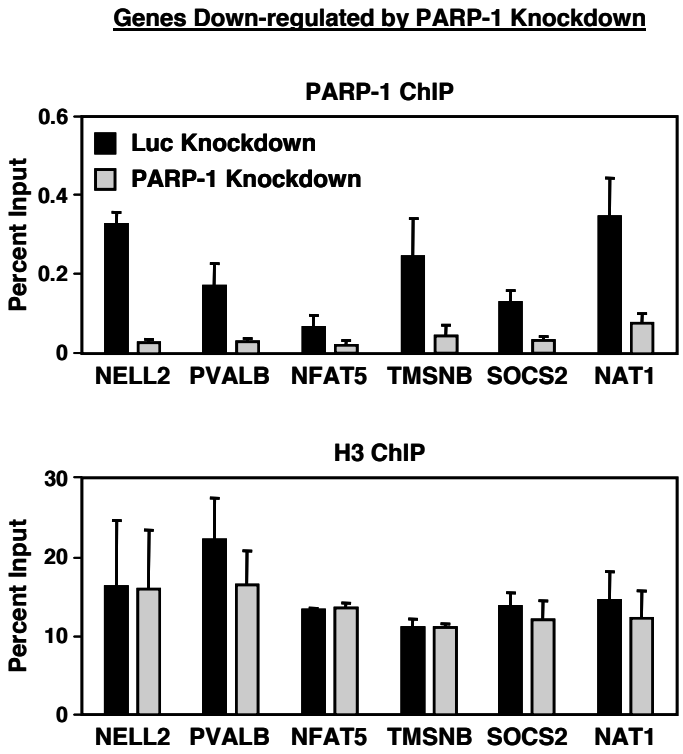

Figure 2.9. Gene-specific analyses showing that H3 levels at promoters to not change upon PARP-1 knockdown. Gene-specific analysis of PARP-1 and H3 promoter binding by ChIP-qPCR in MCF-7 cells with or without PARP-1 knockdown. Each bar = mean + SEM, $n \geq 3$.

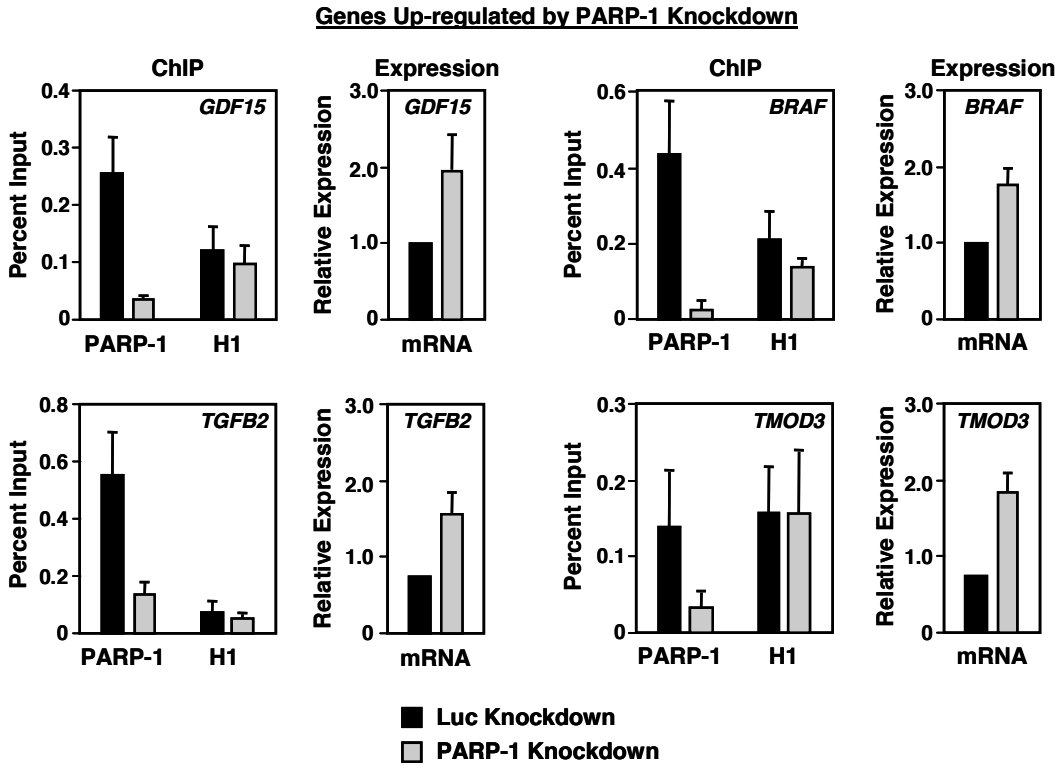

Figure 2.10. Additional gene-specific analyses showing that PARP-1 does not exclude H1 from genes up-regulated by PARP-1 knockdown. Gene-specific analysis of PARP-1 and H1 promoter binding by ChIP-qPCR and mRNA expression by RT-qPCR in MCF-7 cells with or without PARP-1 knockdown. Each bar = mean + SEM, $n \geq 3$.

Our data fit well with and extend the results of previous biochemical and cell-based assays showing a role for PARP-1 in the transcription-related regulation of chromatin structure (Kim, et al., 2004, Tulin and Spradling, 2003, Wacker, et al., 2007) and functional interplay between H1 and PARP-1 (Huletsky, et al., 1989, Ju, et al., 2006, Kim, et al., 2004). Further, our results show that although H1 and PARP-1 have similar nucleosome-binding properties and effects on chromatin structure in vitro (Kim, et al., 2004, Wacker, et al., 2007), they have distinct roles in regulating gene expression outcomes in vivo. Future studies will examine the determinants that direct the specific pattern of H1 and PARP-1 binding at promoters, including the role of PARP-1's NAD^+-dependent enzymatic activity.

2.5 Materials and Methods

Cells lines. MCF-7 human breast cancer cells were kindly provided by Dr. Benita Katzenellenbogen (University of Illinois, Urbana-Champaign). The cells were maintained in MEM supplemented with 5% calf serum and plated for experiments in MEM supplemented with 5% charcoal-dextran treated calf serum. PARP-1-depleted MCF-7 cells were generated by retroviral-mediated gene transfer of two short hairpin RNA sequences specifically targeting the PARP-1 mRNA using the pSUPER.retro system (Oligoengine). Control cells harboring short hairpin RNA sequences directed against luciferase were generated in parallel.

Antibodies. A custom rabbit polyclonal anti-PARP-1 antibody was generated by using an antigen comprising the amino-terminal half of PARP-1 (Kim, et al., 2004). A mouse monoclonal anti-H1 antibody was obtained from Upstate Biotech (05-475). A rabbit polyclonal anti-H3 antibody was obtained from Abcam (ab1791-100). The antibodies were screened for: (1) specificity by Western blotting MCF-7 cell extracts and (2) the

ability to immunoprecipitate their cognate antigens from formaldehyde crosslinked chromatin samples by a ChIP-Western protocol (Kim, et al., 2004). The mouse monoclonal anti-β-actin antibody used for Western blotting was obtained from Sigma-Aldrich (A5316).

Primers.

mRNA expression primers

β-ACTIN forward 5'-AGCTACGAGCTGCCTGAC-3'

β-ACTIN reverse 5'-AAGGTAGTTTCGTGGATGC-3'

GDF15 forward 5'-CTACAATCCCATGGTGCTCA-3'

GDF15 reverse 5'-TATGCAGTGGCAGTCTTTGG-3'

ITPR1 forward 5'- TGCCTCCACAATTCTACG-3'

ITPR1 reverse 5'- TGAATGTCCCACAGTTGC-3'

NAT1 forward 5'-CTTCACCCTCACCCATAGGA-3'

NAT1 reverse 5'-TTTGGGCACAAGCTTTCTCT-3'

NELL2 forward 5'-TGAAGGGAACCACCTACC-3'

NELL2 reverse 5'-ATTTGCCATCCACATACG-3'

NFAT5 forward 5'-ACCTCTTCCAGCCCTACCAT-3'

NFAT5 reverse 5'-CCTCTTCGGTGTTGATGGAT-3'

SOCS2 forward 5'-ACACGTCAGCACCATCTCTG-3'

SOCS2 reverse 5'-TGGCACCGGTACATTTGTTA-3'

TMOD3 forward 5'-GGAAGTAGTAATGGTGTTGACC-3'

TMOD3 reverse 5'-GCTCATCAAATACCGGAAG-3'

PVALB forward 5'-CTGAACGCTGAGGACATC-3'

PVALB reverse 5'-TTCACATCATCCGCACTC-3'

ABHD2 forward: 5' - CACCTCTCTGAGCCTGTTCC- 3'

ABHD2 reverse: 5’ - CGCAGATGTTCAGCAATGTT- 3’

PARP-1 forward: 5’ - GTGTGGGAAGACCAAAGGAA - 3’

PARP-1 reverse: 5’ - TTCAAGAGCTCCCATGTTCA - 3’

TMSL8 forward: 5’ - AACCTGCTATGATGGGTGCT - 3’

TMSL8 reverse: 5’ - CTGCAAAAGCATGCAACTTC - 3’

PFDN1 forward 5’-TGCCTTCTCCCATACATTCC-3’

PFDN1 reverse 5’-CAGGATTATGGCGTCCATCT-3’

ATXN10 forward - 5’-AAGCACCTTTGTGGATCAG-3’

ATXN10 reverse - 5’-ACAGTCATTTCGCACAGG-3’

ChIP primers

ABHD2 promoter forward: 5’ - GCCTCCACTCTGAGGAACAG - 3’

ABHD2 promoter reverse: 5’ - TTGTTCATTGGGCAGTTCAG - 3’

GDF15 promoter forward: 5’ - CTCAGATGCTCCTGGTGTTG - 3’

GDF15 promoter reverse: 5’ - CTCGGAATCTGGAGTCTTCG - 3’

ITPR1 promoter forward: 5’ - GAGCCCTAAGCAGCGTGTAG - 3’

ITPR1 promoter reverse: 5’ - CTCTCCAAGAGCTCCGAATG - 3’

NELL2 promoter forward: 5’ - TCCCCGGAGGAGCAGTCT - 3’

NELL2 promoter reverse: 5’ - CGCCCGAACCTGTTGTAAAG - 3’

SCN1A promoter forward: 5’ - ACCCTCCTCTCTCTCCTTGC - 3’

SCN1A promoter reverse: 5’ - GGGAGGAGGAGAAATTCGTT - 3’

TMSL8 promoter forward: 5’ - CGCGGGAACGCTAACCT - 3’

TMSL8 promoter reverse: 5’ - GTCCTCACCTGAAAGCTTGAAGA - 3’

NVL promoter forward: 5’ - TGCAACCAAACGGATCAATA - 3’

NVL promoter reverse: 5’ - TGAATTAAGTATTAGATTTCCCACTCA - 3’

PTBP2 promoter forward: 5’ - CAATGGCAGAAACAAGAGCA - 3’

PTBP2 promoter reverse: 5’ - CACTCAGCATTCCGTCTTGA - 3’

STC1 promoter forward: 5’ - AAGCCTGCATTGACACCTCT - 3’

STC1 promoter reverse: 5’ - TGCTGACAGTTGGAGGACAG - 3’

PEG10 promoter forward: 5’ - AAGGATTAAACGTGCGGTTG - 3’

PEG10 promoter reverse: 5’ - GGTGGCGATTACGAGGTTTA - 3’

ATXN10 promoter forward: 5’ - GACGCGCCCCTCTTTCTC - 3’

ATXN10 promoter reverse: 5’ - TGTGTTGATGTGGCCGTAACA - 3’

PFDN1 promoter forward: 5’ - CTGGAAGATACGGAGGAGCA - 3’

PFDN1 promoter reverse: 5’ - CTGCGCATGAGTTGGACTAA - 3’

PVALB promoter forward: 5’ - GCTCCCCTATCTGCACACTC - 3’

PVALB promoter reverse: 5’ - CAAAGGCTGTTTGGAAGCTC - 3’

NFAT5 promoter forward: 5’ - ACTTTTGGCTCCACGAACAG - 3’

NFAT5 promoter reverse: 5’ - GCAAAGATGGAGGAAGAACG - 3’

SOCS2 promoter forward: 5’ - TTCAAGCTTTCGAGCAGTGA - 3’

SOCS2 promoter reverse: 5’ - CCCTTAACAATCACGGGAAA - 3’

NAT1 promoter forward: 5’ - CCGGCTGAAATAACCTGGTA - 3’

NAT1 promoter reverse: 5’ - TATGTGCCAGCCACACTTTC - 3’

BRAF promoter forward: 5’ - AGCGCCTTCCTACGTAAACA - 3’

BRAF promoter reverse: 5’ - TCAGCCAATCGTGACCTTC - 3’

TGFB2 promoter forward: 5’ - ACTTTTGGAACTACTGGCCTTTTC - 3’

TGFB2 promoter reverse: 5’ - CAATCTAGTCAATGCCCAACAGAA - 3’

TMOD3 promoter forward: 5’ - GGCACACCCTTTTTGTGATT - 3’

TMOD3 promoter reverse: 5’ - CAGACAGATCAAACCGGTGA - 3’

ITPR1 upstream forward: 5’ - GTGCCACTCTTTTGCTTCAA - 3’

ITPR1 upstream reverse: 5’ - GAGGCACCAACGTTAAAAAGA - 3’

NVL upstream forward: 5’ - AATCAGAGGTCCAGGTCAGG - 3’

NVL upstream reverse: 5’ - AGACAGCAATCCCATGTGTG - 3’

PTBP2 upstream forward: 5’ - TGGCTAGACCACTACAATCTCAA - 3’

PTBP2 upstream reverse: 5’ - TGCTCAATTTTCCATAACATCAAA - 3’

STC1 upstream forward: 5’ - TTGTCAGCAGCAGAGAGAGC - 3’

STC1 upstream reverse: 5’ - CCTGATGAAGCAGCTTAGGG - 3’

PEG10 upstream forward: 5’ - TCTTGAACATGTTTACATGATAGCAC - 3’

PEG10 upstream reverse: 5’ - CACATAGCAGAAAATGATGTAGCC - 3’

ABHD2 upstream forward: 5’ - TGACTCCAAATCCCCTTGTC - 3’

ABHD2 upstream reverse: 5’ - CATTGGTAAGCAGGGGAGAG - 3’

Chromatin immunoprecipitation (ChIP). ChIP was performed essentially as described previously (Kininis, et al., 2007). Briefly, MCF-7 breast cancer cells were grown to ~80 to 90% confluence, cross-linked with 1% paraformaldehyde in PBS for 10 min. at 37°C, and quenched in 125 mM glycine in PBS for 5 min at 4°C. The cells were collected by centrifugation and sonicated in lysis buffer (1% SDS, 10 mM EDTA, 50 mM Tris•HCl, pH 7.9, 1x protease inhibitor cocktail) to generate chromatin fragments of ~500 bp in length. The material was clarified by centrifugation, diluted 10-fold in dilution buffer (0.5% Triton X-100, 2 mM EDTA, 150 mM NaCl, 20 mM Tris•HCl, pH 7.9, 1x protease inhibitor cocktail), and pre-cleared with protein A-agarose beads. The pre-cleared, chromatin-containing supernatant was used in immunoprecipitation reactions with antibodies against PARP-1 or H1, or without antibodies as a control. The immunoprecipitated genomic DNA was cleared of protein and residual RNA by digestion with proteinase K and RNase H, respectively. The DNA was then extracted with phenol:chloroform:isoamyl alcohol and precipitated with ethanol. For gene-specific ChIP analyses, quantitative real-time PCR (qPCR) was used

to determine the enrichment of immunoprecipitated material relative to the input material using gene-specific primer sets to the specified regions. Each ChIP experiment was conduced a minimum of three times with independent chromatin isolates to ensure reproducibility. For the ChIP-chip analyses, the immunoprecipitated genomic DNA was blunted, amplified by ligation-mediated PCR (LM-PCR), and used to probe a custom DNA microarray (Kininis, et al., 2007).

ChIP-chip. LM-PCR amplified genomic DNA samples were used to probe a custom human (HG18) oligonucleotide genomic array from Nimblegen. The custom array contained ~400,000 features (tiling interval of 76 bp for the ~50-mer probes) representing 57 Mb of genomic DNA, including all 44 of the ENCODE regions(2004), as well as an additional 1117 promoter regions. In total, the array contained 1517 annotated RNA polymerase II-transcribed promoters (approximately -25 kb to +5 kb relative to the transcription start site for most promoters). About one quarter of the promoters (i.e., 400) were from the ENCODE regions, while the remaining promoters (i.e., 1117) were selected based on their regulation in "knockdown-expression microarray experiments" by enzymes in the nuclear NAD^+ signaling pathway (e.g., NMNAT-1, NAMPT, SIRT1, PARG, and PARP-1) (Kim, et al., 2005). Detailed information about the genomic regions tiled on the custom array is included with the data submission to NCBI/Gene Expression Omnibus (GEO; see below) or can be obtained by contacting the corresponding author. The PARP-1 and H1 ChIP-chip analyses were run a minimum of two times to ensure reproducibility.

Genomic data analyses. Genomic data analysis was performed using the statistical programming language R (R Development Core Team) (Team, 2006). All data processing scripts are available upon request from the corresponding author and the raw

data sets can be accessed through NCBI/GEO (series record GSE9417). The $\log_2$ ratio data from each of the arrays was subjected to lowess normalization (Smyth and Speed, 2003). A single array error model was generated using a 1 kb moving window with 250 bp steps in which both the mean probe log2 ratio and p-values were calculated for each window. The p-values are from a nonparametric Wilcoxon signed-rank test.

• **Peak and trough finding.** Significant peaks were defined as the center of three consecutive windows with positive means, the center window with a mean greater than either adjacent window, and all windows having p-values less than 0.01. Significant troughs were defined as the center of three consecutive windows with negative means, the center window with a mean less than either adjacent window, and all windows having p-values less than 0.01. The use of these peak/trough selection criteria were justified by our high confirmation rate (CR) and low false positive rate (FPR) as determined by ChIP-qPCR (PARP-1 peak FPR = 0.11; H1 trough FPR = 0.08). The TSS anchored heatmaps used to visualize the ChIP-chip data (Fig. 2.1A) were generated with Java Treeview (Saldanha, 2004). For genes with multiple TSS the most 5' TSS was used.

• **Correlation analyses.** Spearman correlations between PARP-1, H1, H3, and gene expression (Fig. 2.2A) were determined using the ChIP-chip data for each factor from the sliding window centered at -250 bp relative to the TSS, as well as the data from three replicates of MCF-7 expression microarray experiments (Affymetrix, U133A) for the corresponding genes. For ChIP-chip to ChIP-chip correlations, 1512 total genes were used. For ChIP-chip to expression correlations, 1284 total genes were used. To determine the correlation between PARP-1 and H1 at PARP-1-regulated genes only, 108 total genes were used. These genes had a p value < 0.05, a fold change

greater or less then 0.5 or -0.5, respectively, and were flagged present or marginal in two out of the three replicates for both PARP-1 knockdown and control cell lines.

• **Averaging analyses.** The ChIP/input ratios for each window of ChIP-chip data over the 30 kb tiled region (or other specified region) was averaged for all 1517 promoters on the array (or specified subset of promoters). The maximum signal from the PARP-1 peak average analysis is centered at -250 bp relative to the TSS, whereas the minimum signal from the H1 trough average analysis is centered at -750 bp relative to the TSS. The minimum signal from the H3 trough average analysis is centered at +500 bp relative to the TSS.

• **Peak/trough to TSS distances.** The distance of each peak and trough to the closest TSS (e.g., Fig. 2.1B) was determined using RefSeq gene annotations from the UCSC genome browser. A chi squared test was used to determine the significance of the patterns observed in the peak and trough histograms, comparing the peak and trough data to the background pattern obtained by determining the distance of all windows to the closest transcription start site.

• **Expression-based categorization of genes.** For the expression-based categorization (Fig. 2.2B), three replicates of MCF-7 expression microarray data (Affymetrix, U133A) were used to categorize the genes represented on the ChIP-chip array as unambiguously expressed or unexpressed. For a gene on the ChIP-chip array to be marked as unambiguously expressed or unexpressed, all probe sets from all three replicates corresponding to the gene must have been flagged unanimously present or absent, respectively. Any genes on the array not meeting these criteria were marked as ambiguous and were removed from the expression based categorization analysis.

• **ChIP-chip-based categorization of genes.** For the ChIP-chip-based categorization (Fig. 2.6C), genes on the array were placed into one of 4 categories based on two criteria: (1) the presence ($p < 0.01$) or absence ($p > 0.1$) of a significant PARP peak centered within 1500 bp of the TSS and (2) the presence ($p \leq 0.01$) or absence ($p > 0.1$) of a significant H1 trough within 1500 bp of the TSS. Peaks and troughs identified at p-values between 0.01 and 0.1 were labeled as ambiguous due to increased false positive and false negative rates. Genes containing only ambiguous peaks or troughs were not included in the categorization. The significance of the distribution of expressed and unexpressed genes within each category compared to all genes with expression information on the ChIP-chip array was assessed using a chi squared test.

• **Nucleosome mapping by MNase protection.** MNase protection information from a previously published genomic analysis of nucleosome positioning at 3,692 promoters (-1500 to +500) in MCF-7 cells (Ozsolak, et al., 2007) was meta-analyzed and matched to the significant PARP-1 peaks from our ChIP-chip analysis (Fig. 2.5). The $\log_2$ MNase (digested/input) and PARP-1 (IP/input) signals for the overlapping gene set (121 genes) were averaged across the promoter regions. Regions of significant MNase protection were determined by applying a one-tailed t-test to comparisons between adjacent peaks and troughs through the region.

Gene-specific expression analyses. Luciferase knockdown and PARP-1 knockdown MCF-7 cells were seeded at ~1.5×10^5 cells per well in 6-well plates and grown for at least 3 days in the conditions noted above. The cells were collected at about 80 percent confluence, and total RNA was isolated using Trizol Reagent (Invitrogen) according to the manufacturer's protocols. The total RNA was reverse transcribed and subjected to

real-time quantitative PCR using gene-specific primers. All target gene transcripts were normalized to the β-actin transcript. Each experiment was conduced a minimum of three times with independent isolates of total RNA to ensure reproducibility.

REFERENCES

The ENCODE (ENCyclopedia Of DNA Elements) Project. Science 306:636-40.

Berger, S. L. 2002. Histone modifications in transcriptional regulation. Curr Opin Genet Dev 12:142-8.

Boehm, A. K., A. Saunders, J. Werner, and J. T. Lis. 2003. Transcription factor and polymerase recruitment, modification, and movement on dhsp70 in vivo in the minutes following heat shock. Mol Cell Biol 23:7628-37.

Buck, M. J., and J. D. Lieb. 2004. ChIP-chip: considerations for the design, analysis, and application of genome-wide chromatin immunoprecipitation experiments. Genomics 83:349-60.

Heintzman, N. D., R. K. Stuart, G. Hon, Y. Fu, C. W. Ching, R. D. Hawkins, L. O. Barrera, S. Van Calcar, C. Qu, K. A. Ching, W. Wang, Z. Weng, R. D. Green, G. E. Crawford, and B. Ren. 2007. Distinct and predictive chromatin signatures of transcriptional promoters and enhancers in the human genome. Nat Genet 39:311-8.

Huletsky, A., G. de Murcia, S. Muller, M. Hengartner, L. Menard, D. Lamarre, and G. G. Poirier. 1989. The effect of poly(ADP-ribosyl)ation on native and H1-depleted chromatin. A role of poly(ADP-ribosyl)ation on core nucleosome structure. J Biol Chem 264:8878-86.

Ju, B. G., V. V. Lunyak, V. Perissi, I. Garcia-Bassets, D. W. Rose, C. K. Glass, and M. G. Rosenfeld. 2006. A topoisomerase IIbeta-mediated dsDNA break required for regulated transcription. Science 312:1798-802.

Kamakaka, R. T., and S. Biggins. 2005. Histone variants: deviants? Genes Dev 19:295-310.

Kim, M. Y., S. Mauro, N. Gevry, J. T. Lis, and W. L. Kraus. 2004. NAD+-dependent modulation of chromatin structure and transcription by nucleosome binding properties of PARP-1. Cell 119:803-14.

Kim, M. Y., T. Zhang, and W. L. Kraus. 2005. Poly(ADP-ribosyl)ation by PARP-1: 'PAR-laying' NAD+ into a nuclear signal. Genes Dev 19:1951-67.

Kininis, M., B. S. Chen, A. G. Diehl, G. D. Isaacs, T. Zhang, A. C. Siepel, A. G. Clark, and W. L. Kraus. 2007. Genomic analyses of transcription factor binding, histone acetylation, and gene expression reveal mechanistically distinct classes of estrogen-regulated promoters. Mol Cell Biol 27:5090-104.

Kraus, W. L., and J. T. Lis. 2003. PARP goes transcription. Cell 113:677-83.

McBryant, S. J., V. H. Adams, and J. C. Hansen. 2006. Chromatin architectural proteins. Chromosome Res 14:39-51.

Mito, Y., J. G. Henikoff, and S. Henikoff. 2007. Histone replacement marks the boundaries of cis-regulatory domains. Science 315:1408-11.

Ozsolak, F., J. S. Song, X. S. Liu, and D. E. Fisher. 2007. High-throughput mapping of the chromatin structure of human promoters. Nat Biotechnol 25:244-8.

Saldanha, A. J. 2004. Java Treeview--extensible visualization of microarray data. Bioinformatics 20:3246-8.

Simon, J. A., C. A. Sutton, R. B. Lobell, R. L. Glaser, and J. T. Lis. 1985. Determinants of heat shock-induced chromosome puffing. Cell 40:805-17.

Smyth, G. K., and T. Speed. 2003. Normalization of cDNA microarray data. Methods 31:265-73.

Team, R. D. C. 2006. R: A language and environment for statistical computing, R Foundation for Statistical Computing, Vienna, Austria.

Tulin, A., and A. Spradling. 2003. Chromatin loosening by poly(ADP)-ribose polymerase (PARP) at Drosophila puff loci. Science 299:560-2.

Vignali, M., and J. L. Workman. 1998. Location and function of linker histones. Nat Struct Biol 5:1025-8.

Wacker, D. A., K. M. Frizzell, T. Zhang, and W. L. Kraus. 2007. Regulation of chromatin structure and chromatin-dependent transcription by poly(ADP-ribose) polymerase-1: possible targets for drug-based therapies. Subcell Biochem 41:45-69.

Woodcock, C. L., A. I. Skoultchi, and Y. Fan. 2006. Role of linker histone in chromatin structure and function: H1 stoichiometry and nucleosome repeat length. Chromosome Res 14:17-25.

Zhang, Q., D. W. Piston, and R. H. Goodman. 2002. Regulation of corepressor function by nuclear NADH. Science 295:1895-7.

CHAPTER 3

PARP-1 Regulates Chromatin Structure and Transcription Through a KDM5B-Dependent Pathway

3.1 Summary

Poly(ADP-ribose) polymerase-1 (PARP-1) is a ubiquitous and abundant nuclear enzyme that regulates chromatin structure to control gene expression, although the detailed molecular mechanisms of this regulation are unclear. In this study, I examined the functional interplay between PARP-1, histone 3 lysine 4 trimethylation (H3K4me3), and the linker histone H1 in the chromatin-dependent control of gene expression. I find that PARP-1 is required for a series of molecular outcomes at the promoters of target genes whose expression is dependent on PARP-1. Specifically, I show that PARP-1 establishes a permissive chromatin environment at the promoters of these genes by promoting (1) the trimethylation of H3K4 through the poly(ADP-ribosyl)ation and exclusion of KDM5B, an H3K4me3 demethylase, (2) the exclusion of H1, and (3) increased accessibility of the promoter DNA at the TSS. Upon depletion of PARP-1, these outcomes do not occur efficiently. The permissive chromatin environment is required for the loading of the Pol II transcription machinery (e.g., Pol II, TBP, TFIIB) and subsequent transcription. I also find that some cellular signaling pathways use the regulated depletion of PARP-1 from promoters to modulate these molecular outcomes, including gene expression. Collectively, my results assign new functions for PARP-1 in the regulation of chromatin structure and transcription. More broadly, my results help to clarify the molecular mechanisms by which specific chromatin-binding and histone-modifying proteins interact to alter chromatin structure and function to regulate gene transcription.

3.2 Introduction

Chromatin, a repeating array of nucleosomes and nucleosome-binding proteins, is the physiological template for nuclear processes involving genomic DNA. It plays key roles in the regulation of gene transcription by limiting the loading of the RNA polymerase II (Pol II) machinery at gene promoters, the initiation of transcription from transcription start sites (TSSs), and the elongation of transcripts through the bodies of genes (Li et al., 2007; Morse, 2003). Several properties of chromatin contribute to its gene-regulating effects, including its composition (e.g., types and extent of histones modifications, repertoire of nucleosome-bound proteins) and structure (e.g., rotational and translational positioning of nucleosomes, spacing of nucleosomes) (Li et al., 2007; Morse, 2003). Under many conditions, the former can modulate the latter. Although great strides have been made in understanding the molecular mechanisms that underlie chromatin-dependent transcriptional regulation, many fundamental questions remain. For example, the molecular mechanisms by which specific chromatin-binding and histone-modifying proteins interact to alter chromatin structure and function to regulate gene transcription require further analysis.

Nucleosome-binding architectural proteins, such as poly(ADP-ribose) polymerase-1 (PARP-1) and the linker histone H1, promote structural alterations in chromatin and, as a consequence, modulate transcriptional responses (Kraus, 2008; Kraus and Lis, 2003; McBryant et al., 2006; Woodcock et al., 2006). Both PARP-1 and H1 bind at or near the dyad axis of the nucleosome and contact the linker DNA as it exits the nucleosome (Happel and Doenecke, 2009; Kim et al., 2004; Vignali and Workman, 1998). They are also both able to alter nucleosome spacing and promote the compaction of nucleosomal arrays (Kim et al., 2004; Robinson and Rhodes, 2006; Wacker et al., 2007; Woodcock et al., 2006). In the case of PARP-1, this may occur

through a localized mechanism that brings together adjacent nucleosomes (Wacker et al., 2007). Although PARP-1 and H1 elicit grossly similar alterations in chromatin structure in vitro (Kim et al., 2004; Wacker et al., 2007), their effects on chromatin structure may be interpreted differently in vivo (Kraus, 2008). I have shown that PARP-1 and H1 compete for binding to nucleosomes (Kim et al., 2004) and exhibit a reciprocal pattern of binding at actively transcribed promoters: H1 is depleted and PARP-1 is enriched (Krishnakumar et al., 2008). Both PARP-1 and H1 are widely distributed across the genome (Braunschweig et al., 2009; Kim et al., 2004; Krishnakumar et al., 2008; Tulin and Spradling, 2003) and their depletion can promote large scale alterations in chromatin structure (Fan et al., 2005; Lu et al., 2009; Petesch and Lis, 2008; Tulin and Spradling, 2003; Tulin et al., 2002), but their effects on transcription are limited to a subset of specific target genes (Fan et al., 2005; Frizzell et al., 2009; Lu et al., 2009).

Unlike H1, PARP-1 possesses an intrinsic enzymatic activity that catalyzes the polymerization of ADP-ribose units from donor NAD^+ molecules on target proteins (Kim et al., 2005). Although PARP-1 is the major target for PARP-1-mediated poly(ADP-ribosyl)ation (PARylation) in vivo through an automodification reaction, a number of other targets have been also described, including core histones, H1, and a variety of nuclear proteins involved in gene regulation (Kim et al., 2005; Kraus, 2008; Kraus and Lis, 2003). PARylation of protein targets by PARP-1 alters their function, typically in an inhibitory manner (Ju et al., 2006; Ju et al., 2004; Kim et al., 2005; Kraus, 2008; Kraus and Lis, 2003). For example, extensive PARylation of PARP-1 can inhibit its ability to bind nucleosomes (Kim et al., 2004; Wacker et al., 2007), while more modest PARylation of components of the TLE1 corepressor complex can promote its dissociation from target gene promoters (Ju et al., 2004). Although PARP-1 enzymatic activity has been shown to play a key role in the regulation of

transcription in some contexts (Cohen-Armon et al., 2007; Ju et al., 2006; Ju et al., 2004; Kraus, 2008; Kraus and Lis, 2003), in others it is dispensable (Hassa and Hottiger, 2002; Pavri et al., 2005). A clear consensus about the targets and role(s) of PARP-1 enzymatic activity during transcription has yet to emerge.

In addition to nucleosome-binding proteins, covalent posttranslational modifications of the amino-terminal tails of histone proteins, such as acetylation, phosphorylation, and methylation, can affect chromatin structure and function. These modifications can alter the charge of the histone tails and promote structural changes in nucleosomes, as well as create or destroy binding sites for chromatin-regulating proteins (Berger, 2007; Campos and Reinberg, 2009). Different histone modifications 'mark' different functional regions of chromatin. For example, histone H3 lysine 4 trimethylation (H3K4me3) is enriched at TSSs and positively correlates with gene expression (Barski et al., 2007; Bernstein et al., 2005; Guenther et al., 2007; Santos-Rosa et al., 2002; Schneider et al., 2004). This modification creates a binding site for structural modules within a variety of proteins that regulate chromatin structure and transcription (Ruthenburg et al., 2007), including the PHD fingers of BPTF, TAF3, and ING family members (Li et al., 2006; Pena et al., 2006; Shi et al., 2006; Taverna et al., 2006; van Ingen et al., 2008; Vermeulen et al., 2007; Wysocka et al., 2006), the tandem chromodomains of CHD1 (Flanagan et al., 2005; Sims et al., 2005), and the double tudor domain of JMJD2A/KDM4A (Huang et al., 2006). The recruitment of these factors in response to H3K4 trimethylation alters chromatin structure and transcription. Enzymes that remove the H3K4me3 mark, such as the KDM5 family of lysine-specific demethylases (e.g., KDM5B, a.k.a. JARID1B and PLU1), can reverse the actions of the proteins that bind the mark (Allis et al., 2007; Ruthenburg et al., 2007; Yamane et al., 2007).

Although recent studies have linked PARP-1 to the regulation of DNA methylation and histone acetylation (Caiafa et al., 2009; Cohen-Armon et al., 2007), a clear understanding of how the chromatin-modulating effects of PARP-1 are coordinated with various covalent modifications to control transcriptional outcomes is lacking. In the present study, I have examined the mechanisms by which PARP-1 maintains an active chromatin environment at the promoters of target genes by exploring the sequence of events following depletion of PARP-1 that lead to transcriptional repression. At the promoters of positively regulated target genes, PARP-1 depletion leads to an increase in the binding of H1, a decrease in the levels of H3K4me3, a reduction in chromatin accessibility at the TSS, and a decrease in the binding of the Pol II machinery. The decreased levels of H3K4me3 are driven by the recruitment of the lysine-specific demethylase KDM5B. My data indicate that PARP-1 PARylates KDM5B, which in turn inhibits KDM5B binding at promoters and prevents demethylation of H3K4me3. Interestingly, signaling pathways use a strategy analogous to PARP-1 knockdown to repress gene expression, which involves dismissal of PARP-1 from the promoter, an increase in the binding of H1 and KDM5B, a decrease in the levels of H3K4me3, and a decrease in the binding of the Pol II machinery. Collectively, my results elucidate a new pathway for chromatin-dependent gene regulation by PARP-1 involving histone methylation. These results demonstrate a mechanism by which the chromatin-modulating effects of PARP-1 are coordinated with a histone modification to regulate transcription.

Table 3.1. Genes whose regulation was examined in this study.

Gene Symbol	Gene Name	GeneCards® Accession No.[a]	Protein Function[b]	Regulation by PARP-1
ABHD2	Alpha/beta hydrolase domain containing protein 2	GC15P087432	Contains an alpha/beta hydrolase fold, which is found in a very wide range of enzymes. Function unknown.	Not regulated
GDF15	Growth and differentiation factor 15	GC19P018358	Member of the transforming growth factor β superfamily. Regulates tissue differentiation and maintenance.	Negatively regulated
TMSL8	Thymosin-like protein 8	GC0XM101657	By homology, is thought to play a role in the organization of the cytoskeleton by binding to and sequestering actin monomers, thereby inhibiting actin polymerization	Positively regulated
SCN1A	Sodium channel protein type I subunit alpha	GC02M166553	Ion channel that mediates the voltage-dependent sodium ion permeability of excitable membranes	Positively regulated
NELL2	Neural epidermal growth factor-like 2	GC12M043188	A glycoprotein containing several epidermal growth factor (EGF)-like domains. Acts to control cell growth and differentiation, as well oncogenesis.	Positively regulated
ITPR1	Inositol 1,4,5-triphosphate receptor, type 1	GC03P004486	Intracellular channel that mediates calcium release from the endoplasmic reticulum following stimulation by inositol 1,4,5-trisphosphate	Positively regulated

[a] From GeneCards®, a searchable, integrated database of human genes that provides concise genomic, proteomic, transcriptomic, genetic and functional information on all known and predicted human genes. http://www.genecards.org/index.shtml

[b] Based on the GeneCards® description.

Figure 3.1. PARP-1 promotes the binding of RNA Pol II and components of the basal transcription machinery to the promoters of positively regulated target genes.

(A) Western blot showing shRNA-mediated knockdown of PARP-1 with β-actin as an internal standard.

(B) Analysis of mRNA expression for six genes by RT-qPCR in MCF-7 cells with PARP-1 knockdown. The data are normalized to the β-actin transcript and expressed relative to control (Luc) knockdown cells. Each bar represents the mean plus the SEM, $n \geq 3$. The differences observed for all genes except *ABHD2* are significant (Student's t-test, $p \leq 0.05$).

(C - H) ChIP-qPCR analyses of factor or histone levels at the promoters of the PARP-1 target genes from panel A in control (Luc) and PARP-1 knockdown (KD) cells. Each bar represents the mean plus the SEM, $n \geq 3$. The differences observed for the positively regulated genes (i.e., *TMSL8*, *SCN1A*, *NELL2*, *ITPR1*) are significant for panels C - G. The differences observed for the negatively regulated gene (i.e., *GDF15*) are significant for panels C, F, and G (Student's t-test, $p \leq 0.05$).

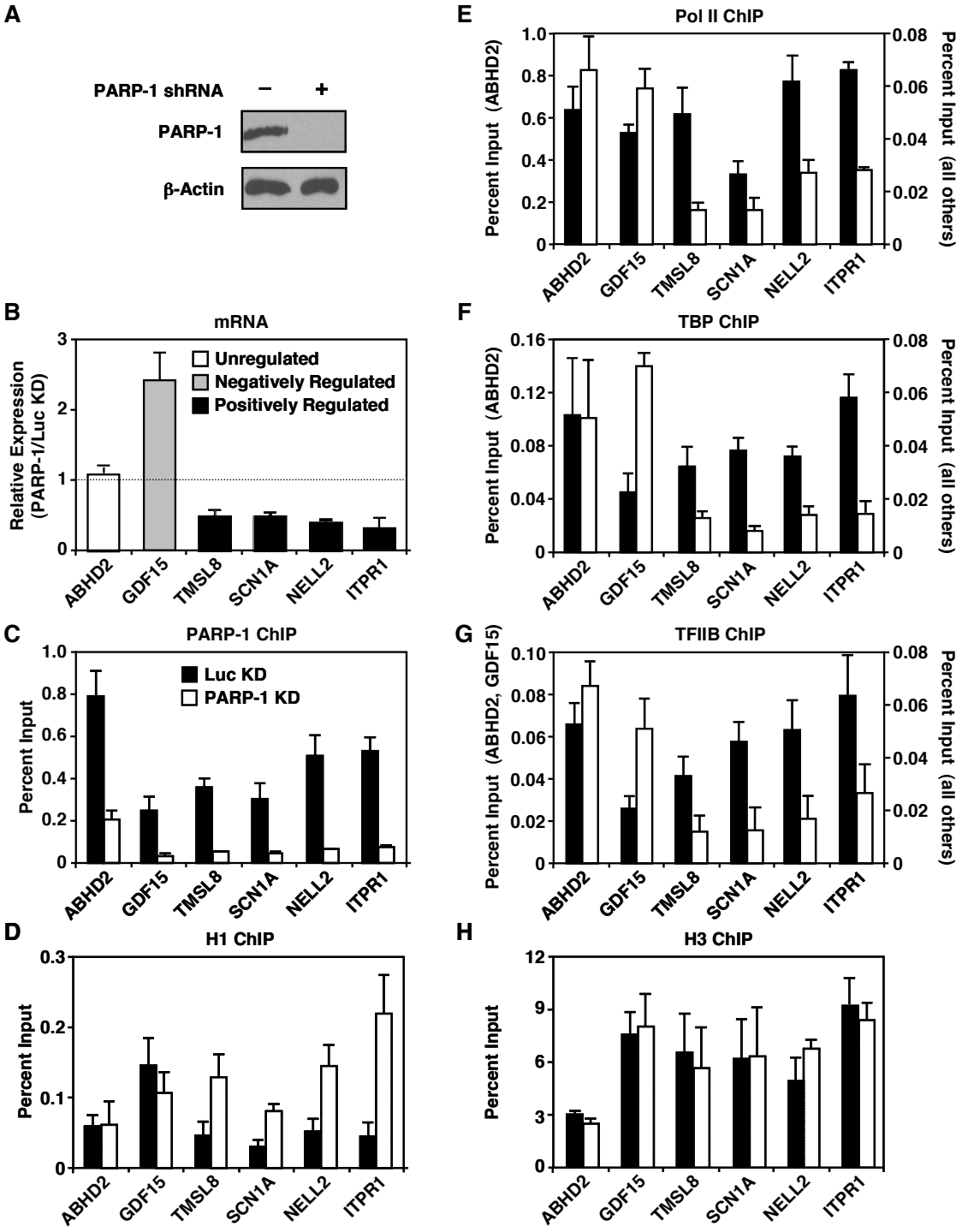
A
PARP-1 shRNA
–
+
PARP-1
β-Actin
B
mRNA
Relative Expression (PARP-1/Luc KD)
Unregulated
Negatively Regulated
Positively Regulated
ABHD2
GDF15
TMSL8
SCN1A
NELL2
ITPR1
C
PARP-1 ChIP
Percent Input
Luc KD
PARP-1 KD
D
H1 ChIP
E
Pol II ChIP
Percent Input (ABHD2)
Percent Input (all others)
F
TBP ChIP
G
TFIIB ChIP
Percent Input (ABHD2, GDF15)
H
H3 ChIP

3.3 Results

PARP-1 promotes the binding of RNA Pol II and components of the basal transcription machinery to the promoters of positively regulated target genes

To better understand how PARP-1 modulates chromatin structure as a means of regulating gene expression, I conducted a series of molecular assays using MCF-7 human breast cancer cells. Given the growing interest in the role of PARP-1 in breast cancer biology (Drew and Plummer, 2009; Frizzell and Kraus, 2009), as well as the considerable gene-specific and genomic data available regarding PARP-1 localization and function in MCF-7 cells (Kim et al., 2005; Kraus, 2008), this is an excellent model system to use. I used shRNA-mediated knockdown to explore PARP-1 function in these cells. As described previously (Frizzell et al., 2009; Krishnakumar et al., 2008), I see a robust knockdown of PARP-1 in this system compared to a control knockdown (luciferase; Luc) (Fig. 3.1A). I focused my studies on a set of previously characterized genes (i.e., *TMSL8*, *SCN1A*, *NELL2*, *ITPR1*; (Frizzell et al., 2009; Krishnakumar et al., 2008) whose efficient expression requires PARP-1 (Fig. 3.1B; "positively regulated" genes - i.e., expression decreases by > 50 percent upon PARP-1 knockdown). Genes in this set function in signaling, oncogenesis, and cell mobility (Supplemental Table S1). For comparison, I also examined genes whose expression is inhibited by PARP-1 (e.g., *GDF15*; "negatively regulated" - i.e., expression increases > 2-fold upon PARP-1 knockdown) or is unaffected by PARP-1 (i.e., ABHD2; "unregulated") (Fig. 3.1B; Table 3.1). Note that terms "positively regulated", "negatively regulated", and "unregulated" are used here as a shorthand for the functional outcomes and do not imply specific mechanisms, although such mechanisms are revealed in the experiments described below.

In my initial studies, I examined the effects of PARP-1 depletion on the binding of the linker histone H1 and components of the Pol II transcription machinery at the promoters of these genes by using chromatin immunoprecipitation (ChIP) assays. As expected, knockdown of PARP-1 caused a dramatic reduction in PARP-1 ChIP signal for all genes tested (Fig. 3.1C). I have shown previously that H1 competes with PARP-1 for binding to promoter-proximal nucleosomes and represses gene transcription by Pol II (Kim et al., 2004; Krishnakumar et al., 2008). For the genes positively regulated by PARP-1, knockdown of PARP-1 caused an increase in H1 binding at the promoter (Fig. 3.1D) without a change in nucleosome density (as determined by histone H3 levels; Fig. 3.1H). This was accompanied by a significant reduction (>60%) in the promoter occupancy of TBP, TFIIB, and Pol II for all four genes in this group (Fig. 3.1, E – G). Opposite effects were observed for the negatively regulated gene *GDF15* (i.e., the increase in gene expression upon PARP-1 knockdown was accompanied by a significant increase in the binding of TBP, TFIIB, and Pol II; Fig 3.1, E - G). As expected, *ABHD2*, a gene whose expression is not affected by PARP-1, showed no changes in these parameters upon PARP-1 knockdown (Fig 3.1, E - G). Taken together, these results indicate that PARP-1 modulates the occupancy of H1, TBP, TFIIB, and Pol II at target promoters to control gene expression.

PARP-1 maintains an open chromatin architecture at the TSSs of positively regulated target genes

Previous studies have shown that PARP-1 can regulate chromatin structure, nucleosome compaction, and the accessibility of DNA in chromatin (Kim et al., 2004; Kraus, 2008; Kraus and Lis, 2003). Based on these results, as well as the data presented in Fig. 3.1, I hypothesized that PARP-1 might act to maintain an open

chromatin architecture at the promoters of positively regulated target genes. To test this hypothesis, I examined the accessibility of promoter DNA surrounding the transcription start sites (TSSs; ca. -300 to +300 bp) to digestion by micrococcal nuclease (MNase). Mononucleosome-sized genomic DNA fragments (~160 bp; Fig. 3.2A) were released by MNase digestion from chromatin isolated from control and PARP-1 knockdown MCF-7 cells. I then used quantitative real-time PCR (qPCR) to tile through the promoter region with overlapping amplicons (21 amplicons for ~600 bp, ~30 bp overlap; Fig. 3.2B) to determine the extent of MNase digestion. As expected, for all genes I observed regions of increased MNase protection on either side of the TSS, likely due to -1 and +1 nucleosomes (Ozsolak et al., 2007; Schones et al., 2008) (Fig. 3.2C). In addition, I observed a dip in protection at or near the TSS, as described previously (Krishnakumar et al., 2008; Ozsolak et al., 2007; Schones et al., 2008). Knockdown of PARP-1 caused a significant increase in the MNase protection (i.e., decreased accessibility or a closed chromatin architecture) at or near the TSS for the positively regulated genes relative to the control knockdown (Fig. 3.2C; *TMSL8*, *SCN1A*, *NELL2*, *ITPR1*). This effect was not observed for *GDF15* or *ABHD2* (Fig. 3.2C). Together, the results from Figs. 3.1 and 3.2 are consistent with a model in which PARP-1 acts to maintain an open chromatin structure at the promoters of positively regulated target genes to allow loading of the transcriptional machinery and subsequent transcription by Pol II.

PARP-1 binding correlates with histone H3 lysine 4 trimethylation at many promoters across the genome

How might PARP-1 regulate promoter chromatin architecture? I considered the possibility of a mechanism involving histone modifications, which have been shown

Figure 3.2. PARP-1 maintains an open chromatin architecture at the TSSs of positively regulated target genes.

MNase protection experiments in control (Luc) and PARP-1 knockdown (KD) MCF-7 cells. qPCR with overlapping amplicons (see Fig. 3.2B) was used to determine the enrichment of MNase digested DNA relative to sonicated genomic DNA ("relative protection") at specific genomic locations spanning from -300 to +300 bp relative to the TSS for each gene indicated. Each point represents the mean ± the SEM, $n \geq 3$. The shaded region indicates statistically significant differences between the Luc and PARP-1 knockdown conditions (Student's T-test, $p \leq 0.05$).

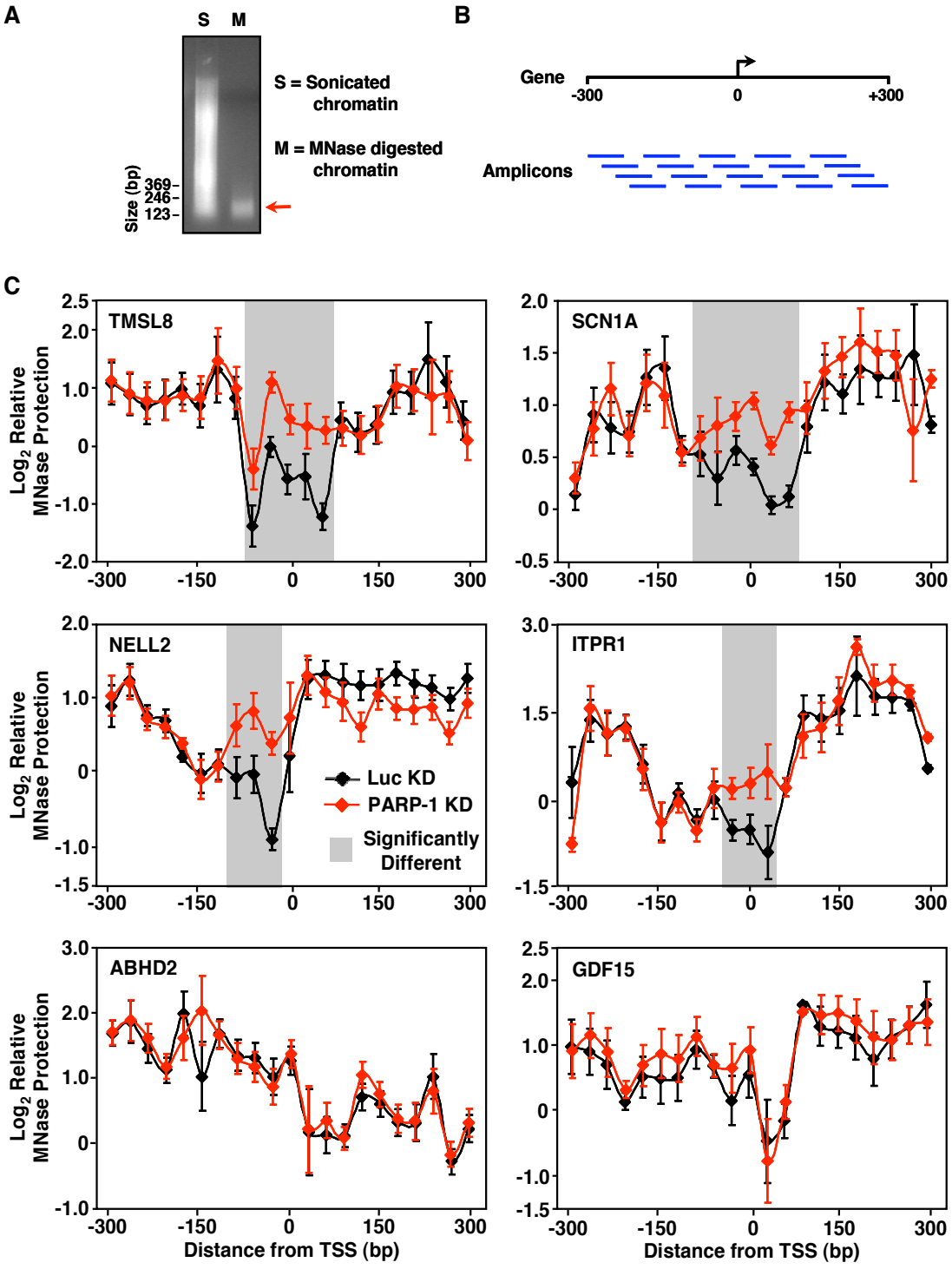
A
S
M
S = Sonicated chromatin
M = MNase digested chromatin
Size (bp)
369
246
123
B
Gene
-300
0
+300
Amplicons
C
TMSL8
SCN1A
NELL2
ITPR1
ABHD2
GDF15
Log2 Relative MNase Protection
Luc KD
PARP-1 KD
Significantly Different
Distance from TSS (bp)

Figure 3.3. PARP-1 binding correlates with histone H3 lysine 4 trimetylation at promoters across the genome.

ChIP-chip analysis of PARP-1, H3K4me3, and H3 at ~23,500 promoters (-3 kb to +3 kb).

(A) Heatmaps showing a visual representation of the ChIP-chip data.

(B) Average PARP-1, H3K4me3, and H3 ChIP-chip signals across promoters either containing or lacking a peak of PARP-1.

(C) Multiple correlation analysis for PARP-1, H3K4me3, and H3 ChIP-chip signals at the TSS. The Spearman correlation coefficients and the p-value are shown.

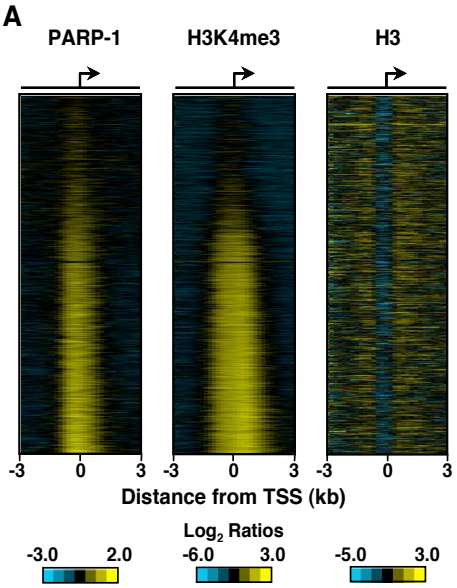

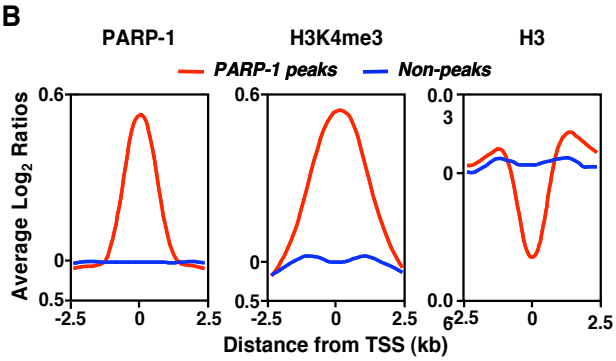

C

Spearman Correlations at the TSS

	PARP-1	H3K4me3	H3	Expr.
PARP-1	1.000	0.595	-0.459	0.419
H3K4me3		1.000	-0.256	0.496
H3			1.000	-0.001
Expr.	$p < 2.2 \times 10^{-16}$			1.000

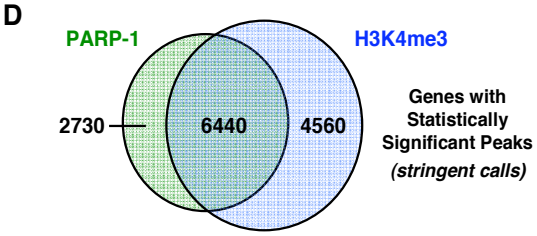

E

	Total Peaks	Overlap
PARP-1	9,170	70%
H3K4me3	11,000	59%

in many contexts to be correlated with specific chromatin states (Berger, 2007; Campos and Reinberg, 2009). I focused on histone H3 lysine 4 trimethylation (H3K4me3), which localizes to promoters and positively correlates with gene expression (Barski et al., 2007; Bernstein et al., 2005; Guenther et al., 2007; Santos-Rosa et al., 2002; Schneider et al., 2004), much like PARP-1 (Krishnakumar et al., 2008). I used ChIP coupled with hybridization to RefSeq promoter arrays (i.e., ChIP-chip) to determine if the binding of PARP-1 to promoters might correlate with H3K4me3 at promoters across the genome. Indeed, the striking pattern of PARP-1 promoter localization that I have observed previously (Krishnakumar et al., 2008) was similar to the pattern of H3K4me3 (Fig. 3.3, A and B). I found statistically significant peaks of both PARP-1 and H3K4me3 at or near the TSSs of about one third of the ~23,500 promoters on the array using stringent peak finding criteria (Fig. 3.3; see Experimental Procedures). PARP-1 and H3K4me3 showed a positive correlation (Spearman's correlation coefficient 0.60, $p < 2.2 \times 10^{-16}$), and both were positively correlated with gene expression (Spearman's correlation coefficients of 0.42 and 0.50, respectively, $p < 2.2 \times 10^{-16}$ for both) (Fig. 3.3C). The strong correlation of PARP-1 and H3K4me3 suggests a functional link between the two. I explored this possibility in the experiments noted below.

PARP-1 prevents KDM5B-dependent demethylation of H3K4me3 at the promoters of positively regulated target genes

To determine if PARP-1 might play an active role in establishing or maintaining H3K4me3 at target gene promoters, I examined the effect of PARP-1 knockdown on H3K4me3 levels. For the positively regulated genes, H3K4me3 levels decreased by more than 65 percent upon PARP-1 knockdown (Fig. 3.5A). For the negatively regulated gene, *GDF15*, the opposite effect was observed, and for the

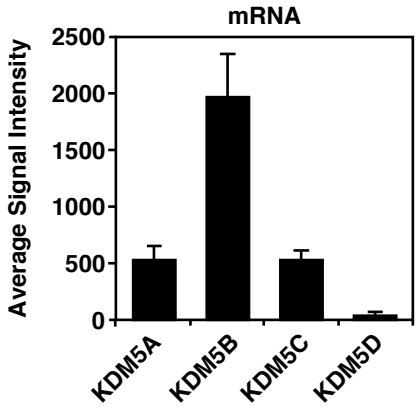

Figure 3.4. KDM5B is the most highly expressed KDM5 isoform in MCF-7 cells. Average signal intensity for KDM5 isoforms from Affymetrix expression arrays hybridized with probes derived from MCF-7 cell total RNA. The Affymetrix data are from the NCBI Gene Expression Omnibus (GEO; http://www.ncbi.nlm.nih.gov/geo/), accession numbers GSM234903, GSM234904, and GSM234905. For each KDM5 isoform, the signal intensities from all probes for one replicate were averaged and then all three replicates were averaged. Standard error of the mean was calculated from the three replicate values.

unegulated gene, *ABHD2*, no effect was observed (Fig. 3.5). These results correlate well with the effects of PARP-1 knockdown on Pol II, TBP, and TFIIB binding noted above (Fig. 3.1). Interestingly, TAF3 (a subunit of the TBP-containing complex TFIID) has been shown to bind to H3K4me3 (Vermeulen et al., 2007). Thus, the PARP-1-dependent reduction in H3K4me3 may reduce TBP binding, leading to a reduction in Pol II occupancy at the promoter, as previously shown (Vermeulen et al., 2007).

I considered the possibility that PARP-1 might regulate promoter H3K4me3 levels by recruiting a histone methyltransferase or by blocking the recruitment of a histone demethylase. A number of methyltransferases in the TRX/MLL family can trimethylate H3K4 in mammalian cells (Berger, 2007), while the KDM5 demethylases (A – D) are the only enzymes known to remove the modification (Nottke et al., 2009; Ruthenburg et al., 2007). Of the four KDM5 isoforms, KDM5B (lysine demethylase 5B; a.k.a. PLU-1 or JARID1B) is the most highly expressed in MCF-7 cells (Fig. 3.4). Thus, in my studies of PARP-1 function in MCF-7 cells, I focused on KDM5B. Knockdown of PARP-1 affected KDM5B binding at the promoters of the six genes tested in a predictable manner that precisely matched the effects on H3K4me3 levels (Fig. 3.5B). For example, PARP-1 knockdown increased KDM5B levels and decreased H3K4me3 levels at the promoters of the positively regulated genes, but not the negatively regulated or unregulated genes. These results suggest that PARP-1 prevents demethylation of H3K4me3 by KDM5B at the promoters of positively regulated target genes.

Figure 3.5. PARP-1 prevents demethylation of H3K4me3 at the promoters of positively regulated target genes by PARylating KDM5B and blocking its recruitment.

(A - D) ChIP-qPCR analysis of H3K4me3 and KDM5B levels at target gene promoters in control (Luc) and PARP-1 knockdown (KD) MCF-7 cells in the absence (panels A and B) or presence (panels C and D) of 5 μM PJ34 for 1.5 hours before collection. Each bar represents the mean plus the SEM, $n \geq 3$. The differences observed for *TMSL8*, *SCN1A*, *NELL2*, *ITPR1* are significant for panels C - G. The differences observed for *GDF15* are significant for panels A and B (Student's t-test, $p \leq 0.05$).

(E and F) PARP-1 binds to and PARylates KDM5B in MCF-7 cells in the absence, but not the presence, of 5 μM PJ34 for 1.5 hours before collection (panel E), and in control knockdown (Luc), but not PARP-1 knockdown, cells (panel F). KDM5B was immunoprecipitated (IP) from nuclear extracts and the immunoprecipitated material was subjected to Western blotting (WB) using antibodies to KDM5B, PARP-1, and PAR. C, non-specific control antibody; K, KDM5B antibody; In, input.

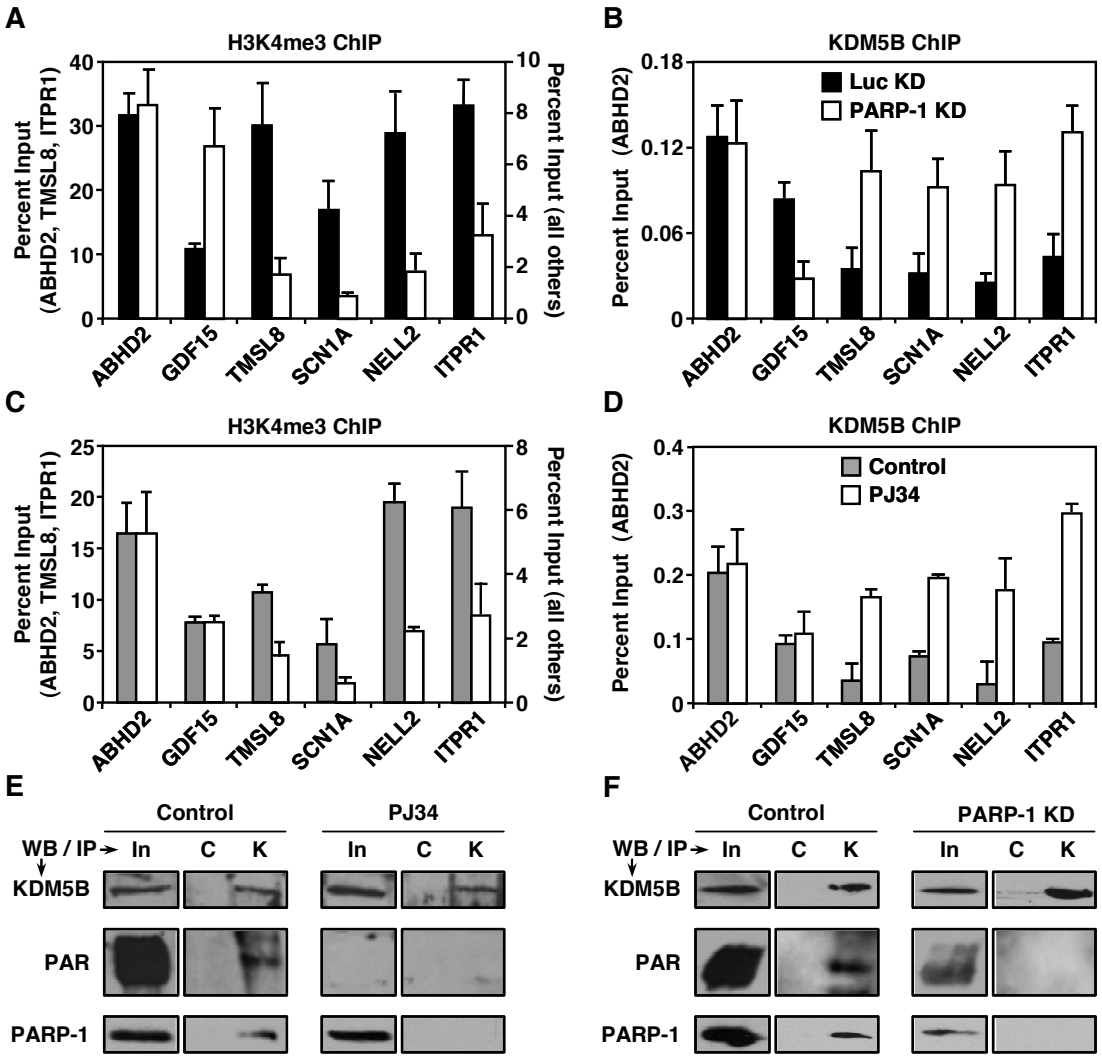
A
H3K4me3 ChIP
Percent Input (ABHD2, TMSL8, ITPR1)
Percent Input (all others)
ABHD2
GDF15
TMSL8
SCN1A
NELL2
ITPR1
B
KDM5B ChIP
Luc KD
PARP-1 KD
Percent Input (ABHD2)
C
H3K4me3 ChIP
D
KDM5B ChIP
Control
PJ34
E
Control
PJ34
WB / IP
In
C
K
KDM5B
PAR
PARP-1
F
Control
PARP-1 KD

Figure 3.6. The PARP-1 inhibitor PJ34 has little or no effect on some PARP-1-dependent molecular outcomes.

(A) Analysis of mRNA expression for six genes by RT-qPCR in MCF-7 cells treated with or without 5 μM PJ34 for 1.5 hours before collection. The data are normalized to the β-actin transcript and expressed relative to untreated cells. Each bar represents the mean plus the SEM, $n \geq 3$. None of the differences are significant (Student's t-test, $p \leq 0.05$).

(B - F) ChIP-qPCR analyses of factor or histone levels at the promoters of the PARP-1 target genes from panel A in MCF-7 cells treated with or without 5 μM PJ34 for 1.5 hours before collection. Each bar represents the mean plus the SEM, $n \geq 3$. None of the differences are significant (Student's t-test, $p \leq 0.05$).

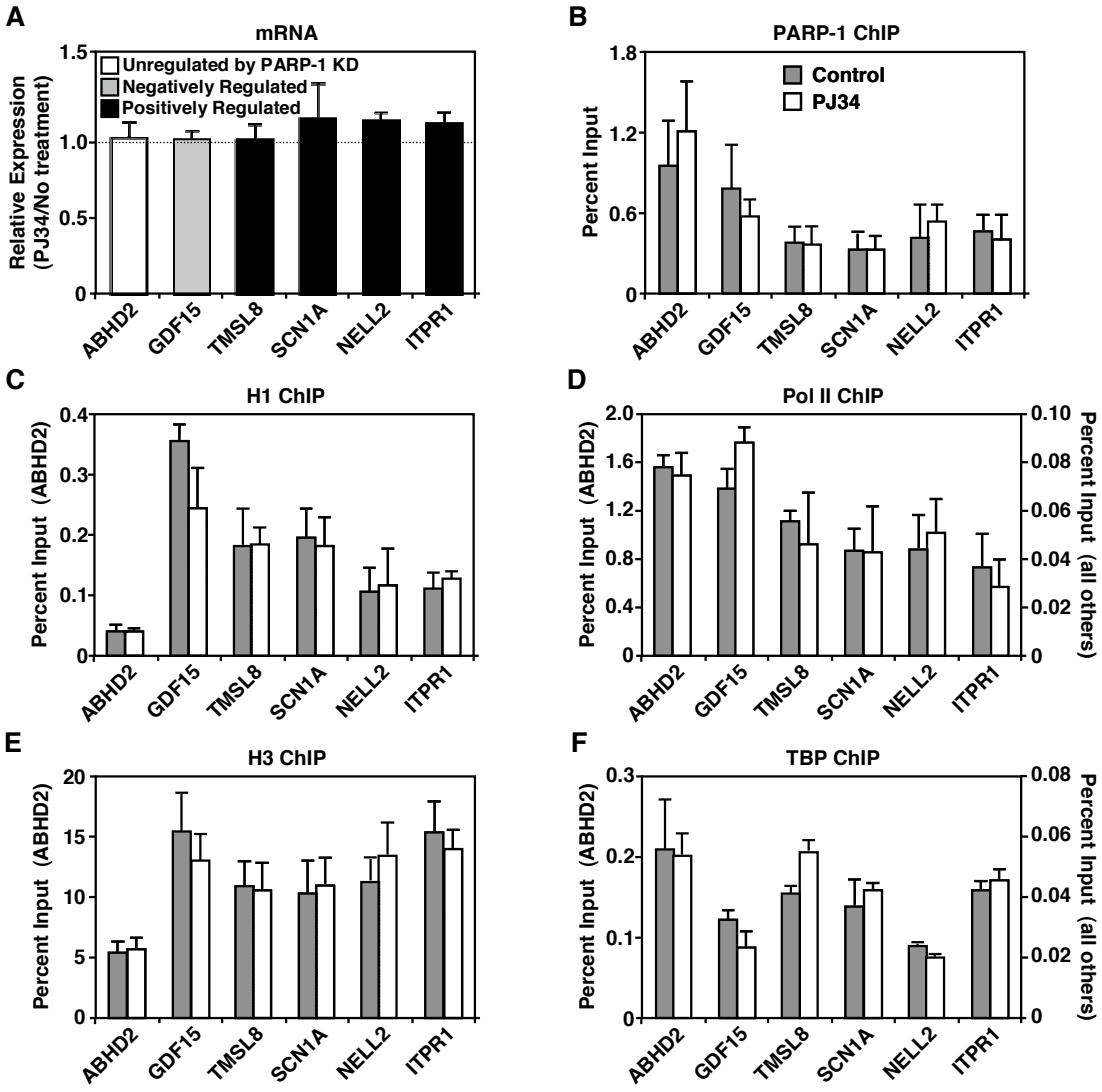
A
mRNA
Unregulated by PARP-1 KD
Negatively Regulated
Positively Regulated
Relative Expression (PJ34/No treatment)
1.5
1.0
0.5
0
ABHD2
GDF15
TMSL8
SCN1A
NELL2
ITPR1
B
PARP-1 ChIP
Control
PJ34
Percent Input
1.8
1.2
0.6
0
C
H1 ChIP
Percent Input (ABHD2)
0.4
0.3
0.2
0.1
0
D
Pol II ChIP
Percent Input (ABHD2)
Percent Input (all others)
2.0
1.6
1.2
0.8
0.4
0
0.10
0.08
0.06
0.04
0.02
E
H3 ChIP
Percent Input (ABHD2)
20
15
10
5
F
TBP ChIP
0.3
0.2
0.1
0.08
0.06
0.04
0.02

PARP-1 catalytic activity is required to prevent the binding of KDM5B at the promoters of positively regulated target genes

PARP-1 is an enzyme that catalyzes the addition of poly(ADP ribose) (PAR) chains on acceptor proteins using NAD^+ as a donor of ADP-ribose (Kim et al., 2005). Previous studies from our lab and others have shown that PARP-1 catalytic activity is required for the PARP-1-dependent expression of some, but not all, target genes (Frizzell et al., 2009; Hassa and Hottiger, 2002; Ju et al., 2006; Kim et al., 2005; Kraus, 2008; Kraus and Lis, 2003; Pavri et al., 2005). In some cases, PARP-1 catalytic activity may be required for one or more steps in the gene regulatory pathway, while the PARP-1 protein itself may be required for other steps. To test this possibility, I determined the effects of the PARP inhibitor, PJ34, on the same target genes and functional endpoints that I examined above. Our lab has shown previously that PJ34 effectively inhibits PARP-1 enzymatic activity in MCF-7 cells (Frizzell et al., 2009). Interestingly, PJ34 had no effect on gene expression or the binding of PARP-1, H1, or Pol II at the promoters of the genes examined (Fig. 3.6). These results indicate that, unlike depletion of PARP-1 protein, inhibition of PARP-1 catalytic activity is not sufficient to inhibit the expression of the positively regulated genes, suggesting that the physical presence of the PARP-1 protein at the promoter is key for maintaining gene expression. However, PJ34 did reduce the levels of H3K4me3 and increase the levels of KDM5B at the same promoters (Fig. 3.5, C and D). Thus, of the various endpoints examined, PARP-1 catalytic activity specifically targets H3K4 trimethylation by KDM5B.

Based on these results, I hypothesized that PARP-1 might interact with and poly(ADP-ribosyl)ate (PARylate) KDM5B in cells, thus preventing KDM5B from binding to promoters. To test this, I immunoprecipitated KDM5B from MCF-7 nuclear extracts and subjected the immunoprecipitated material to Western blotting

Figure 3.7. Generation and confirmation of PARP-1/KDM5B double knockdown cells.

Retrovirus-mediated gene transfer was used to generate MCF-7 cells with stable knockdown (KD) of PARP-1 + Luc (PL), KDM5B + Luc (KL), or PARP-1 + KDM5B (PK), matched with an appropriate control cell line expressing two shRNAs targeting luciferase (LL).

(A) Western blot of nuclear extracts showing the depletion of PARP-1 and KDM5B in the knockdown cell lines noted above. Also shown are Western blots for H3K4me3 and H3.

(B and C) RT-qPCR analysis of PARP-1 (panel B) and KDM5B (panel C) mRNA expression in the knockdown cell lines noted above. Each bar represents the mean plus the SEM, $n \geq 3$. All knockdown effects are significant (ANOVA, $p \leq 0.05$).

(D) ChIP-qPCR analysis in MCF-7 Luc and KDM5B knockdown cells showing that KDM5B knockdown reduces the corresponding ChIP signal at the promoters of two target genes, *ABHD2* and *GDF15*. Each bar represents the mean plus the SEM, $n \geq 3$. The observed effects of knockdown are significant (Student's t-test, $p \leq 0.05$).

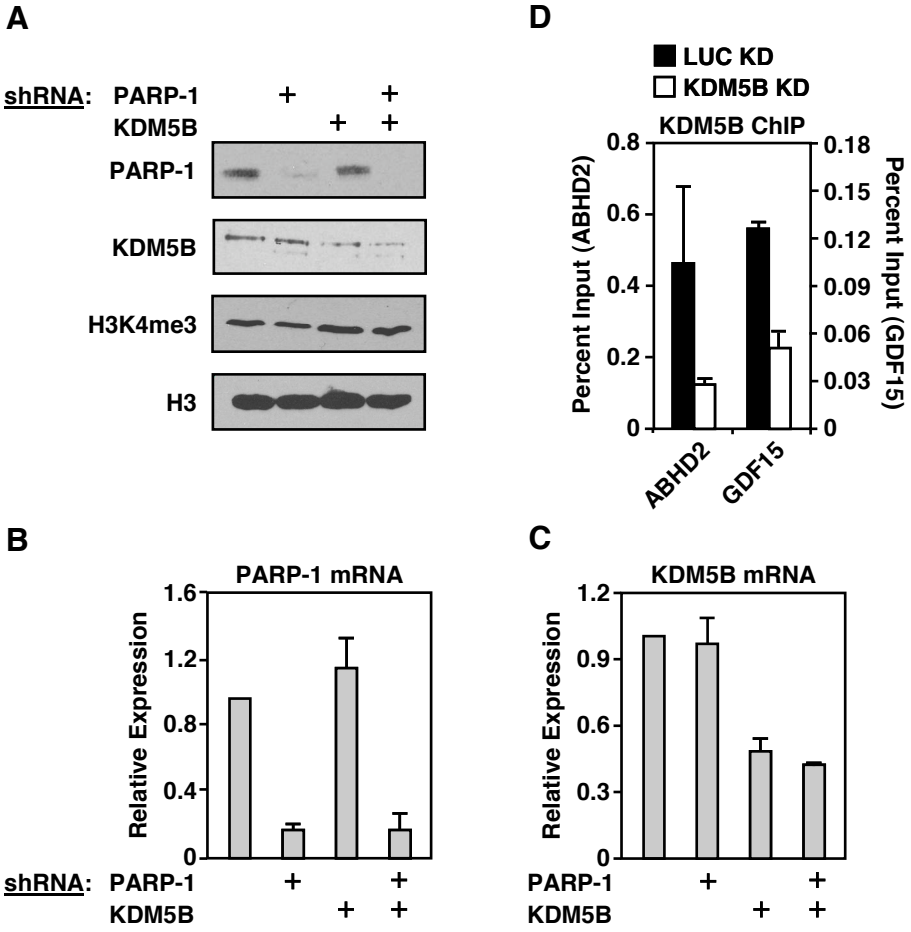
A
shRNA: PARP-1 + +
KDM5B + +
PARP-1
KDM5B
H3K4me3
H3
D
LUC KD
KDM5B KD
KDM5B ChIP
Percent Input (ABHD2)
Percent Input (GDF15)
0.8
0.6
0.4
0.2
0
0.18
0.15
0.12
0.09
0.06
0.03
0
ABHD2
GDF15
B
PARP-1 mRNA
Relative Expression
1.6
1.2
0.8
0.4
0
shRNA: PARP-1 + +
KDM5B + +
C
KDM5B mRNA
Relative Expression
1.2
0.9
0.6
0.3
0
PARP-1 + +
KDM5B + +

using antibodies to KDM5B, PARP-1, and PAR. I found that KDM5B immunoprecipitates PARP-1 and is modified by PARylation (Fig 3.5E). Treatment of the cells with PJ34 (Fig. 3.5E) and knockdown of PARP-1 (Fig. 3.5F) inhibited KDM5B PARylation, indicating that PARP-1 is the enzyme mediating the modification. Taken together, these results indicate that PARP-1 acts to promote H3K4 trimethylation at the promoters of positively regulated target genes by PARylating KDM5B, which blocks its recruitment.

Antagonism of KDM5B-dependent H3K4me3 demethylation by PARP-1 facilitates the expression of positively regulated target genes

To further explore the role of PARP-1-dependent antagonism of KDM5B in target gene expression, I examined the effects of KDM5B knockdown using a previously reported shRNA sequence (Scibetta et al., 2007). According to my model, a key role of PARP-1 is to prevent KDM5B-dependent demethylation of H3K4me3; shRNA-mediated knockdown of PARP-1 allows demethylation of H3K4me3 and subsequent inhibition of transcription of the positively regulated genes. If this model is correct, then depletion of KDM5B should reverse the effects of PARP-1 knockdown. To test this model, I generated a set of cell lines with knockdown of PARP-1 + Luc (PL), KDM5B + Luc (KL), or PARP-1 + KDM5B (PK), matched with an appropriate control cell line expressing two shRNAs targeting luciferase (LL). I confirmed the knockdown of PARP-1 and KDM5B by Western blotting and RT-qPCR (Fig. 3.7, A - C). In addition, I showed that knockdown of KDM5B reduced its signal in ChIP assays (Fig. 3.7D). Although KDM5B knockdown alone had little effect on the expression of positively regulated target genes, it reversed the effect of PARP-1 knockdown (Fig. 3.8A). In contrast, for the negatively regulated gene, *GDF15*, knockdown of KDM5B did not reverse the effect of PARP-1 knockdown, suggesting a

Figure 3.8. Antagonism of KDM5B-dependent H3K4me3 demethylation by PARP-1 promotes a transcriptionally permissive environment at the promoters of positively regulated target genes.

The experiments in this figure used MCF-7 cells with knockdown of PARP-1 + Luc (PL), KDM5B + Luc (KL), or PARP-1 + KDM5B (PK), matched with an appropriate control cell line expressing two shRNAs targeting luciferase (LL).

(A) Analysis of mRNA expression for six genes by RT-qPCR in PARP-1 and KDM5B knockdown MCF-7 cells. The data are normalized to the β-actin transcript and expressed relative to LL cells. Each bar represents the mean plus the SEM, $n \geq 3$. The differences observed for PL relative to LL are significant for all genes except *ABHD2* (ANOVA, $p \leq 0.05$).

(B) ChIP-qPCR analysis of factor, histone, or histone modification levels at the promoter of the PARP-1 target gene, *ITPR1*, in MCF-7 cells with PARP-1 and KDM5B knockdown, as indicated. Each bar represents the mean plus the SEM, $n \geq 3$. The differences observed for PL relative to LL are significant for all ChIPs except H3 (ANOVA, $p \leq 0.05$). Results for additional genes are shown in Supplemental Fig. S4.

(C) MNase protection experiments in MCF-7 cells with PARP-1 and KDM5B knockdown, as indicated, for *ITPR1*. Each point represents the mean ± the SEM, $n \geq 3$. The shaded region indicates statistically significant differences between the LL and PL cells (Student's t-test, $p \leq 0.05$). Results for additional genes are shown in Supplemental Fig. S6.

(D) MNase protection data at the TSS from panel C, above. Each bar represents the mean plus the SEM, $n \geq 3$. The differences observed for PL relative to LL are significant (ANOVA, $p \leq 0.05$).

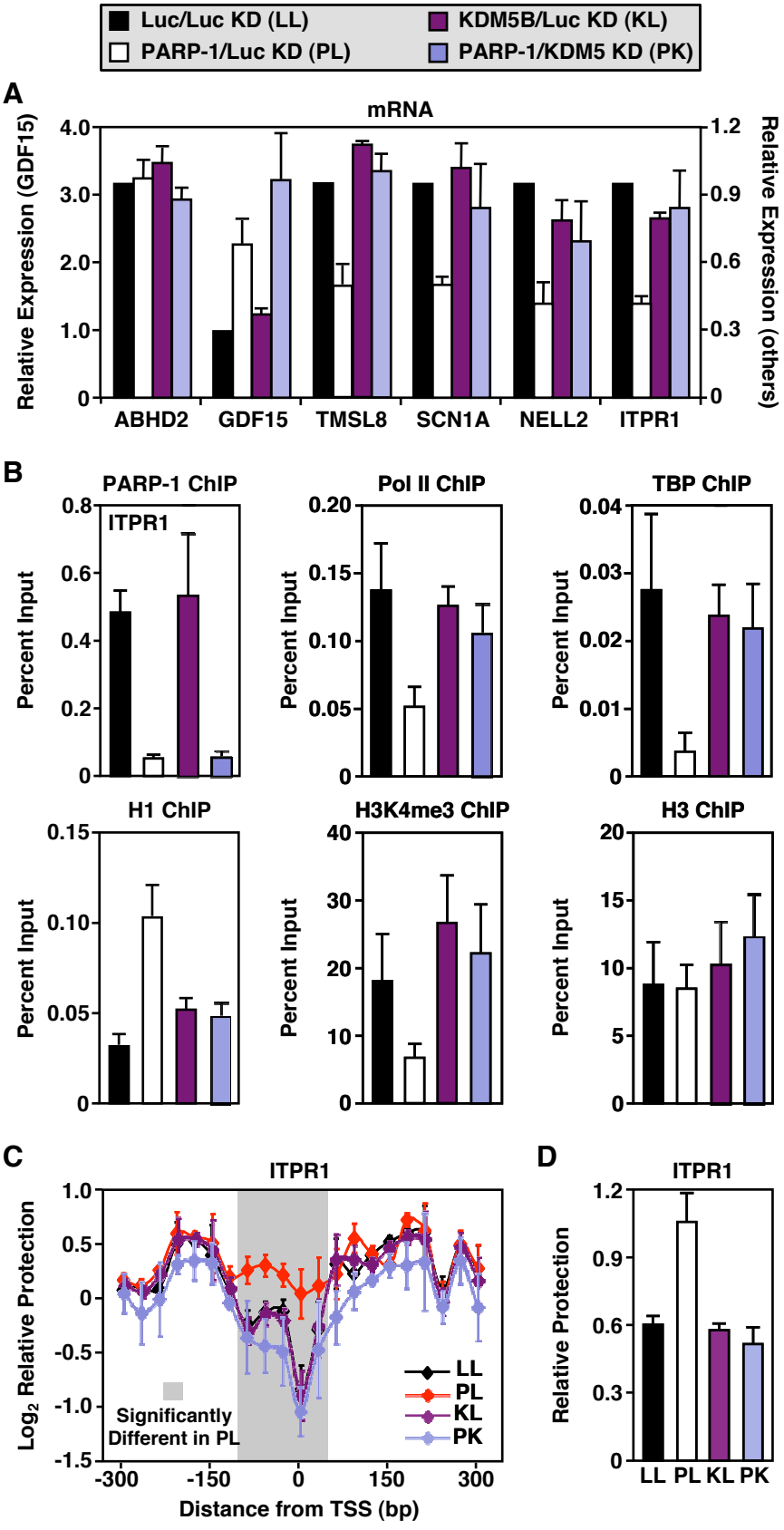
Luc/Luc KD (LL)
PARP-1/Luc KD (PL)
KDM5B/Luc KD (KL)
PARP-1/KDM5 KD (PK)
A
mRNA
Relative Expression (GDF15)
Relative Expression (others)
ABHD2
GDF15
TMSL8
SCN1A
NELL2
ITPR1
B
PARP-1 ChIP
ITPR1
Pol II ChIP
TBP ChIP
H1 ChIP
H3K4me3 ChIP
H3 ChIP
Percent Input
C
ITPR1
Log2 Relative Protection
Significantly Different in PL
LL
PL
KL
PK
Distance from TSS (bp)
D
ITPR1
Relative Protection
LL PL KL PK

Figure 3.9. Antagonism of KDM5B-dependent H3K4me3 demethylation by PARP-1 promotes the recruitment of the Pol II transcription machinery, the exclusion of H1, and the maintenance of H3K4 trimethylation at the promoters of positively regulated target genes.

The experiments in this figure used MCF-7 cells with knockdown of PARP-1 + Luc (PL), KDM5B + Luc (KL), or PARP-1 + KDM5B (PK), matched with an appropriate control cell line expressing two shRNAs targeting luciferase (LL).

(A - C) ChIP-qPCR analysis of PARP-1, Pol II, and TBP at the promoters of six genes, as indicated. Each bar represents the mean plus the SEM, $n \geq 3$. The differences observed for PL and PK relative to LL are significant for all genes in panel A (ANOVA, $p \leq 0.05$). The differences observed for PL relative to LL are significant for all genes except *ABHD2* and *GDF15* in panel B, and all genes except *ABHD2* in panel C (ANOVA, $p \leq 0.05$).

(D – F) ChIP-qPCR analyses of H1, H3K4me3, and H3 at the promoters of six genes, as indicated. Each bar represents the mean plus the SEM, $n \geq 3$. The differences observed for PL relative to LL are significant for all genes except *ABHD2* and *GDF15* in panels A and B (ANOVA, $p \leq 0.05$). The differences in panel F are not significant.

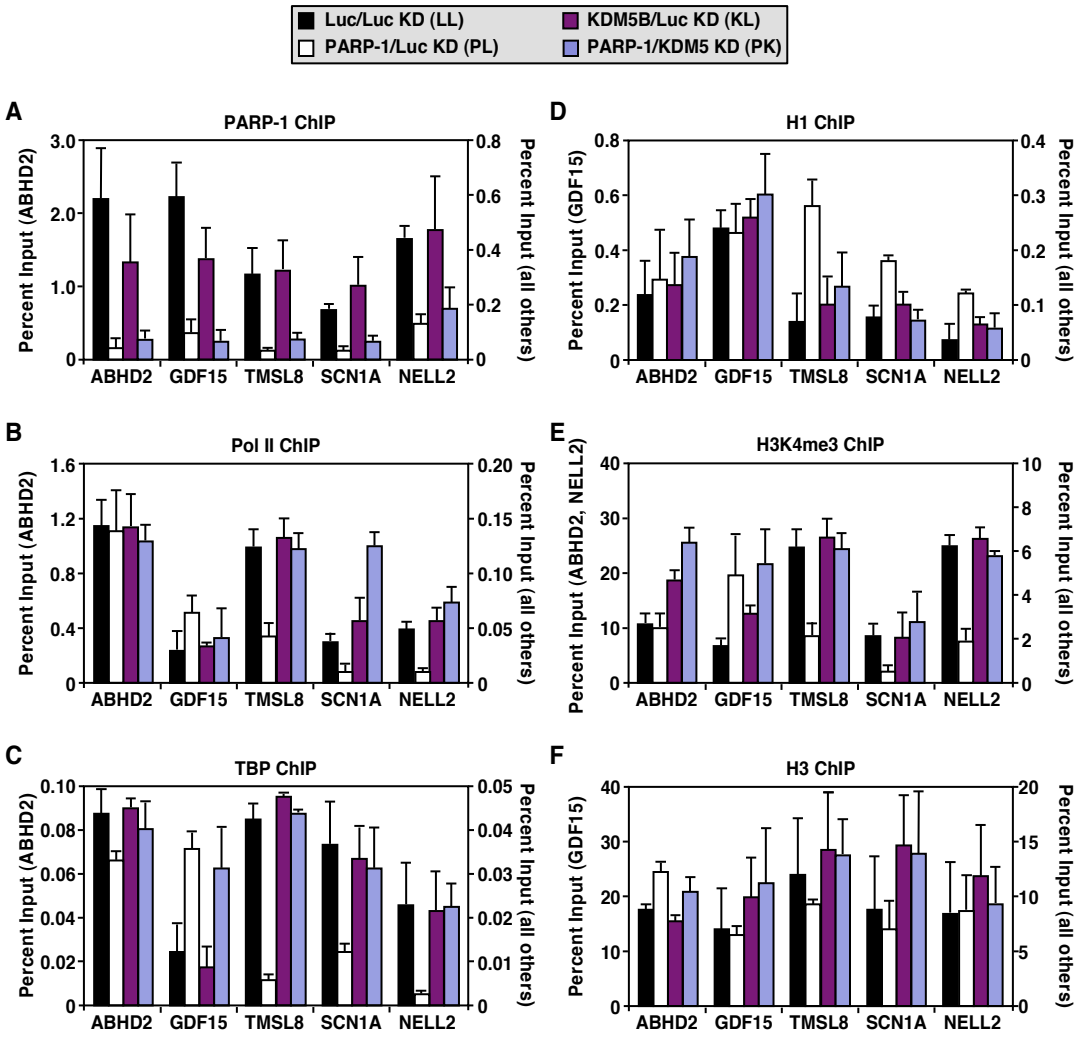
Luc/Luc KD (LL)
PARP-1/Luc KD (PL)
KDM5B/Luc KD (KL)
PARP-1/KDM5 KD (PK)
A
PARP-1 ChIP
Percent Input (ABHD2)
Percent Input (all others)
ABHD2
GDF15
TMSL8
SCN1A
NELL2
D
H1 ChIP
Percent Input (GDF15)
B
Pol II ChIP
E
H3K4me3 ChIP
Percent Input (ABHD2, NELL2)
C
TBP ChIP
F
H3 ChIP

different mode of regulation (Fig. 3.8A). These results indicate that a loss of PARP-1 at the promoters of positively regulated target genes can be overcome by removing KDM5B, consistent with the hypothesis that these two proteins act antagonistically in the same pathway.

Next, to determine the consequences of PARP-1 antagonism of KDM5B, I assayed factor binding (Pol II, TBP, H1) and H3K4 trimethylation at the promoters of the PARP-1 target genes in the double knockdown cells. The results for the positively regulated gene, *ITPR1*, are shown in Figs. 3.8B and 3.8C for illustrative purposes, while the results for additional genes are shown in Fig. 3.9. As I showed above, knockdown of PARP-1 decreased the binding of Pol II and TBP, as well as the levels of H3K4me3, at the promoters of the positively regulated genes, while increasing the binding of H1 (Fig. 3.8B; Fig. 3.9). As I observed with gene expression, knockdown of KDM5B had little effect on its own, but was able to reverse all of the effects of PARP-1 knockdown on the positively regulated genes (Pol II, TBP, H1, H3K4me3; Fig. 3.8B; Fig. 3.9). These results indicate that removal of H3K4me3 is required, but not sufficient (based on the results from Fig. 3.5), for the binding of H1 and the eviction of Pol II from the promoters of positively regulated target genes. Interestingly, knockdown of KDM5B was also able to reverse the effects of PJ34 treatment on H3K4me3 (Fig. 3.10). Together these data support a model in which antagonism of KDM5B binding and H3K4me3 demethylation by PARP-1 facilitates the expression of positively regulated target genes.

Figure 3.10. PARP-1 catalytic activity is required to antagonize the actions of KDM5B.

(A - C) ChIP-qPCR analyses of KDM5B, H3K4me3, and H3 at the promoters of six genes in Luc or KDM5B knockdown (KD) MCF-7 cells with or without of 5 μM PJ34 treatment for 1.5 hours before collection, as indicated. Each bar represents the mean plus the SEM, $n \geq 3$. The differences observed for Luc/PJ34 relative to Luc/Control are significant for all genes except *ABHD2* and *GDF15* in panels A and B (ANOVA, $p \leq 0.05$). The differences in panel C are not significant.

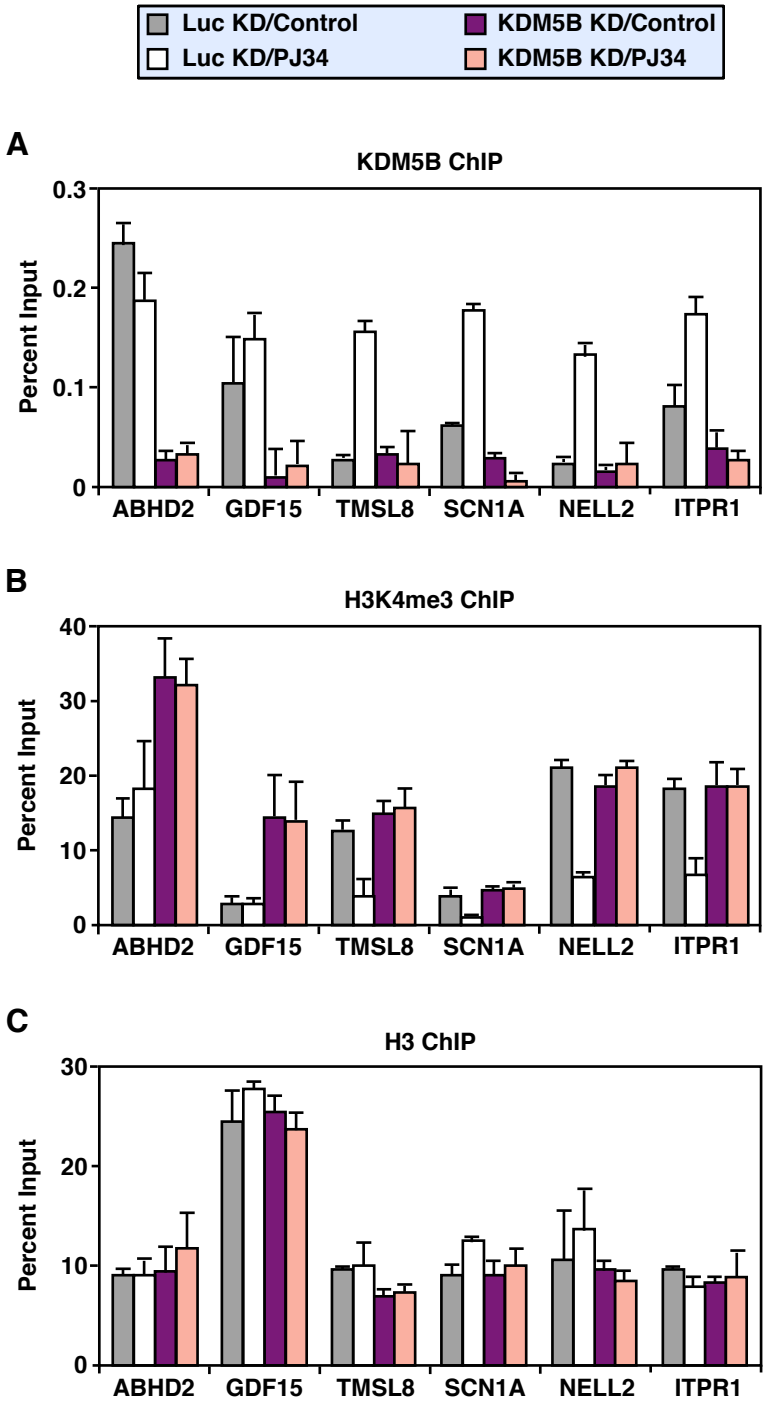
Luc KD/Control
Luc KD/PJ34
KDM5B KD/Control
KDM5B KD/PJ34
A
KDM5B ChIP
Percent Input
0.3
0.2
0.1
0
ABHD2
GDF15
TMSL8
SCN1A
NELL2
ITPR1
B
H3K4me3 ChIP
Percent Input
40
30
20
10
0
ABHD2
GDF15
TMSL8
SCN1A
NELL2
ITPR1
C
H3 ChIP
Percent Input
30
20
10
0
ABHD2
GDF15
TMSL8
SCN1A
NELL2
ITPR1

Antagonism of KDM5B-dependent H3K4me3 demethylation by PARP-1 maintains an open chromatin architecture at the TSSs of positively regulated target genes

In Fig. 3.2, I showed that PARP-1 is required to maintain an open chromatin architecture at the TSSs of positively regulated genes. To determine if PARP-1's antagonism of KDM5B and enhancement of H3K4 trimethylation levels plays a role in this process, I used the MNase protection assay described in Fig. 3.2 with PARP-1 and KDM5B double knockdown cells. As with the gene expression outcomes described above, if my model is correct, then depletion of KDM5B should reverse the effects of PARP-1 knockdown. As seen in Fig. 3.2, PARP-1 knockdown caused a significant increase in the MNase protection (i.e., decreased accessibility or a closed chromatin architecture) relative to the control knockdown at near the TSSs of the positively regulated genes *ITPR1* (Fig. 3.8, C and D) and *SCN1A* (Fig. 3.11A), but not for the unregulated gene *ABHD2* (Fig. 3.11B). Although KDM5B knockdown alone had little effect on the promoter chromatin architecture of *ITPR1* and *SCN1A*, it reversed the effect of PARP-1 knockdown on these genes (Fig. 3.10 C and D; Fig. 3.11A). These results indicate that PARP-1 maintains an open chromatin architecture at the TSSs of positively regulated genes by inhibiting KDM5B-mediated demethylation of H3K4me3.

Removal of PARP-1 from promoters is a mechanism utilized by signaling pathways to negatively regulate gene expression

Having determined a specific role for PARP-1 in maintaining constitutive gene expression in MCF-7 cells under basal growth conditions, I next asked whether the PARP-1-dependent regulatory mechanisms which I uncovered might be applicable to signal-regulated transcription. MCF-7 cells initiate well characterized transcriptional

Figure 3.11. Antagonism of KDM5B-dependent H3K4me3 demethylation by PARP-1 promotes an open chromatin architecture at the promoters of positively regulated target genes.

The experiments in this figure used MCF-7 cells with knockdown of PARP-1 + Luc (PL), KDM5B + Luc (KL), or PARP-1 + KDM5B (PK), matched with an appropriate control cell line expressing two shRNAs targeting luciferase (LL).

(A and B) MNase protection experiments in MCF-7 cells with PARP-1 and KDM5B knockdown, as indicated, for *SCN1A* and *ABHD2*. Each point represents the mean ± the SEM, $n \geq 3$. The shaded region in panel A indicates statistically significant differences between the LL and PL cells (Student's t-test, $p \leq 0.05$).

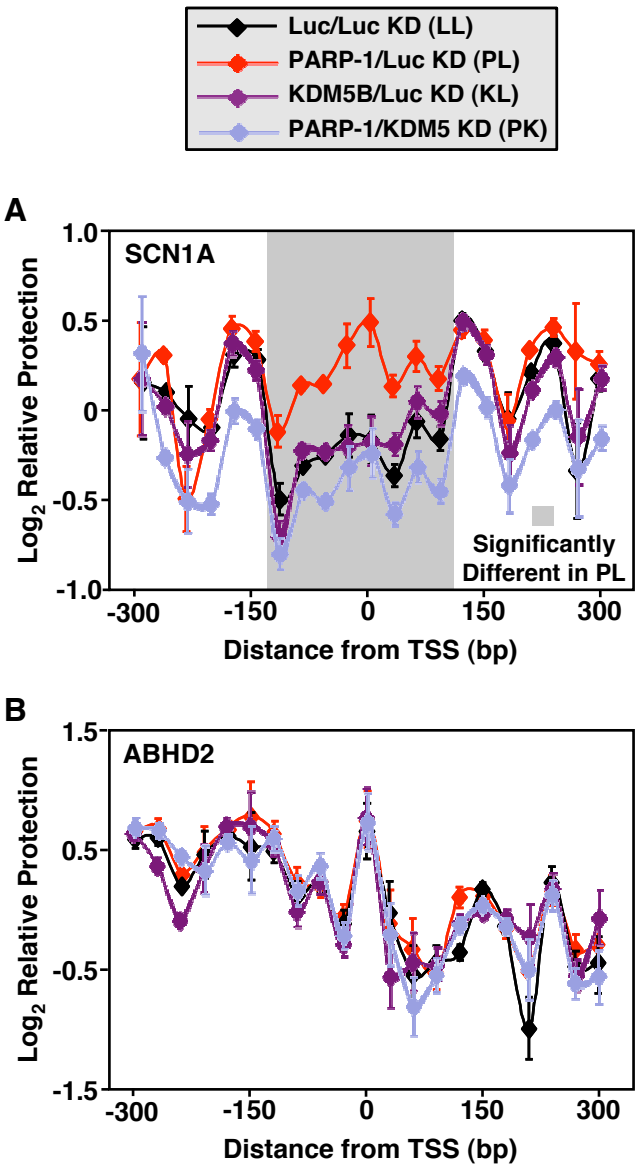
Luc/Luc KD (LL)
PARP-1/Luc KD (PL)
KDM5B/Luc KD (KL)
PARP-1/KDM5 KD (PK)
A
SCN1A
Log2 Relative Protection
1.0
0.5
0
-0.5
-1.0
Significantly
Different in PL
-300
-150
0
150
300
Distance from TSS (bp)
B
ABHD2
Log2 Relative Protection
1.5
0.5
-0.5
-1.5
-300
-150
0
150
300
Distance from TSS (bp)

responses to a wide variety of stimuli, including the phorbol ester 12-O-tetradecanoylphorbol-13-acetate (TPA; a.k.a. phorbol 12-myristate 13-acetate; (Liu and Heckman, 1998)) . TPA, which resembles the natural agonist of protein kinase C, diacylglycerol, is a potent activator of the protein kinase C pathway (Liu and Heckman, 1998). Many genes in MCF-7 cells are responsive to TPA treatment (Cunliffe et al., 2003; Lacroix et al., 2004), including *SCN1A* and *ITPR1* (Fig. 3.12A). The expression of these two genes was inhibited by treatment with TPA (100 ng/ml TPA for 3 hours), an effect that was similar to PARP-1 knockdown (Fig. 3.12A). The expression of *ABHD2*, which I examined for comparison, was unaffected by TPA or PARP-1 knockdown (Fig, 3.12A).

I considered the possibility that TPA-dependent signaling might inhibit the expression of *SCN1A* and *ITPR1* by blocking the localization and/or function of PARP-1 at their promoters. Treatment with TPA promoted the release of PARP-1 from these promoters (Fig. 3.12B), perhaps as a direct target endpoint of the signaling pathway. Given that TPA promoted the release of PARP-1 from the *SCN1A* and *ITPR1* promoters, I expected that TPA might promote the same molecular outcomes as PARP-1 knockdown at these promoters. In this regard, I observed an increase in H1 binding (Fig. 3.12C), a decrease in Pol II and TBP binding (Fig. 3.12, D and E), and a decrease in the levels of H3K4me3 (Fig. 3.12, F and G) upon TPA treatment. Thus, for these endpoints, TPA treatment and PARP-1 knockdown are functionally similar. To determine if KDM5B might be involved in this pathway as well, I monitored H3K4me3 and KDM5B binding at the promoters in response to TPA treatment. As with PARP-1 knockdown, TPA treatment caused a decrease in H3K4me3 levels and an increase in KDM5B binding to the promoters (Fig. 3.12, G and H). Also, I found that TPA-mediated repression of these genes was inhibited by knockdown of KDM5B (Fig. 3.12I). Together, these results indicate that cellular signaling pathways, like

Figure 3.12. Signaling in the PKC pathway promotes the removal of PARP-1 from promoters to negatively regulate gene expression.

(A) Analysis of mRNA expression for three genes by RT-qPCR in MCF-7 cells treated with 100 ng/ml TPA for 3 hours versus MCF-7 cells with PARP-1 knockdown. The data are normalized to the β-actin transcript and expressed relative to untreated LL cells. Each bar represents the mean plus the SEM, $n \geq 3$. The differences observed for all genes except *ABHD2* are significant (ANOVA, $p \leq 0.05$).

(B - H) ChIP-qPCR analysis of factor, histone, or histone modification levels at the promoters of three genes, as indicated, in MCF-7 cells with or without 100 ng/ml TPA treatment for 3 hours. Each bar represents the mean plus the SEM, $n \geq 3$. The differences observed with TPA are significant for *SCN1A* and *ITPR1* for panels C, D, E, G, and H (ANOVA, $p \leq 0.05$).

(I) Analysis of mRNA expression for three genes by RT-qPCR in MCF-7 cells with KDM5B knockdown. The data are normalized to the β-actin transcript and expressed relative to untreated LL cells. Each bar represents the mean plus the SEM, $n \geq 3$. The differences observed for *SCN1A* and *ITPR1* are significant (ANOVA, $p \leq 0.05$).

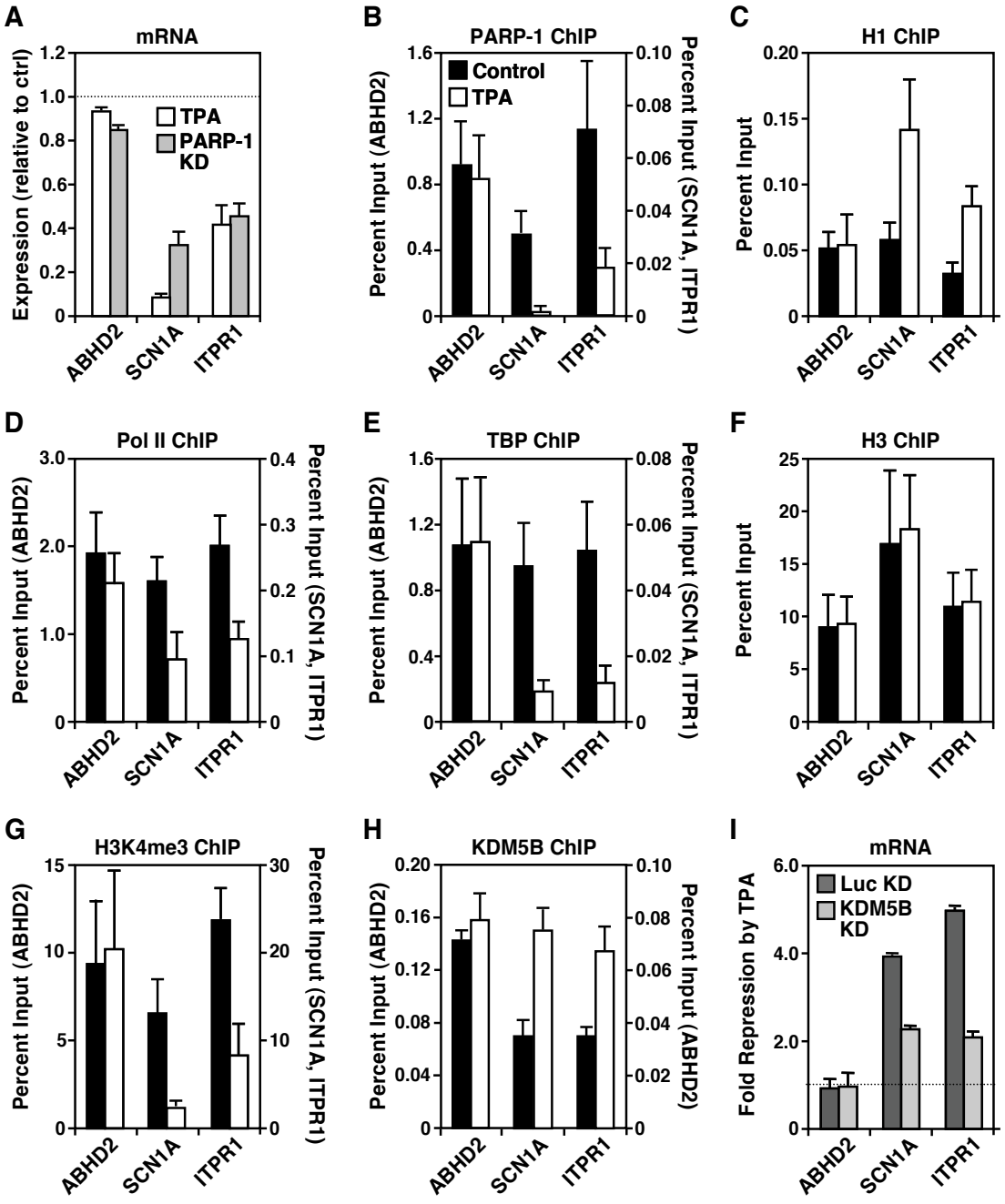
A
mRNA
Expression (relative to ctrl)
TPA
PARP-1 KD
ABHD2
SCN1A
ITPR1
B
PARP-1 ChIP
Control
TPA
Percent Input (ABHD2)
Percent Input (SCN1A, ITPR1)
C
H1 ChIP
Percent Input
D
Pol II ChIP
E
TBP ChIP
F
H3 ChIP
G
H3K4me3 ChIP
H
KDM5B ChIP
Percent Input (ABHD2)
I
mRNA
Luc KD
KDM5B KD
Fold Repression by TPA

those mediated by TPA, can regulate gene expression by abrogating PARP-1 binding at the promoter, which in turn allows H1 binding, KDM5B binding, and the removal of H3K4me3.

Other histone modifications, such as H3K27me3, play a role in mediating PARP-1-dependent transcriptional regulation

During my investigation of various histone modifications, I found that in addition to H3K4me3, PARP-1 depletion also affected the levels of H3K27me3 (histone H3, lysine 27 trimethylation) at target promoters (Fig 3.13A). Based on this data, I investigated the role of the corresponding histone methyltransferase responsible for depositing this particular modification, EZH2 (Enhancer of Zeste Homolog 2, a member of PRC2 [Polycomb Repressive Complex 2]). Upon PARP-1 knockdown EZH2 was recruited to target promoters of positively regulated genes, correlating with a decrease in the modification (Fig. 3.13B). I then examined whether altering levels of H3K4me3 (via knockdown of KDM5B) could affect this modification, and I found that knockdown of KDM5B did not alter H3K27me3, and double knockdown of PARP-1 and KDM5B did not change the effect of PARP-1 knockdown (Fig. 3.13C). Taken together, this suggests that the while PARP-1 acts to maintain low levels of H3K27me3, this occurs either upstream or independently of PARP-1 preventing the binding of KDM5B and the removal. of H3K4me3. Finally, I also found that the increase of H3K27me3 upon removal of PARP-1 from promoters also occurs in the TPA-dependent signaling pathway described previously (Fig. 3.12, 3.13D). It will be interesting to further investigate the role of H3K27me3, EZH2, and other members of the PRC2 complex in PARP-1 dependent transcriptional regulation, as well as the interplay between H3K4me3, H3K27me3 and other chromatin modifications in these regulatory pathways.

Figure 3.13. PARP-1 regulates H3K27me3 levels via modulation of EZH2 recruitment.

(A, B) ChIP-qPCR analyses of H3K27me3 (A) and EZH2 (B) levels at the promoters of the PARP-1 target genes from panel A in control (Luc) and PARP-1 knockdown (KD) cells. Each bar represents the mean plus the SEM, $n \geq 3$. **(C)** The experiments in this panel used MCF-7 cells with knockdown of PARP-1 + Luc (PL), KDM5B + Luc (KL), or PARP-1 + KDM5B (PK), matched with an appropriate control cell line expressing two shRNAs targeting luciferase (LL). ChIP-qPCR analysis of H3K27me3 levels at the promoters of three genes, as indicated, in LL, PL, KL and PK MCF-7. Each bar represents the mean plus the SEM, $n \geq 3$.

(D) ChIP-qPCR analysis of H3K4me3 levels at the promoters of three genes, as indicated, in MCF-7 cells with or without 100 ng/ml TPA treatment for 1 hour. Each bar represents the mean plus the SEM, $n \geq 3$.

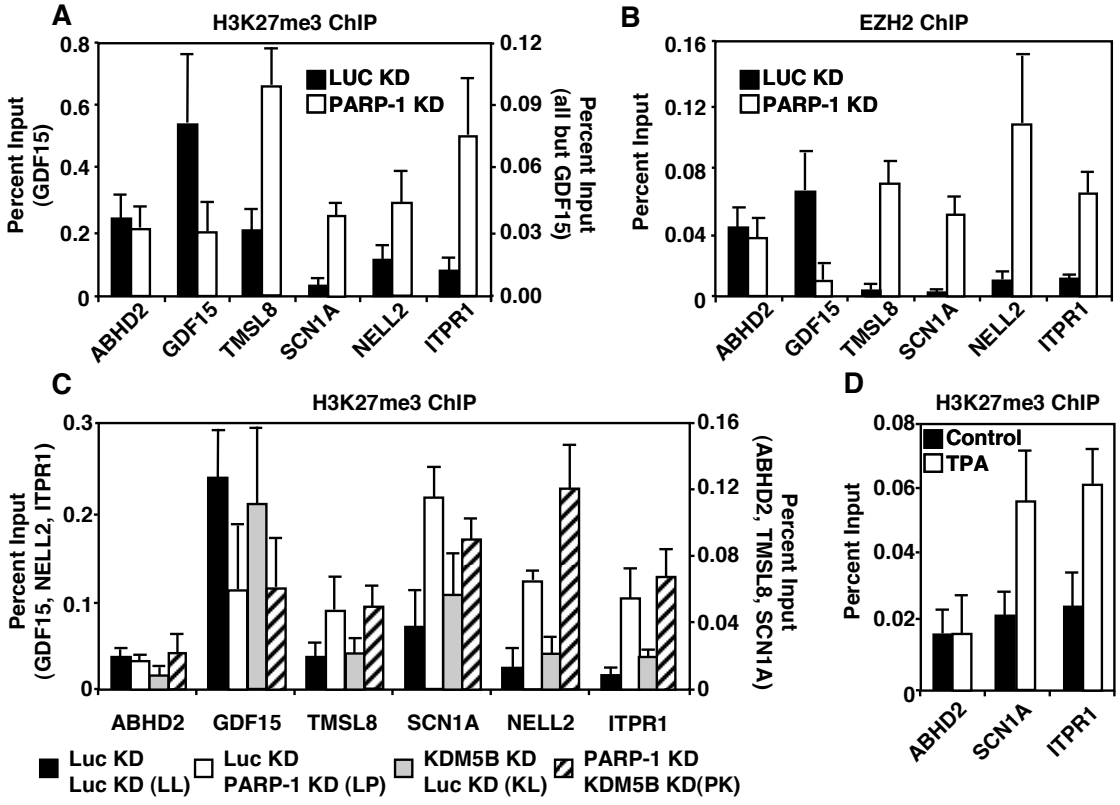
A
H3K27me3 ChIP
LUC KD
PARP-1 KD
Percent Input (GDF15)
Percent Input (all but GDF15)
0.8
0.6
0.4
0.2
0
0.12
0.09
0.06
0.03
0.00
ABHD2
GDF15
TMSL8
SCN1A
NELL2
ITPR1
B
EZH2 ChIP
LUC KD
PARP-1 KD
Percent Input
0.16
0.12
0.08
0.04
0
ABHD2
GDF15
TMSL8
SCN1A
NELL2
ITPR1
C
H3K27me3 ChIP
Percent Input (GDF15, NELL2, ITPR1)
Percent Input (ABHD2, TMSL8, SCN1A)
0.3
0.2
0.1
0
0.16
0.12
0.08
0.04
0
ABHD2
GDF15
TMSL8
SCN1A
NELL2
ITPR1
Luc KD
Luc KD (LL)
Luc KD
PARP-1 KD (LP)
KDM5B KD
Luc KD (KL)
PARP-1 KD
KDM5B KD(PK)
D
H3K27me3 ChIP
Control
TPA
Percent Input
0.08
0.06
0.04
0.02
0
ABHD2
SCN1A
ITPR1

3.4 Discussion

In this study, I explored the role of PARP-1 in the chromatin-dependent control of gene expression. In particular, I examined functional interplay between PARP-1, H3K4 trimethylation, and the linker histone H1. I found that PARP-1 is required for a series of molecular outcomes at the promoters of genes that are positively regulated by PARP-1 (i.e., genes whose expression is dependent on PARP-1) (Fig. 3.14). Specifically, my experiments using shRNA-mediated knockdown showed that PARP-1 establishes a permissive chromatin environment at the promoters of these genes by promoting the (1) trimethylation of H3K4 through the exclusion of KDM5B, (2) exclusion of H1, and (3) accessibility of the promoter DNA at the TSS. Upon depletion of PARP-1, these outcomes do not occur efficiently. The permissive chromatin environment is required for the efficient loading of the Pol II transcription machinery (e.g., Pol II, TBP, TFIIB) and subsequent transcription (Fig. 3.14). Finally, my results indicate that cellular signaling pathways use the regulated depletion of PARP-1 from promoters to inhibit gene expression. Collectively, my results assign new functions for PARP-1 in the regulation of chromatin structure and transcription.

PARP-1 promotes H3K4 trimethylation at the promoters of positively regulated genes by antagonizing KDM5B

PARP-1 has long been known to regulate chromatin structure, perhaps through direct PARylation of core histones or H1, yet the underlying mechanisms and targets have not been clearly determined (Kim et al., 2005; Kraus, 2008; Kraus and Lis, 2003). My results indicate that PARP-1 regulates chromatin in at least two ways. First, it regulates the covalent posttranslational modification of chromatin by promoting H3K4 trimethylation, a histone modification that is positively correlated with gene

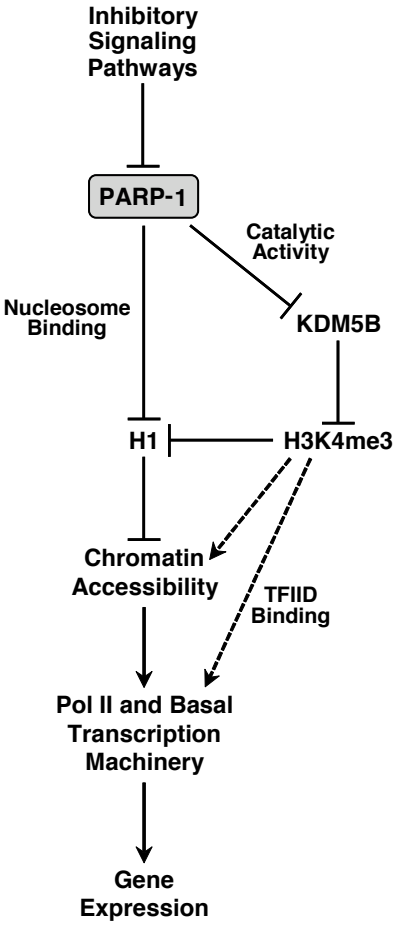

Figure 3.14. Model of PARP-1-dependent gene regulation.

This model is derived from the data shown herein and the literature. PARP-1 acts upstream of a host of molecular events at the promoters of positively regulated target genes to control chromatin architecture and the loading of the Pol II transcriptional machinery. Additional details are provided in the Discussion.

expression (Ruthenburg et al., 2007). Second, it regulates the composition of chromatin by promoting the exclusion of H1, a nucleosome-binding protein associated with gene repression (Happel and Doenecke, 2009). With respect to the former, I have shown herein that PARP-1 promotes the exclusion of the H3K4me3 demethylase KDM5B from promoter chromatin (Fig. 3.5B) through a mechanism that requires PARP-1 catalytic activity (Fig. 3.5D). As such, PARP-1 is able keep the levels of H3K4me3 elevated at the promoters of positively regulated genes, which helps to maintain an active chromatin environment. The intimate interplay between PARP-1 and KDM5B is illustrated by my studies showing that (1) PARP-1 and H3K4me3 colocalize on many promoters across the genome (Fig. 3.3) and (2) the requirement for PARP-1 to maintain a variety of molecular outcomes at the promoters of positively regulated target genes (e.g., Pol II and TBP binding, H1 exclusion, transcription) is abrogated upon KDM5B knockdown (Figs. 3.8, 3.9 and 3.10). In addition, my data suggest that while H3K4me3 demethylation by KDM5B is necessary for reducing gene expression, it is not sufficient, and that PARP-1 protein must also be physically removed from the promoter to allow for H1 binding and subsequent changes in chromatin structure.

How does PARP-1 exclude KDM5B and prevent KDM5B-dependent H3K4me3 demethylation? My results indicate that PARP-1 binds to and PARylates KDM5B (Figs. 3.5E and 3.5F), which inhibits the binding of KDM5B to promoter chromatin (Fig. 3.5D). PARP-1-mediated PARylation has been shown to be an effective mechanism for inhibiting the activity of transcription-related proteins due to its ability to block protein-protein or protein-DNA interactions (Kraus, 2008; Kraus and Lis, 2003). Although not directly tested in my experiments, inhibition of KDM5B enzymatic activity by PARylation is also possible. Previous studies have implicated PARP-1 enzymatic activity in the regulation of factor binding or exchange at target

promoters. For example, PARP-1 enzymatic activity is required to promote the exchange of a TLE1 corepressor complex for a HAT-containing coactivator complex during signal-dependent gene regulation in neuronal cells (Ju et al., 2004). In this regard, PARP-1's effects on KDM5B might be part of a broader process designed to establish a set of histone modification permissive to transcription (i.e., regulating the binding of enzymes that elevate H3K4me3 and H3/H4 acetylation, or reduced H3K27me3). These possibilities will be explored in future studies.

What role might H3K4me3 play in the PARP-1-dependent transcription process? Previous studies have shown that this modification creates a binding site for structural modules within a variety of proteins that regulate chromatin structure and transcription (Ruthenburg et al., 2007), including the PHD fingers of BPTF, TAF3, and ING family members (Li et al., 2006; Pena et al., 2006; Shi et al., 2006; Taverna et al., 2006; van Ingen et al., 2008; Vermeulen et al., 2007; Wysocka et al., 2006), the tandem chromodomains of CHD1 (Flanagan et al., 2005; Sims et al., 2005), and the double tudor domain of JMJD2A/KDM4A (Huang et al., 2006). The binding of H3K4me3 by TAF3, a component of TFIID, has been shown to direct the binding of TFIID to promoters. In this regard, I found that depletion of PARP-1, which reduces the levels of H3K4me3 at positively regulated promoters, also reduces the binding of TBP, another component of TFIID (Fig. 3.1F). These effects of PARP-1 on TBP binding are antagonized by KDM5B, and the requirement for PARP-1 to maintain TBP levels is abrogated upon knockdown of KDM5B (Figs. 3.8B, 3.9). Thus, one aspect of PARP-1-dependent maintenance of H3K3 trimethylation may be the promotion of TFIID binding (Fig. 3.14).

PARP-1 promotes the exclusion of H1 and the formation of open chromatin structures at the promoters of positively regulated genes

In addition to promoting the exclusion of KDM5B, PARP-1 antagonizes the binding of H1 at the promoters of positively regulated target genes (Figs. 3.1D and 3.14), likely through competition for overlapping binding sites on nucleosomes (Kim et al., 2004). PARP-1 catalytic activity is not required for this effect (Fig. 3.6), consistent with the results of previous biochemical assays showing that PARP-1 catalytic activity is not required for the displacement of H1 from nucleosomes (Kim et al., 2004) and PARylation of H1 does not block its binding to chromatin (Poirier et al., 1982). These results are also consistent with my genomic assays showing that PARP-1 and H1 exhibit a reciprocal pattern of binding at promoters across the genome (i.e., H1 is depleted where PARP-1 is enriched) (Krishnakumar et al., 2008). My current results, however, suggest that additional mechanisms may also contribute to the PARP-1-dependent exclusion of H1 from promoter chromatin. For example, the effects of PARP-1 knockdown on H1 binding are abrogated upon KDM5B knockdown (Figs. 3.8B, 3.9), suggesting a role for KDM5B. The actions of KDM5B in this PARP-1-dependent process may be through demethylation of H3K4me3 (Fig. 3.14), or perhaps demethylation of H1 (Kuzmichev et al., 2004; Trojer et al., 2009) or a chromatin- and transcription-related factor (Paik et al., 2007).

A key consequence of PARP-1-dependent antagonism of H1 binding is the maintenance of an open chromatin architecture at the TSSs of positively regulated genes. Previous studies have shown that H1 binding to nucleosomes can promote the formation of a closed chromatin architecture that is repressive to transcription (Happel and Doenecke, 2009; McBryant et al., 2006; Woodcock et al., 2006). In such cases, removal of H1 is required for efficient transcription. In this regard, I found that PARP-1-dependent antagonism of H1 binding correlates with an open chromatin

architecture (Fig. 3.2) and the binding of the Pol II transcription machinery (Pol II, TBP, and TFIIB; Fig. 3.1, E, F and G). My studies suggest a scenario with PARP-1 acting upstream of an ordered series of events including removal of H1, opening of the promoter chromatin architecture, and binding of the Pol II transcription machinery (Fig. 3.14). This is consistent with models proposed in the literature (Li et al., 2007; Morse, 2003).

Requirement for PARP-1 catalytic activity at the promoters of positively regulated target genes

The role of PARP-1 enzymatic activity in transcriptional regulation has been studied in various gene contexts with different transcriptional activators (Frizzell et al., 2009; Kraus, 2008; Kraus and Lis, 2003). In some cases, PARP-1 enzymatic activity was found to be required (e.g., with HES1 and Elk1) (Cohen-Armon et al., 2007; Ju et al., 2004), while in others it was not (e.g., NF-κB and retinoic acid receptor) (Hassa and Hottiger, 2002; Pavri et al., 2005). I found that PARP-1 enzymatic activity is not required for PARP-1-dependent effects on the transcription of positively regulated target genes per se (Fig. 3.6A), but it is required for some of the specific molecular outcomes that I tested. For example, PARP-1 enzymatic activity was required for the promotion of H3K4 trimethylation through inhibition of KDM5B binding (Fig. 3.5, C and D; Fig. 3.10), while it was dispensable for the inhibition of H1, Pol II, and TBP binding (Figs. 3.14; Fig. 3.6 D and F; Table 3.2).

Why might increased KDM5B binding upon PARP-1 knockdown (Fig. 3.5B), which inhibits the transcription of positively regulated target genes (Fig. 3.1B), have a different effect than increased KDM5B binding upon PARP-1 inhibition with PJ34 (Fig. 3.5D), which does not inhibit transcription of those genes (Fig. 3.6)? The answer is likely that with PARP-1 knockdown, the PARP-1 protein is removed, while with

Table 3.2. Requirement for PARP-1 protein and PARP-1 catalytic activity for specific molecular outcomes at the promoters of positively regulated genes.

Outcome[a]	PARP-1 protein required?[b]	PARP-1 catalytic activity required?[c]
Gene expression	Yes (Fig. 3.1B)	No (Fig. 3.6A)
H1 binding	Yes (Fig. 3.1D)	No (Fig. 3.6C)
Pol II binding	Yes (Fig. 3.1E)	No (Fig. 3.6D)
TBP binding	Yes (Fig. 3.1F)	No (Fig. 3.6F)
TFIIB binding	Yes (Fig. 3.1G)	n.d.
Open chromatin architecture at TSS	Yes (Fig. 3.2C)	n.d.
Promoting H3K4 trimethylation	Yes (Fig. 3.5A)	Yes (Fig. 3.5C)
Inhibiting KDM5B binding	Yes (Fig. 3.5B)	Yes (Fig. 3.5D)

[a] Expression was determined by RT-qPCR. H3K4 trimethylation and factor binding were determined by ChIP. Chromatin architecture at the TSS was determined by MNase protection assays.

[b] As determined by PARP-1 knockdown. The figure demonstrating the effect is listed in parentheses.

[c] As determined by PARP-1 inhibition with PJ34. The figure demonstrating the effect is listed in parentheses.

PJ34, it is not (Fig. 3.6). These results suggest that although PARP-1 enzymatic activity might prevent certain steps in the pathway involving KDM5B, the presence of the PARP-1 protein itself is required to inhibit the binding of H1 and allow subsequent steps, such as promoting an open chromatin architecture, facilitating Pol II binding, and allowing transcription (Fig. 3.14). Although the specific molecular role(s) played by PARP-1 enzymatic activity in the transcription process have been difficult to sort out (Cohen-Armon et al., 2007; Frizzell et al., 2009; Hassa and Hottiger, 2002; Ju et al., 2006; Ju et al., 2004; Pavri et al., 2005), my results have helped to discern the distinct molecular roles played by PARP-1 protein and PARP-1 enzymatic activity.

Cellular signaling pathways regulate PARP-1-dependent molecular outcomes at target gene promoters

PARP-1 has been implicated in a number of different signal-dependent gene regulatory pathways, including those mediated by activation of PKC, CaM kinase IIδ, estrogen signaling, retinoic acid signaling, or NF-κB-dependent proinflammatory signaling (Hassa and Hottiger, 2002; Ju et al., 2006; Ju et al., 2004; Kim et al., 2004; Kraus, 2008; Pavri et al., 2005). A previous study has shown that activation of PKC pathways in MCF-7 cells by TPA can stimulate PARP-1-dependent gene expression (Ju et al., 2006). I found that these same pathways can inhibit the expression of a subset of genes positively regulated by PARP-1, including *SCN1A* and *ITPR1* (Fig. 3.12, A and B), which encode signal-regulated ion channels that control sodium and calcium fluxes, respectively (Table 3.1). My molecular analyses indicate that TPA promotes the loss of PARP-1 from the promoters of these genes (Fig. 3.12B). Like shRNA-mediated knockdown of PARP-1, the TPA-dependent reduction of PARP-1 binding at these promoters leads to an increase in the binding of H1 and KDM5B (Fig. 3.12, C and H), as well as a reduction in the binding of Pol II and TBP (Fig. 3.12, D

and E), and the levels of H3K4me3 (Fig. 3.12G). Thus, modulation of PARP-1 binding to chromatin as an endpoint of cellular signaling pathways can provide a means for regulating gene expression outcomes.

PARP-1 and KDM5B have opposing effects in a common molecular pathway: Implications for breast cancers

My results indicate that KDM5B, an enzyme that demethylates H3K4me3, acts antagonistically to PARP-1 at the promoters of genes positively regulated by PARP-1 (Fig. 3.9), and vice versa (Fig. 3.8). Does this molecular antagonism manifest itself in some broader biological outcomes? There is a growing interest in the roles of both KDM5B and PARP-1 in breast cancers. KDM5B was initially isolated as a transcript overexpressed in human breast cancer cell lines (Lu et al., 1999), and as many as 90% of invasive ductal carcinomas express KDM5B (Barrett et al., 2007). Knockdown of KDM5B in MCF-7 cells increases the expression of the negative growth regulator BRCA1 and inhibits cell proliferation by interfering with G1 progression (Scibetta et al., 2007; Yamane et al., 2007). A number of studies have also implicated PARP-1 in the biology of breast cancers, and PARP inhibitors have been shown to be effective in killing breast cancer cells with hereditary mutations in *BRCA1* and *BRCA2* (Frizzell and Kraus, 2009; Lord and Ashworth, 2008). Interestingly, both KDM5B and PARP-1 mRNA levels may increase with increasing tumor grade in breast cancers (Fig. 3.15) (Zhao et al., 2004), suggesting a possible compensation by PARP-1 in an attempt to inhibit the growth promoting effects of KDM5B. The interplay between PARP-1 and KDM5B at the molecular level and in more complex biological processes will be an interesting area of investigation in future studies.

Figure 3.15. PARP-1 and KDM5B mRNA levels increase with increasing tumor grade in breast cancers.

The relative expression levels of PARP-1 and KDM5B in breast cancer samples were obtained from previously published data (Zhao et al., 2004) through Oncomine®. The patients had varying grades of tumors, ranging from 1 to 3, with 3 being the most advanced grade. All samples were compared to normal breast tissue (denoted as "grade 0"). Box limits represent the 25^{th} and 75^{th} percentiles, error bar limits represent the outer-most data points minus the outliers on either side, and the dots represent the upper and lower outlier data points. The differences are statistically significant by Student's t-test ($p < 0.01$).

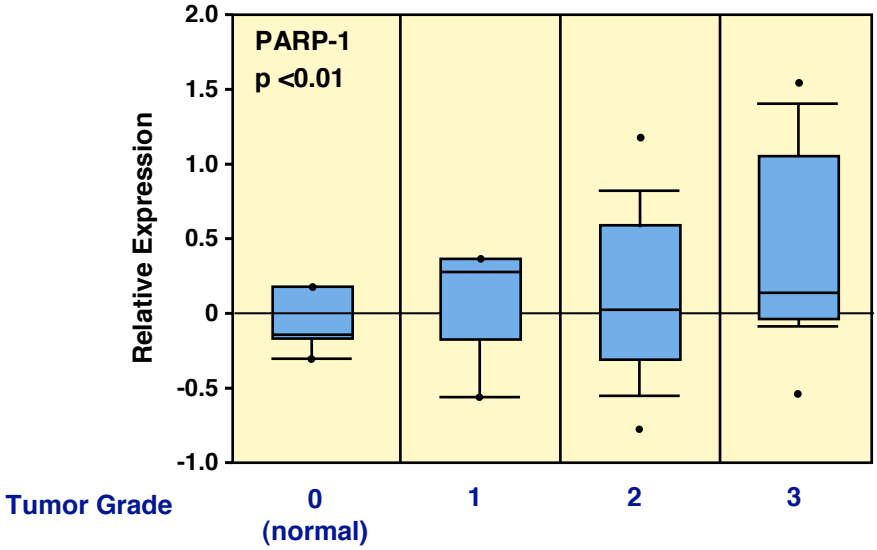

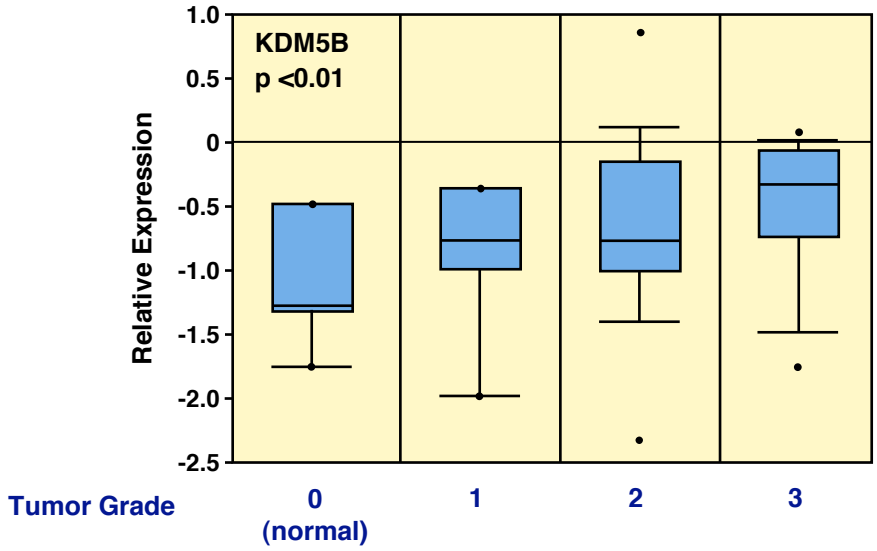

Collectively, my results have defined a functional interplay between PARP-1, H3K4 trimethylation, and the linker histone H1 at the promoters of genes positively

regulated by PARP-1. More broadly, my results have helped to clarify the molecular mechanisms by which specific chromatin-binding and histone-modifying proteins interact to alter chromatin structure and function to regulate gene transcription.

3.5 Materials and Methods

Cells lines, shRNA-mediated knockdown, and treatment with TPA

MCF-7 human breast cancer cells were kindly provided by Dr. Benita Katzenellenbogen (University of Illinois, Urbana-Champaign). The cells were maintained and plated for experiments in MEM supplemented with 5% calf serum. MCF-7 cells with stable shRNA-mediated depletion of PARP-1 and KDM5B were generated by retroviral-mediated gene transfer using the pSUPER.retro system with puromycin- and Geneticin® (G418)-selectable markers (Oligoengine). For experiments with PARP-1 knockdown only, I used cells harboring two short hairpin RNA sequences specifically targeting PARP-1, as described previously (Frizzell et al., 2009). For experiments with multiple factor knockdowns (e.g., PARP-1/KDM5B double knockdown), I used a control-matched set of cells stably expressing (1) an shRNA sequence targeting either PARP-1 (5'-GGGCAAGCACAGTGTCAAA-3') (Frizzell et al., 2009) or KDM5B (5'-GGCATTGAAGCTTGCACCT-3') (Scibetta et al., 2007) plus a control shRNA targeting luciferase (Luc; 5'-GATATGGGCTGAATACAAA-3') (Frizzell et al., 2009) (named PL and KL, respectively; see Fig. 5), (2) separate shRNAs targeting PARP-1 and KDM5B (PK), or (3) two shRNAs targeting luciferase (LL). The cells were selected and maintained under appropriate drug selection (i.e., 0.5 μg/ml puromycin and/or 800 μg/ml G418). For experiments involving TPA (12-O-tetradecanoylphorbol-13-acetate; Biomol, cat. no. PE-160) treatment, the cells were grown as described for the various experiments

noted below and treated with 100 ng/ml TPA dissolved in ethanol or a vehicle control. For experiments with PJ34 (Alexis Biochemicals, cat. no. ALX-270-289), the cells were grown as described and treated for 1 hour with 1 μM.

Antibodies

I used a previously characterized custom rabbit polyclonal anti-PARP-1 antibody for ChIP and Western blotting (Kim et al., 2004). The other ChIP grade antibodies, which were also used for Western blotting as appropriate, were as follows: H1 (Upstate/Millipore, cat. no. 05-475), H3 (Abcam, cat. no. ab1791), H3K4me3 (Abcam, cat. no. ab8580 or ab1012, or Active Motif cat. no. 3915), KDM5B (Abcam, cat. no. ab50958,), Pol II (Santa Cruz, cat. no. SC-899 and SC-900, mixed in a 1:4 ratio), TFIIB (Santa Cruz, cat. no. SC274X), and TBP (Santa Cruz, cat. no. SC273X). For immunoprecipitation experiments, the antibodies were as follows: KDM5B (see above), PAR (Trevigen, cat. no. 4335-AMC-050), and Rabbit IgG (Upstate/Millipore, cat. no. 12-370). Secondary antibodies for Western blotting were as follows: goat anti-rabbit HRP-conjugated IgG (Pierce, cat. no. 31460) and goat anti-mouse HRP-conjugated IgG (Pierce, cat.no. 31430).

mRNA expression analyses

Cells were seeded at ~1.5 x 10^5 cells per well in 6-well plates and grown for at least 3 days in the conditions noted above. The cells were collected at about 80% confluence, and total RNA was isolated using Trizol Reagent (Invitrogen) according to the manufacturer's protocols. The total RNA was reverse transcribed using oligo(dT) and subjected to real-time quantitative PCR using gene-specific primers (see primer sequences listed below; Section 2). All target gene transcripts were normalized to the

β-actin transcript. Each experiment was conducted a minimum of three times with independent isolates of total RNA to ensure reproducibility.

Chromatin immunoprecipitation (ChIP) assays

ChIP was performed essentially as described previously (Kininis et al., 2007). Briefly, cells were grown to ~80 to 90% confluence, cross-linked with 1% formaldehyde in PBS for 10 min. at 37°C, and quenched in 125 mM glycine in PBS for 5 min. at 4°C. For ChIP assays with the KDM5B antibody, I included an additional crosslinking step with 10 mM dimethyl suberimidate (DMS; Pierce, cat. no. 20700) for 10 min. prior to treatment with paraformaldehyde. The cells were collected by centrifugation and sonicated in Lysis Buffer [Tris•HCl pH 7.9, 10 mM EDTA, 50 mM NaCl, 1% SDS, and 1x protease inhibitor cocktail (Roche, cat no. 04 693 124 001)] to generate chromatin fragments of ~500 bp in length. The material was clarified by centrifugation, diluted 10-fold in Dilution Buffer (20 mM Tris•HCl pH 7.9, 2 mM EDTA, 150 mM NaCl, 0.5% Triton X-100, 1x protease inhibitor cocktail), and pre-cleared by incubation with protein A-agarose beads. The pre-cleared, chromatin-containing supernatant was used in immunoprecipitation reactions with antibodies against the factor of interest, or without antibodies as a control. Note that non-specific IgGs gave similar results as the no antibody controls (data not shown). The immunoprecipitated genomic DNA was cleared of protein and residual RNA by digestion with proteinase K and RNase H, respectively. The DNA was then extracted with phenol:chloroform:isoamyl alcohol and precipitated with ethanol. Quantitative real-time PCR (qPCR) was used to determine the enrichment of immunoprecipitated material relative to the input material using gene-specific primer sets to the specified

regions (see primer sequences listed below; Section 2). Each ChIP experiment was conducted a minimum of three times with independent chromatin isolates to ensure reproducibility.

Micrococcal nuclease (MNase) protection assays

Two 15 cm diameter plates of cells seeded at ~5 x 10^5 (for each condition) were grown to ~80 to 90% confluence, cross-linked with 1% formaldehyde in PBS for 10 min. at 37°C, and quenched in 125 mM glycine in PBS for 5 min. at 4°C. The cells were then collected, pelleted by centrifugation, and resuspended in 2 ml of Buffer A (10 mM HEPES pH 7.6, 10 mM KCl, 1.5 mM $MgCl_2$, 0.34 M sucrose, 10% glycerol, 1 mM DTT, 1x protease inhibitor cocktail). Triton-X-100 was added to a final concentration of 0.1 % and the mixture was incubated at 4°C for 8 min. The nuclei were collected by centrifugation (4000 rpm in a refrigerated microcentrifuge for 5 min.) and washed twice with Buffer A. The nuclear pellet was then resuspended in 1 ml of Buffer B (3 mM EDTA, 0.2 mM EGTA, 1 mM DTT, 1x protease inhibitor cocktail) and incubated at 4°C for 30 min. to lyse the nuclei. The chromatin was collected by centrifugation (4500 rpm in a refrigerated microcentrifuge for 5 min.) and washed twice with Buffer B. The pellet was then resuspended in 1 ml of MNase Buffer (50 mM Tris•HCl pH 7.4, 25 mM KCl, 12.5% glycerol, 10 mM $CaCl_2$, 4 mM $MgCl_2$ and 1 mM PMSF). The 1 ml of chromatin was divided into two 500 µl aliquots, and 400 units of MNase were added to one aliquot. Both aliquots were then incubated at 37°C for 8 min., after which EDTA (12.5 mM final concentration) and SDS (0.5% final concentration) were added to stop the reaction. For the control samples (without MNase), the genomic DNA was lightly sheared by sonication (27% amplitude for 3 rounds of 12 seconds using a Branson Sonifier) so that it could be subjected to PCR analysis. All samples were then incubated at 65°C overnight to reverse the

formaldehyde crosslinks. The DNA was cleared of protein and residual RNA by digestion with proteinase K and RNase H, respectively. The DNA was then extracted with phenol:chloroform:isoamyl alcohol and precipitated with ethanol. qPCR with overlapping amplicons (see below) was used to determine the enrichment of MNase digested DNA relative to sonicated genomic DNA ("relative protection") at specific genomic locations (see primer sequences listed below; Section 2). Each experiment was conducted a minimum of three times with independent biological replicates to ensure reproducibility.

Quantitative real-time PCR (qPCR)

Reverse transcribed mRNA, ChIPed DNA, and MNase digested DNA were analyzed by quantitative PCR. Briefly, DNA, 1x SYBR Green PCR master mix, and forward and reverse primers (250 nM) were used in 40 to 45 cycles of amplification (95°C for 15 sec, 60°C for 1 min) following an initial 10 min incubation at 95°C using an Applied Biosystems 7900 HT 384-well Sequence Detection System. Melting curve analysis was performed to ensure that only the targeted amplicon was amplified. The sequences of all primers used for RT-qPCR, ChIP-qPCR, and MNase-qPCR are listed in Section 2 below.

Statistical tests for the gene-specific assays

Each gene-specific experiment (i.e., RT-qPCR, ChIP-qPCR, MNase-qPCR) was conducted a minimum of three times with independent biological replicates to ensure reproducibility. The significance of differences between experimental and control samples was determined using a Student's t-test. Significance and p-values are listed in the figures legends,

Immunoprecipitation of KDM5B and detection of PARylation

Nuclear extract and immunoprecipitation protocols were adapted from Dignam et al. (1983) and Sif et al. (1998), respectively (Dignam et al., 1983; Sif et al., 1998). Two 15 cm diameter plates of cells seeded at ~5 x 10^5 (for each condition) were grown to ~80 to 90% confluence, treated if required, collected, and pelleted by centrifugation. The cells were incubated in Hypotonic Buffer for swelling (10 mM Tris pH 7.9, 20% glycerol, 1.5 mM $MgCl_2$, 0.1 mM EDTA, 10 mM KCl, 1x protease inhibitor cocktail, with 100 μM tannic acid to prevent degradation of existing PAR chains by poly(ADP-ribose) glycohydrolase) and lysed by Dounce homogenization using a 0.4 mm clearance pestle. The nuclei were collected by centrifugation (3000 rpm in a refrigerated microcentrifuge for 5 min.) and extracted in Extraction Buffer (20 mM HEPES pH 7.9, 25% glycerol, 0.42 M NaCl, 1.5 mM $MgCl_2$, 0.2 mM EDTA, and 1x protease inhibitor cocktail) for 10 min. on ice with intermittent agitation. The nuclear extract was clarified by centrifugation (maximum speed in a refrigerated microcentrifuge for 15 min) and diluted with Extraction Buffer lacking NaCl to bring the final NaCl concentration to 0.21 M. The extracts were incubated with 5 μl of KDM5B antibody (or rabbit IgG as a control) and protein A-agarose beads for 16 hours on ice with mixing. The beads were subjected to sequential washes in Wash Buffer (20 mM HEPES pH 7.9, 20% glycerol, 2 mM EDTA) containing 100 mM, 150 mM, or 300 mM KCl for each sequential wash. The beads were heated to 100 °C for 5 min in SDS-PAGE loading buffer to release the bound proteins. The immunoprecipitated material was subjected to Western blotting with the KDM5B (1:1000), PARP-1 (1:2000) and PAR (1:500) antibodies described above. The immunoprecipitation assays were preformed at least twice to ensure reproducibility.

Western blotting of nuclear extracts

Nuclear extracts were prepared as above. The resulting lysate was subjected to SDS-PAGE and Western blotting with antibodies to the following factors: PARP-1 (5 μg of total protein loaded, primary antibody used at 1:2000), H3 (5 μg of total protein loaded, primary antibody used at 1:2000), H3K4me3 (5 μg of total protein loaded, primary antibody used at 1:1000), and KDM5B (20 μg of total protein loaded, primary antibody used at 1:1000).

ChIP-chip

For the ChIP-chip analyses, the immunoprecipitated genomic DNA was blunted, amplified by ligation-mediated PCR (LM-PCR), and used to probe a custom, non-isothermal human (HG18) oligonucleotide genomic array from Nimblegen. The custom array contained ~2,100,000 features (tiling interval of 76 bp for the ~50-mer probes) containing 23,551 annotated RNA polymerase II-transcribed promoters (approximately -3 kb to +3 kb relative to the transcription start site for most promoters). Detailed information about the genomic regions tiled on the custom array is included with the data submission to NCBI/Gene Expression Omnibus (GEO accession number GSE19619). The ChIP-chip analyses were run a minimum of two times to ensure reproducibility.

Genomic data analyses

Genomic data analyses were performed using the statistical programming language R (R Development Core Team, 2006), as previously described (Krishnakumar et al., 2008). All data processing scripts are available upon request from the corresponding author and the raw data sets can be accessed through NCBI/GEO (accession number GSE19619). The $\log_2$ ratio data from each of the arrays was subjected to lowess

normalization (Smyth and Speed, 2003). A single array error model was generated using a 1 kb moving window with 250 bp steps in which both the mean probe log2 ratio and p-values were calculated for each window. The p-values are from a nonparametric Wilcoxon signed-rank test. Significant peaks were defined as the center of three consecutive windows with positive means, the center window with a mean greater than either adjacent window, and all windows having p-values less than 0.016. Correlation analyses, averaging (metagene) analyses, and gene categorization were done as previously described (Krishnakumar et al., 2008).

Primers for ChIP-qPCR, RT-qPCR, and MNase protection

• RT-qPCR:

b-ACTIN mRNA Fwd:	5’ - AGCTACGAGCTGCCTGAC -3 ’
b-ACTIN mRNA Rev:	5’ - AAGGTAGTTTCGTGGATGC - 3’
ABHD2 mRNA Fwd:	5’ - CACCTCTCTGAGCCTGTTCC- 3’
ABHD2 mRNA Rev:	5’ - CGCAGATGTTCAGCAATGTT- 3’
GDF15 mRNA Fwd:	5’ - CTACAATCCCATGGTGCTCA - 3’
GDF15 mRNA Rev:	5’ - TATGCAGTGGCAGTCTTTGG - 3’
ITPR1 mRNA Fwd:	5’ - TGCCTCCACAATTCTACG - 3’
ITPR1 mRNA Rev:	5’ - TGAATGTCCCACAGTTGC - 3’
KDM5B mRNA Fwd:	5’ - CGACAAAGCCAAGAGTCTCC - 3’
KDM5B mRNA Rev:	5’ - CTGCCGTAGCAAGGCTATTC - 3’
NELL2 mRNA Fwd:	5’ - TGAAGGGAACCACCTACC - 3’
NELL2 mRNA Rev:	5’ - ATTTGCCATCCACATACG - 3’
PARP-1 mRNA Fwd:	5’ - GTGTGGGAAGACCAAAGGAA - 3’
PARP-1 mRNA Rev:	5’ - TTCAAGAGCTCCCATGTTCA - 3’

SCN1A mRNA Fwd: 5’ - ATTGAAGGGAACCGATTG- 3’

SCN1A mRNA Rev: 5’ - ATCCCACATCCTTTGCTC- 3’

TMSL8 mRNA Fwd: 5’ - AACCTGCTATGATGGGTGCT - 3’

TMSL8 mRNA Rev: 5’ - CTGCAAAAGCATGCAACTTC - 3’

• ChIP-qPCR:

ABHD2 promoter Fwd: 5’ - GCCTCCACTCTGAGGAACAG - 3’

ABHD2 promoter Rev: 5’ - TTGTTCATTGGGCAGTTCAG - 3’

GDF15 promoter Fwd: 5’ - CTCAGATGCTCCTGGTGTTG - 3’

GDF15 promoter Rev: 5’ - CTCGGAATCTGGAGTCTTCG - 3’

ITPR1 promoter Fwd: 5’ - GAGCCCTAAGCAGCGTGTAG - 3’

ITPR1 promoter Rev: 5’ - CTCTCCAAGAGCTCCGAATG - 3’

NELL2 promoter Fwd: 5’ - TCCCCGGAGGAGCAGTCT - 3’

NELL2 promoter Rev: 5’ - CGCCCGAACCTGTTGTAAAG - 3’

SCN1A promoter Fwd: 5’ - ACCCTCCTCTCTCTCCTTGC - 3’

SCN1A promoter Rev: 5’ - GGGAGGAGGAGAAATTCGTT - 3’

TMSL8 promoter Fwd: 5’ - CGCGGGAACGCTAACCT - 3’

TMSL8 promoter Rev: 5’ - GTCCTCACCTGAAAGCTTGAAGA - 3’

• MNase-qPCR:

(Note: The primers labeled “a” to “u” tile from -300 to +300 bp relative to the TSS with approximately 30 bp spacing)

<u>i) ABHD2</u>

ABHD2a_Fwd: 5’ - GAGCTGGAAGAGGCCATAGA - 3’

ABHD2a_Rev: 5’ - ACCCGAAGGAGAGGAAAAGA - 3’

ABHD2b_Fwd:	5’ - CCTCCACATCTTTTCCTCTCC - 3’
ABHD2b_Rev:	5’ - GAGGAAGAAGGGTCGTGAGTC - 3’
ABHD2c_Fwd:	5’ - TGACTCACGACCCTTCTTCC - 3’
ABHD2c_Rev:	5’ - CAGGGGTGAAATTTGAGGTC - 3’
ABHD2d_Fwd:	5’ - TCACGACCCTTCTTCCTCTC - 3’
ABHD2d_Rev:	5’ - AGGCCGACTGACTGACTCAC - 3’
ABHD2e_Fwd:	5’ - ACCCCTGCGAAATTTGAGTA - 3’
ABHD2e_Rev:	5’ - TAGCTCAGCTGGGGCTCTTA - 3’
ABHD2f_Fwd:	5’ - GGCCTGGACCCATAAGAGC - 3’
ABHD2f_Rev:	5’ - CTGGTAGCTCAGCTGCTGGT - 3’
ABHD2g_Fwd:	5’ - AGCTACCAGCCGACCTCAT - 3’
ABHD2g_Rev:	5’ - AGAGGGCTGGGTAAGGTCA - 3’
ABHD2h_Fwd:	5’ - GTCGACAGCTGACCTTACCC - 3’
ABHD2h_Rev:	5’ - GGGTAATTGTGACCGCAAAC - 3’
ABHD2i_Fwd:	5’ - ACCCAGCCCTCTAAAGCAGT - 3’
ABHD2i_Rev:	5’ - GGGGTGAAGAGACGGGTAAT - 3’
ABHD2j_Fwd:	5’ - GTTTGCGGTCACAATTACCC - 3’
ABHD2j_Rev:	5’ - GGTCGTGTTTGATGTCGATG - 3’
ABHD2k_Fwd:	5’ - CCATCGACATCAAACACGAC - 3’
ABHD2k_Rev:	5’ - ATAAGGCCAGCCCGGAGT - 3’
ABHD2l_Fwd:	5’ - TCAAACACGACCCACCTTCT - 3’
ABHD2l_Rev:	5’ - CTTTAGTCCAGGGACCCAGA - 3’
ABHD2m_Fwd:	5’ - GGGCTGGCCTTATCCAGTAG - 3’
ABHD2m_Rev:	5’ - CATTTGACGGCTTTAGTCCA - 3’
ABHD2n_Fwd:	5’ - CCTGGACTAAAGCCGTCAAA - 3’
ABHD2n_Rev:	5’ - AGTGGAGGCGGGATTCTTAG - 3’

ABHD2o_Fwd:	5’ - TGAGGAGCTCTCCCCTAAGA - 3’
ABHD2o_Rev:	5’ - GATCAGCGAAGCTGTTCCTC - 3’
ABHD2p_Fwd:	5’ - CTAAGAATCCCGCCTCCACT - 3’
ABHD2p_Rev:	5’ - GGATCCATTGATCAGCGAAG - 3’
ABHD2q_Fwd:	5’ - AATGGATCCCCTCCTAGACG - 3’
ABHD2q_Rev:	5’ - CTTGTTCATTGGGCAGTTCA - 3’
ABHD2r_Fwd:	5’ - GATCCCCTCCTAGACGCAAT - 3’
ABHD2r_Rev:	5’ - TTGTTCATTGGGCAGTTCAG - 3’
ABHD2s_Fwd:	5’ - GTGGAGAAGCGGCTGAACT - 3’
ABHD2s_Rev:	5’ - CCCCTAACCACGGAAACC - 3’
ABHD2t_Fwd:	5’ - AAGCGGTTTCCGTGGTTAG - 3’
ABHD2t_Rev:	5’ - TCATGGATATACAGCCGGAAC - 3’
ABHD2u_Fwd:	5’ - GTGGCGGCAGTTACTTGG - 3’
ABHD2u_Rev:	5’ - GGCGCTCATGGATATACAGC - 3’

ii) GDF15

GDF15a_Fwd:	5’ - GGCAGAGAGGCATGACACAT - 3’
GDF15a_Rev:	5’ - TTGGGGTCAAAGGCTAAAGA - 3’
GDF15b_Fwd:	5’ - CCCTTCCTGGCTCCATCTA - 3’
GDF15b_Rev:	5’ - CCCATGGGATTTCCTCTCTT - 3’
GDF15c_Fwd:	5’ - TGCTTCCTTTGTTTTTCACCA - 3’
GDF15c_Rev:	5’ - GACAAGAGTTTAAGAGGTGGCTGT - 3’
GDF15d_Fwd:	5’ - CTTTGACCCCAACCAAAAAG - 3’
GDF15d_Rev:	5’ - GGGAGTCTTTTTGGAGGAAAA - 3’
GDF15e_Fwd:	5’ - CCTTTGACCCCAACCAAAA - 3’
GDF15e_Rev:	5’ - CTGGGAGTCTTTTTGGAGGAA - 3’

GDF15f_Fwd:	5’ - AGGAAATCCCATGGGCATAGA - 3’
GDF15f_Rev:	5’ - AGCCTGGGAGTCTTTTTGGA - 3’
GDF15g_Fwd:	5’ - AACTCTTGTCTGGAATTTTTCACAT - 3’
GDF15g_Rev:	5’ - GGCCTCAGTATCCTCTTCCTC - 3’
GDF15h_Fwd:	5’ - TTTTTCCTCCAAAAAGACTCC - 3’
GDF15h_Rev:	5’ - GGGCGCTCCTAGTAAAGCTA - 3’
GDF15i_Fwd:	5’ - AGGCTGGAATGGTGTCCTC - 3’
GDF15i_Rev:	5’ - TAGGGGGAGGATCTTTAGGTG - 3’
GDF15j_Fwd:	5’ - TACTGAGGCCCAGAAATGTG - 3’
GDF15j_Rev:	5’ - AAACACTCCAATGACCACAGC - 3’
GDF15k_Fwd:	5’ - CCAGAAATGTGCCCTAGCTT - 3’
GDF15k_Rev:	5’ - TAAACACTCCAATGACCACAGC - 3’
GDF15l_Fwd:	5’ - CACCTAAAGATCCTCCCCCTA - 3’
GDF15l_Rev:	5’ - CGTCTCCGCCTGCTCAGT - 3’
GDF15m_Fwd:	5’ - GATCCTCCCCCTAAATACACC - 3’
GDF15m_Rev:	5’ - TCTCCGCCTGCTCAGTCC - 3’
GDF15n_Fwd:	5’ - CAGCTGTGGTCATTGGAGTG - 3’
GDF15n_Rev:	5’ - TTTATAGTCCCCGGACTTTGTC - 3’
GDF15o_Fwd:	5’ - GACTGAGCAGGCGGAGAC - 3’
GDF15o_Rev:	5’ - CCGGACCGGCCTTTATAGT - 3’
GDF15p_Fwd:	5’ - AAAGTCCGGGGACTATAAAGG - 3’
GDF15p_Rev:	5’ - GAGCTGGGACTGACCAGATG - 3’
GDF15q_Fwd:	5’ - ATCTGGTCAGTCCCAGCTCA - 3’
GDF15q_Rev:	5’ - CCATTCACCGTCCTGAGTTC - 3’
GDF15r_Fwd:	5’ - GAACTCAGGACGGTGAATGG - 3’
GDF15r_Rev:	5’ - ACGAGAGCACCAGCAACAC - 3’

GDF15s_Fwd: 5’ - CTCAGATGCTCCTGGTGTTG - 3’

GDF15s_Rev: 5’ - AGGGTCCCGGGAAACTTG - 3’

GDF15t_Fwd: 5’ - AGTTTCCCGGGACCCTCA - 3’

GDF15t_Rev: 5’ - TCTCGGAATCTGGAGTCTTCG - 3’

GDF15u_Fwd: 5’ - CTCCAGATTCCGAGAGTTGC - 3’

GDF15u_Rev: 5’ - AGCCTGGTTAGCAGGTCCTC - 3’

iii) ITPR1

ITPR1a_Fwd: 5’ - AGAAATCCGAGCTCCTAGCC - 3’

ITPR1a_Rev: 5’ - CAAAGTCACCCCTGGGAAG - 3’

ITPR1b_Fwd: 5’ - CCCCAGTGACACCTGGATT - 3’

ITPR1b_Rev: 5’ - GAGCCAGCCGTTCAAAGTC - 3’

ITPR1c_Fwd: 5’ - CTTCCCAGGGGTGACTTTG - 3’

ITPR1c_Rev: 5’ - AGGCTTTCAGGCTGCTGAG - 3’

ITPR1d_Fwd: 5’ - CTTCCCAGGGGTGACTTTG - 3’

ITPR1d_Rev: 5’ - GAGGCTTTCAGGCTGCTG - 3’

ITPR1e_Fwd: 5’ - CAAGGAACAGGCTCAGCAG - 3’

ITPR1e_Rev: 5’ - GGGCTGGGCCCTAAATAGAC - 3’

ITPR1f_Fwd: 5’ - CCCGCACGCGTCTATTTA - 3’

ITPR1f_Rev: 5’ - TAGTCCAAGTAGCGGGTCGT - 3’

ITPR1g_Fwd: 5’ - CAGGGGATTCTGGGACTTGT - 3’

ITPR1g_Rev: 5’ - TAGTCCAAGTAGCGGGTCGT - 3’

ITPR1h_Fwd: 5’ - AGGGGATTCTGGGACTTGTAG - 3’

ITPR1h_Rev: 5’ - GCTTATATAGGCCGGGAAGC - 3’

ITPR1i_Fwd: 5’ - CAGGGGATTCTGGGACTTGT - 3’

ITPR1i_Rev: 5’ - GCTTATATAGGCCGGGAAGC - 3’

ITPR1j_Fwd:	5’ - CGACCCGCTACTTGGACTAC - 3’
ITPR1j_Rev:	5’ - GCAGCACATCCACATGGTTA - 3’
ITPR1k_Fwd:	5’ - CGACCCGCTACTTGGACTAC - 3’
ITPR1k_Rev:	5’ - AGCAGCACATCCACATGGT - 3’
ITPR1l_Fwd:	5’ - ATGTGGATGTGCTGCTGAAG - 3’
ITPR1l_Rev:	5’ - TGCGCTTTCTCTCTCTCCAC - 3’
ITPR1m_Fwd:	5’ - ATGTGGATGTGCTGCTGAAG - 3’
ITPR1m_Rev:	5’ - TTAGGATGGAAGCGGAACAC - 3’
ITPR1n_Fwd:	5’ - GGGGGTGGAGAGAGAGAAAG - 3’
ITPR1n_Rev:	5’ - TCGTTCCGTTAGGATGGAAG - 3’
ITPR1o_Fwd:	5’ - AGGGGGTGGAGAGAGAGAAA - 3’
ITPR1o_Rev:	5’ - GTTAGGATGGAAGCGGAACA - 3’
ITPR1p_Fwd:	5’ - GTGTTCCGCTTCCATCCTAA - 3’
ITPR1p_Rev:	5’ - CGAGGAGAGGGGTTAGCAG - 3’
ITPR1q_Fwd:	5’ - TTCCATCCTAACGGAACGAG - 3’
ITPR1q_Rev:	5’ - CGAGGAGAGGGGTTAGCAG - 3’
ITPR1r_Fwd:	5’ - CCGGGCGCAGAAGTTTTT - 3’
ITPR1r_Rev:	5’ - TGCATGCACATCCATCAAG - 3’
ITPR1s_Fwd:	5’ - CTCTCGGGGAGATCTTGATG - 3’
ITPR1s_Rev:	5’ - GTAAAGGAACCCCCAAATGC - 3’
ITPR1t_Fwd:	5’ - CGGGGAGATCTTGATGGAT - 3’
ITPR1t_Rev:	5’ - AACAACTGCCCGCAGTAAAG - 3’
ITPR1u_Fwd:	5’ - CATGCACTTGGCATGCATTT - 3’
ITPR1u_Rev:	5’ - AAAACAACTGCCCGCAGTAAA - 3’

iv) NELL2

NELL2a_Fwd:	5’ - AAAGACCGCCCATCAACTTA - 3’
NELL2a_Rev:	5’ – TTCTCCCTCCCTCTCTCGAT - 3’
NELL2b_Fwd:	5’ - TTCAATCCCGAAAGGAGGTT - 3’
NELL2b_Rev:	5’ – GTTGCAGCCTCAGCTCTTCT - 3’
NELL2c_Fwd:	5’ - AGAGGGAGGGAGAAGAGCTG - 3’
NELL2c_Rev:	5’ - GTCTCCTGGATGCCAAACC - 3’
NELL2d_Fwd:	5’ - GAGAAGAGCTGAGGCTGCAA - 3’
NELL2d_Rev:	5’ - GGTCTCCTGGATGCCAAAC - 3’
NELL2e_Fwd:	5’ - CTAGACCGGGTTTGGCATC - 3’
NELL2e_Rev:	5’ - GAGGCGGGGTAAGGAGGA - 3’
NELL2f_Fwd:	5’ -CCCTCCCTCCTCCTTACCC - 3’
NELL2f_Rev:	5’ - GAGACGCGCGGAGAGACT - 3’
NELL2g_Fwd:	5’ - GCCCCTCCCTCCTCCTTA - 3’
NELL2g_Rev:	5’ - AGAAAGCTCCGGGAGACG - 3’
NELL2h_Fwd:	5’ - CCCGGAGGAGCAGTCTCT - 3’
NELL2h_Rev:	5’ - CGAACCTGTTGTAAAGGCAGA - 3’
NELL2i_Fwd:	5’ - CGTCTCCCGGAGCTTTCT - 3’
NELL2i_Rev:	5’ - CGCCCGAACCTGTTGTAA - 3’
NELL2j_Fwd:	5’ - TCTGCCTTTACAACAGGTTCG - 3’
NELL2j_Rev:	5’ - ACTCGCACACCCGGTAGA - 3’
NELL2k_Fwd:	5’ - CTGCCTTTACAACAGGTTCG - 3’
NELL2k_Rev:	5’ - TAAAAGCAGCCAAAGACTCG - 3’
NELL2l_Fwd:	5’ - TCTACCGGGTGTGCGAGT - 3’
NELL2l_Rev:	5’ - ATTAGCTCCCGAGCCGAATA - 3’
NELL2m_Fwd:	5’ - GCGAGTCTTTGGCTGCTTT - 3’

NELL2m_Rev: 5’ - GCTCCGTCGGGGAATTAG - 3’

NELL2n_Fwd: 5’ - TTATTCGGCTCGGGAGCTA - 3’

NELL2n_Rev: 5’ - CAATGCGCACATCATTCC - 3’

NELL2o_Fwd: 5’ - TATTCGGCTCGGGAGCTA - 3’

NELL2o_Rev: 5’ - CTCCAATGCGCACATCATT - 3’

NELL2p_Fwd: 5’ - CTGCGTGTGGGAATGATGT - 3’

NELL2p_Rev: 5’ - GCGCGTGAAGAACTTAGACC - 3’

NELL2q_Fwd: 5’ - CTGCGTGTGGGAATGATGT - 3’

NELL2q_Rev: 5’ - GCGCGTGAAGAACTTAGACC - 3’

NELL2r_Fwd: 5’ - CGCATTGGAGGGTCTAAGTT - 3’

NELL2r_Rev: 5’ - ACGCTTTGGTTGCCTAAGAA - 3’

NELL2s_Fwd: 5’ - GAGGCCTCCCTTTTCTTTCT - 3’

NELL2s_Rev: 5’ - GCTGCCTCGGATTTACTGAT - 3’

NELL2t_Fwd: 5’ - TTCTTAGGCAACCAAAGCGTA - 3’

NELL2t_Rev: 5’ - GCGGGAAAATAACGTTTGTC - 3’

NELL2u_Fwd: 5’ - CAGTAAATCCGAGGCAGCAG - 3’

NELL2u_Rev: 5’ - TGGAATCAAGCGGGAAAATA - 3’

v) SCN1A

SCN1Aa_Fwd: 5’ - CCTTTTCCCCTCATCCTTGT - 3’

SCN1Aa_Rev: 5’ - TGTGCGTATAAAGGCAAAGG - 3’

SCN1Ab_Fwd: 5’ - TCCTTTTCCCCTCATCCTTG - 3’

SCN1Ab_Rev: 5’ - TGACACACCCAGAAGATGGA - 3’

SCN1Ac_Fwd: 5’ - CCTTTGCCTTTATACGCACAGTCT - 3’

SCN1Ac_Rev: 5’ - CAGTCTGTGACACACCCAGA - 3’

SCN1Ad_Fwd: 5’ - CTGGGTGTGTCACAGACTGAA - 3’

SCN1Ad_Rev:	5’ - TGGTTCAAATATGGCCTTAATCA - 3’
SCN1Ae_Fwd:	5’ - TTTGATTAAGGCCATATTTGAACC - 3’
SCN1Ae_Rev:	5’ - CAGGAACTGTGCCATGAGTTT - 3’
SCN1Af_Fwd:	5’ - TGATTAAGGCCATATTTGAACCA - 3’
SCN1Af_Rev:	5’ - ACAGGAACTGTGCCATGAGT - 3’
SCN1Ag_Fwd:	5’ - AACTCATGGCACAGTTCCTGTA - 3’
SCN1Ag_Rev:	5’ - CAAATGGTTTCTGTGTTGAGTTT - 3’
SCN1Ah_Fwd:	5’ - AAACTCAACACAGAAACCATTTG - 3’
SCN1Ah_Rev:	5’ - TCCTTAAATTGAAAGGTGATTTCTAA - 3’
SCN1Ai_Fwd:	5’ - AAACTCAACACAGAAACCATTTGT - 3’
SCN1Ai_Rev:	5’ - TTTCTCCTTAAATTGAAAGGTGATTT - 3’
SCN1Aj_Fwd:	5’ - CACCTTTCAATTTAAGGAGAAAACA - 3’
SCN1Aj_Rev:	5’ - TGTCATGAAACATGAGCTAGAGG - 3’
SCN1Ak_Fwd:	5’ - CACCTTTCAATTTAAGGAGAAAACA - 3’
SCN1Ak_Rev:	5’ - TCATGAAACATGAGCTAGAGGA - 3’
SCN1Al_Fwd:	5’ - GCTCATGTTTCATGACAAGAATTT - 3’
SCN1Al_Rev:	5’ - AGGAATACAGATATTTTAAAGAGTGGA - 3’
SCN1Am_Fwd:	5’ - GTCCACTCTTTAAAATATCTGTATTCC - 3’
SCN1Am_Rev:	5’ - TGCATATGAAATTCCTAAAATAAAAGG - 3’
SCN1An_Fwd:	5’ - GGAATTTCATATGCAGAATAAATGGT - 3’
SCN1An_Rev:	5’ - TGCTCCATCTTGTCATCCTG - 3’
SCN1Ao_Fwd:	5’ - TGCAGGATGACAAGATGGAG - 3’
SCN1Ao_Rev:	5’ - TGTCAGGTCCTGGTGGTACA - 3’
SCN1Ap_Fwd:	5’ - TGTACCACCAGGACCTGACA - 3’
SCN1Ap_Rev:	5’ - TTCTGCAATGCGTCTTTCAA - 3’
SCN1Aq_Fwd:	5’ - TCTCTTGCGGCTATTGAAAGA - 3’

SCN1Aq_Rev: 5’ - TTGGGATTCTTTGCCTTTTC - 3’

SCN1Ar_Fwd: 5’ - TGAAAGACGCATTGCAGAAG - 3’

SCN1Ar_Rev: 5’ - GCCATTTTCGTCGTCATCTT - 3’

SCN1As_Fwd: 5’ - AAAAGGCAAAGAATCCCAAA - 3’

SCN1As_Rev: 5’ - GCCATTTTCGTCGTCATCTT - 3’

SCN1At_Fwd: 5’ - AAAAGATGACGACGAAAATGG - 3’

SCN1At_Rev: 5’ - AAGGTTCTTTCCAGCTTCCA - 3’

SCN1Au_Fwd: 5’ - GCCCAAAGCCAAATAGTGAC - 3’

SCN1Au_Rev: 5’ - TGACACCATCTCTGGAGGAA - 3’

vi) TMSL8

TMSL8a_Fwd: 5’ - CTGGCCAAGGATTAGAGCAG - 3’

TMSL8a_Rev: 5’ - GCCCAAGGATGCTGTGATAA - 3’

TMSL8b_Fwd: 5’ - GAGCCCCACTTCCAACCTAC - 3’

TMSL8b_Rev: 5’ - CCGGTATTTAGGCTCTTTCG - 3’

TMSL8c_Fwd: 5’ - GGCCCCAATGGCTATAAAAA - 3’

TMSL8c_Rev: 5’ - GAGGTCCAAGCTGAATGACC - 3’

TMSL8d_Fwd: 5’ - ATACCGGTCATTCAGCTTGG - 3’

TMSL8d_Rev: 5’ - ATCTCGCCCAGTGAGCTTAG - 3’

TMSL8e_Fwd: 5’ - GGTCATTCAGCTTGGACCTC - 3’

TMSL8e_Rev: 5’ - ATCTCGCCCAGTGAGCTTAG - 3’

TMSL8f_Fwd: 5’ - CTAAGCTCACTGGGCGAGAT - 3’

TMSL8f_Rev: 5’ - TCCACATACCCTTCATCCTGA - 3’

TMSL8g_Fwd: 5’ - TCAGGATGAAGGGTATGTGGA - 3’

TMSL8g_Rev: 5’ - GGCCTCTTCCACTGCTTTAG - 3’

TMSL8h_Fwd: 5’ - TGGACCCTCAGGACTAAAGC - 3’

TMSL8h_Rev:	5’ - GGGCTTGGTGAAGTCAGAGC - 3’
TMSL8i_Fwd:	5’ - GGACCCTCAGGACTAAAGCA - 3’
TMSL8i_Rev:	5’ - GGGGCTTGGTGAAGTCAGA - 3’
TMSL8j_Fwd:	5’ - GGTCGGCTCTGACTTCACC - 3’
TMSL8j_Rev:	5’ - GCGTCCACCCTCTCCTCTA - 3’
TMSL8k_Fwd:	5’ - GTCGGCTCTGACTTCACCA - 3’
TMSL8k_Rev:	5’ - CCTCCGCTTGAGTGTACAGA - 3’
TMSL8l_Fwd:	5’ - GATCCTAGAGGAGAGGGTGGA - 3’
TMSL8l_Rev:	5’ - CCTCCTCCGCTTGAGTGT - 3’
TMSL8m_Fwd:	5’ - CTGTACACTCAAGCGGAGGA - 3’
TMSL8m_Rev:	5’ - TCTGATTGGCCAAAGGTTTC - 3’
TMSL8n_Fwd:	5’ - GAAACCTTTGGCCAATCAGA - 3’
TMSL8n_Rev:	5’ - AGTGCTAAGCCACCCAGCAG - 3’
TMSL8o_Fwd:	5’ - GAAACCTTTGGCCAATCAGA - 3’
TMSL8o_Rev:	5’ - CGGACCAGGTTAGCGTTC - 3’
TMSL8p_Fwd:	5’ - CTGCTGGGTGGCTTAGCACT - 3’
TMSL8p_Rev:	5’ - GGGGCTGAGACCCAGACT - 3’
TMSL8q_Fwd:	5’ - AGCGAGTCTGGGTCTCAGC - 3’
TMSL8q_Rev:	5’ - AAGCTTGAAGACTCGTGAAAGG - 3’
TMSL8r_Fwd:	5’ - AGCGAGTCTGGGTCTCAGC - 3’
TMSL8r_Rev:	5’ - AAGCTTGAAGACTCGTGAAAGG - 3’
TMSL8s_Fwd:	5’ - ACAGCCTTTCACGAGTCTTCA - 3’
TMSL8s_Rev:	5’ - CATGGTCCTCTGGCTCCTG - 3’
TMSL8t_Fwd:	5’ - CAGCCTTTCACGAGTCTTCA - 3’
TMSL8t_Rev:	5’ - CATCCCCATGGTCCTCTG - 3’
TMSL8u_Fwd:	5’ - GACCATGGGGATGGGAAG - 3’

TMSL8u_Rev: 5’ - CCAACCTCGGCTCCTCTG - 3’

REFERENCES

Allis, C.D., Berger, S.L., Cote, J., Dent, S., Jenuwien, T., Kouzarides, T., Pillus, L., Reinberg, D., Shi, Y., Shiekhattar, R., *et al*. (2007). New nomenclature for chromatin-modifying enzymes. Cell *131*, 633-636.

Barrett, A., Santangelo, S., Tan, K., Catchpole, S., Roberts, K., Spencer-Dene, B., Hall, D., Scibetta, A., Burchell, J., Verdin, E., *et al*. (2007). Breast cancer associated transcriptional repressor PLU-1/JARID1B interacts directly with histone deacetylases. Int J Cancer *121*, 265-275.

Barski, A., Cuddapah, S., Cui, K., Roh, T.Y., Schones, D.E., Wang, Z., Wei, G., Chepelev, I., and Zhao, K. (2007). High-resolution profiling of histone methylations in the human genome. Cell *129*, 823-837.

Berger, S.L. (2007). The complex language of chromatin regulation during transcription. Nature *447*, 407-412.

Bernstein, B.E., Kamal, M., Lindblad-Toh, K., Bekiranov, S., Bailey, D.K., Huebert, D.J., McMahon, S., Karlsson, E.K., Kulbokas, E.J., 3rd, Gingeras, T.R., *et al*. (2005). Genomic maps and comparative analysis of histone modifications in human and mouse. Cell *120*, 169-181.

Braunschweig, U., Hogan, G.J., Pagie, L., and van Steensel, B. (2009). Histone H1 binding is inhibited by histone variant H3.3. EMBO J *28*, 3635-3645.

Caiafa, P., Guastafierro, T., and Zampieri, M. (2009). Epigenetics: poly(ADP-ribosyl)ation of PARP-1 regulates genomic methylation patterns. FASEB J *23*, 672-678.

Campos, E.I., and Reinberg, D. (2009). Histones: annotating chromatin. Annu Rev Genet *43*, 559-599.

Cohen-Armon, M., Visochek, L., Rozensal, D., Kalal, A., Geistrikh, I., Klein, R., Bendetz-Nezer, S., Yao, Z., and Seger, R. (2007). DNA-independent PARP-1 activation by phosphorylated ERK2 increases Elk1 activity: a link to histone acetylation. Mol Cell *25*, 297-308.

Cunliffe, H.E., Ringner, M., Bilke, S., Walker, R.L., Cheung, J.M., Chen, Y., and Meltzer, P.S. (2003). The gene expression response of breast cancer to growth regulators: patterns and correlation with tumor expression profiles. Cancer Res *63*, 7158-7166.

Drew, Y., and Plummer, R. (2009). The emerging potential of poly(ADP-ribose) polymerase inhibitors in the treatment of breast cancer. Curr Opin Obstet Gynecol.

Fan, Y., Nikitina, T., Zhao, J., Fleury, T.J., Bhattacharyya, R., Bouhassira, E.E., Stein, A., Woodcock, C.L., and Skoultchi, A.I. (2005). Histone H1 depletion in mammals alters global chromatin structure but causes specific changes in gene regulation. Cell *123*, 1199-1212.

Flanagan, J.F., Mi, L.Z., Chruszcz, M., Cymborowski, M., Clines, K.L., Kim, Y., Minor, W., Rastinejad, F., and Khorasanizadeh, S. (2005). Double chromodomains cooperate to recognize the methylated histone H3 tail. Nature *438*, 1181-1185.

Frizzell, K.M., Gamble, M.J., Berrocal, J.G., Zhang, T., Krishnakumar, R., Cen, Y., Sauve, A.A., and Kraus, W.L. (2009). Global analysis of transcriptional regulation by poly(ADP-ribose) polymerase-1 and poly(ADP-ribose) glycohydrolase in MCF-7 human breast cancer cells. J Biol Chem.

Frizzell, K.M., and Kraus, W.L. (2009). PARP inhibitors and the treatment of breast cancer: beyond BRCA1/2? Breast Can Res *11*, 111.

Guenther, M.G., Levine, S.S., Boyer, L.A., Jaenisch, R., and Young, R.A. (2007). A chromatin landmark and transcription initiation at most promoters in human cells. Cell *130*, 77-88.

Happel, N., and Doenecke, D. (2009). Histone H1 and its isoforms: contribution to chromatin structure and function. Gene *431*, 1-12.

Hassa, P.O., and Hottiger, M.O. (2002). The functional role of poly(ADP-ribose)polymerase 1 as novel coactivator of NF-kappaB in inflammatory disorders. Cell Mol Life Sci *59*, 1534-1553.

Huang, Y., Fang, J., Bedford, M.T., Zhang, Y., and Xu, R.M. (2006). Recognition of histone H3 lysine-4 methylation by the double tudor domain of JMJD2A. Science *312*, 748-751.

Inbar-Rozensal, D., Castiel, A., Visochek, L., Castel, D., Dantzer, F., Izraeli, S., and Cohen-Armon, M. (2009). A selective eradication of human non-hereditary breast cancer cells by phenanthridine derived poly(ADP-ribose) polymerase inhibitors. Breast Cancer Research.

Ju, B.G., Lunyak, V.V., Perissi, V., Garcia-Bassets, I., Rose, D.W., Glass, C.K., and Rosenfeld, M.G. (2006). A topoisomerase IIbeta-mediated dsDNA break required for regulated transcription. Science *312*, 1798-1802.

Ju, B.G., Solum, D., Song, E.J., Lee, K.J., Rose, D.W., Glass, C.K., and Rosenfeld, M.G. (2004). Activating the PARP-1 sensor component of the groucho/ TLE1

corepressor complex mediates a CaMKinase IIdelta-dependent neurogenic gene activation pathway. Cell *119*, 815-829.

Kim, M.Y., Mauro, S., Gevry, N., Lis, J.T., and Kraus, W.L. (2004). NAD+-dependent modulation of chromatin structure and transcription by nucleosome binding properties of PARP-1. Cell *119*, 803-814.

Kim, M.Y., Zhang, T., and Kraus, W.L. (2005). Poly(ADP-ribosyl)ation by PARP-1: 'PAR-laying' NAD+ into a nuclear signal. Genes Dev *19*, 1951-1967.

Kininis, M., Chen, B.S., Diehl, A.G., Isaacs, G.D., Zhang, T., Siepel, A.C., Clark, A.G., and Kraus, W.L. (2007). Genomic analyses of transcription factor binding, histone acetylation, and gene expression reveal mechanistically distinct classes of estrogen-regulated promoters. Mol Cell Biol *27*, 5090-5104.

Kraus, W.L. (2008). Transcriptional control by PARP-1: chromatin modulation, enhancer-binding, coregulation, and insulation. Curr Opin Cell Biol *20*, 294-302.

Kraus, W.L., and Lis, J.T. (2003). PARP goes transcription. Cell *113*, 677-683.

Krishnakumar, R., Gamble, M.J., Frizzell, K.M., Berrocal, J.G., Kininis, M., and Kraus, W.L. (2008). Reciprocal binding of PARP-1 and histone H1 at promoters specifies transcriptional outcomes. Science *319*, 819-821.

Kuzmichev, A., Jenuwein, T., Tempst, P., and Reinberg, D. (2004). Different EZH2-containing complexes target methylation of histone H1 or nucleosomal histone H3. Mol Cell *14*, 183-193.

Lacroix, M., Haibe-Kains, B., Hennuy, B., Laes, J.F., Lallemand, F., Gonze, I., Cardoso, F., Piccart, M., Leclercq, G., and Sotiriou, C. (2004). Gene regulation by phorbol 12-myristate 13-acetate in MCF-7 and MDA-MB-231, two breast cancer cell lines exhibiting highly different phenotypes. Oncol Rep *12*, 701-707.

Li, B., Carey, M., and Workman, J.L. (2007). The role of chromatin during transcription. Cell *128*, 707-719.

Li, H., Ilin, S., Wang, W., Duncan, E.M., Wysocka, J., Allis, C.D., and Patel, D.J. (2006). Molecular basis for site-specific read-out of histone H3K4me3 by the BPTF PHD finger of NURF. Nature *442*, 91-95.

Liu, W.S., and Heckman, C.A. (1998). The sevenfold way of PKC regulation. Cell Signal *10*, 529-542.

Lord, C.J., and Ashworth, A. (2008). Targeted therapy for cancer using PARP inhibitors. Curr Opin Pharmacol *8*, 363-369.

Lu, P.J., Sundquist, K., Baeckstrom, D., Poulsom, R., Hanby, A., Meier-Ewert, S., Jones, T., Mitchell, M., Pitha-Rowe, P., Freemont, P., and Taylor-Papadimitriou, J. (1999). A novel gene (PLU-1) containing highly conserved putative DNA/chromatin binding motifs is specifically up-regulated in breast cancer. J Biol Chem *274*, 15633-15645.

Lu, X., Wontakal, S.N., Emelyanov, A.V., Morcillo, P., Konev, A.Y., Fyodorov, D.V., and Skoultchi, A.I. (2009). Linker histone H1 is essential for Drosophila development, the establishment of pericentric heterochromatin, and a normal polytene chromosome structure. Genes Dev *23*, 452-465.

McBryant, S.J., Adams, V.H., and Hansen, J.C. (2006). Chromatin architectural proteins. Chromosome Res *14*, 39-51.

Morse, R.H. (2003). Getting into chromatin: how do transcription factors get past the histones? Biochem Cell Biol *81*, 101-112.

Nottke, A., Colaiacovo, M.P., and Shi, Y. (2009). Developmental roles of the histone lysine demethylases. Development *136*, 879-889.

Ozsolak, F., Song, J.S., Liu, X.S., and Fisher, D.E. (2007). High-throughput mapping of the chromatin structure of human promoters. Nat Biotechnol *25*, 244-248.

Paik, W.K., Paik, D.C., and Kim, S. (2007). Historical review: the field of protein methylation. Trends Biochem Sci *32*, 146-152.

Pavri, R., Lewis, B., Kim, T.K., Dilworth, F.J., Erdjument-Bromage, H., Tempst, P., de Murcia, G., Evans, R., Chambon, P., and Reinberg, D. (2005). PARP-1 determines specificity in a retinoid signaling pathway via direct modulation of mediator. Mol Cell *18*, 83-96.

Pena, P.V., Davrazou, F., Shi, X., Walter, K.L., Verkhusha, V.V., Gozani, O., Zhao, R., and Kutateladze, T.G. (2006). Molecular mechanism of histone H3K4me3 recognition by plant homeodomain of ING2. Nature *442*, 100-103.

Petesch, S.J., and Lis, J.T. (2008). Rapid, transcription-independent loss of nucleosomes over a large chromatin domain at Hsp70 loci. Cell *134*, 74-84.

Poirier, G.G., de Murcia, G., Jongstra-Bilen, J., Niedergang, C., and Mandel, P. (1982). Poly(ADP-ribosyl)ation of polynucleosomes causes relaxation of chromatin structure. Proc Natl Acad Sci U S A *79*, 3423-3427.

Robinson, P.J., and Rhodes, D. (2006). Structure of the '30 nm' chromatin fibre: a key role for the linker histone. Curr Opin Struct Biol *16*, 336-343.

Ruthenburg, A.J., Allis, C.D., and Wysocka, J. (2007). Methylation of lysine 4 on histone H3: intricacy of writing and reading a single epigenetic mark. Mol Cell *25*, 15-30.

Santos-Rosa, H., Schneider, R., Bannister, A.J., Sherriff, J., Bernstein, B.E., Emre, N.C., Schreiber, S.L., Mellor, J., and Kouzarides, T. (2002). Active genes are tri-methylated at K4 of histone H3. Nature *419*, 407-411.

Schneider, R., Bannister, A.J., Myers, F.A., Thorne, A.W., Crane-Robinson, C., and Kouzarides, T. (2004). Histone H3 lysine 4 methylation patterns in higher eukaryotic genes. Nat Cell Biol *6*, 73-77.

Schones, D.E., Cui, K., Cuddapah, S., Roh, T.Y., Barski, A., Wang, Z., Wei, G., and Zhao, K. (2008). Dynamic regulation of nucleosome positioning in the human genome. Cell *132*, 887-898.

Scibetta, A.G., Santangelo, S., Coleman, J., Hall, D., Chaplin, T., Copier, J., Catchpole, S., Burchell, J., and Taylor-Papadimitriou, J. (2007). Functional analysis of the transcription repressor PLU-1/JARID1B. Mol Cell Biol *27*, 7220-7235.

Shi, X., Hong, T., Walter, K.L., Ewalt, M., Michishita, E., Hung, T., Carney, D., Pena, P., Lan, F., Kaadige, M.R., *et al*. (2006). ING2 PHD domain links histone H3 lysine 4 methylation to active gene repression. Nature *442*, 96-99.

Sims, R.J., 3rd, Chen, C.F., Santos-Rosa, H., Kouzarides, T., Patel, S.S., and Reinberg, D. (2005). Human but not yeast CHD1 binds directly and selectively to histone H3 methylated at lysine 4 via its tandem chromodomains. J Biol Chem *280*, 41789-41792.

Taverna, S.D., Ilin, S., Rogers, R.S., Tanny, J.C., Lavender, H., Li, H., Baker, L., Boyle, J., Blair, L.P., Chait, B.T., *et al*. (2006). Yng1 PHD finger binding to H3 trimethylated at K4 promotes NuA3 HAT activity at K14 of H3 and transcription at a subset of targeted ORFs. Mol Cell *24*, 785-796.

Team, R.D.C. (2006). R: A language and environment for statistical computing. In R Foundation for Statistical Computing (Vienna, Austria).

Trojer, P., Zhang, J., Yonezawa, M., Schmidt, A., Zheng, H., Jenuwein, T., and Reinberg, D. (2009). Dynamic Histone H1 Isotype 4 Methylation and Demethylation by Histone Lysine Methyltransferase G9a/KMT1C and the Jumonji Domain-containing JMJD2/KDM4 Proteins. J Biol Chem *284*, 8395-8405.

Tulin, A., and Spradling, A. (2003). Chromatin loosening by poly(ADP)-ribose polymerase (PARP) at Drosophila puff loci. Science *299*, 560-562.

Tulin, A., Stewart, D., and Spradling, A.C. (2002). The Drosophila heterochromatic gene encoding poly(ADP-ribose) polymerase (PARP) is required to modulate chromatin structure during development. Genes Dev *16*, 2108-2119.

van Ingen, H., van Schaik, F.M., Wienk, H., Ballering, J., Rehmann, H., Dechesne, A.C., Kruijzer, J.A., Liskamp, R.M., Timmers, H.T., and Boelens, R. (2008). Structural insight into the recognition of the H3K4me3 mark by the TFIID subunit TAF3. Structure *16*, 1245-1256.

Vermeulen, M., Mulder, K.W., Denissov, S., Pijnappel, W.W., van Schaik, F.M., Varier, R.A., Baltissen, M.P., Stunnenberg, H.G., Mann, M., and Timmers, H.T. (2007). Selective anchoring of TFIID to nucleosomes by trimethylation of histone H3 lysine 4. Cell *131*, 58-69.

Vignali, M., and Workman, J.L. (1998). Location and function of linker histones. Nat Struct Biol *5*, 1025-1028.

Wacker, D.A., Ruhl, D.D., Balagamwala, E.H., Hope, K.M., Zhang, T., and Kraus, W.L. (2007). The DNA binding and catalytic domains of poly(ADP-ribose) polymerase 1 cooperate in the regulation of chromatin structure and transcription. Mol Cell Biol *27*, 7475-7485.

Woodcock, C.L., Skoultchi, A.I., and Fan, Y. (2006). Role of linker histone in chromatin structure and function: H1 stoichiometry and nucleosome repeat length. Chromosome Res *14*, 17-25.

Wysocka, J., Swigut, T., Xiao, H., Milne, T.A., Kwon, S.Y., Landry, J., Kauer, M., Tackett, A.J., Chait, B.T., Badenhorst, P., *et al*. (2006). A PHD finger of NURF couples histone H3 lysine 4 trimethylation with chromatin remodelling. Nature *442*, 86-90.

Yamane, K., Tateishi, K., Klose, R.J., Fang, J., Fabrizio, L.A., Erdjument-Bromage, H., Taylor-Papadimitriou, J., Tempst, P., and Zhang, Y. (2007). PLU-1 is an H3K4 demethylase involved in transcriptional repression and breast cancer cell proliferation. Mol Cell *25*, 801-812.

Zhang, T., Berrocal, J.G., Frizzell, K.M., Gamble, M.J., DuMond, M.E., Krishnakumar, R., Yang, T., Sauve, A.A., and Kraus, W.L. (2009). Enzymes in the NAD+ salvage pathway regulate SIRT1 activity at target gene promoters. J Biol Chem *284*, 20408-20417.

Zhao, H., Langerod, A., Ji, Y., Nowels, K.W., Nesland, J.M., Tibshirani, R., Bukholm, I.K., Karesen, R., Botstein, D., Borresen-Dale, A.L., and Jeffrey, S.S. (2004).

Different gene expression patterns in invasive lobular and ductal carcinomas of the breast. Mol Biol Cell *15*, 2523-2536.

CHAPTER 4

Analysis of NFκB-Dependent Transcription in Human Cardiomyocytes: Roles for PARP-1 and Other Transcription Factors

4.1 Summary

Cardiovascular disease (CVD) is the number one cause of death in the United State, claiming over 800,000 lives per year. Although studies have elucidated a number of molecular mechanisms leading to CVD, many of them still remain unclear. Cardiomyocytes that are subjected to stress signals, such as cytokines (eg. TNFα), activate many different transcriptional pathways to respond to such insults, and one transcription factor that is central to these responses is NFκB. I are using a recently generated immortalized human cardiomyocyte cell line, AC16, to study the mechanisms of NFκB-dependent transcription, as well as the role of other factors in regulating this response. I show that in human cardiomyocytes, the NFκB subunit p65 is significantly recruited to the genome upon TNFα treatment, and NFκB recruitment both up- and down-regulates the expression of a number of genes. These genes specifically reprioritize the transcriptional program of the cells to focus on stress response. Additionally, I find that a majority of the NFκB-dependent genes are likely to involve other transcription factors (including CREB, which has previously been shown to cooperate with NFκB), suggested to us by the lack of a canonical NFκB binding site at a majority of target promoters. Finally I show that Poly (ADP ribose) Polymerase-1 (PARP-1), which has been shown to play a prominent role in the in the regulation of NFκB-dependent transcription, acts as an activator of NFκB, but not a repressor. Together, our data shows that NFκB-dependent transcription is central for human cardiomyocytes to respond to TNFα, but that other factors, including PARP-1 and likely many others, are also critical for this response.

4.2 Introduction

Cardiovascular disease (CVD) is the leading cause of death in the United States (Mehra, 2007). Understanding the regulatory processes that control the biology of cardiomyocytes in normal and disease states is a necessary step in developing better preventative and therapeutic approaches to CVD. Key aspects of cardiomyocytes physiology are determined by the regulation of gene expression. Numerous studies have demonstrated a clear role for sequence-specific DNA-binding transcription factors, such as GATA4, STATs and AP-1 in regulating gene expression outcomes in cardiomyocytes (Epstein and Parmacek, 2005, Fischer and Hilfiker-Kleiner, 2007, Henderson and Tyagi, 2006, Kim and Iwao, 1999). But probably the most established and well-characterized pro-inflammatory transcription factor is the Nuclear Factor Kappa-light-chain-enhancer of activated B cells, or NFκB (Epstein and Parmacek, 2005). NFκB is a dimeric complex of two proteins, one from the Rel class and the other from the NFκB class (Fig. 4.1). Members of the NFκB class are synthesized as precursors with a repression domain, which is cleaved during activation. This allows for dimerization of one member of each of the classes, which then results in an active NFκB complex (Lentsch and Ward, 1999, Lentsch and Ward, 2000). Upon stimulation by various molecules (including Tumor Necrosis Factor Alpha, or TNFα), a signaling cascade is initiated, which ultimately results in the activation of the cytosolic kinase IKKα/β. This kinase phosphorylates IκB, the protein which sequesters NFκB in the cytosol. Upon phosphorylation, IκB is degraded by the proteosome, NFκB translocates into the nucleus, bind chromatin and regulate gene expression (Fig. 4.2) (Lentsch and Ward, 1999, Lentsch and Ward, 2000).

The pathways that regulate NFκB-dependent gene expression are relatively well established, and a number of factors have been implicated as co-regulators for

Figure 4.1. NFκB Family of Proteins. Schematic shown the domain structure of the proteins that comprise the NFκB family. RelA, RelB and cRel proteins (Rel class) can dimerize with NFκB1 or NFκB2 proteins (NFκB class). LZD = Leucine Zipper Domain; GRR = Glycine Rich Region. Figure adapted from (Rangan, et al., 2009).

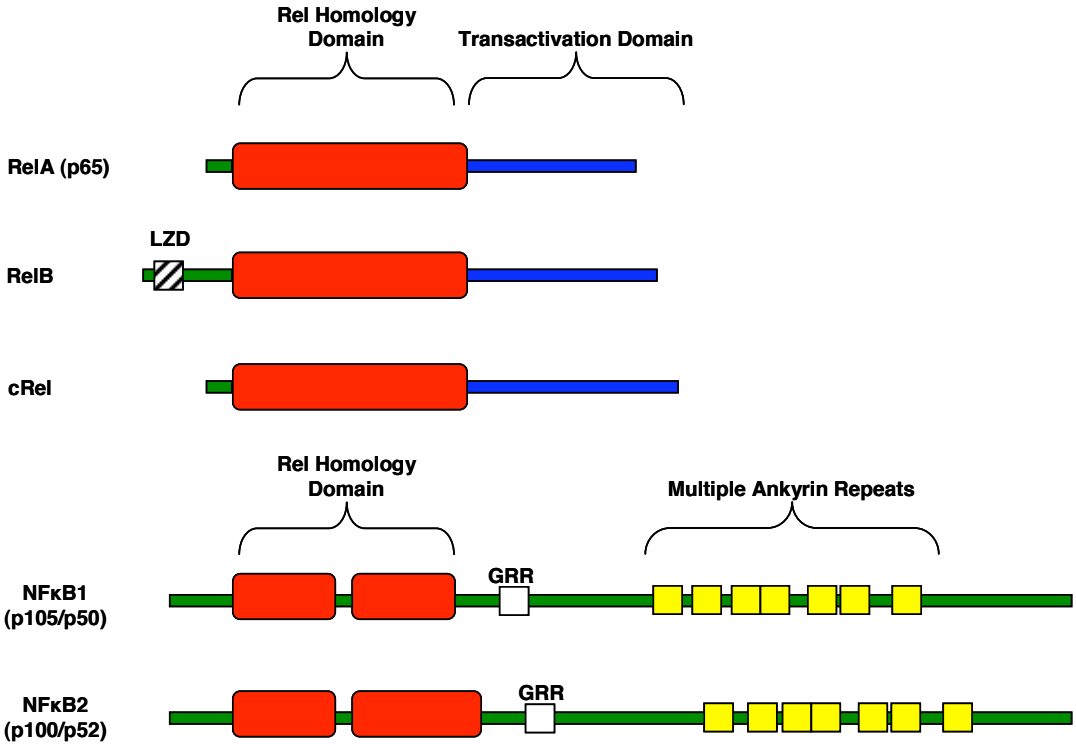
Rel Homology Domain
Transactivation Domain
RelA (p65)
LZD
RelB
cRel
Rel Homology Domain
Multiple Ankyrin Repeats
GRR
NFκB1 (p105/p50)
GRR
NFκB2 (p100/p52)

NFκB-dependent transcription. These include DNA-binding transcription factors such as E2F, AP-2, SP-1 and p53, as well as co-regulators including CBP/p300, HDACs, CARM1, and even IKKα, which until recently was not thought to be chromatin-bound (Chen, et al., 2001, Covic, et al., 2005, Hassa, et al., 2003, Hassa, et al., 2005, Hirano, et al., 1998, Katsel and Greenstein, 2001, Lim, et al., 2007, Meylan, et al., 2009, Yamamoto, et al., 2003, Yang, et al., 2000). Thus, NFκB is a versatile transcription factor that can regulate a variety of biological processes depending on the signaling pathways that are activated, and the co-regulators that are involved.

PARP-1 is involved in regulating the response to a number of stress factors leading to CVD (Molnar, et al., 2006, Pacher and Szabo, 2007, Pillai, et al., 2005, Szabo, et al., 2006). It plays a role at multiple stages of CVD, including the initial acute-phase pro-inflammatory response, and the later apoptotic phase if the cells are damaged beyond recovery. Regarding the latter, cardiomyocytes cultured from PARP-1 knockout mice have been shown to improve mitochondrial functions, and reduced NAD+ consumption (Pacher and Szabo, 2007, Pillai, et al., 2006). Further supporting the involvement of PARP-1 in pro-inflammatory responses, PARP-deficient *Drosophila* have immune defects, and are more susceptible to bacterial infection as their wild-type counterparts (Tulin and Spradling, 2003). These results indicate that PARP-1 inhibitors may be useful as therapeutic tools against heart disease, leading to studies testing PARP inhibitors for this purpose (Pacher and Szabo, 2007). PARP-1 has also been shown to regulate pro-inflammatory transcription in cells that are exposed to stress during CVD. Specifically, PARP-1 can regulate the expression of pro-inflammatory genes, including inducible nitric oxide synthase (iNOS), adhesion molecules (VCAM1, ICAM1) and class II MHCs (Pacher and Szabo, 2007). The mechanism of PARP-1 action at these genes is not fully understood, although recent work has begun to elucidate some of these pathways,

Figure 4.2. NFκB Signaling Pathway. A simplified rendition of the activation pathway of NFκB. Translocation of NFκB into the nucleus is dependent on external signals, resulting in a signaling cascade which activates IKKα/β. Degradation of phosphorylated IκB allows NFκB to translocate into the nucleus, and regulate gene expression. Figure adapted from (Li and Stark, 2002).

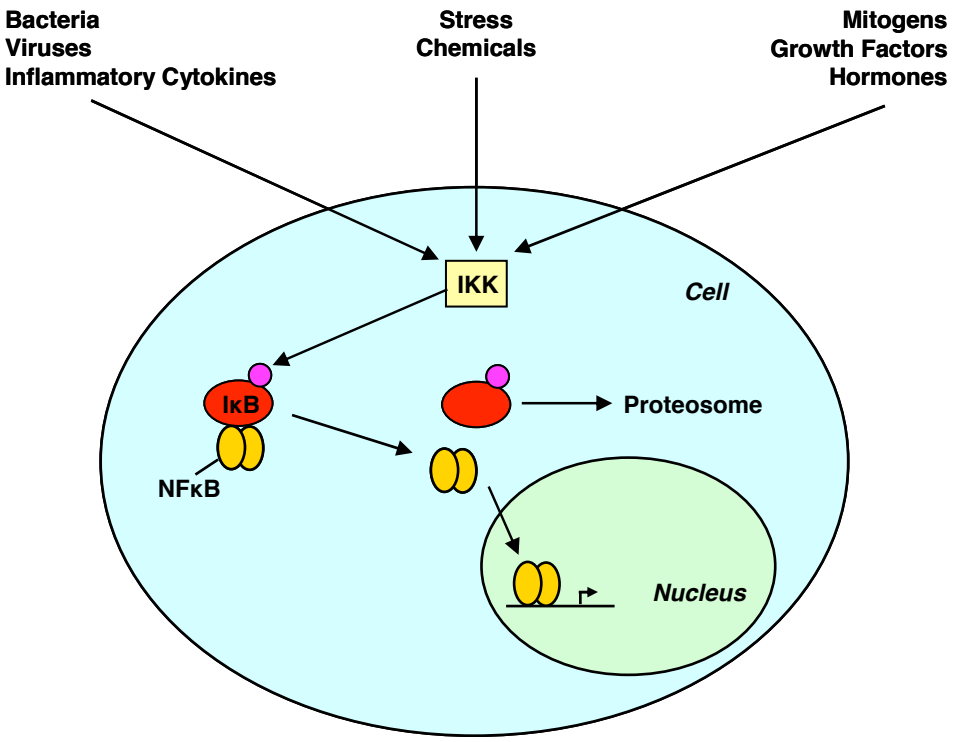
Bacteria
Viruses
Inflammatory Cytokines
Stress
Chemicals
Mitogens
Growth Factors
Hormones
IKK
Cell
IκB
NFκB
Proteosome
Nucleus

which include p300/CBP, and Mediator (Hassa, et al., 2005).

I am interested in the role of PARP-1 and other transcription factors in regulating NFκB-dependent transcription in human cardiomyocytes. Recently, immortalized cardiac cell lines have been developed as a tool for studying the regulation of processes such as gene expression in cardiomyocytes. One example of such a cell line is the immortalized human cardiomyocyte cell line, AC16 (Davidson, et al., 2005). These cells have been immortalized using the SV40 antigen, but were shown to maintain the hallmarks of primary cardiomyocytes, thus making them a useful model system for the study of gene regulation in cardiomyocytes. Using ChIP-chip in AC16 cells, I found that TNFα can stimulate NFκB translocation into the nucleus, as well as its global recruitment onto chromatin. In addition, I found that by categorizing NFκB-recruited genes using RNA Polymerase II ChIP-chip data, I could identify functional categories of genes, which I then show to be regulated by NFκB. I also see that, while up-regulated genes are enriched for NFκB binding sites, the majority of regulated genes do not contain a canonical DNA motif, strongly suggesting cooperation with other transcription factors for recruitment and activity of NFκB. While investigating the mechanisms of NFκB action at gene promoters, I found that PARP-1 is required at genes with a canonical NFκB site that are up-regulated, but not at down-regulated genes. In conclusion, NFκB transcription is critical for stress responses in human cardiomyocytes, and regulation of gene expression via NFκB involves other factors such as PARP-1. Future studies will examine the roles of other transcription factors in regulating the various categories of NFκB-dependent genes, as well as investigate whether PARP-1 affects up-regulated genes lacking a canonical NFκB site.

4.3 Results

AC16 cells are a relatively newly characterized cell line (Davidson, et al., 2005), and although it is known that cardiomyocytes are responsive to stress signals such as TNFα (Natoli, et al., 1998), I wanted to confirm that these immortalized cells had a similar response to primary cardiomyocytes. To this end, I treated the cells with TNFα, and determined whether the prototypic pro-inflammatory transcription factor, NFκB, translocated into the nucleus. I used an antibody against the p65 subunit of NFκB complex, which has previously been reported to be entirely sequestered in the cytosol prior to activation (Lentsch and Ward, 1999, Lentsch and Ward, 2000). I found that at basal levels, there was no p65 in the nucleus, but that upon TNFα treatment, NFκB levels in the nucleus increased drastically (Fig 4.3A). I was also able to demonstrate that using an IKKα/β inhibitor, BAY 11-7085, I could block the translocation of NFκB into the nucleus upon TNFα treatment (Fig. 4.3A). Having established that NFκB activity was as expected in this cell line, I examined the effect of TNFα on the expression of prototypic pro-inflammatory NFκB targets. I measured the change in mRNA levels of six genes upon treatment with TNFα for 30 min and 180 min. All six genes showed a significant increase in expression after 180 min, with two of the genes (TNFA and IL6) having increased expression even at 30 min (Fig. 4.3B). This can be explained by the fact that these two genes encode cytokines (TNFα [which upregulates itself], and Il6). Not only are these genes shorter, but they are also more early-response genes in the pro- inflammatory process (Lentsch and Ward, 2000). In addition, I also used BAY 11-7085 to show that these responses were dependent on NFκB activation. If the cells were pre-treated with the inhibitor, the response to TNFα was either abrogated or greatly reduced (Fig. 4.3B). These data show that TNFα activates a pro-inflammatory response in AC16 cells, and that the transcription factor NFκB plays an important role in this activation. Interestingly,

Figure 4.3. AC16 cells are responsive to TNFα treatment. (A) Western blot of AC16 cytoplasmic and nuclear fractions blotted for NFκB, TFIIB (nuclear marker) and GAPDH (cytoplasmic marker), in control and TNFα-treated cells. In addition, one set of samples was also pre-treated with 10 μg/ml of the IKKα/β inhibitor, BAY-11-7082, for 1 hr. (B-G) Analysis of mRNA expression by RT-qPCR in TNFα-treated AC16 cells relative to vehicle treated cells. Cells were treated with 25 ng/ml TNFα for either 30 min or 180 min. One set of samples was also pre-treated with (labeled Bay) 10 μg/ml of BAY-11-7082 for 1 hr Expression data is standardized to β-actin transcripts. All samples were done in Luciferase Knockdown cells, for comparison with data in Fig. 4.11. Each data point is a mean of $n = 3$. Error bar represents SEM.

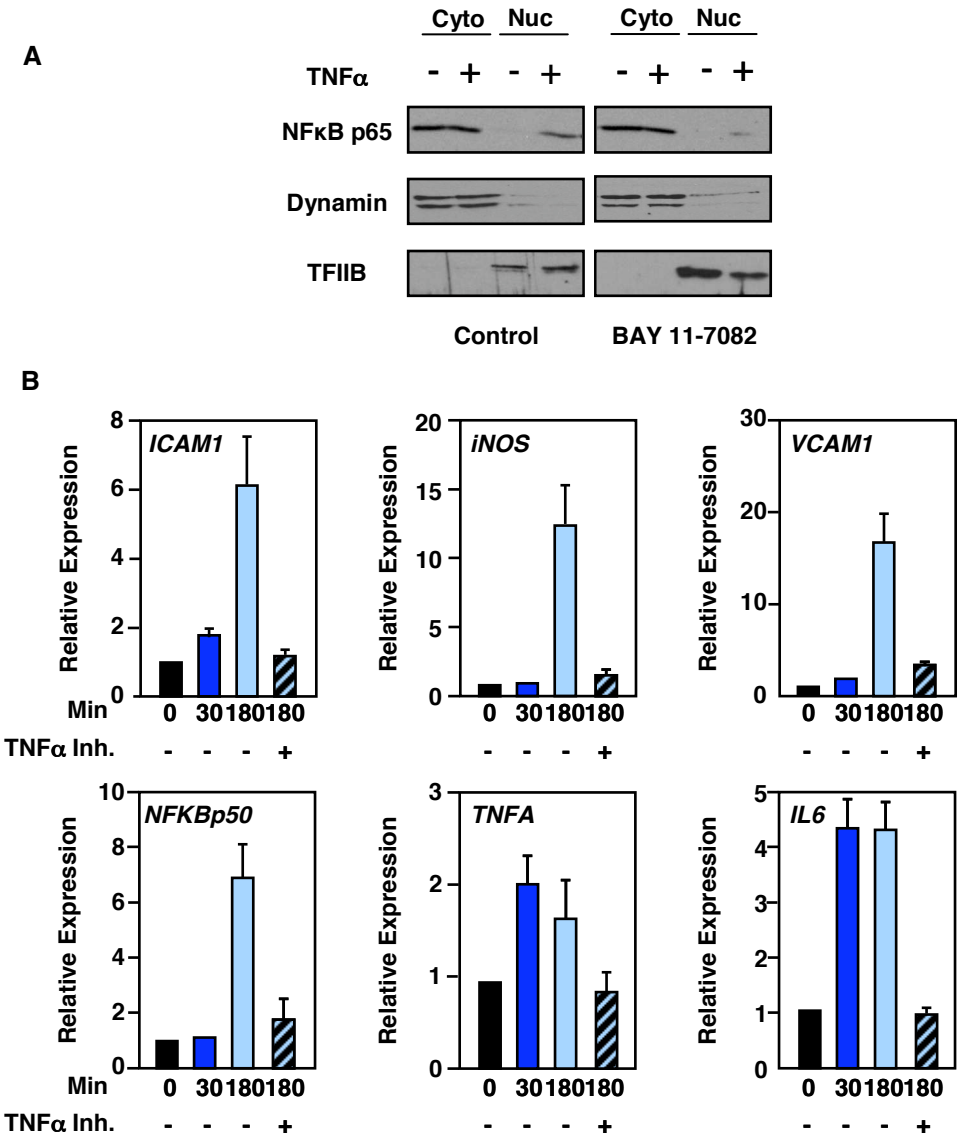
A
Cyto
Nuc
Cyto
Nuc
TNFα
- + - + - + - +
NFκB p65
Dynamin
TFIIB
Control
BAY 11-7082
B
ICAM1
iNOS
VCAM1
NFKBp50
TNFA
IL6
Relative Expression
Min
0 30 180 180
TNFα Inh.
- - - +

when I searched for DNA sequence motifs under significant peaks of NFκB in the TNFα treated cells, I found that the NFκB site itself was not as enriched as a number of other sites (Table 4.1). This result was further investigated, and will be discussed later in this study.

Having established that NFκB translocates to the nucleus upon TNFα as expected, I then wanted to investigate the genomic binding pattern of NFκB in AC16 cells. I used Chromatin Immunoprecipitation coupled with DNA microarrays (ChIP-chip) using a Nimblegen promoter array, to probe 23,551 RefSeq promoters, tiled from -3.2 KB to +3.2 KB from the transcription start site (Fig. 4.4A). While I observed some background binding of NFκB in the basal condition, upon TNFα treatment, there was a drastic global increase in chromatin-bound NFκB (Fig. 4.4A). This result suggested that there was a global response in these cells to treatment with TNFα, which involved NFκB binding to chromatin. I then counted the number of promoters with statistically significant peaks of NFκB, both in the untreated and TNFα-treated condition. There were almost three times as many genes with peaks in the TNFα-treated cells, again demonstrating the global recruitment of NFκB to chromatin (Fig. 4.4B). In fact, genes could be categorized as either "significantly recruited" or "not recruited" based on stringent statistical criteria (Fig. 4.4D and 4.4E).

This was also confirmed by conventional ChIP coupled with quantitative PCR (ChIP-qPCR) (Fig. 4.4C).

As previously mentioned, NFκB is a transcription factor that regulates transcription of numerous genes in various different contexts (Covic, et al., 2005, Hassa, et al., 2003, Lentsch and Ward, 2000, Meylan, et al., 2009). Therefore, I was interested in the functional outcomes of NFκB binding to gene promoters upon TNFα treatment in AC16 cells. In order to address this question, I performed RNA Polymerase II (Pol II) ChIP-chip on the same Nimblegen arrays as were used for

Table 4.1. Enrichment of transcription factor binding sites (based on Transfac®) under statistically significant NFkB peaks

[a]Site	[b]Fold Enrichment
NFY	6.8
SP1	6.7
AP2	6.6
PAX4	6.3
PAX5	6.0
AHRARNT	5.7
EGR1	5.6
TAXCREB	5.5
CREB	5.5
ATF	5.5
NFKB	2.7

[a]Sites within 200bp of statistically significant peaks of NFκB

[b]Enrichments all have pvalues of $p<1x10^{-300}$

Figure 4.4. NFκB is recruited to chromatin upon TNFα treatment in AC16 cells. (A) Heat maps of NFκB ChIP-chip data in control cells, or TNFα-treated cells (25 ng/ml for 30 min), shown from -3 kb to +3 kb relative to the TSS. The data are ordered based on the intensity of the NFκB signal at the promoter in the TNFα-treated sample. (B) Venn diagram showing the number of promoters with statistically significant ($p<0.016$) peaks of NFκB on the ChIP-chip array in control and TNFα-treated cells. (C) Scatter plot of gene-specific ChIP-qPCR analyses of NFκB binding at regions of statistically significant ($p<0.016$) NFκB recruitment upon TNFα treatment, and regions without NFκB recruitment. Each data point is a mean of $n = 3$. Bar represents median. (D) Average Log2 ratios of ChIP-chip data minus and plus TNFα for promoters with statistically significant ($p<0.016$) NFκB recruitment upon TNFα treatment. (E) Same as (D) for promoters without NFκB recruitment.

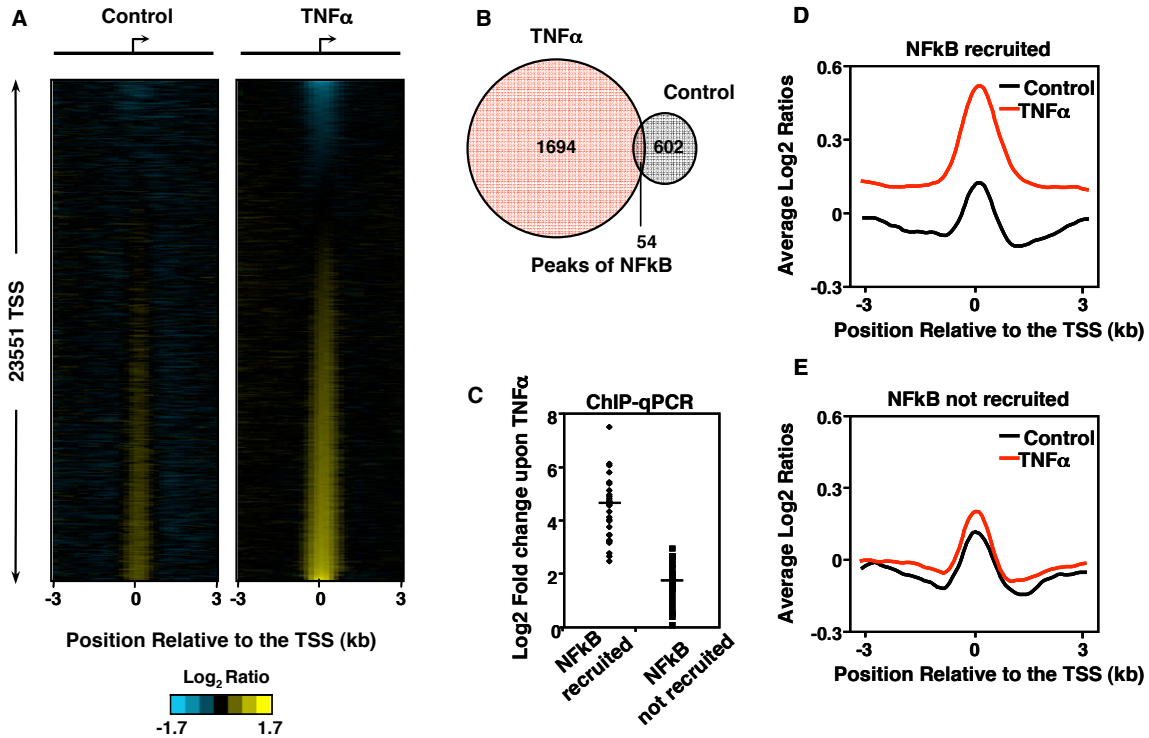
A
Control
TNFα
23551 TSS
-3
0
3
Position Relative to the TSS (kb)
Log2 Ratio
-1.7
1.7
B
TNFα
Control
1694
602
54
Peaks of NFkB
C
ChIP-qPCR
Log2 Fold change upon TNFα
NFkB recruited
NFkB not recruited
D
NFkB recruited
Control
TNFα
Average Log2 Ratios
Position Relative to the TSS (kb)
E
NFkB not recruited
Control
TNFα
Average Log2 Ratios
Position Relative to the TSS (kb)

NFκB. As is demonstrated by the resulting heat maps (Fig. 4.5A), a considerable number of genes contained Pol II bound at the promoter in the untreated condition. Upon TNFα treatment, a large proportion of genes showed significant change in Pol II binding, which can also be seen by averaging all the data (Figs. 4.5A and 4.5B). Specifically, there was a small but significant overall decrease in promoter-proximal Pol II, accompained by an increase in Pol II in the body of the gene (defined as +1KB to +3KB for statistical analyses) (Fig. 4.5B). This suggested that AC16 cells responded in a global manner to TNFα treatment by altering transcription of target genes. The ChIP-chip data for Pol II was also confirmed by ChIP-qPCR (Fig. 4.5C).

Pol II binding information serves as a direct measure of transcriptional activity (specifically Pol II in the body of the gene), but I wanted to ask whether changes in Pol II binding were likely to result in changes at the mRNA level. I made use of three existing data sets for changes in gene expression after 1 hr of TNFα treatment. These data sets are previously published, and use HeLa cells, HuVEC and epidermal keratinocytes (Banno, et al., 2005, Tian, et al., 2005, Wada, et al., 2009). I used stringent fold-cutoff criteria to select the 80 most up-regulated and 80 most down-regulated genes in each of the three data sets, and plotted our AC16 cell Pol II ChIP-chip data for these 160 genes. What I observed was that at the up-regulated genes the ChIP-chip signal in the body of the gene increased significantly, whereas as the down-regulated genes, the peak of Pol II at the promoter virtually disappeared (Fig. 4.5 D, E). This result supports the strength and the relevance of using Pol II ChIP-chip, both in terms of measuring a direct transcriptional response to TNFα, but at the same time, investigating genes that are likely regulated at the mRNA (and therefore protein) level as well.

Having established that NFκB is recruited to the genome upon TNFα treatment, and that Pol II binding is also regulated by TNFα, I wanted to find the

Figure 4.5. RNA Polymerase II (Pol II) distribution on chromatin is altered upon TNFα treatment in AC16 cells. (A) Heat maps of Pol II ChIP-chip data in control cells, or TNFα-treated cells (25 ng/ml for 30 min), shown from -3 kb to +3 kb relative to the TSS. The data are ordered based on the total intensity of the Pol II in the TNFα-treated sample. (B) Average Log2 ratios of Pol II ChIP-chip data minus and plus TNFα for all promoters on the array. (C) Scatter plot of gene-specific ChIP-qPCR analyses of Pol II binding at regions of statistically significant ($p<0.016$) Pol II recruitment to the gene body upon TNFα treatment, regions without Pol II changes and regions of statistically significant ($p<0.016$) Pol II release from the gene body upon TNFα treatment. Each data point is a mean of $n = 3$. Bar represents median. (D) Average Log2 ratios of Pol II ChIP-chip data minus and plus TNFα for the top 80 mRNA transcripts which are up-regulated in HeLa cells, HuVEC and epidermal keratinocytes upon 1 hr treatment with TNFα, based on published expression microarray data (refs). All changes in mRNA transcript levels are 3 fold or greater ($p<0.05$). (E) Same as (D), except for the 80 most down-regulated transcripts.

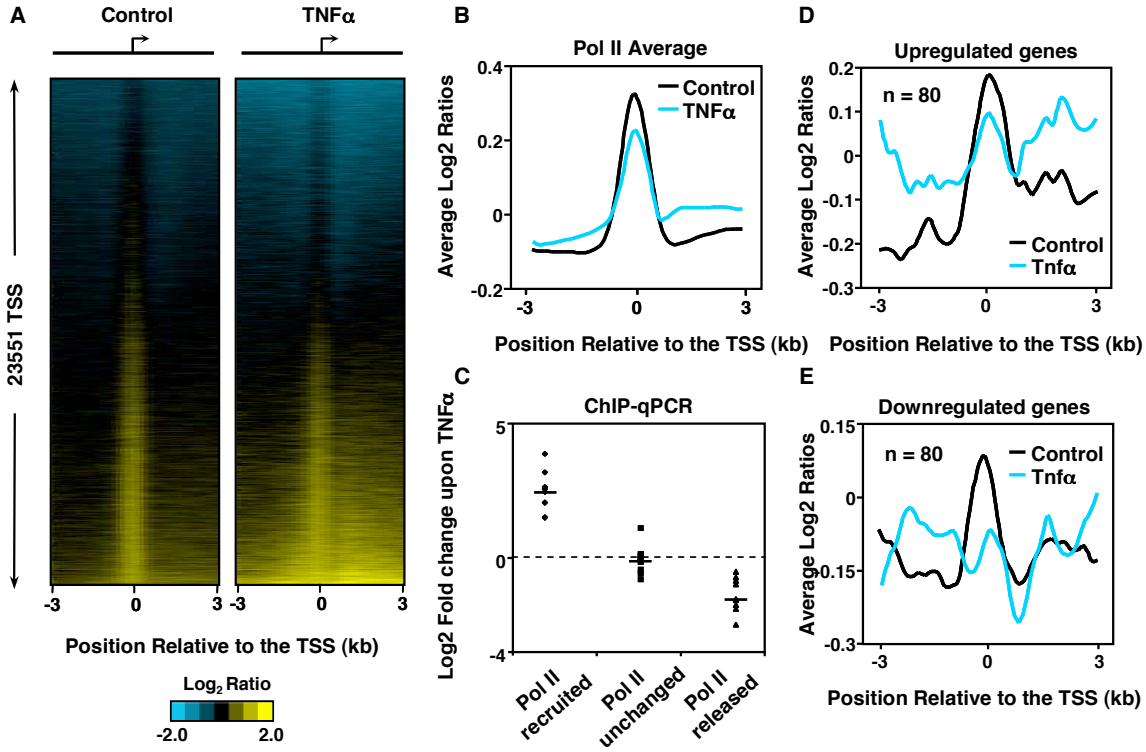
A
Control
TNFα
23551 TSS
-3
0
3
-3
0
3
Position Relative to the TSS (kb)
Log2 Ratio
-2.0
2.0
B
Pol II Average
Control
TNFα
Average Log2 Ratios
0.4
0.2
0
-0.2
-3
0
3
Position Relative to the TSS (kb)
C
ChIP-qPCR
Log2 Fold change upon TNFα
5
0
-4
Pol II recruited
Pol II unchanged
Pol II released
D
Upregulated genes
n = 80
Average Log2 Ratios
0.2
0.1
0
-0.1
-0.2
-0.3
Control
Tnfα
-3
0
3
Position Relative to the TSS (kb)
E
Downregulated genes
n = 80
Average Log2 Ratios
0.15
0
-0.15
-0.3
Control
Tnfα
-3
0
3
Position Relative to the TSS (kb)

intersection between these data sets, or in other words, obtain a list of candidate genes whose transcription is regulated by NFκB binding. Using stringent statistical criteria ($p<0.016$, Fold>2, Wilcoxin sign-rank test), I divided the genes that showed changes in NFκB into three functional categories based on changes in Pol II from +1KB to +3KB (i.e. in the body of the gene): Pol II recruited, Pol II unchanged and Pol II released (these categories will henceforth be referred to as above) (Fig. 4.6 A-C). The functional importance of these categories was determined using gene ontology (GO) analysis (Beissbarth and Speed, 2004). While the Pol II unchanged category contained one non-relevant GO term, both the recruited and released categories yielded a significant number of terms (Fig. 4.6G). When dissecting these terms, it was clear that while the up-regulated category consisted of genes involved in stress responses, such as nitric oxide synthesis and defense mechanism, the down-regulated category mostly comprised "housekeeping" functions, including transcription and metabolism (Fig. 4.6H, Tables 4.2, 4.3 and 4.4). These results demonstrate that TNFα likely regulates a transition of the cell from a basal state to a stress-responsive state, and that this change at is orchestrated by NFκB-dependent changes in transcription. For further proof that these categories contained genes that were ultimately relevant for the cellular response to TNFα, I went back to the mRNA data from HeLa cells, HuVEC and epidermal keratinocytes used in Fig. 4.4 (Banno, et al., 2005, Tian, et al., 2005, Wada, et al., 2009). In the Pol II recruited and released categories, a majority of the genes were up-regulated 1.2 fold or more at the mRNA level in at least 2 of the three above cell lines (Fig. 4.6I). This again confirms that the genes regulated at the transcriptional level are also highly likely to be regulated at the protein level.

Next, I performed motif searches underneath NFκB peaks after TNFα treatment in the three Pol II-sorted categories of genes, and surprisingly, the categories revealed distinct binding behaviors of NFκB. In the Pol II recruited categories, the

Figure 4.6. Categorization of NFκB ChIP-chip data based on Pol II status. Average Log2 ratios of ChIP-chip data for NFκB (A, C, E) and Pol II (B, D, F), minus and plus TNFα, for promoters where NFκB is recruited. Genes were sub-categorized based on Pol II binding, and will henceforth be referred to as such (recruited (A, B), unchanged (C, D) or released (E, F) upon TNFα). Note: unchanged genes were selected based on $p>0.9$, to have similar numbers in each sub-category. (G) Number of significant GO terms ($p<0.1$) obtained for Pol II recruited, unchanged and released genes using GOstat©. (H) Significant GO terms for Pol II recruited and released genes from (G) separated into functional categories. (C) Percentage of genes in Pol II recruited and Pol II released categories that are regulated at least 1.2 fold at the mRNA level in two of the three cell lines in Fig. 4.5 (D,E).

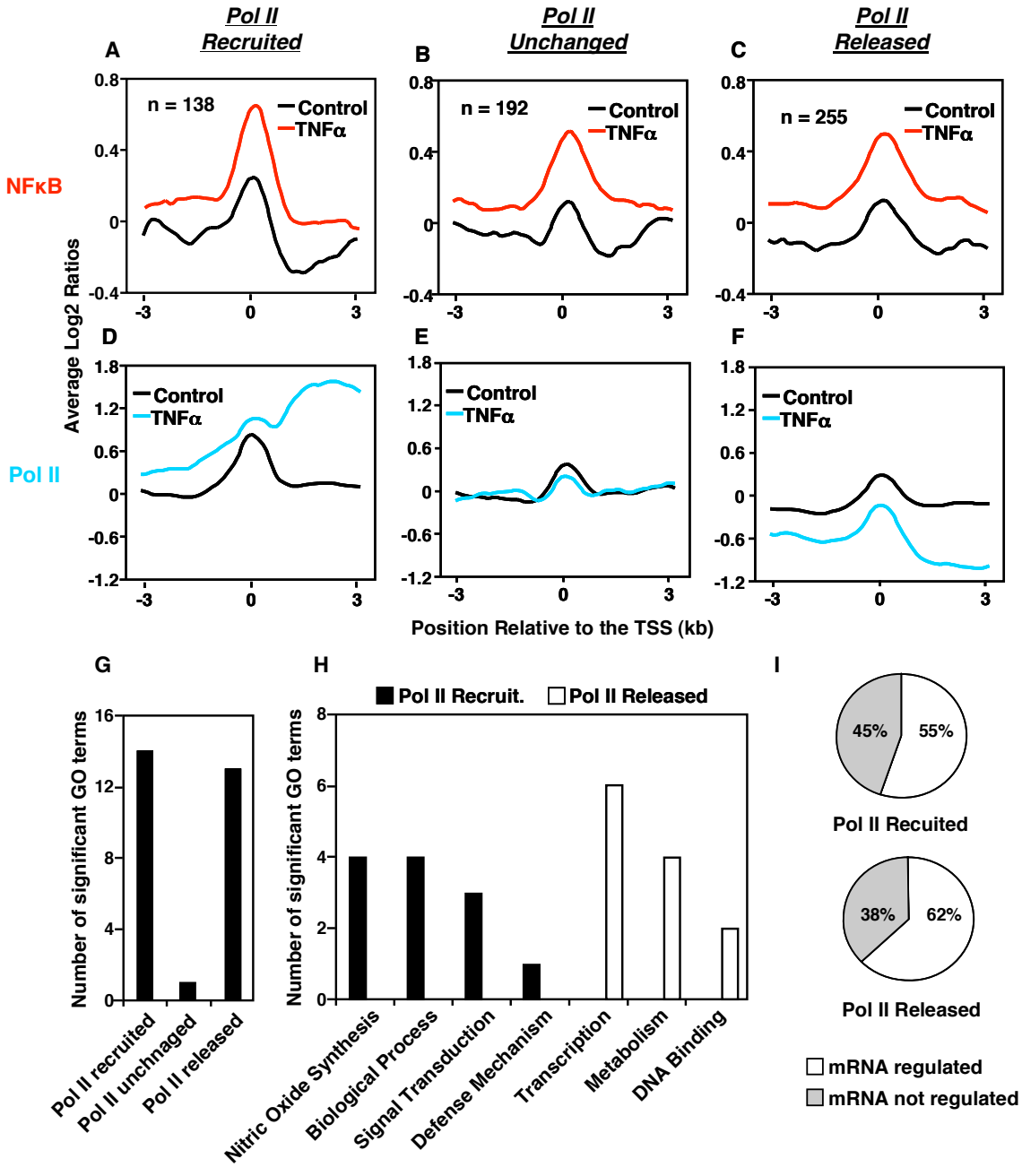
Pol II Recruited
Pol II Unchanged
Pol II Released
A
B
C
D
E
F
n = 138
n = 192
n = 255
Control
TNFα
NFκB
Pol II
Average Log2 Ratios
Position Relative to the TSS (kb)
G
H
I
Number of significant GO terms
Pol II Recruit.
Pol II Released
Pol II recruited
Pol II unchnaged
Pol II released
Nitric Oxide Synthesis
Biological Process
Signal Transduction
Defense Mechanism
Transcription
Metabolism
DNA Binding
45%
55%
Pol II Recuited
38%
62%
Pol II Released
mRNA regulated
mRNA not regulated

most highly enriched binding sites were the reported canonical NFκB sequences (Table 4.6). On the other hand, in the unchanged and released categories, the NFκB sequences were not significantly enriched, and instead, a number of other motifs were identified for a variety of transcription factors (Tables 4.8 and 4.9). Interestingly however, even though the canonical binding site was enriched at Pol II recruited genes, a majority of them still do not contain a known NFκB-binding sequence (Table 4.5). Additionally, when this analysis was performed on the Pol II recruited genes after removing all NFκB canonical binding site-containing regions, a number of other transcription factor binding sites, including CREB, were still significantly enriched (Table 4.7). This analysis reveled that although NFκB can bind its canonical binding site, and does so specifically at up-regulated genes, there are a large number of promoters without a canonical site that are regulated and recruit NFκB, strongly suggesting cooperation between NFκB and other key transcription factors.

Until now, I established that changes in NFκB and Pol II binding can serve to separate regulated genes into functional categories. The next question to address was whether NFκB was in fact regulating the transcriptional changes that I observed in these categories. I therefore selected 5 – 10 genes in each of the three Pol II categories, and examined gene-specific effects on factor binding at these promoters (Table 4.10). I treated the cells with the IKKα/β inhibitor, BAY 11-7085, and discovered that inhibiting NFκB translocation into the nucleus upon TNFα treatment had profound effects on Pol II binding (Fig. 4.7). Specifically, Pol II increase and decrease upon TNFα treatment was abrogated by BAY 11-7085 (Fig. 4.7B) (as was recruitment of NFκB, as expected (Fig. 4.7A)). Therefore, not only is NFκB and Pol II binding altered by exposure of AC16 cells to TNFα, but NFκB is critical for the regulation of up- and down-regulated genes, even at genes that do not contain a canonical NFκB binding site.

Table 4.2. Gene ontology analysis showing enriched terms for genes where both NFκB and RNA Polymerase II are recruited upon TNFα treatment.

Go Term	P value
Cell Communication	0.00421
Positive Regulation of Nitric Oxide Biosynthetic Process	0.00421
Signal Transduction	0.00582
Regulation of Nitric Oxide Biosynthetic Process	0.00582
Nitric Oxide Biosynthetic Process	0.0449
Nitric Oxide Metabolic Process	0.0449
Nitric Oxide Synthase Regulator Activity	0.0499
Positive Regulation of Binding	0.0723
Negative Regulation of Biological Process	0.0905
Positive Regulation of Biosynthetic Process	0.095
Defense Response	0.095
Regulation of Signal Transduction	0.095
Regulation of Biological Process	0.095
Small GTPase Regulator Activity	0.095

Table 4.3. Gene ontology analysis showing enriched terms for genes where NFκB is recruited and RNA Polymerase II is unchanged upon TNFα treatment.

Go Term	P value
Embryonic Development	0.0809

Table 4.4. Gene ontology analysis showing enriched terms for genes where NFκB is recruited and RNA Polymerase II is released upon TNFα treatment.

Go Term	P value
Transcription Factor Activity	3.6e-05
Sequence-Specific DNA Binding	0.0185
Regulation of Transcription	0.0356
DNA Binding	0.0356
Regulation of Transcription, DNA-Dependent	0.0356
Regulation of Nucleic Acid Metabolic Process	0.0461
Transcription, DNA-Dependent	0.0461
RNA Biosynthetic Process	0.0461
Regulation of Gene Expression	0.0502
Transcription	0.0514
Regulation of Cellular Metabolic Process	0.0613
Aminopeptidase Activity	0.0681
Regulation of Metabolic Process	0.091

PARP-1 is a known co-activator of NFκB-dependent transcription, making it a prime candidate for the factors that cooperate with NFκB at target genes in AC16 cells. To test the role of PARP-1 in this cardiomyocyte cell line, I generated two separate shRNA-mediated PARP-1 knockdown cell lines (Fig. 4.8A) (Knockdown cell lines generated and tested with the help of Xin Luo). In both

knockdown cell lines, I tested the response of pro-inflammatory genes (same as in Fig. 4.3) that are known to be regulated by PARP-1 in other cell types. PARP-1 depletion caused a drastic reduction in induction of the mRNAs of these genes upon TNFα treatment compared with control cells, regardless of the time of maximal induction (Fig. 4.8 B –G). Since both cell lines behaved identically, for future experiments I used P1-1 only. Whether or not the catalytic activity of PARP-1 plays a role in NFκB-dependent transcription has been somewhat controversial. It appears to depend on the context and cell type, although more reports than not have suggested that it is not required (Hassa, et al., 2003, Hassa, et al., 2005). In order to test the function of poly(ADP-ribosyl)ation (PARylation) in the response of AC16 cells to TNFα, I pre-treated the cells a PARP catalytic inhibitor, PJ34 (Soriano, et al., 2001), and showed that PARylation was inhibited (Fig 4.9A). I observed that in the PJ34-treated cells, the induction of pro-inflammatory genes was not affected (Fig. 4.9B), suggesting that in human cardiomyocytes, the NFκB-dependent response to TNFα does not depend on PARP-1 catalytic activity alone. Finally, to determine whether PARP-1 localization was significantly altered upon TNFα treatment, I performed a PARP-1 ChIP-chip (which was independently confirmed (Fig. 4.10C)), and saw that overall, there was no drastic change in PARP-1 binding before and after treatment (Fig. 4.10A and 4.10B). PARP-1 has been previously reported in the literature to be a co-activator of NFκB, so to address whether these two proteins were co-localized on chromatin, I started by identifying the promoters that contained a statistically significant peak of PARP-1 and

Table 4.5. Percentage of promoters with TNFα-dependent NFκB recruitment that contain a canonical NFκB binding site. Due to the resolution of ChIP sonication, two different distances from the peak center are shown below.

Category	[a]1kb	[b]400bp
Pol II recruited	38 %	33 %
Pol II unchanged	19 %	13 %
Pol II released	17 %	13 %

[a]NFκB binding site in a 1 kb window surrounding the statistically significant NFκB ChIP-chip peak

[b]NFκB binding site in a 400 bp window surrounding the statistically significant NFκB ChIP-chip peak

Table 4.6. Top 20 Transfac® binding site enrichment for genes where both NFκB and RNA Polymerase II are recruited upon TNFα treatment.

Transfac® Binding Site	Ratio	Site Count
CREL_01	5.901452	30
NFKAPPAB65_01	5.859398	15
NFKAPPAB_01	5.60956	31
EGR1_01	5.266389	33
NGFIC_01	5.154057	34
CREB_01	4.501922	11
SP1_Q6	4.500055	18
NFKB_C	4.490372	26
MAX_01	4.474713	13
STAT3_02	4.401539	10
MAZR_01	4.223586	27
ELK1_02	4.151735	23
ARNT_01	4.147146	20
IK3_01	4.124764	22
SP1_01	4.002718	13
E2F_03	3.963268	13
PAX2_01	3.880892	32
ATF_01	3.874284	23
EGR2_01	3.845436	24
USF_Q6	3.818203	21

Sites are within 200bp on either side of the NFκB peak center, all p values: $p<1x10^{-300}$

Table 4.7. Top 20 Transfac® binding site enrichment for genes where both NFκB and RNA Polymerase II are recruited upon TNFα treatment, after removing all regions which contain a canonical NFκB binding site.

Transfac® Binding Site	Ratio	Site Count
CREB_Q4	4.255078	4
STAT3_02	4.206689	6
NFE2_01	4.128633	14
ELK1_02	4.025716	14
ATF_01	4.025182	15
NFY_Q6	3.940657	13
CREB_01	3.911865	6
NGFIC_01	3.863659	16
EGR1_01	3.812069	15
ARNT_01	3.633502	11
E4BP4_01	3.622731	12
CREBP1_Q2	3.59685	12
NRF2_01	3.553173	12
USF_Q6	3.475422	12
AP1_Q4	3.397627	2
E2F_01	3.222782	11
AP1_01	3.186089	12
SP1_Q6	3.185758	8
PAX5_01	3.180876	20
CEBPB_02	3.170474	10

Sites are within 200bp on either side of the NFκB peak center, all p values: $p<1x10^{-300}$

Table 4.8. Top 20 Transfac® binding site enrichment for genes where NFκB is recruited and RNA Polymerase II is unchanged upon TNFα .

Transfac® Binding Site	Ratio	Site Count
USF_C	6.37998	27
AP1_Q4	6.119471	8
E2F_03	5.249472	24
AHRARNT_01	4.893034	45
MAZR_01	4.487834	40
NMYC_01	4.270084	41
SP1_01	4.196438	19
E2F_02	4.120228	44
USF_01	4.108155	16
MYCMAX_03	4.037753	46
CREB_02	4.024033	17
AHRARNT_02	3.938088	37
HMX1_01	3.861733	39
HEN1_01	3.444987	28
ARNT_01	3.420487	23
ARNT_02	3.356281	30
MYCMAX_01	3.347713	27
MYCMAX_02	3.264825	19
CREB_Q2	3.240882	7
SP1_Q6	3.227477	18

Sites are within 200bp on either side of the NFκB peak center, all p values: $p<1x10^{-300}$

Table 4.9. Top 20 Transfac® binding site enrichment for genes where NFκB is recruited and RNA Polymerase II is released upon TNFα treatment .

Transfac® Binding Site	Ratio	Site Count
AP2ALPHA_01	7.350379	9
PAX4_01	4.397058	58
HEN1_01	4.349422	47
TAXCREB_02	4.30688	50
AREB6_03	4.304521	50
AP2_Q6	4.256468	53
AHRARNT_02	4.242204	53
NFY_01	4.207955	18
SP1_01	4.152074	25
EGR2_01	4.148384	48
NF1_Q6	4.140876	35
E2F_03	4.11141	25
HOX13_01	4.049337	51
AP2GAMMA_01	4.044471	15
CREB_Q4	3.961824	11
AHRARNT_01	3.923472	48
PAX5_01	3.770719	70
EGR3_01	3.732387	43
MIF1_01	3.663757	46
AREB6_02	3.662176	39

Sites are within 200bp on either side of the NFκB peak center, all p values: $p<1x10^{-300}$

Figure 4.7. At NFκB recruited promoters, changes in Pol II upon TNFα treatment are dependent on NFκB. Box plots of gene-specific ChIP-qPCR analyses of Pol II and NFκB binding at regions of statistically significant ($p<0.016$) NFκB recruitment upon TNFα treatment (25 ng/ml for 30 min). Eight promoters were selected from the Pol II recruited and Pol II released sub-categories, and five promoters were selected from the Pol II unchanged sub-category. Of all the promoters, only six in the "Pol II recruited" sub-category have a consensus NFκB binding site. Box limits represent the 25^{th} and 75^{th} percentile, and error bar limits represent the outer-most data points. Each data point is a mean of $n = 3$. Asterisk denotes significance ($p<0.01$) in a Student's T-test. (A) ChIP-qPCR data for NFκB in all three sub-categories, with amplicons spanning the peak of NFκB binding according to the ChIP-chip. (B) ChIP-qPCR data for Pol II in all three sub-categories, with amplicons spanning the body of the genes (>1kb into the gene).

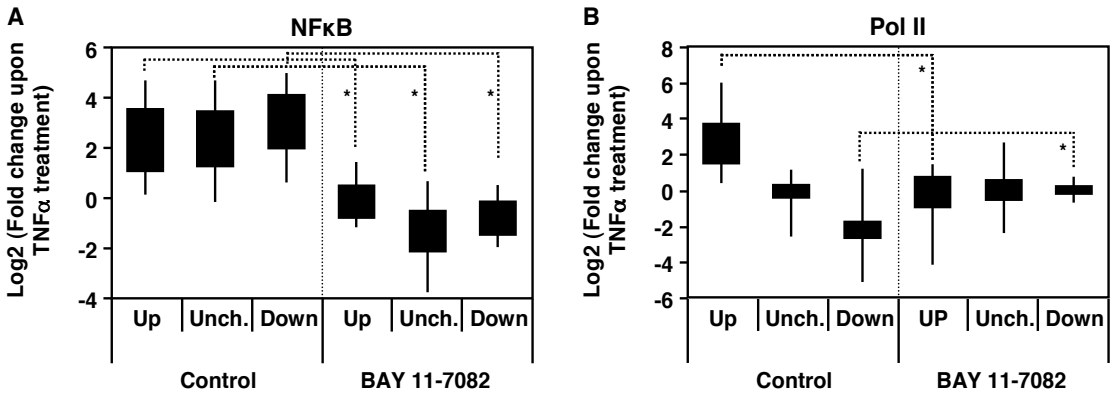
A
NFκB
Log2 (Fold change upon TNFα treatment)
6
4
2
0
-2
-4
Up
Unch.
Down
Up
Unch.
Down
Control
BAY 11-7082
B
Pol II
Log2 (Fold change upon TNFα treatment)
8
6
4
2
0
-2
-4
-6
Up
Unch.
Down
UP
Unch.
Down
Control
BAY 11-7082

Table 4.10. Selected genes for qPCR analysis in Pol II recruited, Pol II unchanged and Pol II released gene categories.

Pol II recruited (n=10)	**Pol II unchanged (n=5)**	**Pol II released (n=9)**
ZC3H12A	JHDM1D	PARD6A
NFKB2	NDUFS6	RASSF7
BIRC3	P2RY11	HCCA2
CADM1	CENPB	FSCN1
NEO1	SLBP	C9orf167
OXSR1		ADCYAP1R1
MAPK6		SLC7A10
CADM1		CALML3
SMURF2		PPP2R5B
TRIM33		

Figure 4.8. PARP-1 is an essential co-activator for the TNFα-dependent increase in key pro-inflammatory NFκB target genes in AC16 cells. (A) Western blot of control and PARP-1 knockdown AC16 whole cell extract blotted for PARP-1 and β-Actin (as a loading control). Two separate PARP-1 knockdown constructs were used to show specificity. (B-G) Analysis of mRNA expression by RT-qPCR in TNFα-treated AC16 cells relative to vehicle treated cells, in control and PARP-1 knockdown cells. Cells were treated with 25 ng/ml TNFα for either 30 min (dark blue) or 180 min (light blue). Expression data is standardized to β-actin transcripts. Each data point is a mean of $n = 3$. Error bar represents SEM.

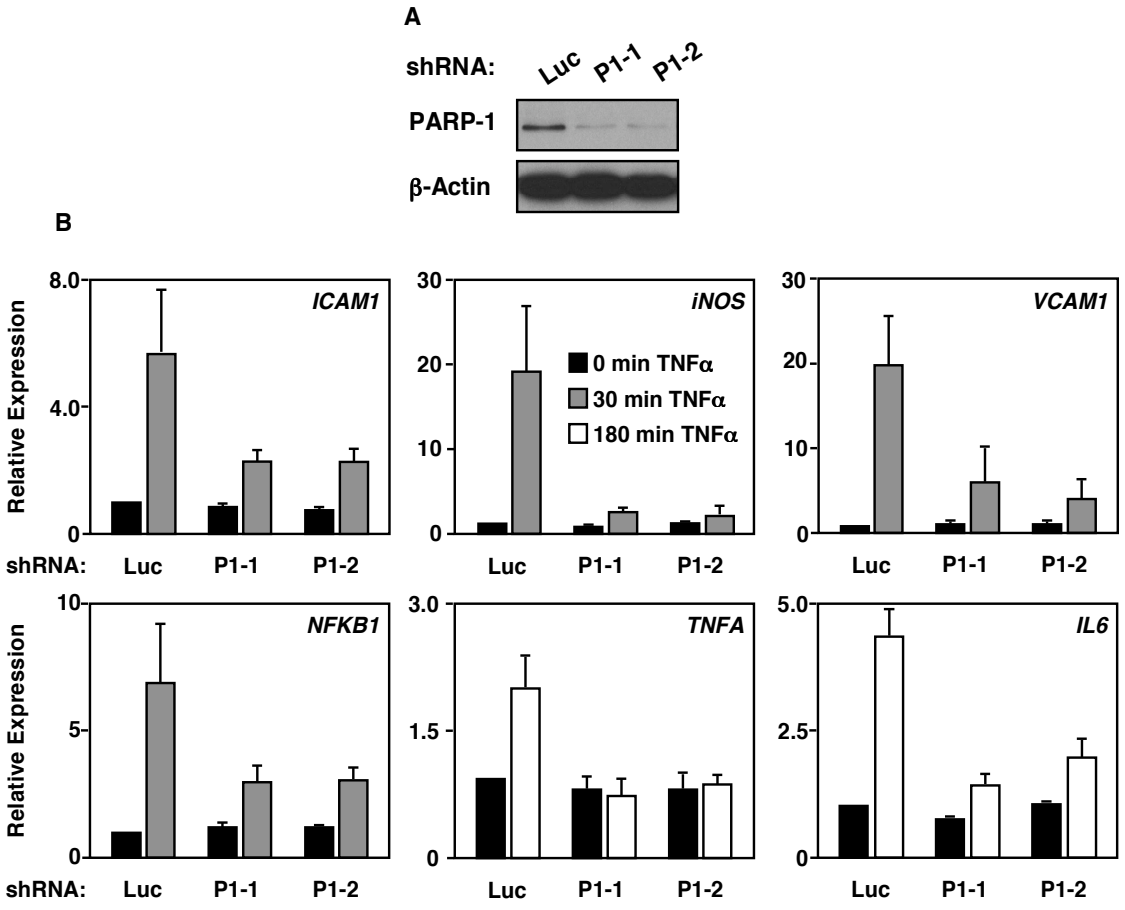
A
shRNA:
Luc
P1-1
P1-2
PARP-1
β-Actin
B
Relative Expression
ICAM1
iNOS
VCAM1
0 min TNFα
30 min TNFα
180 min TNFα
shRNA:
Luc
P1-1
P1-2
NFKB1
TNFA
IL6

Figure 4.9. PARP-1 catalytic activity is not required for TNFα-dependent activation of pro-inflammatory genes in AC16 cells. (A) Western blot of control and PARP-1 inhibitor (PJ34)-treated AC16 whole cell extract blotted for PARP-1, Poly(ADP-ribose) (PAR) and β-Actin (as a loading control). Cells were pre-treated +/- 5 μM PJ34 for 1 hr, as well as +/- hydrogen peroxide (C – control, H – hydrogen peroxide treated) to increase the PAR signal. (B-G) Analysis of mRNA expression by RT-qPCR in TNFα-treated (25 ng/ml for 30 min (dark blue) or 180 min (light blue)) AC16 cells relative to vehicle treated cells, in control and PJ34-treated (5 μM for 1 hr) cells. Expression data is standardized to β-actin transcripts. Each data point is a mean of $n = 3$. Error bar represents SEM.

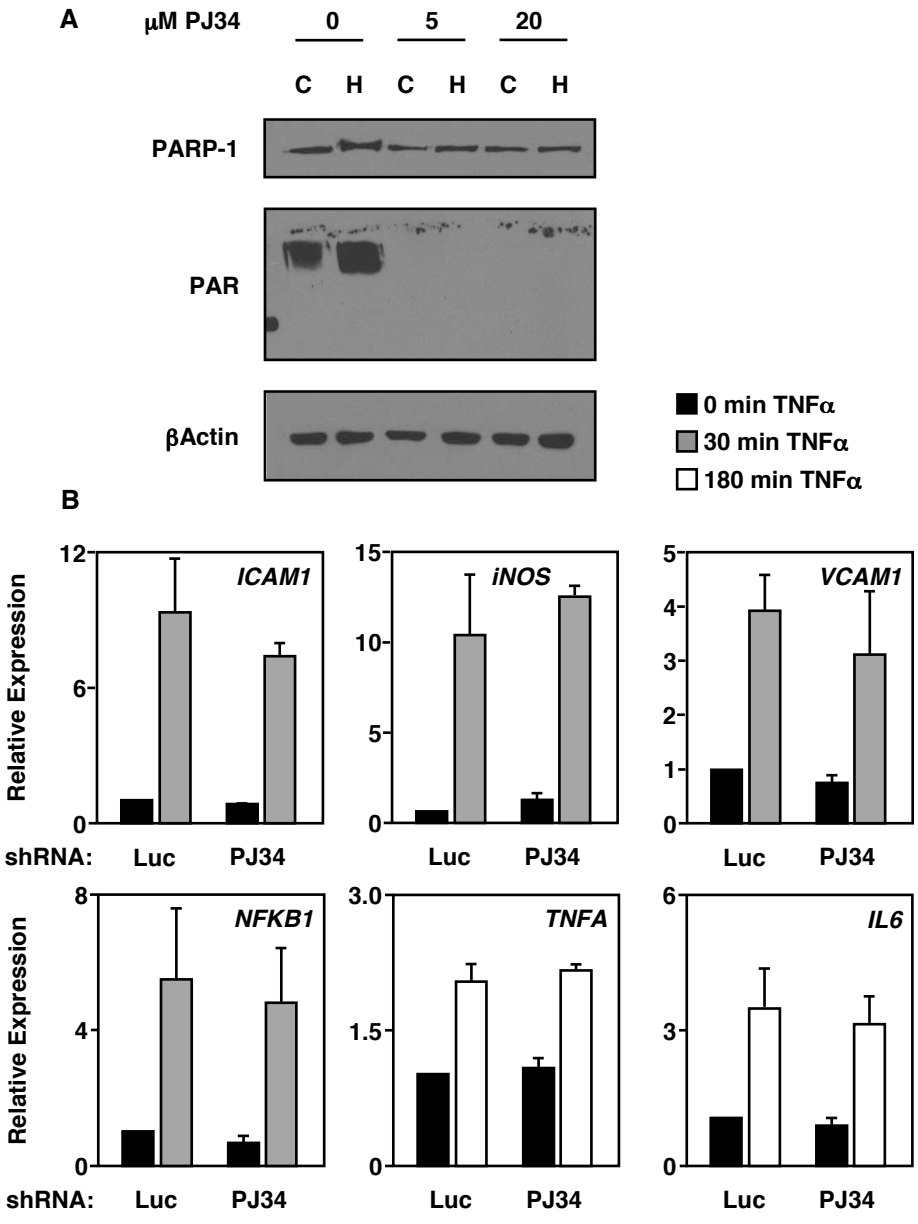
A
μM PJ34
0
5
20
C H C H C H
PARP-1
PAR
βActin
0 min TNFα
30 min TNFα
180 min TNFα
B
Relative Expression
ICAM1
iNOS
VCAM1
NFKB1
TNFA
IL6
shRNA:
Luc
PJ34

of NFκB (Fig. 4.11C). I found that 68% of the promoters that contained a peak of NFκB after TNFα treatment also contained a peak of PARP-1, confirming that they were bound at the same promoters. However, when I asked whether the peaks of PARP-1 and NFκB were within 500 bp of each other, I saw that in the majority of cases, the peaks were not co-localized, supporting our data showing that PARP-1 and NFκB do not affect each other's recruitment to chromatin (Fig. 4.12A). Additionally, we found that of all the TNFα-regulated genes (i.e. Pol II recruited or release), about three quarters did not show co-localization (i.e. peak of binding within 1kb) of PARP-1 and NFκB at their promoters (Fig. 4.12B). Finally we see that at a vast majority of promoters that show recruitment of NFκB upon TNFα treatment, the binding of PARP-1 is unchanged across a 3kb region around the TSS (Fig. 4.12C). These data suggest that may be these proteins have a more complex interaction than a purely co-activator – transcription factor relationship, and this hypothesis is further probed in the discussion section.

Next, I wanted to determine the role of PARP-1 in NFκB-dependent transcription. I began by confirming that the depletion of PARP-1 translated into a significant decrease of PARP-1 on chromatin (Fig. 4.11D), and that BAY 11-7085 does not affect PARP-1 localization at the genes in the three aforementioned Pol II categories (Fig. 4.11E). Also, PARP-1 knockdown does not affect NFκB translocation into the nucleus upon TNFα treatment (Fig 4.11F). I next examined the role of PARP-1 as a co-regulator of the genes in the three categories. I found that, while depleting PARP-1 abrogates the Pol II recruitment in the corresponding category, the binding of Pol II is unchanged at the genes in the released category, suggesting that PARP-1 specifically plays a role as an activator, and not a repressor, in NFκB-dependent transcription (Fig. 4.11G). Although PARP-1 has been shown to act both as an activator and a repressor of gene expression in various contexts (Hassa, et

al., 2003, Hassa, et al., 2005, Ju, et al., 2006, Ju, et al., 2004, Krishnakumar, et al., 2008, Pavri, et al., 2005), it appears to be solely an activator in NFκB-dependent transcription.

My bioinformatic data (Tables 4.7 – 4.9) suggest the involvement of other transcription factors in regulating NFκB-dependent transcription, so in order to follow-up on this result, I looked at the role of the CREB/ATF family of proteins in this pathway. I chose this family since it has previously been reported to play a role in NFκB-dependent transcription (Spooren, et al., , Todorov, et al., 2005), and its members are significantly enriched in relevant classes of my bioinformatic analysis (Tables 4.7 – 4.9). Initially, I confirmed the bioinformatic results experimentally by transient trasfections followed by luciferase reporter gene assays (Fig. 4.13A – Plasmids courtesy of Dr. Nina Heldring). I found that using a plasmid with a CRE (CREB Response Element, the DNA motif bound by CREB/ATF transcription factors) enhance the TNFα-dependent activation of the reported in AC16 cells (Fig. 4.13A). Pre-treating the cells with the NFκB inhibitor BAY 11-7085, or co-transfecting a plasmid expressing a dominant-negative ATF protein (A-ATF) abrogated this response (Fig. 4.13A).

In order to further investigate the role of these family members, I generated a cell line that stably overexpressed a dominant negative version of CREB (A-CREB) as well as another line stably overexpressing A-ATF. (Plasmids for overexpression courtesy of Dr. Nina Heldring). Unfortunately, the overexpression of A-CREB was detrimental to the cells, causing them to die before cells could be collected for experiments. The A-ATF cells, on the other hand, though somewhat slower-growing and less healthy, were able to survive and proliferate. Confirmation of the expression of ATF factors (represented by ATF2) as well as the A-ATF were performed by western blot (Fig. 4.13B, C). I therefore used these cells to

determine whether ATF cooperates with NFκB to regulate tarvget genes. More specifically, at NFκB target genes that have no NFκB consensus site, but have a CRE site, is ATF required for maximal expression of target genes? As a representative of the ATF family, I looked for ATF2 at promoters, and found a subset of genes with ATF2 bound (Fig. 4.13D). I chose to look at one TNFα-upregulated gene (MAPK6), one unregulated gene (JHDM1D), and two downregulated genes (PARD6A and PPP2R5B) that do not have an NFκB consensus site (henceforth referred to as "non-consensus regulated"). I also used NFKB2, an upregulated gene that does have a NFκB consensus site, as a control. Upon expression of A-ATF, ATF2 binding was significantly reduced at these promoters, as expected (Fig. 4.13D). I next looked at NFκB binding at these target genes, and found that while at NFKB2 and JHDM1D (two controls) the recruitement of NFκB was unaffected, at the non-consensus regulated genes, lack of ATF2 at the promoter inhibits NFκB recruitment, consistent with a model in which NFκB and ATF2 cooperate. Also consistent with this model is the reduction of Pol II recruitment and mRNA production in the A-ATF cells (Fig. 4.13F, G). Taken together, these data reveal a role for ATF2 in tethering NFκB p65 to target promoters for transcriptional regulation.

4.4 Discussion

Cardiovascular disease (CVD) is the leading cause of death in the United States, and understanding the molecular mechanisms leading to CVD is key to finding sustainable therapies and taking preventative measures to these pathologies (Mehra, 2007). In this study, I examine the role of the nuclear transcription factor NFκB in mediating the signaling events leading to CVD. I use TNFα-treated human cardiomyocytes (it is known that TNFα is released by a number of cell types during conditions of stress, including cardiomyocytes) to determine a role for NFκB in

regulating RNA Polymerase II (Pol II) in response to stress. Using this system, I have shown herein that NFκB is not only globally recruited to chromatin upon TNFα treatment, but that it is vital in mediating TNFα-dependent changes in gene expression by Pol II. In addition, I have shown that, unexpectedly, the majority of NFκB binding events occur independently of a canonical NFκB binding site, suggesting intricate cooperation with a number of other transcription factors. Finally, I have demonstrated a role for PARP-1 at NFκB target genes that are up-regulated by TNFα, but not the down-regulated ones, suggesting different mechanisms at different target promoters.

NFκB is Recruited to the Genome upon TNFα Treatment. Recruitment of NFκB to the genome after various different stress stimuli is a well-documented phenomenon (Lim, et al., 2007, Schreiber, et al., 2006). I expected to obtain a subset of genes showing NFκB recruitment, but instead, I observed a genomic increase in NFκB binding across many genes (Fig. 4.4). This result was somewhat unexpected based on the rapid time-point at which I performed our experiments, as well as previous data on NFκB binding to the genome (Lim, et al., 2007, Schreiber, et al., 2006). However, to our knowledge, this is the first report of NFκB binding sites at promoters in a human cardiomyocyte cell line, and it is possible that these cells are acutely responsive to stress signals. In fact, based on what is known about the role of NFκB in CVD, it is not entirely surprising to find such a global response (Lentsch and Ward, 1999, Lentsch and Ward, 2000, Valen, 2004). In this study, I have used the p65 (or RelA) subunit as the representative member of the NFκB protein family, but as was discussed previously (Fig. 4.1), there are multiple NFκB proteins that mediate the signaling pathways (Lentsch and Ward, 2000, Vallabhapurapu and Karin, 2009). In fact, a previous study has examined the recruitment of different subunits of NFκB to the genome, and has found that depending on the subunit, they can be bound to the

Figure 4.10. PARP-1 binding to promoters is relatively unaltered upon TNFα treatment in AC16 cells. (A) Heat maps of PARP-1 ChIP-chip data in control cells, or TNFα-treated cells (25 ng/ml for 30 min), shown from -3 kb to +3 kb relative to the TSS. The data are ordered based on the intensity of the PARP-1 at the promoter in the untreated sample. (B) Average Log2 ratios of PARP-1 ChIP-chip data minus and plus TNFα for all promoters on the array. (C) Scatter plot of gene-specific ChIP-qPCR analyses of PARP-1 binding at regions of statistically significant ($p<0.016$) peaks of PARP-1, as well as unbound regions. Note: unbound regions were defined as having $p>0.9$. Each data point is a mean of $n = 3$. Bar represents median.

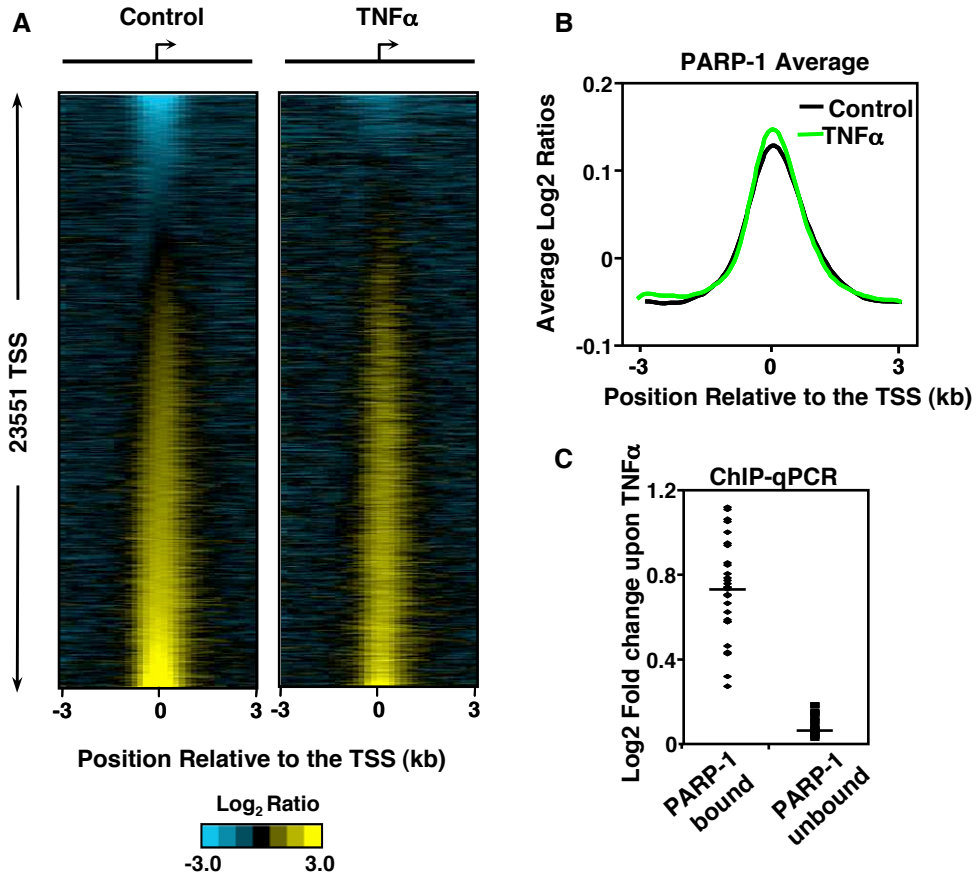
A
Control
TNFα
23551 TSS
-3
0
3
-3
0
3
Position Relative to the TSS (kb)
Log2 Ratio
-3.0
3.0
B
PARP-1 Average
Control
TNFα
Average Log2 Ratios
0.2
0.1
0
-0.1
-3
0
3
Position Relative to the TSS (kb)
C
ChIP-qPCR
Log2 Fold change upon TNFα
1.2
0.8
0.4
0
PARP-1 bound
PARP-1 unbound

Figure 4.11. PARP-1 is unaffected by inhibition of NFκB, and depletion of PARP-1 does not alter NFκB translocation into the nucleus. Box plots of gene-specific ChIP-qPCR analyses of PARP-1 were performed exactly as described in Fig.. 4.7.. Each data point is a mean of $n = 3$. Asterisk denotes significance ($p<0.01$) in a Student's T-test. (A) Cells were treated with 25 ng/ml TNFα for 30 min (or left untreated). ChIP-qPCR data shows knockdown of PARP-1 at the chromatin in all three sub-categories. (B) Cells were treated with 25 ng/ml TNFα for 30 min (or left untreated), either with or without pre-treatment with 10 μg/ml BAY-11-7082 for 1 hr. ChIP-qPCR data shows that PARP-1 binding is unchanged upon TNFα in all three sub-categories. (C) Venn diagram showing overlap of genes with NFκB and PARP-1 peaks. (D) Western blot of AC16 cytoplasmic and nuclear fractions blotted for NFκB, PARP-1, TFIIB (nuclear marker) and GAPDH (cytoplasmic marker), in control and TNFα-treated cells. Data for control cells is duplicated from Fig. 4.1. (E-G) ChIP-qPCR data of PARP-1 (E), NFκB (F), and Pol II (G) binding in all three categories upon TNFα treatment in control (Luc) knockdown and PARP-1 knockdown cells.

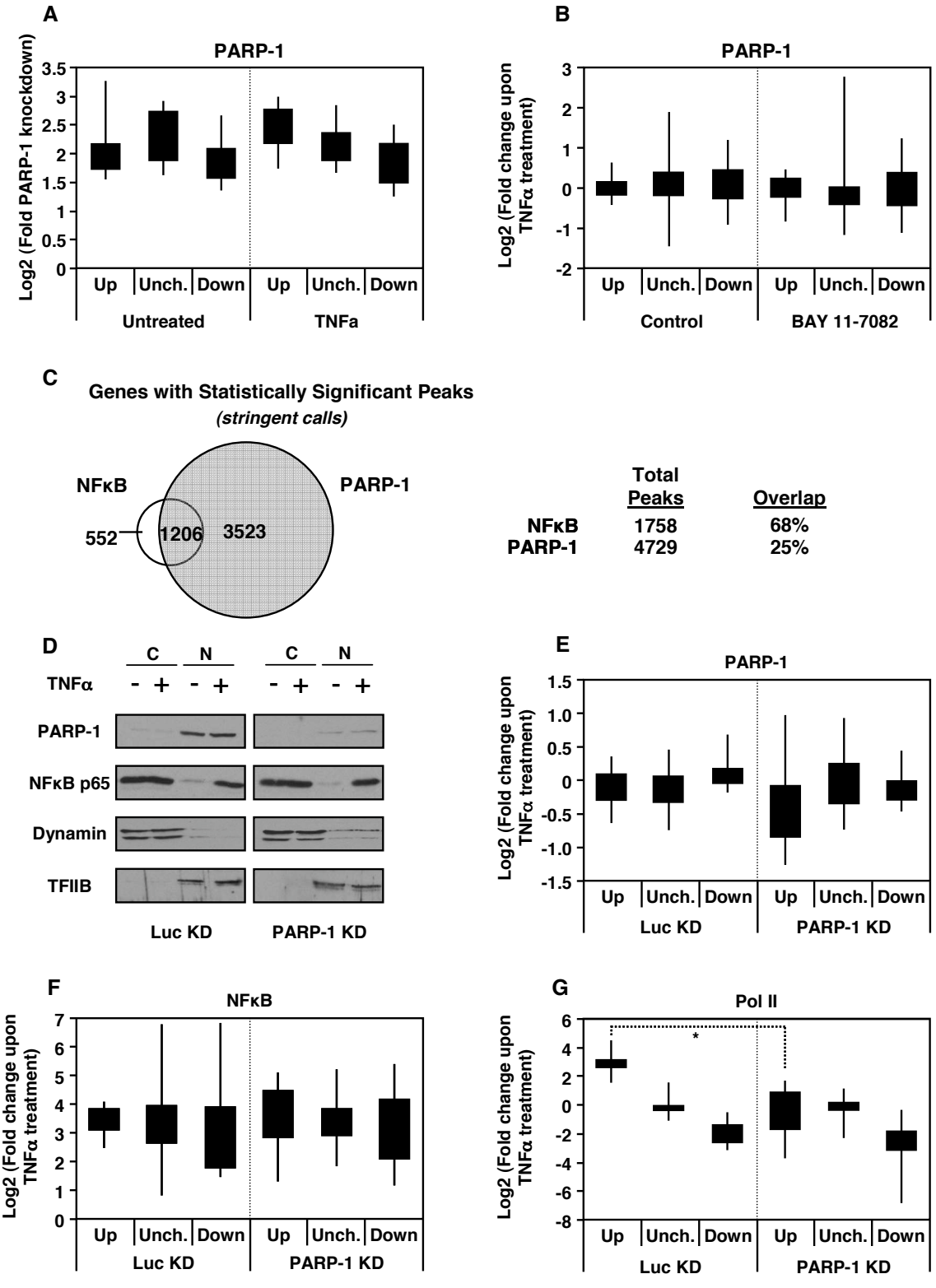
A
PARP-1
Log2 (Fold PARP-1 knockdown)
3.5
3
2.5
2
1.5
1
0.5
0
Up
Unch.
Down
Up
Unch.
Down
Untreated
TNFa
B
PARP-1
Log2 (Fold change upon TNFα treatment)
3
2
1
0
-1
-2
Up
Unch.
Down
Up
Unch.
Down
Control
BAY 11-7082
C
Genes with Statistically Significant Peaks
(stringent calls)
NFκB
PARP-1
552
1206
3523
Total Peaks
Overlap
NFκB 1758 68%
PARP-1 4729 25%
D
C
N
C
N
TNFα
- + - + - + - +
PARP-1
NFκB p65
Dynamin
TFIIB
Luc KD
PARP-1 KD
E
PARP-1
Log2 (Fold change upon TNFα treatment)
1.5
1.0
0.5
0
-0.5
-1.0
-1.5
Up
Unch.
Down
Up
Unch.
Down
Luc KD
PARP-1 KD
F
NFκB
Log2 (Fold change upon TNFα treatment)
7
6
5
4
3
2
1
0
Up
Unch.
Down
Up
Unch.
Down
Luc KD
PARP-1 KD
G
Pol II
Log2 (Fold change upon TNFα treatment)
6
4
2
0
-2
-4
-6
-8
*
Up
Unch.
Down
Up
Unch.
Down
Luc KD
PARP-1 KD

chromatin prior to stimulation, pre-bound and further recruited, or unbound and recruited upon stimulation (Schreiber, et al., 2006). Specifically, in monocytes, p50 and p52 proteins appear to be pre-bound to chromatin, and there isn't much change in their binding upon treatment with lipopolysaccharide (LPS). On the other hand, p65 (the subunit that I examined) appears to be completely absent in the untreated state, and significantly recruited upon LPS treatment. I did, however, find some p65 binding in the AC16 cells prior to TNFα treatment, but there are a number of possible explanations. Firstly, monocytes are an entirely different cell line, and the differences in NFκB could be cell-type specific. Additionally, when I performed Gene Ontology analysis on the genes that contained a peak of p65 prior to TNFα treatment, I did not find any significantly enriched terms, meaning that while there was binding of the factor, it may not be functionally relevant (data not shown). Finally, the stringency of binding site identification can vary from study to study, and despite the fact that our criteria were highly stringent, it is possible that this alternate study applied even greater stringency (which could also explain the differences in binding site numbers). Taken together however, our data as well as the literature suggest that while there may be nuances between cell types, NFκB recruitement to promoters upon stress is a hallmark mechanism of regulating transcription.

TNFα-Dependent Signaling Regulates RNA Polymerase II. TNFα is a pro-inflammatory cytokine which is known to initiate a large number of signaling cascades that result in changes in gene expression, and eventually changes in cell physiology (Kronke, et al., 1992, Schutze, et al., 1992). A majority of cell types are highly responsive to stress signals such as TNFα, but certain cell types are much more likely to require a rapid inflammatory response as a result of TNFα exposure, and one such example is cardiomyocytes during the onset of CVD (Schulz, et al., 2004). It has also

Figure 4.12. PARP-1 is not a classical NFκB co-activator. (A) Pie chart showing percentage of genes at which the PARP-1 peaks +/- TNFα are overlapping (i.e. very little lateral movement of the peak PARP-1 upon TNFα). Also shown is a schematic to illustrate the two categories. (B) Pie charts showing percentage of genes where PARP-1 and NFκB co-localize at promoters (defined as the peak of one factor being with 1kb of the peak of the other) in the Pol II recruited and released categories of genes as previously define Fig. 4.6). Again, a schematic is shown to clarify the definition of co-localized. (C) Pie charts showing percentage of genes with a statistically significant difference in the amount of PARP-1 bound at promoters minus and plus TNFα (Wilcoxin test $p \leq 0.016$).

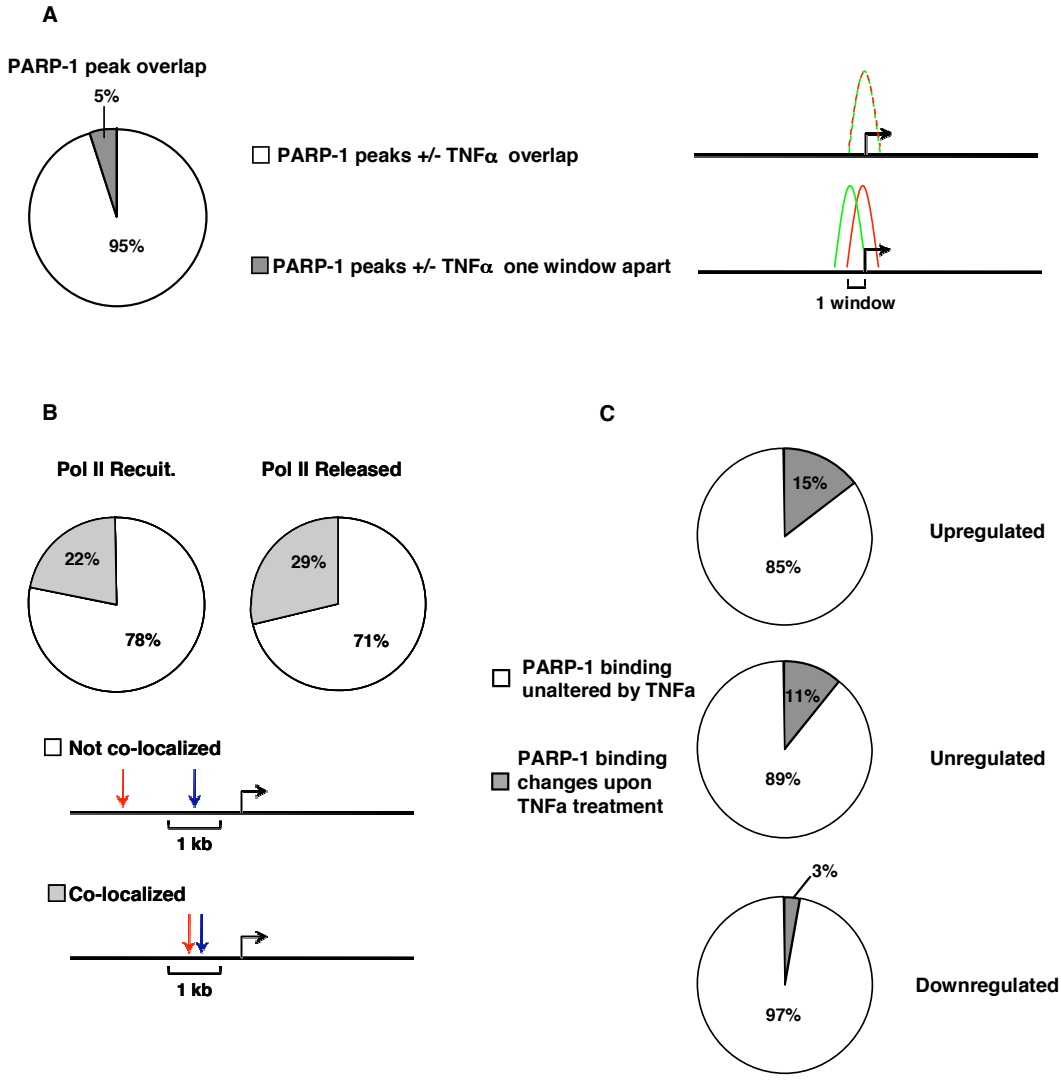
A
PARP-1 peak overlap
5%
95%
PARP-1 peaks +/- TNFα overlap
PARP-1 peaks +/- TNFα one window apart
1 window
B
Pol II Recuit.
Pol II Released
22%
78%
29%
71%
Not co-localized
1 kb
Co-localized
1 kb
C
15%
85%
Upregulated
PARP-1 binding unaltered by TNFa
PARP-1 binding changes upon TNFa treatment
11%
89%
Unregulated
3%
97%
Downregulated

Figure 4.13. ATF2 cooperates with NFκB to regulate TNFα-dependent transcription. (A) Luciferase reporter gene assays using pGL3 with a CRE at the promoter (a No CRE plasmid was used for the control condition). Cells were also either treated with BAY 11-7085 or co-transfected with A-ATF. All data was normalized to βgal. Each data point is a mean of $n = 3$. Error bar represents SEM. (B) Western blot of whole cell extract from AC16 overexpressing Flag tagged A-ATF (or empty vector control), blotted for FLAG and β-Actin (as a loading control) . (C) Western blot of nuclear extract from AC16 plus or minus 25 ng/ml TNFα treatment for 1 hour, blotted for ATF2 and TBP (as a loading control) . (D-F) ChIP-qPCR analyses of ATF2 (D), NFκB (E), and Pol II (F) levels at the promoters of five NFκB target genes (NFKB2 – upregulated, consensus NFκB site; MAPK6 – upregulated, CRE; JHDM1D – unregulated, CRE; PARD6A and PPP2R5B – downregulated, CRE) in control (pQCXIP) and A-ATF overexpressing cells, plus and minus TNFα. (G) Analysis of mRNA expression for the same genes in the same cell lines as (D-F) by RT-qPCR. The data are normalized to the β-actin transcript and expressed relative to control (pQCXIP) cells. Each bar represents the mean plus the SEM, $n \geq 3$.

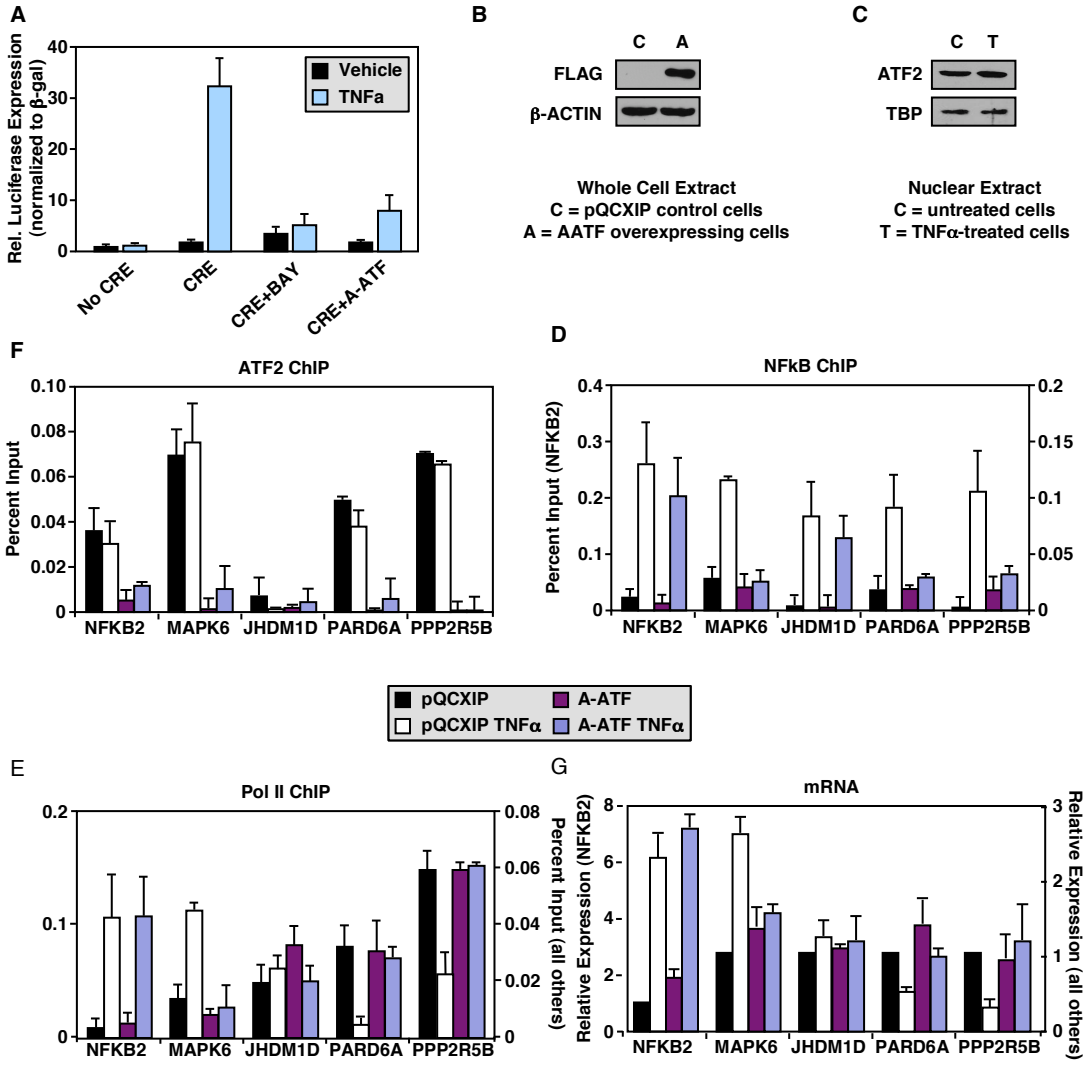
A
Rel. Luciferase Expression (normalized to β-gal)
Vehicle
TNFa
No CRE
CRE
CRE+BAY
CRE+A-ATF
B
C A
FLAG
β-ACTIN
Whole Cell Extract
C = pQCXIP control cells
A = AATF overexpressing cells
C
C T
ATF2
TBP
Nuclear Extract
C = untreated cells
T = TNFα-treated cells
F
ATF2 ChIP
Percent Input
NFKB2
MAPK6
JHDM1D
PARD6A
PPP2R5B
D
NFkB ChIP
Percent Input (NFKB2)
pQCXIP
pQCXIP TNFα
A-ATF
A-ATF TNFα
E
Pol II ChIP
Percent Input (all others)
G
mRNA
Relative Expression (NFKB2)
Relative Expression (all others)

been shown that cardiomyocytes can up-regulate and secrete TNFα themselves when they are stressed ((Comstock, et al., 1998, Maass, et al., 2002), see Fig. 4.3), which means that the TNFα signaling pathways get rapidly propagated in the context of CVD. In our study, I show that TNFα alters the genomic binding pattern of Pol II at gene promoters and into the gene bodies. In fact, I used Pol II density in the gene body to identify transcription regulation, a method which has previously been used in the literature (Welboren, et al., 2009). Furthermore, comparison of our Pol II ChIP-chip with expression data sets from three un-related cell lines confirm the connection between immediate transcriptional responses by Pol II and stable mRNA 30 minutes later (Fig. 4.5 D, E). While our heat maps and average log2 ratio analysis suggest that a large number of genes are up-regulated upon TNFα treatment (Fig. 4.5), I show that a significant number of genes are also down-regulated. This suggests a general re-arrangement of the transcriptional program in response to TNFα, as quickly as 30 minutes after exposure. Interestingly, a recent study used microarrays, ChIP and RNA FISH to show that TNFα causes a wave of Pol II to be released into the body of target genes, and that this wave correlates with the appearance of nascent RNAs (Wada, et al., 2009). This further supports the use of Pol II density in the body of the gene as a measure of transcription. In fact, the authors of this study show that the rate of Pol II movement can be altered by CTCF binding sites and cohesion binding (Wada, et al., 2009). Based on this and on our work shown here, I may be able to use AC16 cells in the future to determine the rate of Pol II travel along gene bodies, which I can correlate with many variables, including factor binding and local chromatin environment. Such analyses should help shed light on what factors affect transcription by Pol II at a highly molecular level.

NFκB Regulates Transcription of Genes that Alter the Physiological State of the Cells. By sub-setting the genes that recruit NFκB based on their Pol II status, I found that genes with NFκB binding upon TNFα treatment revealed different characteristics. Specifically, genes that are up-regulated have a higher enrichment of canonical NFκB binding sites than genes that are down-regulated. This strongly suggests different mechanisms at these two categories of genes, which will be actively investigated in future studies. The Gene Ontology analysis also reveals specific differences between up- and down-regulated genes. Upon TNFα treatment, NFκB up-regulated genes include proteins involved in nitric oxide synthesis (a hallmark of inflammation), signaling and defense mechanisms. Conversely, down-regulated genes include proteins involved in transcription and metabolism. The cells appear to be focusing their efforts on responding to the stress signal, and are down-regulating many of the "housekeeping" processes in order to conserve resources. This is a known phenomenon for stress-response, specifically for heat-shock (Aufricht, 2005). Additionally, infection (which triggers many of the same pathways as treatment with TNFα) also causes massive down-regulation of genes that are used for host maintenance (Prosniak, et al., 2001). Therefore, human cardiomyocytes respond to stress by TNFα by rapidly reprioritizing the transcription that occurs.

NFκB and PARP-1 Function Together to Up-Regulate Genes Upon TNFα Treatment. PARP-1 has been previously shown to cooperate with NFκB to regulate transcription of key pro-inflammatory genes (Hassa, et al., 2003, Hassa, et al., 2005, Pacher and Szabo, 2007, Pillai, et al., 2005, Szabo, et al., 2006, Tulin and Spradling, 2003). Here I confirm a role for PARP-1 in the regulation of NFκB-dependent transcription in cardiomyocytes. I see that while NFκB can both up- and down-

regulate gene expression, PARP-1 appears only to be an activator in this context. This is consistent with what has been previously reported in the literature regarding a role

for PARP-1 in NFκB-dependent transcription. However, PARP-1 has often been labeled as an "NFκB co-activator", which suggests that upon stimulation, PARP-1 is recruited to chromatin by NFκB. This study, on the other hand, suggests that the binding of PARP-1 is not dependent on NFκB (treating with an IKK inhibitor does not affect PARP-1 binding, but blocks NFκB recruitment), but that the activity of NFκB at up-regulated promoters requires PARP-1. Additionally, co-regulators would be expected to co-localize on chromatin, and I show that while PARP-1 and NFκB bind largely to the same promoters, they are not necessarily binding to the same sites, suggesting that the functional interacting between them occurs after they are bound to chromatin (for example, by recruiting other factors) (Fig. 4.12B). Finally, PARP-1 is not recruited to chromatin upon TNFα treatment as you would expect for a co-activator, but is bound prior so stimulation and NFκB recruitment (Fig. 4.12A, C). Our results are not necessarily contradictory to the majority of the literature, but our interpretation takes into account the many different conclusions both from our study and from other studies. For example, work done by another lab demonstrates that PARP-1 interacts with both the p50 and p65 subunits of NFκB, and that the interaction with p50 is strengthened upon stimulation with LPS. First of all, *in vivo*, PARP-1 would only come into contact with p65 after stimulation, and secondly, interaction based on an immunoprecipitation assay with proteins in solution does not necessarily suggest co-localization on chromatin. Additionally, this group shows that PARP-1 acetylation by p300/CBP can increase association of PARP-1 with p50 (interestingly, not p65) and Mediator, and again, this is still consisitent with PARP-1 being pre-bound at these promoters, and recruiting both p300/CBP and Mediator after

stimulation. This may also explain why all the above proteins are found in a complex. Therefore, when I combine my data with the data from these studies, I am able provide an interpretation which explains all the results together, without necessarily requiring that PARP-1 be a classical co-activator of NFκB.

Transcriptional Regulation by NFκB in Cardiomyocytes is Likely to Involve Other Transcription Factors, such as CREB. Based on the motif finding analysis performed on the different classes of NFκB-regulated genes, I concluded that the majority of NFκB binding events did not require a canonical NFκB binding site, suggesting cooperation of NFκB with other DNA-binding transcription factors. It is known that NFκB requires a number of factors for many of its functions (Chen, et al., 2001, Covic, et al., 2005, Hassa, et al., 2003, Hassa, et al., 2005, Katsel and Greenstein, 2001, Lim, et al., 2007, Meylan, et al., 2009, Yamamoto, et al., 2003, Yang, et al., 2000). Although transcription factors are known to cooperate with NFκB (e.g. AP2, SP1, p53), most published work focuses on genes that have both an NFκB site and another site (Katsel and Greenstein, 2001, Lim, et al., 2007, Yang, et al., 2000). For instance, a recent study looked at NFκB p65 binding upon LPS treatment in human monocytes, and found that many NFκB sites were enriched for a flanking E2F1 site (Lim, et al., 2007). They go on to show that NFκB requires E2F1 to regulate target gene expression changes upon LPS treatment, although it was not required to recruit p65 to promoters. This is likely because the targets they looked at also had an NFκB canonical binding site. Here, I have shown a requirement for other transcription factors such as ATF2 to recruit NFκB to promoters which do not contain a canonical NFκB site (Fig. 4.13). Specifically, I can use a dominant negative form of ATF to prevent NFκB binding to promoters upon TNFα treatment, and block transcription by Pol II, strongly suggesting cooperation between these factors. Further

experiments are likely to identify more such factors that cooperate with NFκB to regulate inflammation in cardiomyocytes.

Future perspectives: Increasing Evidence Points to Roles for NFκB in Diverse Physiological Processes. Although the mechanism by which NFκB is activated and regulates gene expression has been studied for decades, it has been considered primarily as a pro-inflammatory transcription factor (Lentsch and Ward, 1999, Lentsch and Ward, 2000, Vallabhapurapu and Karin, 2009). Only recently are I beginning to understand the magnitude of physiological responses that involve, and require, NFκB-dependent pathways. NFκB has recently been shown to be vital in the progression of lung carcinoma (Meylan, et al., 2009). In the background of a p53 mutation and Ras overexpression, NFκB signaling is constitutively activated, promoting tumor formation in mice. The authors briefly show that NFκB target genes are altered in these mutant backgrounds, but mechanisms behind these changes are unclear. It is tempting to speculate that perhaps some of the same factors that cooperate with NFκB during inflammatory responses (PARP-1, CBP, CREB) may be playing a role in carcinogenesis, and this hypothesis warrants further study. It would be too simplistic, however, to imagine that all the pathways would be completely conserved, even if the players are the same. An interesting example of this comes from a study that looks at the cooperation between PARP-1 and NFκB not in stress-regulated transcription, but in the response to DNA damage. In this work, the authors show the importance of PARP-1 catalytic activity in forming a critical DNA repair protein complex (while PARP-1 catalytic activity is not required for TNFα-dependent transcription regulated by NFκB) (Stilmann, et al., 2009). This shows us that understanding NFκB-dependent pathways in one system cannot necessarily predict behaviors in other contexts, but can provide us with candidates to investigate in other

physiological responses. NFκB is also involved in ageing, and interestingly, it is found in the same pathway as another NAD^+-dependent enzyme, the sirtuin SIRT6. But while PARP-1 is a co-activator of NFκB, SIRT6 is an antagonist, and H3K9 deacetylation by SIRT6 at NFκB targets attenuates NFκB signaling and reverses the effect of premature ageing and death seen in SIRT6 knockout mice (Kawahara, et al., 2009). Sirtuins and PARPs are known to compete for NAD^+, which could set the stage for competition between the two enzymes. It will be interesting to determine whether PARP-1 may be playing a role in the ageing phenotype caused by overactivation of NFκB, and whether other transcription factors, including ones in the CREB family that I have already identified as cooperating with NFκB, are also involved. In conclusion, NFκB-regulated pathways are as wide-spread as they are versatile, and understanding the molecular mechanisms that underlie these pathways in different physiological and pathological contexts could greatly increase the chances of developing novel therapies to a variety of diseases and disorders that plague the world today.

4.5 Materials and Methods

Cell lines. AC16 human adult ventricular cardiomyocyte cells purchased from American Type Cell Culture (ATCC) (Davidson, et al., 2005). The cells were maintained in DMEM F-12 supplemented with 12.5% fetal bovine serum. TNFα was purchased at PeproTech (Cat# 300-01A), and the IKKα/β inhibitor BAY-11-7082 was purchased from Calbiochem (Cat# 196870). For relevant experiments, PJ34 was purchased from Alexis Biochemicals (Cat# ALX-270-289). For all TNFα treatments, medium was changed to serum-free DMEM F-12, 24 hrs after plating. PARP-1-depleted AC16 cells were generated by retroviral-mediated gene transfer of two short

hairpin RNA sequences specifically targeting the PARP-1 mRNA using the pSUPER.retro system (Oligoengine) (Frizzell, et al., 2009, Zhang, et al., 2009)]. Control cells harboring a short hairpin RNA sequence directed against luciferase were generated in parallel. A-ATF overexpressing cells were generated using the pQCXIP system (Clonetech), and an empty vector was used to generate a control cell line in parallel (plasmids courtesy of Dr. Nina Helding). Selection for knockdown and overexpressing cells was performed in 0.5 μg/ml puromycin.

Antibodies. A previously characterized custom rabbit polyclonal anti-PARP-1 antibody was used for ChIP and western blotting (Kim, et al., 2004). NFκB p65 ChIP grade antibody was purchased from Abcam (Cat# 7970) All other antibodies were as follows: Pol II (Santa Cruz SC-899 and SC-900, mixed in a 1:4 ratio), TBP (Santa Cruz SC273X), Dynamin (Sigma-Aldrich D4038), PAR (Trevigen 4335-AMC-050) and β-ACTIN (Sigma-Aldrich, A5316).

mRNA expression analyses. Cells were seeded at ~1.5 x 10^5 cells per well in 6-well plates and grown for a day before being left in serum-free medium overnight. The cells were then treated with TNFα, BAY-11-7082, or PJ34 as appropriate (see figure legends), and collected at about 80% confluence. Total RNA was isolated using Trizol Reagent (Invitrogen) according to the manufacturer's protocols. The total RNA was reverse transcribed using oligo(dT) and subjected to real-time quantitative PCR using gene-specific primers (see primer sequences listed below; Section 2). All target gene transcripts were normalized to the β-actin transcript. Each experiment was conducted a minimum of three times with independent isolates of total RNA to ensure reproducibility.

Transient transfection and reporter gene assays. Cells were seeded at ~1.5 x 10^5 cells per well in 6-well plates and grown for a day before changing the medium to serum-free, and transfecting the following plasmids using the GeneJuice system (EMD Biosciences): pCMV-βgal, pCMV empty or A-ATF, pGL3 promoter only or promoter with CRE (plasmids courtesy of Dr. Nina Heldring). The following day, cells were treated with TNFα for 4 hours, after which they were collected, lysed in ProMega 5X Lysis Buffer, and the supernatant was collected by centrifugation. Parallel luciferase and βgal assays were performed. Control cells were left untreated.

Primers

ChIP primers

ICAM1_TSS_Fwd	5'-CGGTGTAGACCGTGATTCAA-3'
ICAM1_TSS_Rev	5'-TCCGGAATTTCCAAGCTAAA-3'
INOS_TSS_Fwd	5'-TGGTTTCCAAAGGGAGTGTC-3'
INOS_TSS_Rev	5'-TGAAGAGGCACCACACAGAG-3'
VCAM1_TSS_Fwd	5'-ACACACAGGTGGGACACAAA-3'
VCAM1_TSS_Rev	5'-CCAAGGATCACGACCATCTT-3'
TNF_TSS_Fwd	5'-GCTTGTGTGTCCCCAACTTT-3'
TNF_TSS_Rev	5'-AACCAGCGGAAAACTTCCTT-3'
NFKBp50_TSS_Fwd	5'-CTCGACGTCAGTGGGAATTT-3'
NFKBp50_TSS_Rev	5'-GCGAAACCTCCTCTTCCTG-3'
IL6_TSS_Fwd	5'-TGCACTTTTCCCCCTAGTTG-3'
IL6_TSS_Rev	5'-TCATGGGAAAATCCCACATT-3'
ZC3H12A_TSS_Fwd	5'-CGTGCTTATCTTGCGCATAC-3'
ZC3H12A_TSS_Rev	5'-CTTCCTGCTCCGCTCCTC-3'
ZC3H12A_1kb_Fwd	5'-GTTTTGGGAGGGAGGTTAGG-3'

ZC3H12A_1kb_Rev	5'-GACAGGCTTCTCTCCACAGG-3'
NFKB2_-1kb_Fwd	5'-ACACACATGCACACGGAGAC-3'
NFKB2_-1kb_Rev	5'-CGGGTGAGCGTATCTTGAGT-3'
NFKB2_TSS_Fwd	5'-CCCTTGGTATTTTCGGGACT-3'
NFKB2_TSS_Rev	5'-GGAAGGGGCAGGAAAGTTAG-3'
NFKB2_2kb_Fwd	5'-AGCAAGAGGCCAAAGAACTG-3'
NFKB2_2kb_Rev	5'-AGGGAGAAGGAGCCATCACT-3'
BIRC3_-0.5kb_Fwd	5'-TGCAAAGGAGAACTGCATGA-3'
BIRC3_-0.5kb_Rev	5'-AGCTGCAGAAGTCCAGCATT-3'
BIRC3_1kb_Fwd	5'-AGGCAGAAAGAAAAGGCACA-3'
BIRC3_1kb_Rev	5'-CATGCAGCACATCCATTTTT-3'
CADM1_TSS_Fwd	5'-GGCTTCTGCTGTTGCTCTTC-3'
CADM1_TSS_Rev	5'-ACACCTACCTGTGGGGATCA-3'
CADM1_3kb_Fwd	5'-GGCTGACTTTTGCTTGCTTT-3'
CADM1_3kb_Rev	5'-TGCGGCTATTCAATCTGATG-3'
NEO1_TSS_Fwd	5'-TCACTCTCGGGGAAGAGATG-3'
NEO1_TSS_Rev	5'-CAGGCAGTAGAGCCAGAAGG-3'
NEO1_2kb_Fwd	5'-TGAGGAGTGGGTAGGAGTGG-3'
NEO1_2kb_Rev	5'-GCAGAGCGGTTTACAGGAAG-3'
MAPK6_TSS_Fwd	5'- GGAGACCTGAGCCGACACT-3'
MAPK6_TSS_Rev	5'- CACACACACTCACGGGACTT-3'
MAKP6_2kb_Fwd	5'- ACAGCCAACGTTTAGCAAGG-3'
MAKP6_2kb_Rev	5'- CAGCCCCACTCTTAAACTGC-3'
JHDM1D_TSS_Fwd	5'-TGCGATATCTGCAAGGACTG-3'
JHDM1D_TSS_Rev	5'-GGCTGGAGGGGGTTTATTTA-3'
JHDM1D_1.5kb_Fwd	5'-TATTTGGGTGTTGTGGCAAA-3'

JHDM1D_1.5kb_Rev	5'-GGAAACCGGCTTCAACTAAA-3'
NDUFS6_TSS_Fwd	5'-AGAAGGTCACGCACACTGG-3'
NDUFS6_TSS_Rev	5'-GGAGGAAGGTGCATCCTGTA-3'
NDUFS6_2kb_Fwd	5'-TTCCAGAGCTACAGGGCATT-3'
NDUFS6_2kb_Rev	5'-CCCATCAAACCACACAACAG-3'
P2RY11_TSS_Fwd	5'-GGGATTCTGGAGCCATACAA-3'
P2RY11_TSS_Rev	5'-TTCCAGGAAGAAACCAGGTG-3'
P2RY11_2kb_Fwd	5'-CAATGCATAACCCTGGCTCT-3'
P2RY11_2kb_Rev	5'-TCCCTGGACACGAGTTCTTT-3'
CENPB_TSS_Fwd	5'-CTGACGTTCCGGGAGAAG-3'
CENPB_TSS_Rev	5'-GGATTCTCCTCCACCTCCTG-3'
CENPB_2kb_Fwd	5'-CTTTGCCATGGTCAAGAGGT-3'
CENPB_2kb_Rev	5'-TGTCCAAGACCTCGAACTCC-3'
SLBP_TSS_Fwd	5'-CCCACATAAAGGCGGTTG-3'
SLBP_TSS_Rev	5'-GGCAGAGAGCGCAGAGTAGA-3'
SLBP_2kb_Fwd	5'-ATGGGAAGTTGTGAGGCTTG-3'
SLBP_2kb_Rev	5'-TGCCTCCCATGTAGACTCCT-3'
PARD6A_TSS_Fwd	5'-TAGCATCGTCGAGGTGAAGA-3'
PARD6A_TSS_Rev	5'-AGGGGAGAAAGAGGGAATTG-3'
PARD6A_2kb_Fwd	5'-GGTCCTTGTGTGTCCCAGTT-3'
PARD6A_2kb_Rev	5'-GGAAGTTCTCCCCAATGTCA-3'
RASSF7_TSS_Fwd	5'-CGCCCACACCTGTAGTCT-3'
RASSF7_TSS_Rev	5'-CATTGGCTGCCTCTGTCAC-3'
RASSF7_2kb_Fwd	5'-CCCCTCACCTATGGCATCT-3'
RASSF7_2kb_Rev	5'-GCTCCTGAACAGCCAGGTC-3'
HCCA2_TSS_Fwd	5'-CGGTGAGGCCTGAGTCTCTA-3'

HCCA2_TSS_Rev	5'-TCCTCTACAGGGCTTCCAGA-3'
HCCA2_2kb_Fwd	5'-AGGAGTGGGTTCACACCAAG-3'
HCCA2_2kb_Rev	5'-AGATCGGGGTCCTGAGTTCT-3'
FSCN1_TSS_Fwd	5'-CTCGTCTACTGCCACCATGA-3'
FSCN1_TSS_Rev	5'-AGGTACTTGTTGCCGCAGTT-3'
FSCN1_2kb_Fwd	5'-TACCCTCTGGTGAACCCATC-3'
FSCN1_2kb_Rev	5'-TCGGGGAGAATCTGAGAAAG-3'
C9orf167_-1.5kb_Fwd	5'-CACCCCTGTAGATGGGAGAA-3'
C9orf167_-1.5kb_Rev	5'-CCCTATGGGTCAAAGGTGAA-3'
C9orf167_TSS_Fwd	5'-ACCCCCTGACTCACTTCCTT-3'
C9orf167_TSS_Rev	5'-CGGAGTAGAGGAAGCTCTGG-3'
C9orf167_2kb_Fwd	5'-GTGAGGGCTTCTTTCCTGAC-3'
C9orf167_2kb_Rev	5'-GCCTCCACTACAGGAGGTTC-3'
ADCYAP1R1_TSS_Fwd	5'-CGTCCTTTGCGGAGTCTG-3'
ADCYAP1R1_TSS_Rev	5'-GCGACCCTTACCTGCTCACT-3'
ADCYAP1R1_2kb_Fwd	5'-AAGGATCCCTCTCCTGCACT-3'
ADCYAP1R1_2kb_Rev	5'-GGTCCCAAAGTGTTTCTCCA-3'
SLC7A10_TSS_Fwd	5'-AGATCTGCCCCAAGTCCTCT-3'
SLC7A10_TSS_Rev	5'-CTCCCCCACCTCCCTTAAA-3'
SLC7A10_2kb_Fwd	5'-CCTTCAGTTCCTTCCTGCTG-3'
SLC7A10_2kb_Rev	5'-CCTGGCTCAGTGTTCAAGGT-3'
CALML3_-0.8_Fwd	5'-AGCAGGAGGTCTGTCCTTGA-3'
CALML3_-0.8_Rev	5'-TGATCGAGGAATGCAAACAA-3'
CALML3_TSS_Fwd	5'-AGCTGACTGAGGAGCAGGTC-3'
CALML3_TSS_Rev	5'-GTCCCCATCCTTGTCAAACA-3'
CALML3_1.5_Fwd	5'-ATACGCTGGCAGCAAAGAGT-3'

CALML3_1.5_Rev	5'-ACTTCACAACCAGGGAGCAC-3'
PPP2R5B_TSS_Fwd	5'-TGGTCTGGCAGCTCACTTTA-3'
PPP2R5B_TSS_Rev	5'-GCTGCTCAGGATGACATCAA-3'
PPP2R5B_2kb_Fwd	5'-AGGAGATGGCACAAGAGCAT-3'
PPP2R5B_2kb_Rev	5'-GGCAGACCCTCCTAATCTCC-3'
TRIM33_TSS_Fwd	5'-TTCGCTCTCTCGCTAGCTCT-3'
TRIM33_TSS_Rev	5'-CTTTGTTTTCCGCCATGTTT-3'
TRIM33_2.5kb_Fwd	5'-TGGGGTGTAGGGAGGATAAA-3'
TRIM33_2.5kb_Rev	5'-GCTTCTCCAACAACCAAAGC-3'

mRNA primers

ICAM1mRNA_Fwd	5'-AGCTTCTCCTGCTCTGCAAC-3'
ICAM1mRNA_Rev	5'-AATCCCTCTCGTCCAGTCG-3'
iNOSmRNA_Fwd	5'-TGGATGCAACCCCATTGTC-3'
iNOSmRNA_Rev	5'-CCCGCTGCCCCAGTTT-3'
VCAM1mRNA_Fwd	5'-CGAGACCACCCCAGAATCTA-3'
VCAM1mRNA_Rev	5'-GGTGCTGCAAGTCAATGAGA-3'
TNFmRNA_Fwd	5'-AACCTCCTCTCTGCCATCAA-3'
TNFmRNA_Rev	5'-GGAAGACCCCTCCCAGATAG-3'
NFKBp50mRNA_Fwd	5'-CTGGAAGCACGAATGACAGA-3'
NFKBp50mRNA_Rev	5'-CCTTCTGCTTGCAAATAGGC-3'
IL6_mRNA_Fwd	5'-GGTACATCCTCGACGGCATCT-3'
IL6_mRNA_Rev	5'-GTGCCTCTTTGCTGCTTTCAC-3'
NFKB2mRNA_Fwd	5'- AGGTCTACTGGAGGCCCTGT-3’
NFKB2mRNA_Rev	5'- CTTGTCTCGGGTTTCTGGAC-3’
JHDM1DmRNA_Fwd	5'- CGAGGGGACTGTTCTTCTTG -3’

JHDM1DmRNA_Rev	5'- CTTCCGGACTGAAAGGACAC -3’
PARD6AmRNA_Fwd	5'- GTTGCCAACAGCCATAACCT -3’
PARD6AmRNA_Rev	5'- CAGGTCACTGCTGTCATCGT -3’
MAP6KmRNA_Fwd	5'- ATCTATTCCCCATCCCAAGG -3’
MAP6KmRNA_Rev	5'- AAGAGACTGCGATGCCACAT -3’
PPP2R5B_mRNA_Fwd	5'- CCAGAGTGGCTTCTGAGGAC -3'
PPP2R5B_mRNA_Rev	5'- AGCATTCTGTTGCCAAGACC -3'

Chromatin immunoprecipitation (ChIP). ChIP was performed essentially as described previously (Kininis, et al., 2007, Krishnakumar, et al., 2008). Briefly, cells were grown to ~70% confluence, and left in serum-free medium overnight. Cells were then treated with relevant chemicals (eg. TNFα 25 ng/ml for 30 min., with or without pre-treatment with 10 μg/ml BAY-11-7082), cross-linked with 1% paraformaldehyde in PBS for 10 min. at 37°C, and quenched in 125 mM glycine in PBS for 5 min. at 4°C. The cells were collected by centrifugation and sonicated in lysis buffer (1% SDS, 10 mM EDTA, 50 mM Tris•HCl, pH 7.9, 1x protease inhibitor cocktail) to generate chromatin fragments of ~500 bp in length. The material was clarified by centrifugation, diluted 10-fold in dilution buffer (0.5% Triton X-100, 2 mM EDTA, 150 mM NaCl, 20 mM Tris•HCl, pH 7.9, 1x protease inhibitor cocktail), and pre-cleared with protein A-agarose beads. The pre-cleared, chromatin-containing supernatant was used in immunoprecipitation reactions with antibodies against the factor of interest, or without antibodies as a control. The immunoprecipitated genomic DNA was cleared of protein and residual RNA by digestion with proteinase K and RNase H, respectively. The DNA was then extracted with phenol:chloroform:isoamyl alcohol and precipitated with ethanol. Quantitative real-time PCR (qPCR) was used to determine the enrichment of immunoprecipitated material relative to the input material

using gene-specific primer sets to the specified regions. Each ChIP experiment was conduced a minimum of three times with independent chromatin isolates to ensure reproducibility.

ChIP-chip. LM-PCR amplified genomic DNA samples were used to probe a custom human (HG18) oligonucleotide genomic array from Nimblegen. The custom array contained ~2,100,000 features (tiling interval of 75 bp for the ~50-mer probes), including 23,551 promoter regions (approximately -3 kb to +7 kb relative to the transcription start site for most promoters). The ChIP-chip analyses were run a minimum of two times to ensure reproducibility.

Genomic data analyses. Genomic data analyses were performed using the statistical programming language R (R Development Core Team) as previously described (Krishnakumar, et al., 2008, Team, 2006). The $\log_2$ ratio data from each of the arrays was subjected to lowess normalization. A single array error model was generated using a 800 bp moving window with 200 bp steps in which both the mean probe log2 ratio and p-values were calculated for each window. The p-values are from a nonparametric Wilcoxon signed-rank test. Significant peaks were defined as the center of three consecutive windows with positive means, the center window with a mean greater than either adjacent window, all windows having p-values less than 0.016, and the middle window having a signal intensity greater than 0.5. Correlation analyses, averaging (metagene) analyses, and gene categorization were done as described in Chapter 2/3.

Motif Finding Analysis. Transcription factor binding sites (Transfac® motifs) were identified in regions with statistically significant peaks of factor binding (as defined in

each specific analysis, usually 400 bp around the peak) using the UCSC Genome Browser feature Galaxy®. Following this, the enrichment of each binding site over the background regions (defined as all the regions on our ChIP-chip promoter array) was obtained, and the significance of this enrichment was calculated using a Fisher-exact test.

REFERENCES

Aufricht, C. 2005. Heat-shock protein 70: molecular supertool? Pediatr Nephrol 20:707-13.

Banno, T., A. Gazel, and M. Blumenberg. 2005. Pathway-specific profiling identifies the NF-kappa B-dependent tumor necrosis factor alpha-regulated genes in epidermal keratinocytes. J Biol Chem 280:18973-80.

Beissbarth, T., and T. P. Speed. 2004. GOstat: find statistically overrepresented Gene Ontologies within a group of genes. Bioinformatics 20:1464-5.

Chen, L., W. Fischle, E. Verdin, and W. C. Greene. 2001. Duration of nuclear NF-kappaB action regulated by reversible acetylation. Science 293:1653-7.

Comstock, K. L., K. A. Krown, M. T. Page, D. Martin, P. Ho, M. Pedraza, E. N. Castro, N. Nakajima, C. C. Glembotski, P. J. Quintana, and R. A. Sabbadini. 1998. LPS-induced TNF-alpha release from and apoptosis in rat cardiomyocytes: obligatory role for CD14 in mediating the LPS response. J Mol Cell Cardiol 30:2761-75.

Covic, M., P. O. Hassa, S. Saccani, C. Buerki, N. I. Meier, C. Lombardi, R. Imhof, M. T. Bedford, G. Natoli, and M. O. Hottiger. 2005. Arginine methyltransferase CARM1 is a promoter-specific regulator of NF-kappaB-dependent gene expression. EMBO J 24:85-96.

Davidson, M. M., C. Nesti, L. Palenzuela, W. F. Walker, E. Hernandez, L. Protas, M. Hirano, and N. D. Isaac. 2005. Novel cell lines derived from adult human ventricular cardiomyocytes. J Mol Cell Cardiol 39:133-47.

Epstein, J. A., and M. S. Parmacek. 2005. Recent advances in cardiac development with therapeutic implications for adult cardiovascular disease. Circulation 112:592-7.

Fischer, P., and D. Hilfiker-Kleiner. 2007. Survival pathways in hypertrophy and heart failure: the gp130-STAT axis. Basic Res Cardiol 102:393-411.

Frizzell, K. M., M. J. Gamble, J. G. Berrocal, T. Zhang, R. Krishnakumar, Y. Cen, A. A. Sauve, and W. L. Kraus. 2009. Global analysis of transcriptional regulation by poly(ADP-ribose) polymerase-1 and poly(ADP-ribose) glycohydrolase in MCF-7 human breast cancer cells. J Biol Chem.

Hassa, P. O., C. Buerki, C. Lombardi, R. Imhof, and M. O. Hottiger. 2003. Transcriptional coactivation of nuclear factor-kappaB-dependent gene

expression by p300 is regulated by poly(ADP)-ribose polymerase-1. J Biol Chem 278:45145-53.

Hassa, P. O., S. S. Haenni, C. Buerki, N. I. Meier, W. S. Lane, H. Owen, M. Gersbach, R. Imhof, and M. O. Hottiger. 2005. Acetylation of poly(ADP-ribose) polymerase-1 by p300/CREB-binding protein regulates coactivation of NF-kappaB-dependent transcription. J Biol Chem 280:40450-64.

Henderson, B. C., and S. C. Tyagi. 2006. Oxidative mechanism and homeostasis of proteinase/antiproteinase in congestive heart failure. J Mol Cell Cardiol 41:959-62.

Hirano, F., H. Tanaka, Y. Hirano, M. Hiramoto, H. Handa, I. Makino, and C. Scheidereit. 1998. Functional interference of Sp1 and NF-kappaB through the same DNA binding site. Mol Cell Biol 18:1266-74.

Ju, B. G., V. V. Lunyak, V. Perissi, I. Garcia-Bassets, D. W. Rose, C. K. Glass, and M. G. Rosenfeld. 2006. A topoisomerase IIbeta-mediated dsDNA break required for regulated transcription. Science 312:1798-802.

Ju, B. G., D. Solum, E. J. Song, K. J. Lee, D. W. Rose, C. K. Glass, and M. G. Rosenfeld. 2004. Activating the PARP-1 sensor component of the groucho/ TLE1 corepressor complex mediates a CaMKinase IIdelta-dependent neurogenic gene activation pathway. Cell 119:815-29.

Katsel, P. L., and R. J. Greenstein. 2001. Identification of overlapping AP-2/NF-kappa B-responsive elements on the rat cholecystokinin gene promoter. J Biol Chem 276:752-8.

Kawahara, T. L., E. Michishita, A. S. Adler, M. Damian, E. Berber, M. Lin, R. A. McCord, K. C. Ongaigui, L. D. Boxer, H. Y. Chang, and K. F. Chua. 2009. SIRT6 links histone H3 lysine 9 deacetylation to NF-kappaB-dependent gene expression and organismal life span. Cell 136:62-74.

Kim, M. Y., S. Mauro, N. Gevry, J. T. Lis, and W. L. Kraus. 2004. NAD+-dependent modulation of chromatin structure and transcription by nucleosome binding properties of PARP-1. Cell 119:803-14.

Kim, S., and H. Iwao. 1999. Activation of mitogen-activated protein kinases in cardiovascular hypertrophy and remodeling. Jpn J Pharmacol 80:97-102.

Kininis, M., B. S. Chen, A. G. Diehl, G. D. Isaacs, T. Zhang, A. C. Siepel, A. G. Clark, and W. L. Kraus. 2007. Genomic analyses of transcription factor binding, histone acetylation, and gene expression reveal mechanistically distinct classes of estrogen-regulated promoters. Mol Cell Biol 27:5090-104.

Krishnakumar, R., M. J. Gamble, K. M. Frizzell, J. G. Berrocal, M. Kininis, and W. L. Kraus. 2008. Reciprocal binding of PARP-1 and histone H1 at promoters specifies transcriptional outcomes. Science 319:819-21.

Kronke, M., S. Schutze, P. Scheurich, and K. Pfizenmaier. 1992. TNF signal transduction and TNF-responsive genes. Immunol Ser 56:189-216.

Lentsch, A. B., and P. A. Ward. 1999. Activation and regulation of NFkappaB during acute inflammation. Clin Chem Lab Med 37:205-8.

Lentsch, A. B., and P. A. Ward. 2000. The NFkappaBb/IkappaB system in acute inflammation. Arch Immunol Ther Exp (Warsz) 48:59-63.

Li, X., and G. R. Stark. 2002. NFkappaB-dependent signaling pathways. Exp Hematol 30:285-96.

Lim, C. A., F. Yao, J. J. Wong, J. George, H. Xu, K. P. Chiu, W. K. Sung, L. Lipovich, V. B. Vega, J. Chen, A. Shahab, X. D. Zhao, M. Hibberd, C. L. Wei, B. Lim, H. H. Ng, Y. Ruan, and K. C. Chin. 2007. Genome-wide mapping of RELA(p65) binding identifies E2F1 as a transcriptional activator recruited by NF-kappaB upon TLR4 activation. Mol Cell 27:622-35.

Maass, D. L., D. P. Hybki, J. White, and J. W. Horton. 2002. The time course of cardiac NF-kappaB activation and TNF-alpha secretion by cardiac myocytes after burn injury: contribution to burn-related cardiac contractile dysfunction. Shock 17:293-9.

Mehra, R. 2007. Global public health problem of sudden cardiac death. J Electrocardiol 40:S118-22.

Meylan, E., A. L. Dooley, D. M. Feldser, L. Shen, E. Turk, C. Ouyang, and T. Jacks. 2009. Requirement for NF-kappaB signalling in a mouse model of lung adenocarcinoma. Nature 462:104-7.

Molnar, A., A. Toth, Z. Bagi, Z. Papp, I. Edes, M. Vaszily, Z. Galajda, J. G. Papp, A. Varro, V. Szuts, Z. Lacza, D. Gero, and C. Szabo. 2006. Activation of the poly(ADP-ribose) polymerase pathway in human heart failure. Mol Med 12:143-52.

Natoli, G., A. Costanzo, F. Guido, F. Moretti, and M. Levrero. 1998. Apoptotic, non-apoptotic, and anti-apoptotic pathways of tumor necrosis factor signalling. Biochem Pharmacol 56:915-20.

Pacher, P., and C. Szabo. 2007. Role of poly(ADP-ribose) polymerase 1 (PARP-1) in cardiovascular diseases: the therapeutic potential of PARP inhibitors. Cardiovasc Drug Rev 25:235-60.

Pavri, R., B. Lewis, T. K. Kim, F. J. Dilworth, H. Erdjument-Bromage, P. Tempst, G. de Murcia, R. Evans, P. Chambon, and D. Reinberg. 2005. PARP-1 determines specificity in a retinoid signaling pathway via direct modulation of mediator. Mol Cell 18:83-96.

Pillai, J. B., M. Gupta, S. B. Rajamohan, R. Lang, J. Raman, and M. P. Gupta. 2006. Poly(ADP-ribose) polymerase-1-deficient mice are protected from angiotensin II-induced cardiac hypertrophy. Am J Physiol Heart Circ Physiol 291:H1545-53.

Pillai, J. B., A. Isbatan, S. Imai, and M. P. Gupta. 2005. Poly(ADP-ribose) polymerase-1-dependent cardiac myocyte cell death during heart failure is mediated by NAD+ depletion and reduced Sir2alpha deacetylase activity. J Biol Chem 280:43121-30.

Prosniak, M., D. C. Hooper, B. Dietzschold, and H. Koprowski. 2001. Effect of rabies virus infection on gene expression in mouse brain. Proc Natl Acad Sci U S A 98:2758-63.

Rangan, G., Y. Wang, and D. Harris. 2009. NF-kappaB signalling in chronic kidney disease. Front Biosci 14:3496-522.

Schreiber, J., R. G. Jenner, H. L. Murray, G. K. Gerber, D. K. Gifford, and R. A. Young. 2006. Coordinated binding of NF-kappaB family members in the response of human cells to lipopolysaccharide. Proc Natl Acad Sci U S A 103:5899-904.

Schulz, R., S. Aker, S. Belosjorow, and G. Heusch. 2004. TNFalpha in ischemia/reperfusion injury and heart failure. Basic Res Cardiol 99:8-11.

Schutze, S., T. Machleidt, and M. Kronke. 1992. Mechanisms of tumor necrosis factor action. Semin Oncol 19:16-24.

Soriano, F. G., L. Virag, and C. Szabo. 2001. Diabetic endothelial dysfunction: role of reactive oxygen and nitrogen species production and poly(ADP-ribose) polymerase activation. J Mol Med 79:437-48.

Spooren, A., R. Kooijman, B. Lintermans, K. Van Craenenbroeck, L. Vermeulen, G. Haegeman, and S. Gerlo. Cooperation of NFkappaB and CREB to induce synergistic IL-6 expression in astrocytes. Cell Signal 22:871-81.

Stilmann, M., M. Hinz, S. C. Arslan, A. Zimmer, V. Schreiber, and C. Scheidereit. 2009. A nuclear poly(ADP-ribose)-dependent signalosome confers DNA damage-induced IkappaB kinase activation. Mol Cell 36:365-78.

Szabo, C., P. Pacher, and R. A. Swanson. 2006. Novel modulators of poly(ADP-ribose) polymerase. Trends Pharmacol Sci 27:626-30.

Team, R. D. C. 2006. R: A language and environment for statistical computing, R Foundation for Statistical Computing, Vienna, Austria.

Tian, B., D. E. Nowak, M. Jamaluddin, S. Wang, and A. R. Brasier. 2005. Identification of direct genomic targets downstream of the nuclear factor-kappaB transcription factor mediating tumor necrosis factor signaling. J Biol Chem 280:17435-48.

Todorov, V. T., S. Volkl, J. Friedrich, L. A. Kunz-Schughart, T. Hehlgans, L. Vermeulen, G. Haegeman, M. L. Schmitz, and A. Kurtz. 2005. Role of CREB1 and NF{kappa}B-p65 in the down-regulation of renin gene expression by tumor necrosis factor {alpha}. J Biol Chem 280:24356-62.

Tulin, A., and A. Spradling. 2003. Chromatin loosening by poly(ADP)-ribose polymerase (PARP) at Drosophila puff loci. Science 299:560-2.

Valen, G. 2004. Signal transduction through nuclear factor kappa B in ischemia-reperfusion and heart failure. Basic Res Cardiol 99:1-7.

Vallabhapurapu, S., and M. Karin. 2009. Regulation and function of NF-kappaB transcription factors in the immune system. Annu Rev Immunol 27:693-733.

Wada, Y., Y. Ohta, M. Xu, S. Tsutsumi, T. Minami, K. Inoue, D. Komura, J. Kitakami, N. Oshida, A. Papantonis, A. Izumi, M. Kobayashi, H. Meguro, Y. Kanki, I. Mimura, K. Yamamoto, C. Mataki, T. Hamakubo, K. Shirahige, H. Aburatani, H. Kimura, T. Kodama, P. R. Cook, and S. Ihara. 2009. A wave of nascent transcription on activated human genes. Proc Natl Acad Sci U S A 106:18357-61.

Welboren, W. J., M. A. van Driel, E. M. Janssen-Megens, S. J. van Heeringen, F. C. Sweep, P. N. Span, and H. G. Stunnenberg. 2009. ChIP-Seq of ERalpha and RNA polymerase II defines genes differentially responding to ligands. EMBO J 28:1418-28.

Yamamoto, Y., U. N. Verma, S. Prajapati, Y. T. Kwak, and R. B. Gaynor. 2003. Histone H3 phosphorylation by IKK-alpha is critical for cytokine-induced gene expression. Nature 423:655-9.

Yang, C. R., C. Wilson-Van Patten, S. M. Planchon, S. M. Wuerzberger-Davis, T. W. Davis, S. Cuthill, S. Miyamoto, and D. A. Boothman. 2000. Coordinate modulation of Sp1, NF-kappa B, and p53 in confluent human malignant melanoma cells after ionizing radiation. FASEB J 14:379-90.

Zhang, T., J. G. Berrocal, K. M. Frizzell, M. J. Gamble, M. E. DuMond, R. Krishnakumar, T. Yang, A. A. Sauve, and W. L. Kraus. 2009. Enzymes in the NAD+ salvage pathway regulate SIRT1 activity at target gene promoters. J Biol Chem 284:20408-17.

Concluding Remarks

Although PARP-1 has been studied for a number of years, only recently are we beginning to understand the physiological roles that PARP-1 plays *in vivo (Kraus, 2008)*. Specifically, recent studies have unveiled a prominent role for PARP-1 as a modulator of chromatin structure and transcription, and in this work, we have identified novel mechanisms by which PARP-1 achieves this regulation, in two different biological systems *(Caiafa, et al., 2009, Hassa and Hottiger, 2002, Ju, et al., 2006, Krishnakumar, et al., 2008, Pavri, et al., 2005)*. Based on our data, we have formed a model of how we think PARP-1 acts at target promoters (Fig. 5). We show in breast cancer cells that PARP-1 binds to the promoters of active genes and excludes the binding of repressor proteins from the promoter, including linker histone H1 and the histone demethylase KDM5B *(Krishnakumar, et al., 2008)*. Work from other labs has shown that PARP-1 can also recruit activator proteins, which fits with our model of PARP-1's role at promoters *(Hassa and Hottiger, 2002, Ju, et al., 2006, Pavri, et al., 2005)* For some of these proteins, PARP-1 catalytic activity is vital for regulating their localization, as is the case for KDM5B. By coordinating repressor and activator protein binding at target promoters, PARP-1 is able to create a favorable chromatin environment (i.e. suitable positioning of nucleosomes) to promote the binding of Pol II and associated basal transcription machinery, which results in increased transcription.

In addition to maintaining basal transcription, PARP-1 is also involved in organizing the transcriptional response to a number of different signaling pathways, and cooperates with DNA-binding transcription factors to this end, one of which is NFκB *(Hassa and Hottiger, 2002, Ju, et al., 2006, Pavri, et al., 2005)*. NFκB is a major transcription factor involved in regulating the inflammatory pathways that are

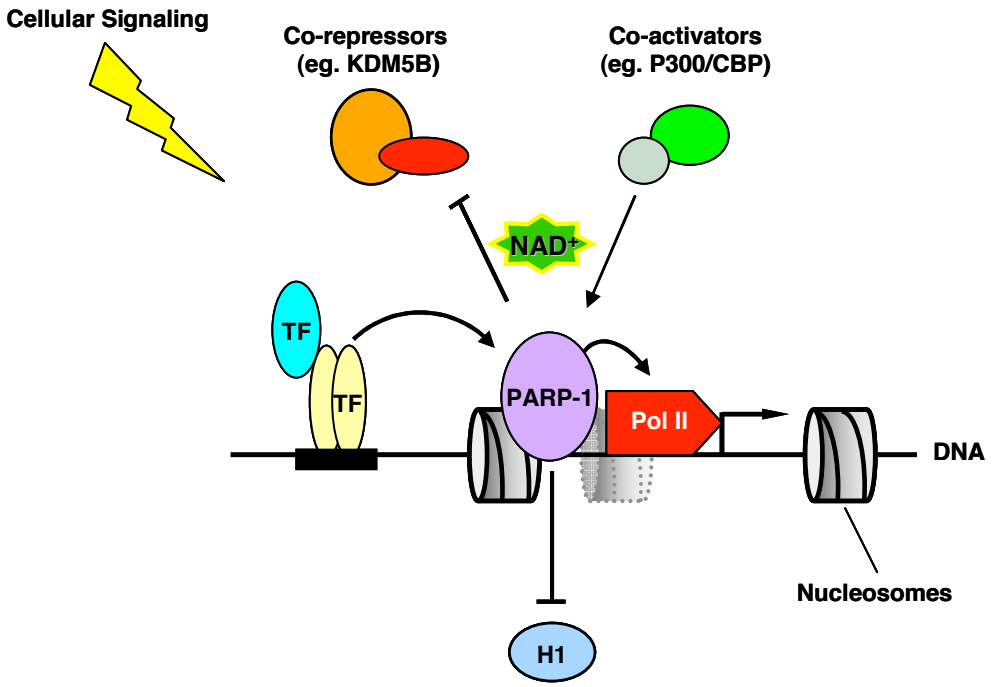

Figure 5. Model of PARP-1-dependent regulation of chromatin structure and transcription at target promoters. Schematic of a prototypic target gene. TSS (Transcription start site) of the gene is depicted by a bent arrow. TF = Transcription factor. Black bar = Transcription factor binding site.

triggered as a result of CVD. Here, I looked at how TNFα-stimulated NFκB-dependent transcription is regulated in human cardiomyocytes, and I confirm a role for PARP-1 as an activator. Interestingly, I see that while PARP-1 and NFκB are found primarily at an overlapping set of promoters, they do not directly co-localize, as may be the case if PARP-1 were a classical co-activator of NFκB. Furthermore, PARP-1 is pre-bound at target genes, and preventing NFκB recruitment by inhibiting IKKα/β does not affect PARP-1 binding, suggesting that PARP-1 may be playing a more chromatin-based role in this system, in a manner similar to what I observed in breast cancer cells. In addition, the lack of NFκB canonical binding sites under a majority of the NFκB peaks at promoters suggests cooperation with additional transcription factors, and I will be focusing on how NFκB, PARP-1 and these other factors all coordinate the intricate response to TNFα that I observe in these cells. In conclusion, PARP-1 is involved in variety of signaling and transcriptional pathways and is able to coordinate responses to a number of different stimuli. It will be interesting to determine the level of conservation of the PARP-1-dependent pathways I have observed in this study, and how we can expand on these roles by investigating additional biological systems. We are, however, only seeing the tip of the iceberg, and it is very likely that in the years to come, the common themes that connect all the different functions of PARP-1 in various systems will become much more evident. Identifying these commonalities is going to be critical to be able to capitalize on the therapeutic potential of PARP-1, and other PARP family members. As we are slowly realizing, they are a poorly-tapped but very rich resource for the future of medicine.

REFERENCES

Caiafa, P., T. Guastafierro, and M. Zampieri. 2009. Epigenetics: poly(ADP-ribosyl)ation of PARP-1 regulates genomic methylation patterns. FASEB J 23:672-8.

Hassa, P. O., and M. O. Hottiger. 2002. The functional role of poly(ADP-ribose)polymerase 1 as novel coactivator of NF-kappaB in inflammatory disorders. Cell Mol Life Sci 59:1534-53.

Ju, B. G., V. V. Lunyak, V. Perissi, I. Garcia-Bassets, D. W. Rose, C. K. Glass, and M. G. Rosenfeld. 2006. A topoisomerase IIbeta-mediated dsDNA break required for regulated transcription. Science 312:1798-802.

Kraus, W. L. 2008. Transcriptional control by PARP-1: chromatin modulation, enhancer-binding, coregulation, and insulation. Curr Opin Cell Biol 20:294-302.

Krishnakumar, R., M. J. Gamble, K. M. Frizzell, J. G. Berrocal, M. Kininis, and W. L. Kraus. 2008. Reciprocal binding of PARP-1 and histone H1 at promoters specifies transcriptional outcomes. Science 319:819-21.

Pavri, R., B. Lewis, T. K. Kim, F. J. Dilworth, H. Erdjument-Bromage, P. Tempst, G. de Murcia, R. Evans, P. Chambon, and D. Reinberg. 2005. PARP-1 determines specificity in a retinoid signaling pathway via direct modulation of mediator. Mol Cell 18:83-96.